



**Design and PLC Implementation of Nonlinear PID Controllers for
Control of Nonlinear Processes**

by

NOMZAMO TSHEMESE

Thesis submitted in fulfillment of the requirements for the degree

Master of Technology: Electrical Engineering

in the Faculty of Engineering

at the Cape Peninsula University of Technology

Supervisor: Prof. R. Tzoneva

Co-supervisor: Mr. C. Kriger

Bellville Campus

December 2014

DECLARATION

I, Nomzamo Tshemese, declare that the contents of this dissertation/thesis represent my own unaided work, and that the dissertation/thesis has not previously been submitted for academic examination towards any qualification. Furthermore, it represents my own opinions and not necessarily those of the Cape Peninsula University of Technology.

Signed

Date

ABSTRACT

A new control strategy for control of the nonlinear process of Dissolved Oxygen (DO) concentration in the aerobic tank of wastewater treatment process is proposed. It provides means to improve the performance of the Linear Proportional Integration and Derivative (LPID) controller by extending it to a Nonlinear Proportional Integration and Derivative (NLPID) controller.

The aim of the thesis is to develop methods, algorithms and software for design, simulation, and programmable logic controller (PLC) implementation of NLPID controllers in order to control the nonlinear process of dissolved oxygen. The thesis investigates the possibilities the widely used in theory and industry methods for the design of the LPID controllers for linear processes as Ziegler- Nichols and Pole Placement, to be applied to the design of NLPID controllers for the nonlinear process of DO concentration. Three cases are considered:

Case 1: Application of the values of the parameters the linear PID controller designed by the Ziegler-Niched method for the linearized DO process model to be used as parameters of the nonlinear PID controllers to control the DO nonlinear process.

Case 2: Application of the values of the parameters of the linear PID controller designed by the Pole placement method for the linearized DO process model, to be used as parameters of the nonlinear PID controller to control the nonlinear DO process.

Case 3: Novel, proposed in the thesis, method based on the Pole placement method for direct design of the parameters of the linear and nonlinear PID controllers to control the nonlinear DO process.

Software is developed to simulate in MATLAB environment the behavior of the closed loop DO process for the considered cases of controller designs. The results of the simulations show that in the Case1 and the Case 2 it is not possible to use the values of the LPID controller parameters designed for the linearized DO process, directly to control the nonlinear process by the NPID controllers. Additional tuning for some of the parameters is needed. The simulation in the Case 3 shows the excellent behaviors of the closed loop system for all linear and nonlinear PID controllers which prove that the new method is effective and applicable.

Real-time simulations of the closed loop system are done in a TwinCAT 3 simulation environment of the Bechhoff EX5020 PLC. The deliverables of the thesis are applicable to many type nonlinear processes in chemical, manufacturing, and other industries.

ACKNOWLEDGMENTS

I wish to thank:

- My creator for giving courage, wisdom and strength for guiding me throughout my studies.
- I would like to express my gratitude to my Supervisor, Prof. R. Tzoneva, whose encouragement, guidance, and support helped me throughout my course of study, and it would not have been possible without your support.
- I would like to thank my Co-supervisor Mr. C. Kriger for his support to successfully complete this study.
- I am grateful to my entire family, especially my husband for his encouragements, motivation and support.
- The staff members and post graduate students of the RTDS and CSAEMS research centers at the Cape Peninsula University of Technology.
- Acknowledgements can go on and on, but some people will still be left out. To those I have unknowingly left out, but were helpful to me, please accept my gratitude.

The financial assistance of the National Research Foundation towards this research is acknowledged. Opinions expressed in this thesis and the conclusions arrived at, are those of the author, and are not necessarily to be attributed to the National Research Foundation.

DEDICATION

I wish to dedicate this thesis to my mother Emelina, my husband Leonard and my children Elethu, and Snelitha for their patience and support.

TABLE OF CONTENTS

Declaration	ii
Abstract	iii
Acknowledgements	iv
Dedication	v
Table of contents	vi
List of Figures	xiii
List of Tables	xxix
List of Appendices	xxxii
Glossary	xxxii
Mathematical Notations	xxxiii

CHAPTER ONE: INTRODUCTION

1.1	Introduction	1
1.2	Awareness of the problem	3
1.3	Problem Identification	4
1.4	Statement of the Problem	5
1.4.1	Design based sub-problems	5
1.4.2	Real time implementation sub-problems	6
1.5	Aim and Objectives	6
1.6	Hypothesis	7
1.7	Research approach and Techniques	7
1.8	Research Assumptions	7
1.9	Research Significance	8
1.10	Thesis Outline	9
1.11	Conclusion	10

CHAPTER TWO: LITERATURE REVIEW

2.1	Introduction	11
2.2	Literature search to perform an overview of the Activated Sludge Wastewater Treatment Process and the methods for design of nonlinear controllers	12
2.3	Wastewater Treatment Plant (WWTP) Description	14
2.3.1	Common layout of WWTP	14
2.3.2	The process of Activated Sludge	15
2.3.3	Significant zones of the Activated Sludge Process	17
2.3.3.1	Carbon Removal	17

2.3.3.2	Nitrogen Removal	17
2.3.3.3	Phosphorus Removal	17
2.3.4	Dissolved Oxygen Concentration Process Overview	18
2.4	Activated Sludge Models	19
2.4.1	Benchmark Model of the Activate Sludge Wastewater Treatment Plant	19
2.4.2	Historical overview of the Activated Sludge Biological Models development	20
2.5	Literature Review of the methods for design of nonlinear controllers for nonlinear plants	22
2.5.1	Feedback Linearization methods	22
2.5.2	Linear and nonlinear PID controllers	24
2.5.2.1	<i>Linear PID controllers</i>	24
2.5.2.2	<i>Nonlinear PID</i>	27
2.5.3	Lyapunov theory of stability	29
2.5.4	Adaptive control	30
2.5.5	Optimal control	30
2.5.6	Model Predictive Control	31
2.5.7	Pole Placement method	32
2.5.8	Ziegler and Nichols control design method	32
2.5.9	Review of the existing papers in a Table form	33
2.6	Discussion on the findings from the literature review	42
2.7	New International Electro-technical Commission (IEC) 61499 standard and PLC controller implementation	43
2.8	Conclusion	45

CHAPTER THREE: DISSOLVED OXYGEN CONCENTRATION MODELING AND SIMULATION

3.1	Introduction	46
3.2	Description of the Benchmark Process based on ASM1 biological model	47
3.3	Dissolved Oxygen Mathematical Model	48
3.3.1	Oxygen Transfer Function and Uptake rate	49
3.3.2	An exponential model of K_{La}	50
3.4	Dissolved Oxygen simulation model	52
3.4.1	Description	52
3.4.2	Matrix Laboratory and Simulink	52
3.4.3	Simulation Input data and Biological Process Model Parameters	53
3.4.4	Dissolved Oxygen Simulation Results	54
3.5	Analysis and Discussion of the results	62
3.5.1	Conclusion of the discussion	63
3.6	Conclusion	64

CHAPTER FOUR: APPLIED LINEAR AND NONLINEAR CONTROL THEORY

4.1	Introduction	65
4.2	Control History	66
4.2.1	Control Overview and Theory	67
4.2.2	Standard Control Theory	67
4.2.3	Controller Specifications	68
4.2.4	Control Theory Ending	69
4.3	Closed-loop System transfer function	69
4.3.1	PID Control Description	69
4.3.1.1	Linear PID Controller	70
4.4	Nonlinear Control Theory	72
4.4.1	Why Nonlinear control	72
4.4.1.1	Improvement of existing control systems	73
4.4.1.2	Investigation analysis of solid nonlinearities	73
4.4.1.3	Uncertainties of the model	73
4.4.1.4	Design Simplicity and Nonlinear Control Description	74
4.5	Mathematical model of Differential Tracker	75
4.6	Mathematical Model of the nonlinear PID Controller	77
4.7	Conclusion	79

CHAPTER FIVE: DEVELOPMENT OF METHODS FOR DESIGN AND TUNING OF NLPID CONTROLLERS

5.1	Introduction	80
5.2	The need for designing the Nonlinear PID Controller	80
5.2.1	Nonlinear PID Controllers	81
5.2.1.1	The first selected NLPID controller: (NLPID1)	82
5.2.1.2	The second selected nonlinear PID controller: (NLPID2)	83
5.3	Ziegler-Nichols Design Methods	84
5.3.1	Ziegler-Nichols (Z-N) tuning method for design of the LPID controller and its application to NLPID controllers	85
5.3.2	Simulink Block Diagrams	87
5.3.2.1	Closed loop DO process model under the LPID controller	87
5.3.2.2	Simulink Block Diagram of the closed loop system based on the NLPID1 controller	87
5.3.2.3	Simulink model of the closed loop DO process under the NLPID2 controller	88

5.3.3	Simulation results	89
5.3.3.1	Simulation results of the closed loop nonlinear DO process under the LPID controller designed by the Ziegler-Nichols Method	89
5.3.3.2	Simulation results of the closed loop DO process under the NLPID1 controller designed by the Ziegler-Nichols Method	90
5.3.3.2.1	Characteristics analysis and discussion	99
5.3.3.3	Simulation results of the closed loop nonlinear DO process under the NLPID2	100
5.3.3.3.1	Discussion	108
5.4	Conclusion	109

CHAPTER SIX: APPLICATION OF THE POLE-PLACEMENT METHOD FOR DESIGN OF THE PARAMETERS OF THE LPID AND NLPID CONTROLLERS FOR THE CASE OF THE LINEARIZED MODEL OF THE DO PROCESS

6.1	Introduction	110
6.2	Application of the Pole-Placement method for design of a linear PID controller's parameters	111
6.2.1	Linearization of the nonlinear model of the DO Process	111
6.2.2	Characteristic equation of the closed loop system	113
6.2.3	The desired poles and desired characteristic equation	114
6.2.4	Calculation of the linear PID controller's parameters	114
6.3	Simulation of the linearized and nonlinear closed loop DO process under the LPID controller	115
6.3.1	Simulation results of the closed loop linearized DO process under the linear PID controller	116
6.3.2	Simulation results of the closed loop nonlinear DO process behaviour under the designed LPID controller	117
6.3.2.1	Discussion	125
6.4	Simulations of the closed loop nonlinear DO process based on the two NLPID controllers	125
6.4.1	Closed loop linearized and nonlinear DO process Simulink Block Diagrams based on the NLPID1 and NLPID2 controllers	126
6.4.2	Simulation results for the closed loop linear and nonlinear DO process based on the NLPID1 and NLPID2 controllers	128

6.4.2.1	Simulation results for the linearized DO model under the NLPID1 controller	128
6.4.2.2	Simulation results for the nonlinear DO model behaviour under the NLPID1 controller	131
6.4.2.2.1	Discussion	137
6.4.2.3	Simulation results for the closed loop linear DO process behaviour under the NLPID2 controller	138
6.4.2.4	Simulation results for the closed loop nonlinear DO process behaviour under the NLPID2 controller	140
6.4.2.4.1	Discussion	146
6.5	Conclusion	147

CHAPTER SEVEN: APPLICATION OF THE POLE-PLACEMENT METHOD TO DESIGN LPID AND NLPID CONTROLLERS FOR THE NONLINEAR DO PROCESS MODEL

7.1	Introduction	148
7.2	Procedure for the design of the LPID and NLPID Controllers Parameters for the nonlinear DO process based on the Pole-Placement method	148
7.3	Design of the LPID controller parameters for the nonlinear DO process model	149
7.3.1	FSOLVE function based on the Levenberg-Marquardt Algorithm	151
7.3.2	Simulink block diagram of the closed loop system under the LPID controller	153
7.3.2.1	Simulation results of the closed loop nonlinear DO process based on the LPID controller	154
7.3.2.2	Discussion on the simulation results based on the LPID controller	159
7.4	Design of the NLPID1 controller parameters for the nonlinear DO process	160
7.4.1	Simulink Block Diagram of the DO closed loop system under the NLPID1 controller	162
7.4.2	Simulation results of the closed loop nonlinear DO process based on the NLPID1 controller	163
7.4.3	Discussion on the simulation results based on the NLPID1 controller for the different operation conditions	168
7.5	Design of the NLPID2 controller parameters for the nonlinear DO process	169
7.5.1	Simulink Block Diagram of the closed loop system under the NLPID2 controller	171
7.5.2	Simulation results of the nonlinear DO process under the NLPID2 controller	172
7.5.3	Discussion on the simulation results obtained under the NLPID2 controller	178
7.6	Conclusion	179

CHAPTER EIGHT: REAL-TIME SIMULATIONS OF THE CLOSED LOOP DO SYSTEM IN PLC USING A MODEL TRANSFORMATION TECHNIQUE

8.1	Introduction	180
8.2	Programmable Logic Controller (PLC) history	180
8.3	PLC hardware and software	181
8.3.1	Advantages and disadvantages of using PLC	182
8.3.2	Programmable Logic Controller Hardware	183
8.3.2.1	Central Processing Unit (CPU)	183
8.3.2.2	Input/Output (I/O) modules	184
8.3.2.3	Framework or backplane	184
8.3.2.4	Power Supply	185
8.3.2.5	Programming device	185
8.3.3	PLC Software	185
8.4	Beckhoff CX50x0 Programmable Logic Controllers	185
8.4.1	CX5020-Embedded PC series	186
8.5	TwinCAT development software	187
8.5.1	TwinCAT Architecture	188
8.5.1.1	eXtended Automation Engineering (XAE)	189
8.5.1.2	Engineering (XAE)-Matlab/Simulink integration	190
8.5.2	Code generation algorithm	191
8.5.2.1	eXtended Automation Runtime (XAR)	194
8.6	Model Transformation and Real-time Results	195
8.6.1	Generating a TwinCAT module from a Simulink model for the DO closed loop system	196
8.6.1.1	Generate a TwinCAT module procedure	196
8.6.1.2	The generated TwinCAT module as a TwinCAT project	198
8.6.2	Simulink Model to TwinCAT Transformation of the closed loop DO process system under the NLPID1 controller	200
8.6.3	Implementation in Real-Time using the NLPID1 controller	201
8.6.3.1	Real-time results for the DO closed loop system under the NLPID1 controller	201
8.6.3.2	Discussion on the real-time simulation results of the closed loop system with the NLPID1 controller when using different set points	211
8.6.4	Implementation in Real-Time using the NLPID2 controller	211
8.6.4.1	Results from the real-time simulation of the closed loop system with NLPID2 controller	215
8.6.4.2	Discussion on the real-time simulation results of the closed loop system using the NLPID2 controller designed by the two design methods for different set points values	221
8.7	Complete Result Discussion	221

8.8	Conclusion	222
-----	------------	-----

CHAPTER NINE: CONCLUSION AND FUTURE RECOMMENDATION

9.1	Introduction	223
9.2	Aims and Objectives	223
9.3	Thesis deliverables	224
9.3.1	Modeling and Simulation	225
9.3.2	Review of control theory for design of nonlinear controllers	225
9.3.3	Controller Design and Implementation	225
9.3.3.1.	The Ziegler-Nichols method for design of the LPID controller	225
9.3.3.2	Pole Placement method for design of the LPID controller based on the linearized DO model	226
9.3.3.3	Novel Pole Placement based method for direct design of the parameters of the LPID and NLPID parameters are unknown	226
9.3.4	Matlab codes for Simulation	226
9.3.5	Real-Time simulation of the closed loop system models	228
9.4	Importance of the deliverables	229
9.5	Application of the nonlinear PID controllers	230
9.6	Application of the thesis results	230
9.7	Future recommendation	231
9.8	Publication	231
9.9	Conclusion	231
	BIBLIOGRAPHY	232

LIST OF FIGURES

Figure 2.1:	Bar graph showing the number of papers for design of nonlinear controllers for nonlinear plants per year	13
Figure 2.2:	A common layout of a Waste Water Treatment Plant	14
Figure 2.3:	Typical Activated Sludge Process	16
Figure 2.4:	Activated sludge process	17
Figure 2.5:	Lay-out of the benchmark simulation platform plant	20
Figure 2.6	Input-Output linearization	23
Figure 2.7:	Structure of the PID NN Controller	25
Figure 2.8:	Typical structure of the PID	26
Figure 3.1:	Benchmark activated sludge process	48
Figure 3.2:	Typical shape of the oxygen transfer function (KLa(u)) as a function of the airflow rate (u).	50
Figure 3.3:	Dissolved Oxygen Simulink model diagram	54
Figure 3.4a:	DO concentration open loop response using $s_{o,in} = 0.01\text{mg/L}$ and $r_{so} = -294.8954\text{mg/L/day}$	56
Figure 3.4b:	DO concentration open loop response using $s_{o,in} = 0.01\text{mg/L}$ and $r_{so} = -294.8954\text{mg/L/day}$	56
Figure 3.5:	DO concentration open loop response using $s_{o,in} = 0.01\text{mg/L}$ and $r_{so} = -309.6402\text{mg/L/day}$	56
Figure 3.6:	DO concentration open loop response using $s_{o,in} = 0.01\text{mg/L}$ and $r_{so} = -280.1506\text{mg/L/day}$	57
Figure 3.7:	DO concentration open loop response using $s_{o,in} = 0.01\text{mg/L}$ and $r_{so} = -324.3849\text{mg/L/day}$	57
Figure 3.8:	DO concentration open loop response using $s_{o,in} = 0.01\text{mg/L}$ and $r_{so} = -264.4059\text{mg/L/day}$	57
Figure 3.9:	DO concentration open loop response using $s_{o,in} = 0.01\text{mg/L}$ and $r_{so} = -442.3431\text{mg/L/day}$	58
Figure 3.10:	DO concentration open loop response using $s_{o,in} = 0.01\text{mg/L}$ and $r_{so} = -147.4477\text{mg/L/day}$	58
Figure 3.11:	DO concentration open loop response using $s_{o,in} = 0.8\text{mg/L}$ and $r_{so} = -309.6402\text{mg/L/day}$	58
Figure 3.12:	DO concentration open loop response using $s_{o,in} = 0.8\text{mg/L}$ and $r_{so} = -309.6402\text{mg/L/day}$	59

	$r_{so} = -280.1506 \text{ mg/L/day}$	
Figure 3.13:	DO concentration open loop response using $s_{o,in} = 0.8 \text{ mg/L}$ and $r_{so} = -324.3849 \text{ mg/L/day}$	59
Figure 3.14:	DO concentration open loop response using $s_{o,in} = 0.8 \text{ mg/L}$ and $r_{so} = -264.4059 \text{ mg/L/day}$	59
Figure 3.15:	DO concentration open loop response using $s_{o,in} = 0.8 \text{ mg/L}$ and $r_{so} = -442.3431 \text{ mg/L/day}$	60
Figure 3.16:	DO concentration open loop response using $s_{o,in} = 0.8 \text{ mg/L}$ and $r_{so} = -147.4477 \text{ mg/L/day}$	60
Figure 3.17:	DO concentration open loop response using $s_{o,in} = 2 \text{ mg/L}$ and $r_{so} = -309.6402 \text{ mg/L/day}$	60
Figure 3.18:	DO concentration open loop response using $s_{o,in} = 2 \text{ mg/L}$ and $r_{so} = -280.1506 \text{ mg/L/day}$	61
Figure 3.19:	DO concentration open loop response using $s_{o,in} = 2 \text{ mg/L}$ and $r_{so} = -324.3849 \text{ mg/L/day}$	61
Figure 3.20:	DO concentration open loop response using $s_{o,in} = 2 \text{ mg/L}$ and $r_{so} = -264.4059 \text{ mg/L/day}$	61
Figure 3.21:	DO concentration open loop response using $s_{o,in} = 2 \text{ mg/L}$ and $r_{so} = -442.3431 \text{ mg/L/day}$	62
Figure 3.22:	DO concentration open loop response using $s_{o,in} = 2 \text{ mg/L}$ and $r_{so} = -147.4477 \text{ mg/L/day}$	62
Figure 4.1:	Time domain LPID controller structure	70
Figure 4.2:	Closed-loop NLPID controller with a DT	76
Figure 5.1:	DO concentration open loop response using $s_{o,in} = 0.01 \text{ mg/L}$ and $r_{so} = -294.8954 \text{ mg/L/day}$	86
Figure 5.2:	Closed Loop diagram of the DO process with the linear PID controller	87
Figure 5.3:	Closed loop diagram of the DO process with the NLPID1 controller	88
Figure 5.4:	Closed loop diagram of the DO process with the NLPID2 controller	89
Figure 5.5:	DO concentration closed loop behaviour using a set-point of 2 mg/L and $r_{so} = -294.8954 \text{ mg/L/day}$	90
Figure 5.6:	Closed loop response of the DO process under the NLPID1 controller using the designed parameters, when the set-point is 2 mg/L ,	91

$$s_{o,in} = 0.8 \text{ mg/L and } r_{so} = -294.8954 \text{ mg/L/day}$$

Figure 5.7:	Closed loop DO process response under the NLPID1 controller using the designed parameters, when the set-point is 2.7 mg/L and $r_{so} = -294.8954 \text{ mg/L/day}$	91
Figure 5.8:	Closed loop response of the NLPID1 controller, when the set-point is 2 mg/L and $s_{o,in} = 0.8 \text{ mg/L}$, $r_{so} = -294.8954 \text{ mg/L/day}$	92
Figure 5.9:	Closed loop DO process response under the NLPID1 controller, when the set-point is 2 mg/L, $s_{o,in} = 0.8 \text{ mg/L}$ and $r_{so} = -294.8954 \text{ mg/L/day}$	92
Figure 5.10:	Closed loop DO process response under the NLPID1 controller, when the set-point is 2.7 mg/L and $r_{so} = -294.8954 \text{ mg/L/day}$	94
Figure 5.11:	Closed loop DO process response under the NLPID1 controller, when the set-point is 2.7 mg/L and $r_{so} = -309.6402 \text{ mg/L/day}$	94
Figure 5.12:	Closed loop DO process response under the NLPID1 controller, when the set-point is 2.7 mg/L and $r_{so} = -280.1506 \text{ mg/L/day}$	94
Figure 5.13:	Closed loop DO process response under the NLPID1 controller, when the set-point is 2.7 mg/L and $r_{so} = -442.3431 \text{ mg/L/day}$	95
Figure 5.14:	Closed loop DO process response under the NLPID1 controller, when the set-point is 2.7 mg/L and $r_{so} = -147.4477 \text{ mg/L/day}$	95
Figure 5.15:	Closed loop DO process response under the NLPID1 controller, when the set-point is 2 mg/L and $r_{so} = -294.8954 \text{ mg/L/day}$	95
Figure 5.16:	Closed loop DO process response under the NLPID1 controller, when the set-point is 2 mg/L and $r_{so} = -309.6402 \text{ mg/L/day}$	96
Figure 5.17:	Closed loop DO process response under the NLPID1 controller, when the set-point is 2 mg/L and $r_{so} = -280.1506 \text{ mg/L/day}$	96
Figure 5.18:	Closed loop DO process response under the NLPID1 controller, when the set-point is 2 mg/L and $r_{so} = -442.3431 \text{ mg/L/day}$	96
Figure 5.19:	Closed loop DO process response under the NLPID1 controller, when the set-point is 2 mg/L and $r_{so} = -147.4477 \text{ mg/L/day}$	97
Figure 5.20:	Closed loop DO process response under the NLPID1 controller, when the set-point is 1.7 mg/L and $r_{so} = -294.8954 \text{ mg/L/day}$	97
Figure 5.21:	Closed loop DO process response under the NLPID1 controller, when the set-point is 1.7 mg/L and $r_{so} = -309.6402 \text{ mg/L/day}$	97
Figure 5.22:	Closed loop DO process response under the NLPID1 controller, when the set-point is 1.7 mg/L and $r_{so} = -280.1506 \text{ mg/L/day}$	98
Figure 5.23:	Closed loop DO process response under the NLPID1 controller, when the set-point is 1.7 mg/L and $r_{so} = -442.3431 \text{ mg/L/day}$	98
Figure 5.24:	Closed loop DO process response under the NLPID1 controller, when the	98

	set-point is 1.7 mg/L and $r_{so} = -147.4477 \text{ mg/L/day}$	
Figure 5.25:	Closed loop DO process response under the NLPID2 controller, when the set-point is 2 mg/L and $s_{oin} = 0.8 \text{ mg/L}$	100
Figure 5.26:	Closed loop DO process response under the NLPID1 controller, when the set-point is 2.7 mg/L , $s_{oin} = 0.01 \text{ mg/L}$ and $r_{so} = -294.8954 \text{ mg/L}$	101
Figure 5.27:	Closed loop DO process response under the NLPID1 controller, when the set-point is 2 mg/L , $s_{oin} = 0.01 \text{ mg/L}$ and $r_{so} = -294.8954 \text{ mg/L}$	101
Figure 5.28:	Closed loop DO process response under the NLPID2 controller, when the set-point is 2.7 mg/L , $s_{oin} = 0.01 \text{ mg/L}$ and $r_{so} = -294.8954 \text{ mg/L/day}$	102
Figure 5.29:	Closed loop DO process response under the NLPID2 controller, when the set-point is 2.7 mg/L , $s_{oin} = 0.01 \text{ mg/L}$ and $r_{so} = -309.6402 \text{ mg/L/day}$	103
Figure 5.30:	Closed loop DO process response under the NLPID2 controller, when the set-point is 2.7 mg/L , $s_{oin} = 0.01 \text{ mg/L}$ and $r_{so} = -280.1506 \text{ mg/L/day}$	103
Figure 5.31:	Closed loop DO process response under the NLPID2 controller, when the set-point is 2.7 mg/L , $s_{oin} = 0.01 \text{ mg/L}$ and $r_{so} = -442.3431 \text{ mg/L/day}$	103
Figure 5.32:	Closed loop DO process response under the NLPID2 controller, when the set-point is 2.7 mg/L , $s_{oin} = 0.01 \text{ mg/L}$ and $r_{so} = -147.4477 \text{ mg/L/day}$	104
Figure 5.33:	Closed loop DO process response under the NLPID2 controller, when the set-point is 2 mg/L , $s_{oin} = 0.8 \text{ mg/L}$ and $r_{so} = -294.8954 \text{ mg/L/day}$	104
Figure 5.34:	Closed loop DO process response under the NLPID2 controller, when the set-point is 2 mg/L , $s_{oin} = 0.8 \text{ mg/L}$ and $r_{so} = -309.6402 \text{ mg/L/day}$	104
Figure 5.35:	Closed loop DO process response under the NLPID2 controller, when the set-point is 2 mg/L , $s_{oin} = 0.8 \text{ mg/L}$ and $r_{so} = -280.1506 \text{ mg/L/day}$	105
Figure 5.36:	Closed loop DO process response under the NLPID2 controller, when the set-point is 2 mg/L , $s_{oin} = 0.8 \text{ mg/L}$ and $r_{so} = -442.3431 \text{ mg/L/day}$	105
Figure 5.37:	Closed loop DO process response under the NLPID2 controller, when the set-point is 2 mg/L , $s_{oin} = 0.8 \text{ mg/L}$ and $r_{so} = -147.4477 \text{ mg/L/day}$	105
Figure 5.38:	Closed loop DO process response under the NLPID2 controller, when the set-point is 1.7 mg/L , $s_{oin} = 0.8 \text{ mg/L}$ and $r_{so} = -294.8954 \text{ mg/L/day}$	106
Figure 5.39:	Closed loop DO process response under the NLPID2 controller, when the	106

	set-point is 1.7 mg/L , $s_{oin} = 0.8 \text{ mg/L}$ and $r_{so} = -309.6402 \text{ mg/L/day}$	
Figure 5.40:	Closed loop DO process response under the NLPID2 controller, when the set-point is 1.7 mg/L , $s_{oin} = 0.8 \text{ mg/L}$ and $r_{so} = -280.1506 \text{ mg/L/day}$	106
Figure 5.41:	Closed loop DO process response under the NLPID2 controller, when the set-point is 1.7 mg/L , $s_{oin} = 0.8 \text{ mg/L}$ and $r_{so} = -442.3431 \text{ mg/L/day}$	107
Figure 5.42:	Closed loop DO process response under the NLPID2 controller, when the set-point is 1.7 mg/L , $s_{oin} = 0.8 \text{ mg/L}$ and $r_{so} = -147.4477 \text{ mg/L/day}$	107
Figure 6.1:	Block diagram of the closed loop system	113
Figure 6.2:	Simulink diagram of the linearized closed loop DO process using the Linear PID controller	116
Figure 6.3:	Simulink block diagram for the linear PID control of the nonlinear DO process	116
Figure 6.4:	Linearized DO process response under the LPID controller, when the set-point is 2 mg/L	117
Figure 6.5:	Linearized DO process response under the LPID controller, when the set-point is 2.7 mg/L	117
Figure 6.6:	Closed loop nonlinear DO process response under the un-tuned LPID controller, when the set-point is 2 mg/L , $s_{oin} = 0.01 \text{ mg/L}$ and $r_{so} = -294.8954 \text{ mg/L/day}$	118
Figure 6.7:	Closed loop nonlinear DO process response under the tuned LPID controller, when the set-point is 2.7 mg/L , $s_{oin} = 0.01 \text{ mg/L}$ and $r_{so} = -294.8954 \text{ mg/L/day}$	119
Figure 6.8:	Closed loop nonlinear DO process response under the tuned LPID controller, when the set-point is 2.7 mg/L , $s_{oin} = 0.01 \text{ mg/L}$ and $r_{so} = -294.8954 \text{ mg/L/day}$	119
Figure 6.9:	Closed loop nonlinear DO process response under the tuned LPID controller, when the set-point is 2.7 mg/L , $s_{oin} = 0.01 \text{ mg/L}$ and $r_{so} = -309.6402 \text{ mg/L/day}$	120
Figure 6.10:	Closed loop nonlinear DO process response under the tuned LPID controller, when the set-point is 2.7 mg/L , $s_{oin} = 0.01 \text{ mg/L}$ and $r_{so} = -280.1506 \text{ mg/L/day}$	120
Figure 6.11:	Closed loop nonlinear DO process response under the tuned LPID controller, when the set-point is 2.7 mg/L , $s_{oin} = 0.01 \text{ mg/L}$ and $r_{so} = -442.3431 \text{ mg/L/day}$	120

Figure 6.12:	Closed loop nonlinear DO process response under the tuned LPID controller, when the set-point is 2.7 mg/L, $s_{oin} = 0.01 \text{ mg/L}$ and $r_{so} = -147.4477 \text{ mg/L/day}$	121
Figure 6.13:	Closed loop nonlinear DO process response under the tuned LPID controller, when the set-point is 2 mg/L, $s_{oin} = 0.8 \text{ mg/L}$ and $r_{so} = -294.8954 \text{ mg/L}$	121
Figure 6.14:	Closed loop nonlinear DO process response under the tuned LPID controller, when the set-point is 2 mg/L, $s_{oin} = 0.8 \text{ mg/L}$ and $r_{so} = -309.6402 \text{ mg/L/day}$	121
Figure 6.15:	Closed loop nonlinear DO process response under the tuned LPID controller, when the set-point is 2 mg/L, $s_{oin} = 0.8 \text{ mg/L}$ and $r_{so} = -280.1506 \text{ mg/L/day}$	122
Figure 6.16:	Closed loop nonlinear DO process response under the tuned LPID controller, when the set-point is 2 mg/L, $s_{oin} = 0.8 \text{ mg/L}$ and $r_{so} = -442.3431 \text{ mg/L/day}$	122
Figure 6.17:	Closed loop nonlinear DO process response under the tuned LPID controller, when the set-point is 2 mg/L, $s_{oin} = 0.8 \text{ mg/L}$ and $r_{so} = -147.4477 \text{ mg/L/day}$	122
Figure 6.18:	Closed loop nonlinear DO process response under the tuned LPID controller, when the set-point is 1.7 mg/L, $s_{oin} = 0.8 \text{ mg/L}$ and $r_{so} = -294.8954 \text{ mg/L/day}$	123
Figure 6.19:	Closed loop nonlinear DO process response under the tuned LPID controller, when the set-point is 1.7 mg/L, $s_{oin} = 0.8 \text{ mg/L}$ and $r_{so} = -309.6402 \text{ mg/L/day}$	123
Figure 6.20:	Closed loop nonlinear DO process response under the tuned LPID controller, when the set-point is 1.7 mg/L, $s_{oin} = 0.8 \text{ mg/L}$ and $r_{so} = -280.1506 \text{ mg/L/day}$	123
Figure 6.21:	Closed loop nonlinear DO process response under the tuned LPID controller, when the set-point is 1.7 mg/L, $s_{oin} = 0.8 \text{ mg/L}$ and $r_{so} = -442.3431 \text{ mg/L/day}$	124
Figure 6.22:	Closed loop nonlinear DO process response under the tuned LPID controller, when the set-point is 1.7 mg/L, $s_{oin} = 0.8 \text{ mg/L}$ and $r_{so} = -147.4477 \text{ mg/L/day}$	124
Figure 6.23:	Structure for Matlab/Simulink simulation of the closed loop DO process based on the NLPID controllers with parameters designed for the LPID controller and the linearized process model	126
Figure 6.24:	Simulink diagram of the closed loop linearized DO process under the NLPID1 controller	127

Figure 6.25:	Simulink diagram of the closed loop nonlinear DO process under the NLPID1 controller	127
Figure 6.26:	Simulink diagram of the closed loop linearized DO process using the NLPID2 controller	127
Figure 6.27:	Simulink diagram of the closed loop nonlinear DO process under the NLPID2 controller	128
Figure 6.28:	Closed loop linear DO process response under the NLPID1 controller, when the set-point is 2 mg/L	128
Figure 6.29:	Closed loop linear DO process response under the NLPID1 controller, when the set-point is 2 mg/L	129
Figure 6.30:	Closed loop linear DO process response under the NLPID1 controller, when the set-point is 2 mg/L	129
Figure 6.31:	Closed loop linear DO process response under the NLPID1 controller, when the set-point is 2 mg/L	130
Figure 6.32:	Closed loop linear DO process response under the NLPID1 controller, when the set-point is 2.7 mg/L	130
Figure 6.33:	Closed loop linear DO process response under the NLPID1 controller, when the set-point is 1.7 mg/L	131
Figure 6.34:	Closed loop DO process response under the NLPID1 controller, when the set-point is 2.7 mg/L, $s_{o,in} = 0.01\text{ mg/L}$ and $r_{so} = -294.8954\text{ mg/L/day}$	132
Figure 6.35:	Closed loop DO process response under the NLPID1 controller, when the set-point is 2.7 mg/L, $s_{o,in} = 0.01\text{ mg/L}$ and $r_{so} = 309.6402\text{ mg/L/day}$	132
Figure 6.36:	Closed loop linear DO process response under the NLPID1 controller, when the set-point is 2.7 mg/L, $s_{o,in} = 0.01\text{ mg/L}$ and $r_{so} = 280.1506\text{ mg/L/day}$	133
Figure 6.37:	Closed loop DO process response under the NLPID1 controller, when the set-point is 2.7 mg/L, $s_{o,in} = 0.01\text{ mg/L}$ and $r_{so} = -442.3431\text{ mg/L/day}$	133
Figure 6.38:	Closed loop DO process response under the NLPID1 controller, when the set-point is 2.7 mg/L, $s_{o,in} = 0.01\text{ mg/L}$ and $r_{so} = -147.4477\text{ mg/L/day}$	133
Figure 6.39:	Closed loop DO process response under the LPID controller, when the set-point is 2 mg/L, $s_{o,in} = 0.8\text{ mg/L}$ and $r_{so} = -294.8954\text{ mg/L/day}$	134
Figure 6.40:	Closed loop DO process response under the NLPID1 controller, when the set-point is 2 mg/L, $s_{o,in} = 0.8\text{ mg/L}$ and $r_{so} = -309.6402\text{ mg/L/day}$	134
Figure 6.41:	Closed loop DO process response under the NLPID1 controller, when the set-point is 2 mg/L, $s_{o,in} = 0.8\text{ mg/L}$ and $r_{so} = -280.1506\text{ mg/L/day}$	134

Figure 6.42:	Closed loop DO process response under the NLPID1 controller, when the set-point is 2 mg/L , $s_{o,in} = 0.8\text{ mg/L}$ and $r_{so} = -442.3431\text{ mg/L/day}$	135
Figure 6.43:	Closed loop DO process response under the NLPID1 controller, when the set-point is 2 mg/L , $s_{o,in} = 0.8\text{ mg/L}$ and $r_{so} = -147.4477\text{ mg/L/day}$	135
Figure 6.44:	Closed loop DO process response under the LPID controller, when the set-point is 1.7 mg/L , $s_{o,in} = 0.8\text{ mg/L}$ and $r_{so} = -294.8954\text{ mg/L/day}$,	135
Figure 6.45:	Closed loop DO process response under the NLPID1 controller, when the set-point is 1.7 mg/L , $s_{o,in} = 0.8\text{ mg/L}$ and $r_{so} = -309.6402\text{ mg/L/day}$	136
Figure 6.46:	Closed loop DO process response under the NLPID1 controller, when the set-point is 1.7 mg/L , $s_{o,in} = 0.8\text{ mg/L}$ and $r_{so} = 280.1506\text{ mg/L/day}$	136
Figure 6.47:	Closed loop DO process response under the NLPID1 controller, when the set-point is 1.7 mg/L , $s_{o,in} = 0.8\text{ mg/L}$ and $r_{so} = 442.3431\text{ mg/L/day}$	136
Figure 6.48:	Closed loop DO process response under the LPID controller, when the set-point is 1.7 mg/L , $s_{o,in} = 0.8\text{ mg/L}$ and $r_{so} = 147.4477\text{ mg/L/day}$	137
Figure 6.49:	Closed loop linearised DO process response under the NLPID2 controller, when the set-point is 2 mg/L	138
Figure 6.50:	Closed loop linearised DO process response under the NLPID2 controller, when the set-point is 2 mg/L	139
Figure 6.51:	Closed loop linearised DO process response under the NLPID2 controller, when the set-point is 2.7 mg/L	139
Figure 6.52:	Closed loop DO process response under the NLPID2 controller, when the set-point is 2 mg/L , $s_{o,in} = 0.8\text{ mg/L}$ and $r_{so} = -294.8954\text{ mg/L/day}$ (Figure 6.52: (a) better tuned controller parameters for NLPID2 and (b) nonlinear DO response under the NLPID2 when the tuned for NLPID1 parameters are used in NLPID2 controller)	140
Figure 6.53:	Closed loop DO process response under the NLPID2 controller, when the set-point is 2.7 mg/L , $s_{o,in} = 0.01\text{ mg/L}$ and $r_{so} = -294.8954\text{ mg/L/day}$	141
Figure 6.54:	Closed loop DO process response under the NLPID2 controller, when the set-point is 2.7 mg/L , $s_{o,in} = 0.01\text{ mg/L}$ and $r_{so} = -309.6402\text{ mg/L/day}$	141
Figure 6.55:	Closed loop DO process response under the NLPID2 controller, when the set-point is 2.7 mg/L , $s_{o,in} = 0.01\text{ mg/L}$ and $r_{so} = -280.1506\text{ mg/L/day}$	141
Figure 6.56:	Closed loop DO process response under the NLPID2 controller, when the set-point is 2.7 mg/L , $s_{o,in} = 0.01\text{ mg/L}$ and	142

$$r_{so} = -442.3431 \text{ mg/L/day}$$

- Figure 6.57:** Closed loop DO process response under the NLPID2 controller, when the set-point is 2.7 mg/L , $s_{o,in} = 0.01 \text{ mg/L}$ and $r_{so} = -147.4477 \text{ mg/L/day}$ 142
- Figure 6.58:** Closed loop DO process response under the NLPID2 controller, when the set-point is 2 mg/L , $s_{o,in} = 0.8 \text{ mg/L}$ and $r_{so} = -294.8954 \text{ mg/L/day/day}$ 142
- Figure 6.59:** Closed loop DO process response under the NLPID2 controller, when the set-point is 2 mg/L , $s_{o,in} = 0.8 \text{ mg/L}$ and $r_{so} = -309.6402 \text{ mg/L/day}$ 143
- Figure 6.60:** Closed loop DO process response under the NLPID2 controller, when the set-point is 2 mg/L , $s_{o,in} = 0.8 \text{ mg/L}$ and $r_{so} = -280.1506 \text{ mg/L/day}$ 143
- Figure 6.61:** Closed loop DO process response under the NLPID2 controller, when the set-point is 2 mg/L , $s_{o,in} = 0.8 \text{ mg/L}$ and $r_{so} = -442.3431 \text{ mg/L/day}$ 143
- Figure 6.62:** Closed loop DO process response under the NLPID2 controller, when the set-point is 2 mg/L , $s_{o,in} = 0.8 \text{ mg/L}$ and $r_{so} = -147.4477 \text{ mg/L/day}$ 144
- Figure 6.63:** Closed loop DO process response under the NLPID2 controller, when the set-point is 1.7 mg/L , $s_{o,in} = 0.8 \text{ mg/L}$ and $r_{so} = -294.8954 \text{ mg/L/day}$ 144
- Figure 6.64:** Closed loop DO process response under the NLPID2 controller, when the set-point is 1.7 mg/L , $s_{o,in} = 0.8 \text{ mg/L}$ and $r_{so} = -309.6402 \text{ mg/L/day}$ 144
- Figure 6.65:** Closed loop DO process response under the NLPID2 controller, when the set-point is 1.7 mg/L , $s_{o,in} = 0.8 \text{ mg/L}$ and $r_{so} = -280.1506 \text{ mg/L/day}$ 145
- Figure 6.66:** Closed loop DO process response under the NLPID2 controller, when the set-point is 1.7 mg/L , $s_{o,in} = 0.8 \text{ mg/L}$ and $r_{so} = -442.3431 \text{ mg/L/day}$ 145
- Figure 6.67:** Closed loop DO process response under the NLPID2 controller, when the set-point is 1.7 mg/L , $s_{o,in} = 0.8 \text{ mg/L}$ and $r_{so} = -147.4477 \text{ mg/L/day}$ 145
- Figure 7.1:** Flow diagram to solve the Equation (7.5) according K_p and T_i 151
- Figure 7.2:** Closed Loop diagram of the nonlinear DO process with the linear PID controller 153
- Figure 7.3:** Closed loop DO process response under the LPID controller, when the set-point is 2.7 mg/L and $r_{so} = -294.8954 \text{ mg/L/day}$ 154
- Figure 7.4:** Closed loop DO process response under the LPID controller, when the set-point is 2.7 mg/L and $r_{so} = -309.6402 \text{ mg/L/day}$ 155

Figure 7.5:	Closed loop DO process response under the LPID controller, when the set-point is 2.7 mg/L and $r_{so} = -280.1506 \text{ mg/L/day}$	155
Figure 7.6:	Closed loop DO process response under the LPID controller, when the set-point is 2.7 mg/L and $r_{so} = -442.3431 \text{ mg/L/day}$	155
Figure 7.7:	Closed loop DO process response under the LPID controller, when the set-point is 2.7 mg/L and $r_{so} = -147.4477 \text{ mg/L/day}$	156
Figure 7.8:	Closed loop DO process response under the LPID controller, when the set-point is 2 mg/L and $r_{so} = -294.8954 \text{ mg/L/day}$	156
Figure 7.9:	Closed loop DO process response under the LPID controller, when the set-point is 2 mg/L and $r_{so} = -309.6402 \text{ mg/L/day}$	156
Figure 7.10:	Closed loop DO process response under the LPID controller, when the set-point is 2 mg/L and $r_{so} = -280.1506 \text{ mg/L/day}$	157
Figure 7.11:	Closed loop DO process response under the LPID controller, when the set-point is 2 mg/L and $r_{so} = -442.3431 \text{ mg/L/day}$	157
Figure 7.12:	Closed loop DO process response under the LPID controller, when the set-point is 2 mg/L and $r_{so} = -147.4477 \text{ mg/L/day}$	157
Figure 7.13:	Closed loop DO process response under the LPID controller, when the set-point is 1.7 mg/L and $r_{so} = -294.8954 \text{ mg/L/day}$	158
Figure 7.14:	Closed loop DO process response under the LPID controller, when the set-point is 1.7 mg/L and $r_{so} = -309.6402 \text{ mg/L/day}$	158
Figure 7.15:	Closed loop DO process response under the LPID controller, when the set-point is 1.7 mg/L and $r_{so} = -280.1506 \text{ mg/L/day}$	158
Figure 7.16:	Closed loop DO process response under the LPID controller, when the set-point is 1.7 mg/L and $r_{so} = -442.3431 \text{ mg/L/day}$	159
Figure 7.17:	Closed loop DO process response under the LPID controller, when the set-point is 1.7 mg/L and $r_{so} = -147.4477 \text{ mg/L/day}$	159
Figure 7.18:	Simulink diagram of the closed loop DO process using the NLPID1 controller	162
Figure 7.19:	Closed loop DO process response under the NLPID1 controller, when the set-point is 2.7 mg/L and $r_{so} = -294.8954 \text{ mg/L/day}$	163
Figure 7.20:	Closed loop DO process response under the NLPID1 controller, when the set-point is 2.7 mg/L and $r_{so} = -309.6402 \text{ mg/L/day}$	163
Figure 7.21:	Closed loop DO process response under the NLPID1 controller, when the set-point is 2.7 mg/L and $r_{so} = -280.1506 \text{ mg/L/day}$	164
Figure 7.22:	Closed loop DO process response under the NLPID1 controller, when the set-point is 2.7 mg/L and $r_{so} = -442.3431 \text{ mg/L/day}$	164
Figure 7.23:	Closed loop DO process response under the NLPID1 controller, when the set-point is 2.7 mg/L and $r_{so} = -147.4477 \text{ mg/L/day}$	164

Figure 7.24:	Closed loop DO process response under the NLPID1 controller, when the set-point is 2 mg/L and $r_{so} = -294.8954 \text{ mg/L/day}$	165
Figure 7.25:	Closed loop DO process response under the NLPID1 controller, when the set-point is 2 mg/L and $r_{so} = -309.6402 \text{ mg/L/day}$	165
Figure 7.26:	Closed loop DO process response under the NLPID1 controller, when the set-point is 2 mg/L and $r_{so} = -280.1506 \text{ mg/L/day}$	165
Figure 7.27:	Closed loop DO process response under the NLPID1 controller, when the set-point is 2 mg/L and $r_{so} = -442.3431 \text{ mg/L/day}$	166
Figure 7.28:	Closed loop DO process response under the NLPID1 controller, when the set-point is 2 mg/L and $r_{so} = -147.4477 \text{ mg/L/day}$	166
Figure 7.29:	Closed loop DO process response under the NLPID1 controller, when the set-point is 1.7 mg/L and $r_{so} = -294.8954 \text{ mg/L/day}$	166
Figure 7.30:	Closed loop DO process response under the NLPID1 controller, when the set-point is 1.7 mg/L and $r_{so} = -309.6402 \text{ mg/L/day}$	167
Figure 7.31:	Closed loop DO process response under the NLPID1 controller, when the set-point is 1.7 mg/L and $r_{so} = -280.1506 \text{ mg/L/day}$	167
Figure 7.32:	Closed loop DO process response under the NLPID1 controller, when the set-point is 1.7 mg/L and $r_{so} = -442.3431 \text{ mg/L/day}$	167
Figure 7.33:	Closed loop DO process response under the NLPID1 controller, when the set-point is 1.7 mg/L and $r_{so} = -147.4477 \text{ mg/L/day}$	168
Figure 7.34:	Simulink diagram of the DO closed loop system using the NLPID2 controller	171
Figure 7.35:	Closed loop DO process response under the NLPID2 controller, when the set-point is 2.7 mg/L and $r_{so} = -294.8954 \text{ mg/L/day}$	172
Figure 7.36:	Closed loop DO process response under the NLPID2 controller, when the set-point is 2.7 mg/L and $r_{so} = -309.6402 \text{ mg/L/day}$	172
Figure 7.37:	Closed loop DO process response under the NLPID2 controller, when the set-point is 2.7 mg/L and $r_{so} = -280.1506 \text{ mg/L/day}$	173
Figure 7.38:	Closed loop DO process response under the NLPID2 controller, when the set-point is 2.7 mg/L and $r_{so} = -442.3431 \text{ mg/L/day}$	173
Figure 7.39:	Closed loop DO process response under the NLPID2 controller, when the set-point is 2.7 mg/L and $r_{so} = -147.4477 \text{ mg/L/day}$	173
Figure 7.40:	Closed loop DO process response under the NLPID2 controller, when the set-point is 2 mg/L and $r_{so} = -294.8954 \text{ mg/L/day}$	174
Figure 7.41:	Closed loop DO process response under the NLPID2 controller, when the set-point is 2 mg/L and $r_{so} = -309.6402 \text{ mg/L/day}$	174
Figure 7.42:	Closed loop DO process response under the NLPID2 controller, when the set-point is 2 mg/L and $r_{so} = -280.1506 \text{ mg/L/day}$	174

Figure 7.43:	Closed loop DO process response under the NLPID2 controller, when the set-point is 2 mg/L and $r_{so} = -442.3431 \text{ mg/L/day}$	175
Figure 7.44:	Closed loop DO process response under the NLPID2 controller, when the set-point is 2 mg/L and $r_{so} = -147.4477 \text{ mg/L/day}$	175
Figure 7.45:	Closed loop DO process response under the NLPID2 controller, when the set-point is 1.7 mg/L and $r_{so} = -294.8954 \text{ mg/L/day}$	175
Figure 7.46:	Closed loop DO process response under the NLPID2 controller, when the set-point is 1.7 mg/L and $r_{so} = -309.6402 \text{ mg/L/day}$	176
Figure 7.47:	Closed loop DO process response under the NLPID2 controller, when the set-point is 1.7 mg/L and $r_{so} = -280.1506 \text{ mg/L/day}$	176
Figure 7.48:	Closed loop DO process response under the NLPID2 controller, when the set-point is 1.7 mg/L and $r_{so} = -442.3431 \text{ mg/L/day}$	176
Figure 7.49:	Closed loop DO process response under the LPID controller, when the set-point is 1.7 mg/L and $r_{so} = -147.4477 \text{ mg/L/day}$	177
Figure 7.50:	Real –time application of the NLPID controller parameters design	179
Figure 8.1:	Historical diagram of the PLC development	181
Figure 8.2:	Classic part of the PLC	183
Figure 8.3:	Typical PLC scans cycle	184
Figure 8.4:	Classic PLC framework	185
Figure 8.5:	General CX50x0 DIN rail Industrial PCs	186
Figure 8.6:	Diagram of the CX5020	186
Figure 8.7:	eXtended Automation Architecture (XAA)	188
Figure 8.8:	eXtended Automation Architecture (XAA)	189
Figure 8.9:	extended Automation Engineering (XAE)	190
Figure 8.10:	Typical Code generation Process	192
Figure 8.11:	From Matlab/Simulink to TwinCAT	193
Figure 8.12:	Debugging in TwinCAT3	194
Figure 8.13:	Modular structure of the TwinCAT 3 runtime environment	195
Figure 8.14:	Simulink model	196
Figure 8.15:	Model Explorer browser for System Configuration	197
Figure 8.16:	Code Generation	197
Figure 8.17:	Simulink model transformation process to TwinCat representation	198
Figure 8.18:	Setup the priority and a cycle time for the object “NLPID_DO”	199
Figure 8.19:	Simulink model transformed to TwinCat module actively working in a PLC CX5020	199
Figure 8.20:	Transformed Simulink closed loop model to the TwinCAT closed loop model	200
Figure 8.21:	Real-time PLC simulation results of the closed loop system with NLPID1 (PP1) controller when the set-point is 2.7 mg/L , $s_{o,in} = 0.01 \text{ mg/L}$ and	202

$$r_{so} = -294.8954 \text{ mg/L/day}$$

- Figure 8.22:** Real-time PLC simulation results of the closed loop system with NLPID1 (PP1) controller when the set-point is 2.7 mg/L , $s_{o,in} = 0.01 \text{ mg/L}$ and $r_{so} = -442.3431 \text{ mg/L/day}$ 202
- Figure 8.23:** Real-time PLC simulation results of the closed loop system with NLPID1 (PP1) controller when the set-point is 2.7 mg/L , $s_{o,in} = 0.1 \text{ mg/L}$ and $r_{so} = -147.4477 \text{ mg/L/day}$ 202
- Figure 8.24:** Real-time PLC simulation results of the closed loop system with NLPID1 (PP1) controller when the set-point is 2 mg/L , $s_{o,in} = 0.8 \text{ mg/L}$ and $r_{so} = -294.8954 \text{ mg/L/day}$ 203
- Figure 8.25:** Real-time PLC simulation results of the closed loop system with NLPID1 (PP2) controller when the set-point is 2 mg/L , $s_{o,in} = 0.8 \text{ mg/L}$ and $r_{so} = -442.3431 \text{ mg/L/day}$ 203
- Figure 8.26:** Real-time PLC simulation results of the closed loop system with NLPID1 (PP1) controller when the set-point is 2 mg/L , $s_{o,in} = 0.8 \text{ mg/L}$ and $r_{so} = -147.4477 \text{ mg/L/day}$ 203
- Figure 8.27:** Real-time PLC simulation results of the closed loop system with NLPID1 (PP1) controller when the set-point is 1.7 mg/L , $s_{o,in} = 0.8 \text{ mg/L}$ and $r_{so} = -294.8954 \text{ mg/L/day}$ 204
- Figure 8.28:** Real-time PLC simulation results of the closed loop system with NLPID1 (PP1) controller when the set-point is 1.7 mg/L , $s_{o,in} = 0.8 \text{ mg/L}$ and $r_{so} = -442.3431 \text{ mg/L/day}$ 204
- Figure 8.29:** Real-time PLC simulation results of the closed loop system with NLPID1 (PP1) controller when the set-point is 1.7 mg/L , $s_{o,in} = 0.8 \text{ mg/L}$ and $r_{so} = -147.4477 \text{ mg/L/day}$ 204
- Figure 8.30:** : Two curves of the closed loop DO process response under the NLPID1 (PP1) controller, when the set-point is 2.7 mg/L , $s_{o,in} = 0.01 \text{ mg/L}$ and $r_{so} = -442.3431 \text{ mg/L/day}$: Figure 8.30A- Simulink results and Figure 8.30B Real-time PLC results 205
- Figure 8.31:** Real-time simulation of the closed loop system with NLPID1 (PP2) controller when the set-point is 2.7 mg/L , $s_{o,in} = 0.01 \text{ mg/L}$ and $r_{so} = -294.8954 \text{ mg/L/day}$ 206
- Figure 8.32:** Real-time simulation of the closed loop DO process response under the NLPID1 (PP2) controller, when the set-point is 2.7 mg/L and $r_{so} = -442.3431 \text{ mg/L/day}$ 206
- Figure 8.33:** Real-time simulation of the closed loop DO process response under the NLPID1 (PP2) controller, when the set-point is 206

$$2.7 \text{ mg/L}, s_{o,in} = 0.01 \text{ mg/L} \text{ and } r_{so} = -147.4477 \text{ mg/L/day}$$

- Figure 8.34:** Real-time simulation of the closed loop DO process response under the NLPID1 controller, when the set-point is 2 mg/L , $s_{o,in} = 0.8 \text{ mg/L}$ and $r_{so} = -294.8954 \text{ mg/L/day}$ 207
- Figure 8.35:** : Real-time simulation of the closed loop DO process response under the NLPID1 controller, when the set-point is 2 mg/L , $s_{o,in} = 0.8 \text{ mg/L}$ and $r_{so} = -442.3431 \text{ mg/L/day}$ 207
- Figure 8.36:** Real-time simulation of the closed loop DO process response under the NLPID1 (PP2) controller, when the set-point is 2 mg/L , $s_{o,in} = 0.8 \text{ mg/L}$ and $r_{so} = -147.4477 \text{ mg/L/day}$ 207
- Figure 8.37:** Real-time simulation of the closed loop DO process response under the NLPID1 (PP2) controller, when the set-point is 1.7 mg/L , $s_{o,in} = 0.8 \text{ mg/L}$ and $r_{so} = -294.8954 \text{ mg/L/day}$ 208
- Figure 8.38:** Real-time simulation of the closed loop DO process response under the NLPID1 (PP2) controller, when the set-point is 1.7 mg/L , $s_{o,in} = 0.8 \text{ mg/L}$ and $r_{so} = -442.3431 \text{ mg/L/day}$ 208
- Figure 8.39:** Real-time simulation of the closed loop DO process response under the NLPID1 (PP2) controller, when the set-point is 1.7 mg/L , $s_{o,in} = 0.8 \text{ mg/L}$ and $r_{so} = -147.4477 \text{ mg/L/day}$ 208
- Figure 8.40:** Two carves of the closed loop DO process response under the NLPID1 (PP2) controller, when the set-point is 2 mg/L , $s_{o,in} = 0.8 \text{ mg/L}$ and $r_{so} = -147.4477 \text{ mg/L/day}$ (Figure 8.40a- Simulink results and Figure 8.40b Real-time PLC results) 209
- Figure 8.41:** Model Transformations for the closed loop system with the NLPID2 controller 211
- Figure 8.42:** PLC Real-time simulation of the closed loop system with the NLPID2 (PP1) controller when the set-point is 2.7 mg/L , $s_{o,in} = 0.01 \text{ mg/L}$ and $r_{so} = -294.8954 \text{ mg/L/day}$ 212
- Figure 8.43:** PLC Real-time simulation of the closed loop system with the NLPID2 (PP1) controller when the set-point is 2.7 mg/L , $s_{o,in} = 0.01 \text{ mg/L}$ and $r_{so} = -442.3431 \text{ mg/L/day}$ 212
- Figure 8.44:** PLC Real-time simulation of the closed loop system with the NLPID2 (PP1) controller when the set-point is 2.7 mg/L , $s_{o,in} = 0.1 \text{ mg/L}$ and $r_{so} = -147.4477 \text{ mg/L/day}$ 213
- Figure 8.45:** PLC Real-time simulation of the closed loop system with the NLPID2 (PP1) controller when the set-point is 2 mg/L , $s_{o,in} = 0.8 \text{ mg/L}$ and $r_{so} = -294.8954 \text{ mg/L/day}$ 213

Figure 8.46:	PLC Real-time simulation of the closed loop system with the NLPID2 (PP1) controller when the set-point is 2 mg/L , $s_{o,in} = 0.8 \text{ mg/L}$ and $r_{so} = -442.3431 \text{ mg/L/day}$	213
Figure 8.47:	PLC Real-time simulation of the closed loop system with the NLPID2 (PP1) controller when the set-point is 2 mg/L , $s_{o,in} = 0.8 \text{ mg/L}$ and $r_{so} = -147.4477 \text{ mg/L/day}$	214
Figure 8.48:	PLC Real-time simulation of the closed loop system with the NLPID2 (PP1) controller when the set-point is 1.7 mg/L , $s_{o,in} = 0.8 \text{ mg/L}$ and $r_{so} = -294.8954 \text{ mg/L/day}$	214
Figure 8.49:	PLC Real-time simulation of the closed loop system with the NLPID2 (PP1) controller when the set-point is 1.7 mg/L , $s_{o,in} = 0.8 \text{ mg/L}$ and $r_{so} = -442.3431 \text{ mg/L/day}$	214
Figure 8.50:	PLC Real-time simulation of the closed loop system with the NLPID2 (PP1) controller when the set-point is 1.7 mg/L , $s_{o,in} = 0.8 \text{ mg/L}$ and $r_{so} = -147.4477 \text{ mg/L/day}$	215
Figure 8.51:	Two curves for comparison of the closed loop DO process response under the NLPID2 (PP1) controller, when the set-point is 2 mg/L , $s_{o,in} = 0.8 \text{ mg/L}$ and $r_{so} = -147.4477 \text{ mg/L/day}$ (Figure 8.51a-Simulink results and Figure 8.51b Real-time PLC results)	215
Figure 8.52:	Real-time PLC simulation results of the closed loop system with NLPID2 (PP2) controller when the set-point is 2.7 mg/L , $s_{o,in} = 0.01 \text{ mg/L}$ and $r_{so} = -294.8954 \text{ mg/L/day}$	216
Figure 8.53:	Real-time PLC simulation results of the closed loop system with NLPID2 (PP2) controller when the set-point is 2.7 mg/L , $s_{o,in} = 0.01 \text{ mg/L}$ and $r_{so} = -442.3431 \text{ mg/L/day}$	216
Figure 8.54:	Real-time PLC simulation results of the closed loop system with NLPID2 (PP2) controller when the set-point is 2.7 mg/L , $s_{o,in} = 0.01 \text{ mg/L}$ and $r_{so} = -147.4477 \text{ mg/L/day}$	216
Figure 8.55:	Real-time PLC simulation results of the closed loop system with NLPID2 (PP2) controller when the set-point is 2 mg/L , $s_{o,in} = 0.8 \text{ mg/L}$ and $r_{so} = -294.8954 \text{ mg/L/day}$	217
Figure 8.56:	Real-time PLC simulation results of the closed loop system with NLPID2 (PP2) controller when the set-point is 2 mg/L , $s_{o,in} = 0.8 \text{ mg/L}$ and $r_{so} = -442.3431 \text{ mg/L/day}$	217
Figure 8.57:	TwinCat 3 Real-time simulation of the closed loop DO process response under the NLPID2 controller, when the set-point is 2 mg/L and	217

$$r_{so} = -147.4477 \text{ mg/L}$$

- Figure 8.58:** Real-time PLC simulation results of the closed loop system with NLPID2 (PP2) controller when the set-point is 1.7 mg/L , $s_{o,in} = 0.8 \text{ mg/L}$ and $r_{so} = -294.8954 \text{ mg/L/day}$ 218
- Figure 8.59:** Real-time PLC simulation results of the closed loop system with NLPID2 (PP2) controller when the set-point is 1.7 mg/L , $s_{o,in} = 0.8 \text{ mg/L}$ and $r_{so} = -442.3431 \text{ mg/L/day}$ 218
- Figure 8.60:** Real-time PLC simulation results of the closed loop system with NLPID2 (PP2) controller when the set-point is 1.7 mg/L , $s_{o,in} = 0.8 \text{ mg/L}$ and 218
- Figure 8.61:** Two curves of the closed loop DO process response under the NLPID2 (PP2) controller, when the set-point is 1.7 mg/L , $s_{o,in} = 0.8 \text{ mg/L}$ and $r_{so} = -294.8954 \text{ mg/L/day}$ (Figure 8.61a- Simulink and Figure 8.61b- Real-time PLC) 219

LIST OF TABLES

Table 2.1:	Description of Activated Sludge Models	21
Table 2.2:	Linear and Nonlinear controllers for nonlinear processes	34
Table 3.1:	Different models for oxygen transfer function	49
Table 3.2:	Process parameters from benchmark structure	53
Table 3.3:	Changes of the disturbances in the process	55
Table 3.4:	DO open loop characteristics behaviour	63
Table 5.1:	Ziegler-Nichols step response method table	86
Table 5.2:	NLPID1 Parameters obtained by tuning	93
Table 5.3:	Parameters variation for the DO set point and the DO process disturbances	93
Table 5.4:	Closed loop nonlinear DO process characteristics under the NLPID1 controller	99
Table 5.5:	NLPID2 Parameters obtained by tuning	102
Table 5.6:	Closed loop DO process characteristics under the NLPID2	108
Table 6.1:	Variation for the DO set point and the DO process disturbances	118
Table 6.2:	Results obtained when the tuned LPID controller parameters are used to control the nonlinear DO process	124
Table 6.3:	Closed loop linearised DO process characteristics under the NLPID1 controller	131
Table 6.4:	Closed loop nonlinear DO process characteristics under the NLPID1 controller	137
Table 6.5:	Closed loop linearised DO process characteristics under the NLPID2 controller	139
Table 6.6:	Closed loop the nonlinear DO process characteristics under the NLPID2 controller	146
Table 6.7:	Comparison of the obtained closed loop nonlinear DO process specifications of the designed LPID and NLPID controllers	147
Table 7.1:	Obtained K_p, T_i for the linear PID controller	152
Table 7.2:	Selected controller parameters for nonlinear DO process under the linear PID controller	153
Table 7.3:	Variation for the DO set point and the DO process disturbances	154
Table 7.4:	Nonlinear DO process characteristics under the LPID controller	160
Table 7.5:	Obtained NLPID1 controller parameters designed based on the nonlinear DO process	161
Table 7.6:	The chosen NLPID1 controller parameters for the nonlinear DO process	162
Table 7.7:	Closed loop characteristics obtained when the NLPID1 is used to control the nonlinear DO process	168
Table 7.8:	Controller Parameter designed based on the nonlinear DO process	170
Table 7.9:	Selected NLPID2 controller parameter designed based for the nonlinear DO process	171

Table 7.10:	Results Obtained when a NLPID2 is used to control nonlinear DO	177
Table 7.11:	Comparison of the obtained closed loop DO process specifications of the designed LPID and NLPID controllers	178
Table 8.1:	CX5020 technical data sheet from (www.beckhoff.com)	187
Table 8.2:	Table 8.2: XAE and XAR	189
Table 8.3:	DO process disturbances and set points values to be applied in real-time	201
Table 8.4:	Comparison between DO process characteristics behaviour obtained under the NLPID1 controller parameters designed by the PP1 and PP2 methods	210
Table 8.5:	Comparison between the DO process characteristics behaviour obtained under the NLPID2 controller parameters designed by the PP1 and PP2 methods	220
Table 9.1:	Matlab script file developed	226
Table 9.2:	Simulink Environment Models	228
Table 9.3:	TwinCAT 3 Environment Models	228

LIST OF APPENDICES

Appendix A:	MATLAB PROGRAM FOR DO OPEN LOOP PROCESS MODEL script file - <i>DO_Last.m</i>	239
Appendix B	MATLAB PROGRAM FILES FOR CONTROLLER DESIGN PARAMETERS OF THE LINEAR AND NONLINEAR PID CONTROLLERS	240
Appendix B1	Matlab script - LPID_DO.m	240
Appendix B2	Matlab script - NLPID1withDOzn.m	240
Appendix B3	Matlab script - NLPID2zn_DO.m	241
Appendix B4	Matlab script - LPIDpp1.m	242
Appendix B5	Matlab script - NLPID1pp1withDOPar.m	242
Appendix B6	Matlab script - NLPID2pp1_DOPar.m	243
Appendix B7	Matlab script - findLPIDpar.m	243
Appendix B8	MATLAB PROGRAM for calculation of the controller parameters using the calculation procedure for pole placement2 method based on the NLPID2 controller given in Chapter 7	244
Appendix B8a	Matlab script - Findnlpid1par_PP2.m	244
Appendix B8b	Matlab <i>function file</i> – <i>myfun1</i>	246
Appendix B8c	Matlab script – <i>NLPID1PP2par_DO</i>	247
Appendix B9:	MATLAB PROGRAM for calculation of the controller parameters using the calculation procedure for pole placement2 method based on the NLPID2 controller given in Chapter 7	248
Appendix B9a	Matlab script - Matlab script – <i>findnlpid2par</i>	248
Appendix B9b	Matlab <i>function file</i> - <i>myfun2</i>	250
Appendix B9c	Matlab script - <i>NLPID2PP2par_DO</i>	250
Appendix C	Simulink Models	251
Appendix C1	Simulink - DO model.mdl	251
Appendix C2	Simulink - LPIDwithDO.mdl	252
Appendix C3	Simulink - NLPID1withDOmodel	253
Appendix C4	Simulink - NLPID2withDOmodel.mdl	254
Appendix D	PLC Hardware	254

GLOSSARY

Terms/Abbreviations	Definition/ Explanation
AE	Aerobic
AN	Anoxic
ASM1	Activated Sludge Model 1
ASM2	Activated Sludge Model 2
ASM3	Activated Sludge Model 3
ASP	Activated Sludge Process
BNR	Biological Nutrient Removal
BOD	Biochemical Oxygen Demand
COD	Chemical Oxygen Demand
DO	Dissolved Oxygen
IAWQ	International Association on Water Quality
I/O	Input/output
MATLAB	Matrix Laboratory
OUR	Oxygen Uptake Rate
PID	Proportional Integral Derivative
PLC	Programmable Logic Controller
RBOS	Readily Biodegradable Organic Substrate
SIMULINK	Simulation and Link
WWT	Wastewater Treatment
WWTP	Wastewater Treatment Plants

Mathematical Notation

Symbols	Explanation
Q_r	Return flow rate of aerobic tank
Q_w	Wastage flow rate of aerobic tank
Q_{air}	Airflow rate of aerobic tank
N	Nitrogen
H_2O	Water
NH_3	Ammonia
NH_4^+	Ammonium
NO_3	Nitrate
NO_2	Nitrite
s_o	DO concentration in the aeration tank
O_2	Gaseous Oxygen
K_{La}	Oxygen transfer function
$s_{O,sat}$	Saturated value of the DO concentration in wastewater
$u(t)$	Control input
r_{SO}	Respiration rate or Oxygen Uptake Rate
$s_{O,in}$	DO concentration of the input flow
V	Volume of the wastewater
s_{OL}	DO concentration in the liquid phase
K_{LaL}	Oxygen transfer coefficient based on liquid volume
Q_{in}	Flow rate of the liquid entering the system
Q_{out}	Flow rate of the liquid leaving the system
K_{LaG}	Oxygen transfer coefficient based on gas volume
Q_{in}	Input flow rate for the aeration tank
$r_{SO,end}$	Endogenous Oxygen uptake rate
$r_{SO,ex}$	Exogenous Oxygen uptake rate
s_O^{sp}	DO concentration set-point in the aeration tank

$\varepsilon(t)$	Predictor error
K_S	Half-saturation (hetero.growth)
μ_H	Maximum heterotrophic growth rate
K_{OH}	Half-saturation (hetero.oxygen)
K_{NO}	Half-saturation (nitrate)
b_H	Heterotrophic decay
η_g	Anoxic growth rate correction factor
η_h	Anoxic hydrolysis rate correction factor
K_h	Maximum specific hydrolysis rate
K_x	Half-saturation (hydrolysis)
μ_A	Maximum autotrophic growth rate
K_{NH}	Half-saturation (auto. growth)
b_A	Autotrophic decay
K_{OA}	Half-saturation (auto.oxygen)
k_a	Ammonification rate
x	Soluble inert organic matter
s_s	Readily biodegradable substrate
x_l	Particulate inert organic matter
x_s	Slowly biodegradable substrate
x_{BH}	Active heterotrophic biomass
x_{BA}	Active autotrophic biomass
x_p	Particulate product arising from biomass decay
s_{NO}	Nitrate and nitrite nitrogen
s_{NH}	$\text{NH}_4^+ + \text{NH}_3$ nitrogen
s_{ND}	Soluble biodegradable organic nitrogen
x_{ND}	Particulate biodegradable organic nitrogen
Y_H	Heterotrophic yield
Y_A	Autotrophic yield
$f(t)$	Nonlinear function

w

Disturbance vector

CHAPTER ONE

INTRODUCTION

1.1 Introduction

Clean water is a necessity for life of almost all creatures on earth. For example:

- i. Clean water is critical to plants and animals that live in water.
- ii. Human beings, who live, work and play close to water.
- iii. Water birds that use water catchment areas for resting and feedings.
- iv. Groups of fish which use water to habituate, and
- v. Water is used for various applications such as domestic, commercial, public supply, industrial production, energy production, mining, agricultural, etc.

For health concerns and environmental conservation, water has to be treated before it enters to a receiver. Installing water treatment equipment not only improves the quality of the water but also raises the hygienic standard of the environment. Environmental protection is a priority in all countries.

Wastewater treatment plants are designed to handle a previously designed load and flow. These conditions infrequently appear in reality. It is well known that the plant operates under dynamic conditions, which is the reason that control is needed. The function of the wastewater treatment plants (WWTP) is to speed up the natural process by which the water purifies itself. The main objective is to produce an effluent meeting the required standards at the lowest possible cost. The problem solution for wastewater treatment (WWT) is very important these days, because of fast population increase and industrial development. This examination considers new applications of control routines that plan to enhance the operation of the activated sludge handle in wastewater treatment plants.

The need for control of the Dissolved Oxygen (DO) concentration in a wastewater treatment plant (WWTP) is becoming more and more important. Harsh environmental and health regulations together with a demand for cost effective ways of wastewater treatment have made control technology in Wastewater Treatment Plants (WWTP) an important priority (Shijian GE *et al.*, 2012). DO is the amount of oxygen in the wastewater aeration tank of the WWTP and it plays a vital role of controlling WWTP. Oxygen dissolves in water through mixing the wastewater with the air blown by the aeration system. DO concentration in the aerobic part of an activated sludge process should be

sufficiently high to supply enough oxygen to the microorganisms in the sludge (Ostace *et al.*, 2010). But an excessive high DO leads to high energy consumption and may also worsen the sludge quality. Necessities for treated wastewater are getting to be logically more and stricter. This, in mix with expanding loads, and restricted accessibility of area, calls for more effective techniques for wastewater treatment plants. In this proposition, control methods are created keeping in mind the end goal to enhance the proficiency of the actuated discharge process by proper control of the DO process.

The measure of oxygen needed by the microorganisms to oxidize the natural materials and to keep up remaining broke up oxygen working levels ought to be exchanged to the air circulation tank in the Activated Sludge Process (ASP). On the off chance that Dissolved Oxygen (DO) focus is not sufficient for the development of micro-living being, filamentous organic entity may prevail, and the settling capacity and nature of the enacted muck may be poor.

In practice, the DO concentration in the aeration tank is generally maintained at about 1.5 to 4 mg/L in all areas of the aeration tank; 2 mg/L is a commonly used value. If the value is above 4 mg/L; operations significantly does not improve, but increase the aeration costs considerably. Therefore, the DO concentration in the aeration tank of an ASP is one of the most important operating parameters to be controlled for the efficient operating cost as well as the good effluent water quality. Even though the dissolved oxygen dynamics is relatively simple, there are some difficulties to control the DO for the disturbances as influent flow and organic loads fluctuation, nonlinearity of the oxygen transfer function and a sensor noise, etc.

Daily variation of the influent loads induces the continuous change in the respiration rate and the oxygen transfer rate, which makes the DO dynamics time-varying one. The time-varying DO dynamics is the main reason for controlling the DO concentration. Moreover, the oxygen transfer rate is higher for low DO concentrations and approaches zero towards the saturated concentration. This nonlinearity together with the time varying oxygen transfer rate makes any conventional controller to perform poorly. A PID controller that is well tuned in the afternoon may have poor performance at midnight. This has motivated the use of the various advanced control techniques (Vanrolleghem, 2003).

A new control strategy for control of the DO concentration in the aerobic tank of a wastewater treatment process is developed. It provides means to improve the

performance of the Linear Proportional Integral and Derivative (LPID) controller by extending it to a Nonlinear Proportional, Integral and Derivative (NLPID) controller. Differential trackers are introduced to obtain a low-noise derivative of the controller input signals. The focus of this thesis is to develop methods for design of nonlinear controllers for the concentration of the DO in the aeration tank of the WWTP and to implement the designed controllers in the frameworks of a Programmable Logic Controller (PLC).

The Chapter describes the awareness of research problem in part 1.2, the research problem is given in part 1.3, and its statement in part 1.4, the project aim and objectives are given in part 1.5, the hypothesis is formulated in part 1.6.

1.2 Awareness of the Problem

Wastewater is the water that the people dispose from their homes, offices and industry. It is water that is not appropriate for human or animal consumption. Wastewater Treatment Plant speeds up the natural process whereby water purifies itself. In a modern wastewater treatment plant the wastewater is generally processed in several steps before it is released to the recipient. Lindberg, (1997) gives a survey of the common practices. The problem for effective and optimal control of wastewater treatment plants is very important lately, because of the increased requirements to the quality of the effluent (Shijian *et al.*, 2012). The activated sludge process is a type of wastewater process characterized with complex dynamics and proper control design and implementation strategies are necessary and important for it to function. Wastewater treatment processes (WWTP) is the nonlinear process that has been chosen for the research investigations throughout this thesis.

Caraman *et al.*, (2005) claim that WWTP are essentially alterable in light of the huge varieties in the influent wastewater stream rate, fixation, and organization. The versatile conduct of the WWTP included microorganism's forces further troubles regarding the time-shifting procedure parameters. Scientific models and machine reproductions are fundamental to anticipate, depict and control the convoluted conduct of these procedures. Sustainable solutions to the problems of wastewater treatment require development of adequate information systems for control and supervision of the process. DO concentration (DO) control is the mostly used strategy in the Activated Sludge Process (ASP) control.

1.3 Problem Identification

Strict environmental and health regulations together with a demand for cost effective ways of wastewater treatment have made control technology in Wastewater Treatment Plants (WWTP) an important priority. DO concentration in the aerobic part of an activated sludge process should be sufficiently high to supply enough oxygen to the microorganisms in the sludge. But an extreme high DO level leads to high energy consumption and may also deteriorate the sludge quality (Wahab, 2007). Necessities for treated wastewater are getting to be progressively more stringent. This, in blend with expanding loads, and constrained accessibility of area, calls for more effective strategies for wastewater treatment plants.

Nonlinear processes like Wastewater treatment are inherently dynamic because of the expansive varieties in the influent wastewater stream rate, focus, and piece. The versatile conduct of the included microorganisms forces further troubles as far as the time-shifting procedure parameters. Numerical models and machine recreations are fundamental to anticipate, describe and control the muddled conduct of these techniques. There are various types of nonlinear controllers. Investigations of the thesis are based of Nonlinear PID (NLPID) controllers as a counter part of the Linear PID (LPID) controllers widely used in industry and WWTPs, and normally implemented by Programmable Logic Controllers. The linear PID controllers cannot fully cope with the nonlinear behavior of the DO process and the idea is to be substituted by NLPIDs. The problem arises how to design the parameters of the Nonlinear PID controllers in such a way that they will control the nonlinear processes effectively. In the thesis methods for design of two types of NLPID controllers are developed in order to improve the efficiency of the activated sludge process; as follows:

- Different methods that can be used for design of the parameters for NLPID controllers are developed for the DO process control.
- Simulation of the closed loop system is accomplished in Matlab/Simulink software environment.
- Real -Time control implementations and simulation of the developed closed loop systems are done using the TwinCat 3 Beckoff Automation software and CX5020 Beckoff PLC (based on IEC 61499 function block programing).

1.4 Statement of the Problem

The research problem in the thesis is to design nonlinear PID controllers to control the activated sludge process (ASP) in the waste water plant (WWP) such that the requirements for the effluent concentration of wastewater are satisfied.

The research problem is solved by using:

1. COST Benchmark plant structure as a nonlinear process to be controlled (Copp, 2000).
2. ASM 1- biological model for description of the DO process model
3. Ziegler-Nichols method for design of the PID controllers.
4. Pole-Placement technique for design of linear PID controller
5. Pole-Placement for design of a NLPID controller using a nonlinear DO model.
6. Matlab/Simulink software environment simulations
7. TwinCAT 3 Engineering and Real-Time Environment simulations of the closed loop systems
8. Beckhoff CX5020 PLC for real-time simulation.

1.4.1 Design based sub-problems

The research problem is divided in the following sub-problems:

Sub-problem 1: Activated sludge process study.

To study, acquire knowledge and understand everything about the activate sludge process technology, physiochemical dependencies, mass balances and their description by the original ASM1 model.

Sub-problem 2: Dissolved Oxygen model simulation.

Development of MATLAB/Simulink programs for model simulation. Study the process behavior for different disturbances.

Sub-problem 3: Ziegler-Nichols and Pole-placement method investigations

- Ziegler-Nichols (ZN) tuning method for design of the LPID controller.
- Pole-Placement method for design of LPID controller based on the linearized DO model
- Pole-Placement method for design of LPID and NLPID controllers based on the nonlinear DO model
- Simulation and Comparison of the closed loop system behavior.

1.4.2 Real time implementation sub-problems

Sub-problem 4: TwinCAT software study.

Develop a model transformation technique in order to transfer the developed models of the closed loop systems from Simulink to TwinCAT 3 software environment.

Sub-problem 5: Uploading the transformed models to Beckhoff PLC.

After developing model transformation from Simulink to TwinCAT (software to software communication), TwinCAT 3 engineering environment is used for upload the transformed models into a Beckhoff CX5020 PLC for real-time simulation.

Sub-problem 6: Real-time simulation of the closed loop system

The uploaded transformed files are used for real-time simulation of the closed loop DO systems.

1.5 Aim and Objectives of the thesis

Aim:

The aim of this thesis is to develop methods, algorithms and software for design, and Programmable Logic Controller (PLC) implementation of nonlinear Proportional, Integral and Derivative (NLPID) controllers in order to control the nonlinear process of Dissolves Oxygen (DO) as part of the Activated Sludge Process (ASP) in wastewater treatment

Objectives:

- To investigate the operation of the nonlinear process to be controlled.
- To develop and simulate the nonlinear model of the DO process.
- To investigate different PID controller structures and to select two nonlinear PID controllers for the purpose of the research investigations.
- To apply the Ziegler-Nichols and the Pole-Placement methods for design of the Linear PID (LPID) controller based on the linearized DO model.
- To develop Pole-Placement method for design of a LPID controller based on the nonlinear DO model (for design of the LPID controller parameters) and method for design of a NLPID control parameters based on the nonlinear DO model (for design of the NLPID controller parameters).
- To simulate the closed loop system in Matlab/Simulink. Comparison analysis between linear and nonlinear PID controllers performance based on the different methods of design.
- Implementation of the two NLPID controllers in PLC (Beckhoff CX5020 which supports the IEC 61499 standard) through TwinCAT 3 software environment.
- To implement the real-time control, Simulation of the designed closed loop in the environment of Beckhoff CX5020.

1.6 Hypothesis

This research project also aims to prove that the nonlinear controllers can give better performance when they are used to control the nonlinear system than that of the linear controllers. The hypothesis is connected with the possibilities of development and application of the methods and technologies of the modern control to the WWTP as follows:

- Different model control design method can be applied to design NLPID controller parameters in order to control nonlinear processes of DO using modern control and computer technologies
- Software integration of Simulink and TwinCAT 3 gives possibilities of implementing the nonlinear controller and DO process in real-time.
- The application of PC and PLC technologies can produce better real-time results from the control of the DO process in comparison with the manual and classical control methods.

1.7 Research approach and Techniques

Mathematical models and computer simulations are essential to predict, describe and control the complicated behavior of WWT processes. Sustainable solutions to the problems of nonlinear processes require development of adequate systems for control and supervision of the process.

The research approach has the following phases

- Literature review and data acquisition.
- Process model development and simulations
- Design of the controllers structure and parameters
- Investigation and verification of the designed systems by simulation in Matlab/Simulink.
- Transformation of the designed closed loop systems to the real-time environment of TwinCAT 3.
- Investigation and verification of the real-time closed loop models through real – time simulation
- Description and comparison of the results.

1.8 Research Assumptions

The thesis assumptions are based on the different aspects/elements of the research work that need to be done. Therefore, the following assumptions are considered:

The wastewater process conforms to the present control technology.

The inflow rate and waste concentrations are the main process disturbances for the whole process.

The oxygen uptake rate (OUR) is the main disturbance for the dissolved oxygen concentration process.

The differential trackers improve the performance of the nonlinear controllers.

1.9 Research Significance

Traditionally there has been very little emphasis on wastewater control systems; as a result most wastewater treatment plants are only equipped with simple control systems. These systems are mainly used for on *and off* control and for monitoring purpose. Dissolved Oxygen (DO) is the most commonly monitored and controlled variable of the activated sludge process (ASP). DO sensors are used to monitor and to transfer the measurements of DO to a computer. Simultaneously, a programmable logic controller (PLC) controls the amount of DO supplied to the aeration tanks. Typically, a PLC is set to regulate DO value to 2 mg/l. Lindberg, *et. all*, (1996).

A high DO concentration in the internally re-circulated water makes the process less efficient. If the DO content is too low, the environment is not stable and the sludge will not be properly treated. Hence, both for economical and process reasons, it is of interest to control the DO process properly Lindberg, (1997). The problem in controlling the DO is that the process changing aspects are nonlinear. This means that high control performance for all operating conditions may be hard to achieve with a linear controller, because linear controllers are designed for a linear process, but the process of the dissolved oxygen in wastewater treatment is a non-linear one. Secondly the parameters of the controller are not determined according to the operating conditions of the process at the moment of control. Thirdly the set-point is selected according to some normal system requirements, not according to the operating conditions of the process at the moment of control. Therefore, the nonlinear characteristics of the oxygen transfer function need to be taken into account when designing the controller.

Significance of the research findings of the thesis are that:

1. The specifics of the nonlinear behavior of the DO process are taken into account for the design of the controllers of the process
2. Nonlinear PID controllers are designed and the simulation results show that they contribute to better performance of the DO process.

3. Transformation procedure is developed for the uploading of the nonlinear controllers directly from Matlab environment to the real-time PLC environment which simplifies the programming of the PLC
4. Real-time simulations of the designed closed loop systems brought knowledge that the new IEC 61499 PLC technology can be applied to control the DO process.

1.10 Thesis Outline

This thesis is made up of nine chapters:

Chapter 2: gives an overview of the methods for modeling, estimation and control of the process for dissolving of oxygen in wastewater. Discussion of the use of different linear and nonlinear controller and estimation of nonlinear plants is done. In particular, the activated sludge process modeling and control is considered. Nonlinear controllers that give high performance for all operating conditions of the nonlinear plant are discussed.

Chapter 3: introduces the structure of the activated sludge process (ASP) and the description of the COST Benchmark process based on the ASM1 biological model. The mass-balance model of the dissolved oxygen concentration for the Benchmark layout is also given together with development of the mathematical model of the oxygen transfer function as an exponential model of the air flow rate.

Chapter 4: shortly describes the general control theory used for the analysis and design of nonlinear control systems.

Chapter 5: apply the Ziegler-Nichols method to design the linear PID controller parameters and the designed and tuned linear PID controller parameters are used in the nonlinear PID controllers for the nonlinear DO process control.

Chapter 6: presents the application of the pole placement method to design linear PID controller parameters based on the linearized DO process model. The designed LPID controller parameters are used for the control of the linear and nonlinear DO process model. In this chapter the NLPID controllers are used to control the linear DO model and nonlinear DO model through the parameters designed for LPID and tuned for NLPID controllers.

Chapter 7: presents the development of the pole placement procedure for design of a LPID controller based on the nonlinear DO model (for design of the LPID controller

parameters) and procedure for design of a NLPID control parameters based on the nonlinear DO model (for design of the NLPID controller parameters)

Chapter 8: describes and presents the real-time implementation structures of the closed loop systems based on the two NLPID controllers. First a model transformation technique is developed to transfer the developed models of the controllers and the corresponding closed loop system directly from Matlab/Simulink environment to the TwinCAT3 environment. Secondly the TwinCAT 3 runtime environment is used for uploading the transferred models in Beckhoff CX5020 PLC. The real-time closed loop system results are displayed in TwinCAT software environment.

Chapter 9: provides the thesis deliverables, conclusion, and future recommendations for development of nonlinear controllers in industry.

1.11 Conclusion

This chapter describes the importance of wastewater treatment and provides a general suggestion of control strategy that can be used for control of the DO concentration in the aerobic tank. Three different controller design procedure are introduced in this chapter through the aim and objective of this thesis.

The next chapter (Chapter 2) is based on the literature review on the design and implementation of nonlinear controllers in industry.

CHAPTER TWO: LITERATURE REVIEW

2.1 Introduction

In the present world the continuous improvement idea is to take care of water, because the value of water is relative to the value of life (Ostace *et. al*, 2010). The objective of a Wastewater Treatment Plant (WWTP) is to remove impurity driving forces from the wastewater through physical, chemical and bio-chemical processes. Current wastewater treatment plants make use of biological nitrogen removal, which relies on using nitrifying and denitrifying bacteria so as to remove the nitrogen from the wastewater. Due to the strict effluent legislation set by municipalities in various nations, essential innovations are becoming necessary for control of Waste Water Treatment Plants (WWTP). Activated sludge WWTP is the most common type of the modern Waste Water Treatment (WWT). The activated sludge process consists of numerous biochemical reactions behaving nonlinearly (Han *et al.*, 2008). The reactions include mechanisms which are useful for reduction of carbonaceous materials and other unwanted compounds in wastewater (Reemtsma, and Jekel., 1997).

Rosemount Analytical, (2009) indicates that Seventy-three percent of the populace is joined with a district wastewater gathering and treatment framework, at the same time as the other 27 percent utilizes on location contaminated frameworks. At the point when water has been utilized as a part of any of these ways, it changes its innovation and becomes a wastewater which is also called sewage and has to be cleaned up before it can come back to the nature for utilization. All types of water are recycled in one way or another. Wastewater is one type of disposing of hazards to the environment. Today it is necessary to recycle the water to keep up practical supplies of safe drinking water for future creation. To clean up or treat wastewater for reuse, it is very much essential to know what the chemical hazards present in the wastewater are and analyze the problems they may cause, and how the cleaning process will be handled today.

This Chapter gives an historical overview of the activated sludge process (ASM) and of the methods for its control. Then the overview of the process of DO concentration, and of the existing benchmark models is done. Literature search and literature review are shown in a form of a bar graph and in a table form. Later a discussion of the different control methods is done. The following parts are discussed in this Chapter as follows:

Section 2.1 gives a general introduction of the Wastewater Treatment Process (WWTP), in section 2.2 Literature search to perform an overview of the activated sludge WWTP and the methods for design of nonlinear controllers is described, section 2.3 delivers some descriptions of the WWTP, Activated Sludge Models (ASM) are described in section 2.4, Literature review of the different techniques used for design of the nonlinear controllers for the nonlinear plants is provided in section 2.5, and the final section 2.6 is the conclusion

2.2 Literature search to perform an overview of the Activated Sludge Wastewater Treatment Process and the methods for the design of nonlinear controllers

Wastewater contains many pollutants and is usually referred in terms of chemical demand, total suspended solids, and total nitrogen and ammonia. Influent passes through an anaerobic tank and an anoxic tank, in which nitrate is decreased to nitrogen and organic carbon is expended. Within air circulation tank, additional utilization of natural carbon takes place and smelling salts are changed to nitrate. The sedimentation gives back an intense stream of activated sludge to the anaerobic tank as passing elucidates gushing by the channel to the cleansing tank for un-activation of destructive microorganisms (Ye *et al.*, 2009). Dissolved Oxygen (DO) concentration control focuses on natural WWTP. Deficient or overload oxygen in the air circulation tank will prompt crumbling of enacting slop. The process of oxygen exchange is nonlinear and hence it is necessary to design an appropriate controller for its operation.

In general the target of a control framework is to make any operating procedure yield act in a required manner by controlling the plant input. The questions that arise are *which variables should be measured, which inputs should be manipulated, and which link should be made between them?* It depends on the variables that can “optimize the process”. There may be many issues involved, and to be trade those off against each other in a systematic manner is necessary to develop a good control structure as proposed in (Skogestad and Jacobsen, 1995). These days the problem for design of the WWTP cannot give an improved solution for the operation of the process, improvements can be done only through development of new control strategies. Along these ways, the control issue of the process is turned into a control optimization issue, according to the original ideas proposed in (Wahab *et al.*, 2007).

Wastewater treatment and accumulation has taken after ways of remarkable and investigative actions. From a remarkable point of view, as population growth is high, so has the requirement for quality water is expanded. Experimentally, as general wellbeing issues and the understanding of the reasons that can flare-up the sickness, for example, cholera and diarrhea have been found, the construction of foundation and advancement of techniques that can be utilized to end these issues by appropriate design of controllers used in the WWTP becomes very important.

The chapter describes an overview on the Activated sludge wastewater treatment process and on the methods for design nonlinear controllers capable to be used to control this process. A literature search using the following key words is done, as follows: Activated Sludge Process, Dissolved Oxygen, nonlinear controllers and nonlinear processes. The Figure 2.1 presents a graph of the number of reviewed papers proposing methods and algorithms for design of nonlinear controllers for nonlinear plants per year, from 1942 to 2014.

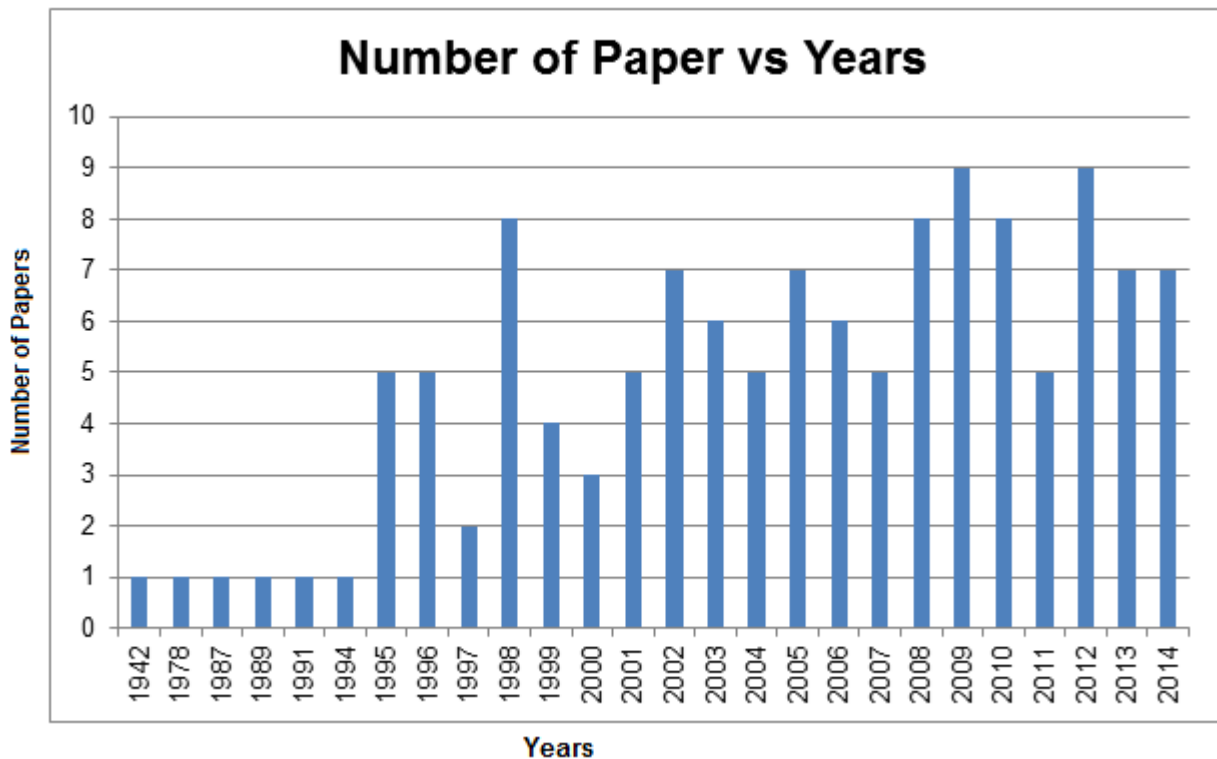


Figure 2.1: Bar graph showing the number of papers for design of nonlinear controllers for nonlinear plants per year

2.3 Wastewater Treatment Plant (WWTP) Description

Wastewater treatment is strictly related to the standards and expectations set for the effluent quality of water worldwide (Gaonkar & Kande, 2014). The consideration of WWTP aims to reach great developments in the quality of the wastewater. WWT is the methodology of expelling the contaminants from wastewater. It incorporates physical, concoction and nature methodology. Its target is to create a treated waste matter and slop suitable for release. The sludge might likewise be reused. The sludge is frequently coincidentally defiled with lethal natural and inorganic compounds. Ordinarily, sewage treatment includes three stages, called primary, secondary and tertiary treatment.

2.3.1 Common layout of WWTP

Many different steps are handled in the wastewater treatment process before the water is released to the beneficiary. Lindberg, (1999) and Geo, (2009) provide an analysis of the accepted practices. A typical representation of WWTP is presented in Figure 2.2. The four section blocks show different stages that are performed in the process of the wastewater treatment.

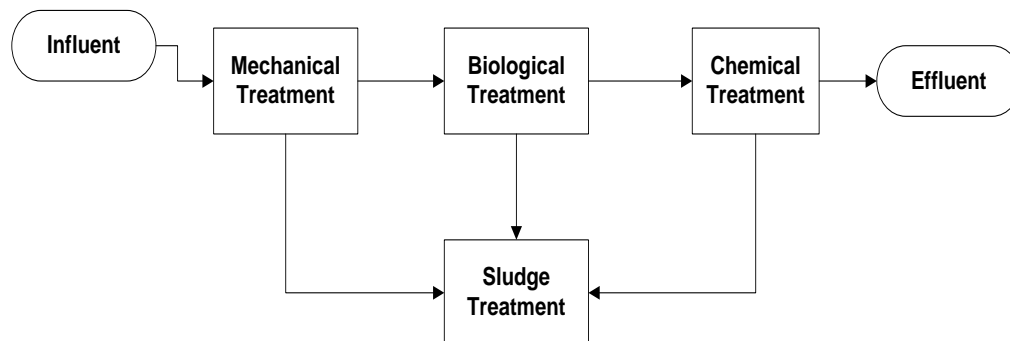


Figure 2.2: A common layout of a Waste Water Treatment Plant

Step 1: Mechanical treatment

Massive substance like scraps are first put together on a framework. Thereafter the big fragments like sand are eliminated in the sand filter and small elements are eliminated in a primary settler.

Step 2: Biological treatment

In the biological treatment process the wastewater treatment plant microorganisms have the ability to cast down the organic matter and in some configurations nutrients are also eliminated. Although different biological processes are present,

the activated sludge process is the most used process in large wastewater treatment plants.

Step 3: Chemical treatment

To remove Phosphorus from the wastewater in the beginning of pre-precipitation, a condensation chemical is added and it deviate phosphate into insoluble fractions. These chemicals also activate the formation of flocks. As stated by Rodrigo, (1999) the biological process in which microorganisms oxidize and clarify organic matter is in the process of activated sludge. As shown in Figure 2.2 microorganisms go into the system through the influent wastewater. To maintain the microbiological population, sludge from the optional pioneer is re-circulated over to the circulated air through (aerated) tank. Large quantity of sludge is evacuated to both maintain a strategic distance from sewage because of in-gushing water and to keep up a sensible suspended solids concentration (Lindberg *et al.*, 1996).

Step 4: Sludge Treatment Process

It is very important that the chlorination for purifying and bad smell elimination is integrated before the water is released to the receiver. Sludge treatment is handled from the different relative blocks in the ASP. The sludge has organic material which needs to be balanced to avoid smell and reduce the pathogenic content. This balancing process is usually done in anaerobic digesters (Muga, 2009).

2.3.2 The process of Activated Sludge

Spring, (2003) claims that activated sludge was originally developed in England prior 1900s, but without the extensive popularity in US up to the 1940s. In these days there are numeral innovations that have advanced the process of activated sludge.

A main activated sludge process consists of many co-dependent factors:

- The biological reaction takes place inside an aeration tank.
- The aeration tank which has an aeration source with the intention to bring oxygen and mixing
- In the clarifier tank, the rock-solid clear and get disconnected from treated wastewater.
- The process of gathering any solid and putting them back to the aeration tank is known as Return Activated Sludge (RAS), or eliminate the solids

from the activated sludge known as the process of Waste Activated Sludge (WAS).

Dynamic microorganisms go through the aeration tank and they reproduce rapidly with sufficient sustenance and oxygen. The wastewater achieves the end of the tank following 4 to 10 hours. The microorganisms utilized a large portion of the natural matter for this time to deliver new cells and the living beings settle to the base of the clarifier tank to separate from the clean water. This sludge is pumped once again to the air circulation tank and is blended with the approaching wastewater or expelled from the framework as access, and this procedure is called wasting. The moderately clear fluid over the slime is sent for further treatment as needed. Typical illustration of the process is shown in Figure 2.3 (Spring, 2003)

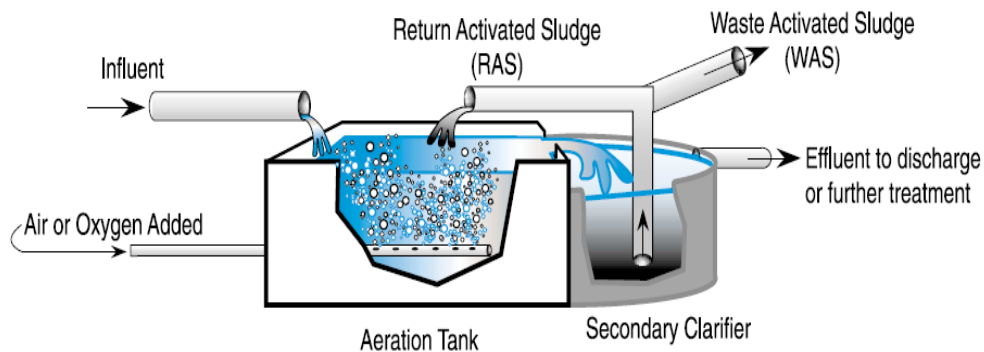


Figure 2.3: Typical Activated Sludge Process (Spring, 2003)

Essential guideline behind all activated slime techniques is that as microorganisms develop they outline some particles that clump together (e.g. Figure 2.3). These particles called flocs are permitted settling to the base of the tank, exit from a generally clear fluid free of natural substance and suspended solids, (Ito, 2004) and (Ostace et al., 2010). Screened wastewater is blended with varying amounts of reused fluid containing a high extent of organic form taken from an auxiliary illuminating tank, and it turns into an item called blended fluid. This mixture is blended and infused with extensive amounts of air, so as to give oxygen and maintain solids in suspension. In a while, blended liquid streams to the clarifier and is permitted to settle. A segment of the microbes is detached as it settles, and the part of the cleaned water streams on for additional treatment. The ensuing settled solids are taken back to the initial tank to start the procedure over again.

2.3.3 Significant zones of the Activated Sludge Process

During the activated sludge process the micro-organisms are kept suspended either by blowing air in the tank or by use of agitators (Lindberg, 1997). Oxygen is used by the microorganisms to oxidize organic matter. Lee, et. al., (2002) proposed that the activated sludge process must have three zones as shown in Figure 2.4 in order to create conditions that are favorable to the growth of bacteria.

The zones are:

Anaerobic Zone: This zone is deficient in nitrate and oxygen.

Anoxic Zone : This zone is deficient in oxygen only.

Aerobic Zone : This zone has both oxygen and nitrate present.

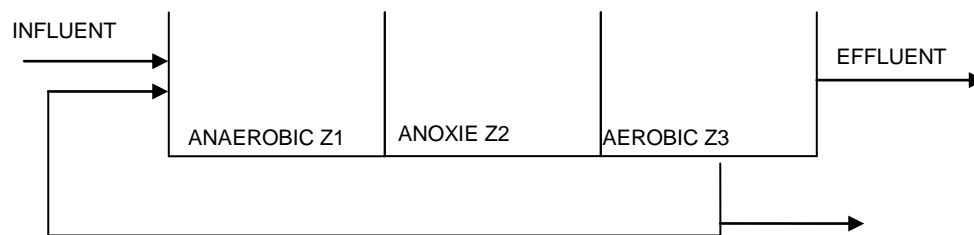


Figure 2.4: Activated sludge process

The zones are used to remove carbon, nitrogen and phosphorus.

2.3.3.1 Carbon Removal:

Carbon in the wastewater is found in an organic form and inorganic compounds, which are removed by the redox reaction. Performed by the microorganisms called Heterotrophs, this reaction causes carbon dioxide to be released to the atmosphere and therefore it removes carbon.

2.3.3.2 Nitrogen Removal:

Nitrogen in the wastewater is in the form of ammonia and an organic form which is converted into nitrate in the aerobic zone. It has an advantage to have the anoxic zone after the aerobic zone in which organisms called Autotrophs are used to convert nitrate to nitrogen gas in the anoxic zone, (Ostace *et al.*, 2010).

2.3.3.3 Phosphorus Removal

Phosphorus in the wastewater is found in microorganisms called Poly-phosphate. The microorganisms can either keep or release phosphorus depending on the

favorable conditions (Macnab, 2014). The stored phosphate is released with the wasted sludge in the WWT process.

Activated sludge is a process for treating sewage and industrial wastewater using air and a biological matter composed of bacteria and protozoans. This process (ASP) is the biological treatment process used in larger or small wastewater plants and these plants are capable of producing a high quality effluent (Ye et al., 2010). Therefore the use of ASP has the advantage of reasonable operating cost, maintenance with low construction cost and the relatively small land requirement and is broadly utilized by vast urban communities and groups where extensive volumes of wastewater must be profoundly treated financially.

The common terms used in the activated sludge model developed for the purpose of control are:

- i. State variables - State variables include the different fractions of the Chemical Oxygen Demand (COD), biomass and diverse sorts of supplements, both natural and inorganic.
- ii. Dynamic processes - Dynamic processes list the distinctive organic techniques that are demonstrated,
- iii. Parameters - Parameters illustrate the circumstances of the natural framework, for example, development and rot rate, half-immersion coefficient for hydrolysis, etc.

2.3.4 Dissolved Oxygen Concentration Process Overview

The microscopic organisms continually require energy so as to develop and to help crucial life exercises. Developing cells use substrate and supplements found outside the cell film for development and energy in a procedure. Oxygen is used by microorganisms called autotrophs to oxidize organic matter. The autotrophs are used to grow only with dissolved oxygen and use inorganic carbon as substrate. Some bacteria can use or not use dissolved oxygen and are called heterotrophs. The major part of bacteria in the activated sludge process use natural carbon as little organic molecules. The biomass growth rate depends on many variables, such as the amount of biomass, substrate, temperature, potential hydrogen (pH), etc.

Dissolved Oxygen (DO) concentration is among the principal control parameters in the activated sludge systems (Lindberg and Carlsson, 1996). Oxygen plays an integral part in activated sludge process. If the associated aeration is done in an

optimal way it will lead to substantial reduction of the energy consumption (Vanrolleghem, 2003). Continuous and reliable DO monitoring can improve plant efficiency, lower the operating costs and decrease the risk of unwanted odor events (Ye *et al.*, 2010). Dissolved Oxygen (DO) concentration control is the most used control strategy in the control of the activated sludge process and influences both the effluent quality and the economical operation of the plant. This research work focuses on the controlling DO concentration in the aeration tank of the Activated Sludge Process (ASP).

Dissolved oxygen (DO) is added to the air circulation bowl known as aeration tank, so as to improve the oxidation transform by giving oxygen to high-impact microorganisms that convert an organic waste into inorganic (Ye *et al.*, 2010). To metabolize sustenance and duplicate, every microorganism must have no less than 0.1 to 0.3 mg/L DO (Copp *et al.*, 1999). Most plants keep up around 2 mg/L of DO and the microscopic organisms contained inside the flocs can utilize this oxygen. Once the concentration of the DO is excessively low, the environment is not steady for the microorganisms. They will die because of the anaerobic zones in the aerobic tank and the sludge will not be suitably treated. Nowadays, most of the plants remunerate by adding very high measures of DO to their procedure. In the event that DO levels get to be excessively high, energy is wasted, excessive air circulation gear experiences unnecessary utilization, and unwanted organisms called filamentous are promoted.

2.4 Activated Sludge Models (ASM)

2.4.1 Benchmark Model of the Activate Sludge Wastewater Treatment Plant

The Benchmark Simulation Model (BSM) based on the ASM1 biological model has five biological reactors connected in series manner as shown in Figure 2.5 (Ostace *et al.*, 2010). The benchmark wastewater treatment plant model shown in Figure 2.5 is proposed by the European Cooperation in the field of Scientific and Technical research, and is known as a product of COST action 624 and COST action 682. The action was done to evaluate the control strategies in the wastewater treatment plants and is strictly in agreement with the benchmark methods, especially from the side of control performances (Alex *at al.*, 2008). The first two units are anoxic and the last three units are aerated reactors. Each anoxic reactor has a volume of 1000 m³ and each aerated reactor has a volume of 1333 m³. The total biological volume is 5999 m³. The reactors are followed by a secondary settler, which has an area of 1500 m² and a depth of 4 m.

The organic methods that are occurring in the tanks are displayed utilizing International Association on Water Quality Activated Sludge Model no.1 (IAWQ ASM1), a biological model proposed in Henze *et al.*, (1987). Copp *et al.*, (1999) state that the Activated Sludge Model (ASM1) has thirteen state variables and eight dynamic processes represented by a set of normal differential equations which describe the forceful changes of the state variables.

According to Wahab *et al.*, (2007) the procedure of undignified the biodegradable matter can be separated in two phases. They are:

- Nitrification and
- Denitrification.

A suitably high concentration of DO is expected to fulfill the nitrification prepare in the oxygen consuming tanks, while an excessively high DO content will unfavorably affect the de-nitrification process in the anoxic tanks.

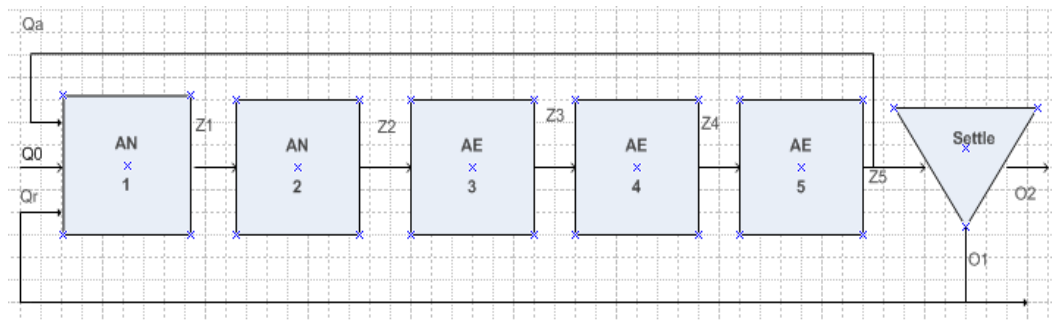


Figure 2.5: Lay-out of the benchmark simulation platform plant (Henze et al., 2002)

Sludge recycles flow rate, external carbon dosing, dissolved oxygen concentration and internal recycle flow rate are frequently investigated as manipulated variables in WWTP by Alex *et al.*, (2008).

2.4.2 Historical overview of the Activated Sludge Biological Model development

The universal name Activated Sludge model (ASM) is for a gathering numerical methods or procedure to model activated sludge biological framework. The investigation here is facilitated by a task gathering of the International Water Association (IWA). Activated sludge models are utilized as part of the investigate exploration to study organic method in theoretical schemes. They can likewise be connected to full scale wastewater treatment plants for optimization, and balanced reference information for slop generation and supplements in the effluent.

In 1983, International Water Quality Associations (IWQA) was formed (Henze *et al.*, 1987). They started to create a generalized framework for mathematical models that could be used to model activated sludge for nitrogen removal. Their main goal was to develop a models of which the complexity was as low as possible, simple to represent, and able to accurately predict the biological processes. Activated Sludge model no.1 (ASM1) started to be used in activated sludge modeling before IWA was formed, although each investigate collection worked on mathematical frameworks of the activated sludge and formed their model, these models were ground incompatible. This fact therefore catalyzed the joint investigate and had a most important impact on activated sludge modeling (Keskitalo and Leiviska, 2010).

The IWA started working on activated sludge process modeling and developed prosper models (ASM1, ASM2, ASM2d, and ASM3) for the WWTP, as given in Table 2.1.

Table 2.1: Description of Activated Sludge Models

Abbreviation	Description	Differences	Limitations
ASM1 (Barbu <i>et al.</i> , 2005)	A simplest model that can describe Carbon oxidization, nitrification and denitrification accurately.	Main difference between the ASM1 and ASM3 are the piece of limit polymers and the altered of improvement rot advancement model to development endogenous breath display in the ASM3. ASM1 has less 13 state variables, less than the ASM2 model with 19 state variables.	The later modification which was done to correct defects, were recognized in ASM1 and to improve parameter identification. The main drawback of ASM1 model is its complexity.
ASM2 (Henze <i>et al.</i> , 1999).	The development of this model aims to incorporate a report of biological phosphorus removal.	Activated Sludge Model2 is more difficult than the Asm1 and has extra segments and procedures to represent organic phosphorus evacuation. Apart from heterotrophic and nitrifying living beings ASM2 has phosphorus-gathering organic entities. Finally ASM2 explain element or chemical precipitation of phosphorus.	As the frameworks are less interconnected, identification of the model is expected to be better. The equations for phosphorus removal were added to ASM1 model, the result being a more complex model called ASM2.
ASM2d (Henze <i>et al.</i> , 1999).	Explanation of organic phosphorus elimination was not finished in ASM2. As a result of that incompleteness the model was enhanced in ASM2d.	In ASM2d there are important extensions to ASM2 such as adding of the denitrifying phosphorus accumulating organisms.	The model is valid for municipal wastewater only, pH should be near neutral, the temperature is expected to be in the range of 15 -20 °C.
ASM3	This model was developed to describe a biological	The decay process of ASM1 is replaced with the concept of endogenous respiration in	ASM3 has made the identification of the model better.

	nitrogen removal.	ASM3.	
--	-------------------	-------	--

ASM1 was the establishment for various expansions. These augmentations incorporate better forecast of nitrogen and phosphorus evacuation and are broadly utilized as a part of augmented models including ASM2, ASM2d, and ASM3P. ASM1 model is further used in biological phosphorus removal (Sanchez and Katebi, 2003). An enhanced version of ASM1 model is selected as a case study in this thesis. The version also named as ASM2 was created to incorporate organic (and synthetic) phosphorus evacuation. As investigative comprehension developed in the late 1990s, ASM2 was stretched out into ASM2d, basically by the expansion of anoxic tank and in addition high-impact uptake of phosphorus. Utilization of the model outside of these limitations is not recommended (Henze *et al.*, 1999).

2.5 Literature Review of the methods for the design of nonlinear controllers for nonlinear plants

Control problems of the nonlinear frameworks have particular, specific consideration all through the most recent four decades. Many impressive efforts were committed to the examination of the structural properties to see better the strategy for methods to control the nonlinear systems. Control of DO is a common problem encountered by the range of industrial systems, such as chemical, biochemical industries and wastewater treatment, due to its high nonlinearity. In the literature review there are included different methods for design of control of nonlinear processes: Input/State linearization, Input/output linearization, Lyapunov method, PID controllers, etc. Review of the application of some of these methods is done below.

2.5.1 Feedback Linearization methods

The literature investigation has shown that there are cases where versatile direct control plans would not perform well when confronted with a very nonlinear procedure. This is on the grounds that the versatile instrument may not be sufficiently quick to track changes in procedure qualities. A suitably design of nonlinear controller would then be expected to perform better.

The literature reviews different types of model based controllers: Fuzzy, neural network, PID, these and other model-based controllers are presented and discussed in Table 2.2 later. Another rising field is that of nonlinear controller design by the use of differential geometric concepts (Slotine and Li, 1991). Furthermore the study of the feedback linearization together with continuous-time recurrent neural networks has been performed. (Singh *et al.*, 2013)

There are two basic important approaches of feedback linearization: Input-Output feedback linearization in which case, the input-output relationship of the resulted closed loop system has to be linear and Input-State feedback linearization in which the relationship between the input and the states of the closed loop system must be linear. The schematic representation of the input/output feedback linearization is shown in following Figure 2.6

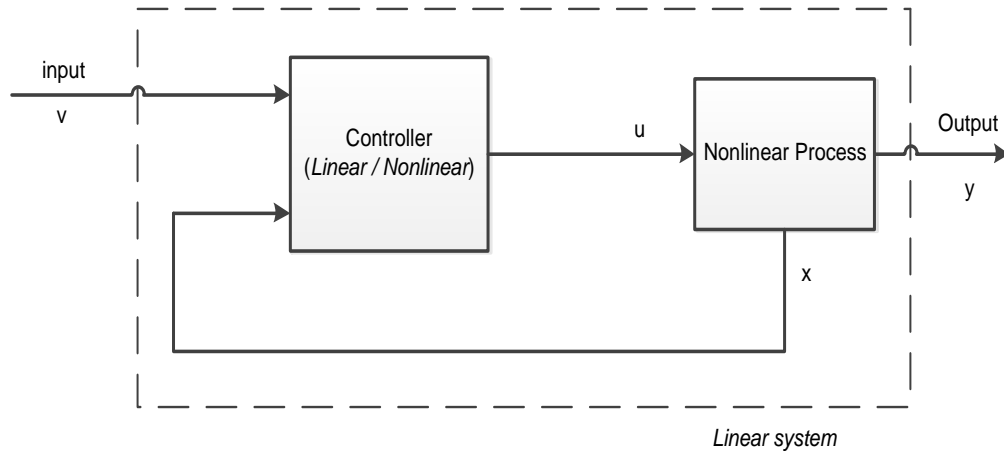


Figure 2.6: Input-Output linearization

In Figure 2.6 the relationship between u and y is nonlinear and between y and v is linear; in addition the relationship between u and v , u and x is also nonlinear where v is a reference input for the nonlinear controller. In the case of continuous-time framework, there exists a number of ways for the design of nonlinear controllers by feedback linearization.

The majority of the feedback linearization methods is based on the input-output linearization or input-space linearization. The main objective of input-output (I/O) linearization approach is to linearize the system between the transformed inputs (v) and the actual outputs (y), detailed discussion are stated in (Kravaris and Chung, 2011) and (Nketoane, 2009)

In the linearization of the state equations the following nonlinear system can be considered:

$$\begin{aligned} \dot{x}(t) &= f(x(t)) + g(x(t))u(t) \\ y(t) &= h(x(t)) \end{aligned} \tag{2.1}$$

Where x is the state vector, u is the input vector, y is output of the system and the smooth vector fields are represented by f , g and h . In a general form g is a

$n \times m$ matrix whose columns are smooth vector fields that can have a required order of continuous partial derivatives. The purpose of input-output linearization is to obtain a nonlinear control in the form:

$$u = a(x) + b(x)v \quad (2.2)$$

Where a and b can represent any variable parameters in such a way that the resulting closed loop control system is linear and results in a linear transfer function, and can be represented in Laplace domain

The output derivative of Equation 2.1 is shown in Equation 2.3 also by means of the Lie derivative:

$$\dot{y}(t) = \frac{\partial h}{\partial x} [f(x(t)) + g(x(t))u(t)] = L_f h(x(t)) + L_g h(x(t))u(t) \quad (2.3)$$

Where $L_f h(x(t)) = \frac{\partial h}{\partial x} f(x(t))$ and $L_g h(x(t)) = \frac{\partial h}{\partial x} g(x(t))$ are called Lie derivative of h along f and g functions. Further definitions for the Lie derivatives can be seen in Muga, (2009).

Taking the essential control $v(t)$, as any suitable linear combination of past outputs in addition to the reference empowers a random task of the closed-loop poles of the linearized by the nonlinear controller system. Therefore, Feedback linearization is a nonlinear counterpart to the pole placement method. (Astrom and Wittenmark, 1995).

2.5.2 Linear and nonlinear PID controllers

2.5.2.1 Linear PID controllers

This section talks over the linear PI and PID controllers based on different algorithms such as Neural Networks (NN), state space etc (Singh *et al.*, 2013) PI and PID controllers remain to be the common methods in industrial applications, because of their effortlessness in execution and understanding. It has been noticed that the linear PI and PID controllers result from the application of model-based controller design technique to direct linear first and second-order systems. In a common way, as can be presumed from the names, a PI controller holds proportional and integral action, and a PID controller which is proportional, integral, and derivative action. The general linear PI and PID controller models are described as follows:

$$u(t) = K_p e(t) + K_i \int e(t) dt \quad (2.4)$$

$$u(t) = K_p e(t) + K_i \int e(t) dt + K_d \dot{e}(t) dt \quad (2.5)$$

Where k_p , k_i , k_d are the PID controller parameters

The standard PID neural network controller design is shown by a feed forward neural network as follows: (Lu *et al.*, 2012)

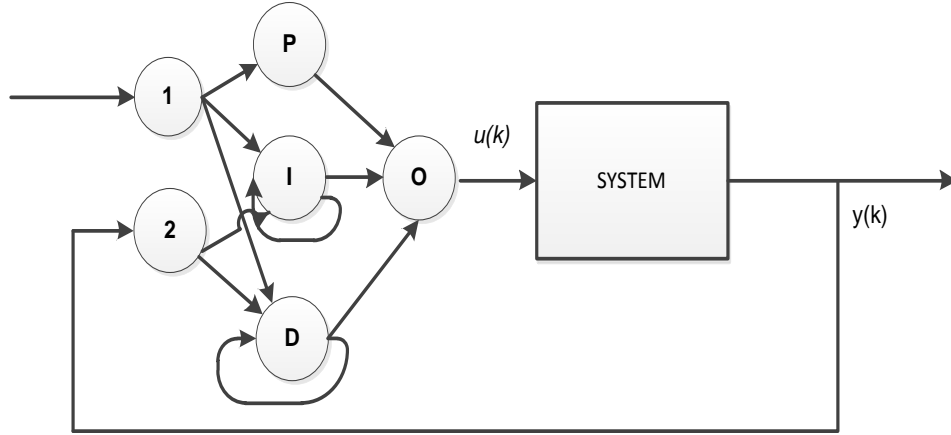


Figure 2.7: Structure of the PID NN Controller (Lu *et al.*, 2012)

$$u_n(k) = K_{pn} e_{pn}(k) + K_{in} e_{in}(k) + K_{dn} e_{dn}(k) \quad (2.6)$$

Where:

$$e_{pn}(k) = r(k) - y(k)$$

$$e_{in}(k) = \sum_{j=1}^k e_j(k) \Delta T \quad (2.7)$$

$$e_{dn}(k) = (e_{pn}(k) - e_{pn}(k-1)) / \Delta T$$

According to Liu and Daley, (2001) if there is a requirement to advance the PID controller's performance, the optimal PID controller design is the option to use. The PID controller is assumed to be of the basic form

$$u(t) = K_p (e(t) + K_i \int_0^t e(t) dt + K_d \frac{de(t)}{dt}) \quad (2.8)$$

Where K_p , K_i and K_d are control parameters, $e(t) = r(t) - y(t)$ is the difference between the reference input $r(t)$ and the output $y(t)$, and $u(t)$ is the control input.

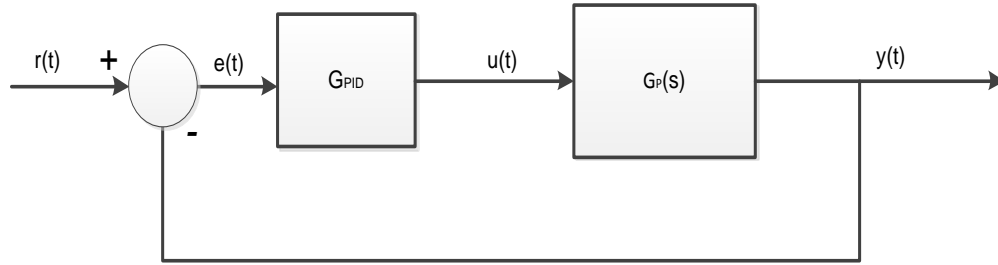


Figure 2.8: Typical structure of the PID

Consider the plant equation shown in Figure 2.7. ($G_p(s)$) is controlled by a linear PID controller. The Equation (2.8) engages certain requirements based on the specifications for a control system design associated with the time response of the system.

$$G(s) = \frac{\omega_n^2}{s^2 + 2\zeta\omega_n s + \omega_n^2} \quad (2.9)$$

Where the parameter ω_n is the natural frequencies, and ζ is the damping ratio. To receive a good closed-loop time response, the following performance function requirement is to be considered when designing a PID controller (Liu and Daley, 2001):

$$J(K_p, K_i, K_d) = \int_0^{\infty} (y_{step}(t) - y_{step}^d(t))^2 dt \quad (2.10)$$

Where: $y_{step}^d(t)$ is the desired step response produced by the transfer function of the system $G(s)$, and $y_{step}(t)$ the step response of the process with the PID controller. Ever since in industrial processes it is frequently not permitted to attempt diverse PID controller parameters on the plant for the purpose of security, $y_{step}^d(t)$ is replaced by the step reaction of the model with the PID controller. In this way, the optimal PID controller configuration may be expressed:

$$\min_{K_p, K_i, K_d} J(K_p, K_i, K_d) \quad (2.11)$$

They continue to state that, some statistics considerations demonstrate that the execution function J is the most proper decision for information fitting when lapses in the information have a typical distribution. The function J is frequently favored in light of the fact that it is realized that the best fitting count is direct to illuminate. But, the way out to the minimisation of equation (2.11) might not give good control results for the system. In that case, some other performance functions have to be taken into account (Liu and Daley, 2001).

2.5.2.2 Nonlinear PID

The investigation shows that the controllers, resulting from nonlinear model-based control theory can be put in a convenient form, more open to industrial implementation. As the LPID controllers are more understandable and very much utilizable in many process control systems, the addition of nonlinear functions in a LPID controller to form NLPID controller can be useful in many nonlinear industrial applications.

The algorithm of the NLPID controller is based on the introduction of nonlinear functions of the control error and an inherent part of the controller. The aim is to achieve a desired better output response of the plant in comparison to this using the conventional PID controller. The nonlinear PID controller has been reconstructed using a nonlinear function proposed by Jiang, *et al.*, (2009), as follows:

$$u = K_p \left[f(e, \alpha_p, \delta_p) + \frac{1}{T_i} f\left(\int e, \alpha_i, \delta_i\right) + T_d f(\dot{e}, \alpha_d, \delta_d) \right] \quad (2.12)$$

Where: K_p, T_i and T_d - are the controller gains similar to these of the linear PID (LPID) controller. $f(e, \alpha_p, \delta_p)$, $f\left(\int e, \alpha_i, \delta_i\right)$ and $f(\dot{e}, \alpha_d, \delta_d)$ - represent nonlinear functions of the PID controller error as given in Equations (2.13) to (2.15).

$$f(e, \alpha_p, \delta_p) = |e(t)|^{\alpha_p} \cdot \text{sign}(e(t)) \quad (2.13)$$

$$f\left(\int e, \alpha_i, \delta_i\right) = \left| \int e(t) dt \right|^{\alpha_i} \cdot \text{sign}\left(\int e(t) dt\right) \quad (2.14)$$

$$f(\dot{e}, \alpha_d, \delta_d) = \left| \frac{de(t)}{dt} \right|^{\alpha_d} \cdot \text{sign}\left(\frac{de(t)}{dt}\right) \quad (2.15)$$

The generalized equation of the nonlinear function is proposed by (Jiang et al., 2009) and (Zaidner et al., 2010) and is given by Equation (2.16)

$$y = f(e, \alpha, \delta) = \begin{cases} \text{sign}(e) \cdot |x|^\alpha, & \text{when } |e| > \delta \\ \delta^{\alpha-1} \cdot e, & \text{when } |e| \leq \delta \end{cases} \quad (2.16)$$

Where: $e(t) = r(t) - y(t)$ and r is the process setpoint and y is the process output. α and δ are two parameters of the nonlinear function $f(\bullet)$, δ is a parameter used to

determine the linear range of the function f , α is the nonlinear degree of the function (Jiang, 2009).

The NLPID controller uses nonlinear functions to replace the linear one in the conventional PID controller. The comparison of the linear PID error e with the nonlinear PID controller function $f(e, \alpha, \delta)$ shows that the use of the function $f(e, \alpha, \delta)$ produces high control gain for small values of the error e and small control gain for large values of the error e .

Since the investigation show that a large percent of practical control techniques among industrial processes is linked to the PID controllers (Wright, 2001) in the case any development of this type of controller could possible result to a positive improvement on all associated industrial process. Also, it is known that most of the developed industrial processes, i.e. thermal, pressure, PH, and flow are nonlinear and can have long time delays. The paper of Zaidner, *et al.*, (2010) reviews one of the nonlinear PID methods, and suggests optional tuning rules accompanied by simulation results. According to what was mentioned to be delivered in this paper, as the design of the Nonlinear PID controllers for stability and control of a noisy model, the better noise rejection for a noise model was not successfully achieved, but it was suggested to combine a NLPID with a Tracking Differentiator in order to control and stabilize systems with noise model in their future work. The PLC implementation was not shown, as they claimed.

To upgrade the execution of a conventional altered addition PID controlled framework, an Enhanced Nonlinear-PID (EN-PID) controller is proposed by (Su *et al.*, 2005) and is joining a sector-bounded by nonlinear gain function and two nonlinear Tracking Differentiators (TDs) into the accessible altered increase PID control building design. To accomplish the high strength against noise, these two nonlinear following differentiators are utilized to choose high- quality differential flag in the surrounding area of estimation commotion. The nonlinear gain is a function of the error and follows up on the error to create the scaled error for quick reaction. Simulation results performed on a robot controller are introduced to exhibit the better execution of the created EN-PID controller in examination with the ordinary settled addition PID controller

2.5.3 Lyapunov theory of stability

When having a system to be controlled, the most important question is about its various properties, whether it is stable or not-stable, because an unstable control system is typically unusable and possibly dangerous. Today, the Lyapunov's linearization method has come to represent the theoretical justification of linear control, while the Lyapunov's direct method has become the most important tool for nonlinear system analysis and design. Together, the linearization method and the direct method form what is known as Lyapunov stability theory (Slotine and Li, 1991). A nonlinear dynamic system can usually be represented by a set of nonlinear differential equations.

The Lyapunov theory of stability is based on the construction of a Lyapunov functions for the system under study. The Lyapunov function is assumed to be done by a quadratic form and for the case of a nonlinear controller design it is selected as follows (Nketoane, 2009):

$$V(e) = e^T(t)Pe(t) \quad (2.17)$$

Where $P \in \mathbf{R}^{n \times n}$ is a positive definite real symmetrical matrix, $e(t)$ is the state system error variable in time domain.

In order to select the nonlinear controller, the first derivative of the function of Lyapunov according the trajectory of the error equation has to be negative, as follows

$$\begin{aligned} \dot{V}(e) = \dot{e}^T(t)Pe + e^T(t)P\dot{e}(t) = [Ae(t) + Ax(t) - f(x(t), u(t)) + Bv(t)]^T Pe(t) + \\ + e^T(t)P[Ae(t) + Ax(t) - f(x(t), u(t)) + Bv(t)] < 0 \end{aligned} \quad (2.18)$$

The nonlinear expression of the controller is calculated from the above equation.

Lyapunov theory includes two methods presented by Lyapunov: indirect method and the direct method. The indirect method, or linearization method, states that the stability properties of a nonlinear system in the close region of a stability point are essentially the same as those of its linearized approximation. The direct method is a powerful tool for nonlinear system analysis, and is mainly called Lyapunov analysis (Slotine and Li, 1991) and (Luo and Si, 2013). In the investigation of Lyapunov theory, the Lyapunov second method of stability assessment was found, this method is based on power considerations, which does not require solution of the systems equations. It involves searching for a function of Lyapunov, which satisfies certain requirements of the system.

Abdelhadi *et al.*, (2014) use a direct design method to identify a pH model from real data by using an application of Local Linear Model Networks (LLMN) and then develop a nonlinear control system for the process. The identified LLMN model of the pH process is tested as an independent model and used for the control simulations. The conventional feedback Proportional Integral (PI) controller parameters for different operating points, identified by the LLMN model, are designed by using a direct design method. These local controllers are then combined into a LLMN controller. Results show the ability of LLMNs for nonlinear system identification and the designed nonlinear control structure results in a good performance.

2.5.4 Adaptive control

Adaptive control is a method used for the control design approach to deal with uncertain systems or time-varying systems. Vanrolleghem, (2003) states that adaptive control uses on-line identification of the system parameters or adjustment of the controller gains, by this means of obtaining strong robustness properties. The adaptive algorithms proposed in Li and Zeng, (2008) are rapidly solving the system of nonlinear equations. The results show that the approach proposed has much higher accuracy than the neural network method and Broyden's method used in this paper.

Singh *et al.*, (2013) this paper presents an approach for velocity and orientation tracking control of a *non-holonomic* mobile robot based on an adaptive controller. The developed PID controller is based on analog neural networks. The feed-forward neural network controller is trained on-line to find the inverse kinematics model, which controls the outputs of the mobile robot system. The proposed controller shows a better performance because of its capability of continuous online learning.

2.5.5 Optimal control

Optimal control is a control method in which the control signal optimizes a certain cost index. Optimization is one of the outstanding recognized branches of mathematics that has an aim of finding the values for variables in order to make the most profit or to decrease the costs subject to some constraints, Andrei (2005).

Ant Colony Optimization (ACO) algorithmic approach has been introduced for optimizing the parameters of a nonlinear PID controller (Hai-bin *et al.*, 2006). From

the results of simulation, it can be concluded that the nonlinear PID controller using the improved ACO algorithm is very effective. The results show a good control and robust performance with some overshoots and settlement. The controller can be improved and be generally used for real-time control of different types of processes.

An optimal-tuning nonlinear PID controller design strategy is proposed by Liu and Daley, (2000) for hydraulic systems. In this paper a nonlinear PID controller which includes the inverse of the dead zone is introduced in order to cancel the dead zone, since the presence of a dead zone in the hydraulic position control system makes difficult to achieve high-precision tracking using only linear controllers. This paper addresses a number of design methods such as: nonlinear modelling, nonlinear PID control, and optimal-tuning PID design. The nonlinear model for the process is estimated using the recursive least-squares method (Liu and Daley, 2000). But the introduction of the inverse of the dead zone to the controller has given unexpected overshoot, long settling time to the closed-loop hydraulic system, now to overcome this optimal-tuning PID controller design for industrial process is proposed by Liu and Daley, (2001) and Predictive control techniques is proposed by (Liu and Daley, 2001).

2.5.6 Model Predictive Control (MPC):

A nonlinear model predictive control (NMPC) focused around a piecewise direct wiener model is exhibited by Shafiee et al, (2006), the nonlinear increase of this specific wiener model is approximated utilizing the piecewise straight abilities. This methodology holds all the intrigued properties of the traditional straight MPC and keeps calculations simple to settle because of the accepted structure of the nonlinear increase. The displayed control plan is connected to a pH balance methodology and reproduction results are contrasted with straight model predictive control. Results from the simulations demonstrate that the nonlinear controller has better execution without any overshoot in examination with linear/ direct MPC, furthermore less steady-state error in following the set point.

Yoo *et al.*, (2004) propose a nonlinear control plan to keep up the poor dissolved oxygen level of an activated sludge framework. Without any linearization or model degeneration, it can straightforwardly fuse the nonlinear DO procedure model with on-line estimation of the breath rate (R) and the oxygen exchange (K_{La}).

Simulation results show that the proposed control scheme is very effective to be used. Since it incorporates the process disturbance and nonlinearity in the controller design, the suggested method can efficiently deal with the operating condition changes that occur frequently in the wastewater treatment process.

2.5.7 Pole Placement method:

Pole Placement is a method used in feedback control system theory to place the closed-loop poles of a plant in pre-determined locations in the s-plane.

Mathematically once the system transfer function is defined, the desired transfer function should be also defined, and then each coefficient in the same order in polynomial is compared to be the same. This pole placement control method results in the desired system response and is easy to fine the gain mathematically, but the accuracy of the system transfer function is significantly important and is expensive to implement in the high order system.

Hasanien *et al.*, (2009) use a digital pole placement controller for permanent magnet synchronous motor (PMSM). The advanced pole placement controller in this paper is utilized for velocity control of the motor. The dynamic reaction of the (PMSM) with the proposed controller is calculated over the beginning process under the full load torque and under burden aggravation. The effectiveness of the proposed advanced digital pole placement controller is then contrasted with that of the traditional PI controller. The proposed controller is utilized as part of request to conquer the nonlinearity issue of PMSM and the parameter varieties

2.5.8 Ziegler and Nichols control design method:

Copeland, (2008) state that, In 1942 Ziegler and Nichols, described simple mathematical procedures for tuning PID controllers. These procedures are now accepted as standard in control systems practice. Ziegler-Nichols formulae for specifying the controllers are based on plant step responses.

As most of the PID tuning rules were developed many years ago, the direct use of Ziegler–Nichols rule in the nonlinear controllers still needs to be investigated. The achievement of a direct design for nonlinear control parameters through Ziegler-Nichols can help to avoid the tuning process which is time consuming.

2.5.9 Review of the existing papers in a Table form

The following table shows a sample of papers describing controllers design for WWTP, dissolved oxygen concentration and other linear and nonlinear processes in industry. Different control strategies, methods for design of linear and nonlinear controllers are also reviewed in Table 2.2.

Table 2.2: Linear and Nonlinear controllers for nonlinear processes

Paper	Problem Formulation	Models		Algorithm for design of the controller	PLC – SCADA Implementation		Applications		Advantages/Disadvantages	
		Plant	Controller		PLC	SCADA	Simulation/Industrial setup	Used Controllers & Plants	Advantages	Disadvantages
(Zhao et al., 1994)	Design Nonlinear optimal control of an alternating activated sludge process.	Pilot Plant model of ASM1	Nonlinear optimal control techniques based on state space model and a new strategy of nitrogen removal.	Newton-Raphson optimization. Least squares algorithm.	No	No	Simulation was done but, the platform of simulation was not mentioned.	1 nonlinear optimal state space controller and 1 Plant.	Optimal nonlinear control approach is successful and effective for improved nitrogen removal in the WWTP.	Results show an improvement still need to be made for the nitrogen removal.
(Rodrigo et al., 1999)	Nonlinear control design for an activated sludge aeration process.	Activated sludge aeration process:	Aeration fuzzy PID controller.	Fuzzy techniques. Neural networks used to obtain fuzzy membership functions. fuzzy PID controller using fuzzy rules.	No	No	Only simulation	One process model. 4 controllers: fuzzy, Internal model control (IMC), Cohen and Coon and ITAE (Integral of the Time weighted Absolute Error) tuned PID controllers.	The nonlinear fuzzy PID controller quickly improves its response and reaches the set-point, even before the IMC and ITAE tuned PID controllers	Trial and error procedure is time consuming.
(Liu and Daley, 2000)	An optimal PID controller design to satisfy some desired time-domain performance requirements.	Hydraulic position control system.	A nonlinear PID (NLPID) control scheme with the inverse of the dead zone.	Optimal-tuning recursive least-squares. Nonlinear modelling, nonlinear PID control, and optimal-tuning PID control design.	No	No	Simulations using Lab-dSPACE, Matlab/ Simulink and Real time workshop.	1 Process model and 2 types of controllers.	Designed optimal PID parameters satisfy the desired system specifications.	This strategy needs slightly more computation to search for the optimal PID parameters, compared with a fixed parameter controller.
(Jiang and Gao, 2001)	Design a nonlinear PID for class of truck ABS Problems. Tuning method.	Brake system dynamics and Wheel velocity models	NLPID, LPID and Loop shaping controllers.	Nonlinear filter approach and NLPID algorithms for on-line tuning.	No	No	Industrial Simulator, On-line testing and adjustment.	3 Controllers: LPID, NLPID and Loop shaping are used respectively to control Anti-lock Brake System (ABS).	Using NLPID controller to truck ABS problem gives short stopping distance and better velocity performance than these obtained with LPID.	The tuning of the controller is done purely on trial and error basis.

(Panagopoulos et al., 2002)	Linear problem. Design the controller parameters, so that the system behaves well with respect to changes such as load disturbance or set point change.	Name not mentioned only, it is linear, time invariant.	PID design formulated as a parameter optimization problem.	Linear partial differential algorithm.	No	No	Simulation Lab setup only.	1 controller designed to capture demands on load disturbance rejection, set point response, and noise and model uncertainty.	Can capture demands on load disturbance rejection, set-point response, measurement noise and model uncertainty.	The disadvantages of the used control type, it can only work successfully to linear process.
(Sanchez and Katebi 2003)	Design of Predictive Control of DO in an Activated Sludge Wastewater Treatment Plant	ASM1	PI, Model Predictive Control, and Pole-placement control, using subspace identification of DO process model.	Composite and Augmented models Predictions. Kalman filter compared to a state observer.	No	No	Simulation only. No real implementation was done.	2 Controllers are used respectively to control dissolved oxygen. Comparison is based on the disturbance estimation,	The controllers (Model Predictive Control and Pole-placement) perform very well and improve the performance compared to a single PI loop.	This paper assumes a constant disturbance model.
(Mhaskar et al., 2004)	A two-level, optimization-based method for deriving tuning guidelines for PID controllers.	Nonlinear chemical reactor model. ASM1 model.	Nonlinear PID Controller and Optimal-tuning linear PID Control.	Classical Tuning Methods. Linearizing controller. Internal Model Control (IMC)-based and Ziegler-Nichols tuning rules	No	No	Simulation has been performed but software is not mentioned. (It seems as Matlab)	1 nonlinear plant and 2 controller: linear and nonlinear PID	Proposed tuning method can achieve closer response of the closed loop reactor model through nonlinear controller.	The proposed method of linear PID cannot give accurate results, tuning is needed which time is consuming.
(Ito, 2004)	Design of a dissipative approach to control a Biological Wastewater Treatment Plants based on entire nonlinear process models.	Biological WWTP model: Activated Sludge Model NO.1	Dissipative flow controller. Attenuating targets via positive control	Dissipation inequality and model-based controller design dissipation property.	No	No	Rigorous simulations in MATLAB/Simulink	One Plant.	Proposed dissipative control is better than the proportional flow control in various points.	This method is able to control the system, but didn't consider the on-line unmeasurable variables.
(Oliveira et al., 2004)	Design of a stable adaptive controller for driving aerobic fermentation processes near maximum oxygen transfer capacity.	Aerobic fermentations near maximum oxygen transfer capacity.	Adaptive control	Model reference adaptive controller (MRAC) is designed based on a phenomenological model of the process.	No	No	Software used for simulation is not mentioned.	One Plant and 1 controller.	Results show that the adaptive controller is accurate, stable and robust to disturbances.	Tuning of design parameters and variables estimation in this method can be time consuming.

(Yoo et al., 2004)	Propose design of a nonlinear controller to maintain the dissolved oxygen level of an activated sludge system.	Biological Wastewater Treatment Process based on DO model.	Generic Model Control and PI control.	Kalman filter. Nonlinear model-based control algorithm.	No	No	Lab real time simulator.	Nonlinear Model-based controller used to control DO plant.	Model-based DO controller can cope well with the operating condition changes that occur frequently in the WWTP	The PID controller shows a large offset as it is a linear controller applied in a nonlinear system.
(Su, et al., 2005)	Enhanced NLPID controller design that exhibits improved performance than the conventional linear PID.	Nonlinear robot manipulator model.	Linear and Nonlinear PID. 2 nonlinear tracking differentiators are used to select high-quality differential signal.	EN_PID Ziegler- Nichols criterion Popov stability criterion	No	No	Matlab simulation	Plant model and 1 NLPID controller.	It is high robustness against noise & superior performance over the conventional fixed gain PID controller.	No real implementation completed
(Barbu et al., 2005)	Mathematical modeling for design of PI controller for operation of biological wastewater treatment.	ASM1 model of the wastewater treatment process.	PI type controller based on decoupling procedure for unobservable and observable disturbance.	PI control algorithm with feed-forward control structure. Model simplified through linearization (state space equation).	No	No	Simulation using Matlab/Simulink	1 Controller and one Plant models.	A robust control method is used to benefit in variable characterization by varying functioning systems and uncertainties..	Linear controller cannot give assure performances for a system (rain, normal or drought) if the functioning point changes significantly.
(Peng and Cheng, 2005)	To design NLPID controller for Superconducting Magnetic Energy Storage unit, to improve the stability of the power system	Generally, the superconducting magnetic energy storage (SMES) unit is used as a torque modulation stabilizer.	NLPID controller and Tracking Differentiators.	Nonlinear feedback rule that can understand dynamic feedback compensation.	No	No	Simulation in Matlab environment.	2 NLPID controllers with the same nonlinear function are used in order to reduce the parameters design for the controller nonlinear configuration. 1 Plant.	It can effectively enhance both dynamic performance of the power system power angle stability and the voltage of the place at which the SMES unit is.	Software implementation part is not perfectly shown.
(Hai-bin et al., 2006)	Application of an Ant Colony Optimization method for design of the NPID controller.	Quadratic Assignment Problem based on how real ants find a shortest path in	Nonlinear PID Parameter Optimization Using Ant Colony Optimization	Novel Approach to Nonlinear PID controller using the Ant Colony Optimization (ACO) algorithm.	No	No	Simulated using Flight Simulation Turntable.	1 controller tested with 1 plant model.	It has good control and robust performance, and can be widely used to control different kinds of object and process.	A good NLPID, but with complex functions to understand.

		nature searching for food.								
(Qi et al., 2006)	Design of nonlinear adaptive PID controller. The aim is to construct and optimize NLPID controller by adopting genetic algorithm (GA).	Name not mentioned, but it is a nonlinear system.	Nonlinear adaptive PID controller.	Genetic algorithm to calculate the optimal value of the NLPID controller.	No	No	Simulation only applied.	Ziegler-Nichols tuning method for PID and GA-PID. Nonlinear system.	Using GA makes the nonlinear function easy to be optimized.	Steps and methodology used to archive the results are not perfect shown.
(Wahab, et al., 2007)	Multivariable PID Control design for Wastewater Systems.	ASM1 model.	Linear PID and Multivariable PID Control	Davison, Penttinen-Koivo method. Maciejowski method	No	No	Simulation	4 Different. Controllers tested in 1 Plant.	Results show that the Davison, Penttinen-Koivo method gives the best performance.	To use tuning method without any calculations can be time consuming.
(Holenda, et al., 2008)	MPC is investigated on two examples using systematic evaluation criteria	State-space models of the aeration process based on DO model.	Model Predictive Controller (MPC).	Linear state-space controller design.	No	No	Simulation environment only.	MPC controller effectively used to control DO in 1 WWTP.	Results show that model predictive control can be effectively applied in the control of DO concentration of WWTP.	Need to avoid imposing constraints on the manipulated variable.
(Kandare, 2008)	Nonlinear processes. Control of oxygen and energy optimization in the reactors of biological phase. Quadratic APC	Biological reactor	PID and Adaptive Prediction	Adaptive Predictive algorithm.	No	No	Lab simulation	2 Controllers for 1 Plant.	Using pressure set point optimization module help to reduce the energy consumption (up to 27%).	The final results were not close enough to the set-point and oscillations are not eliminated.
(Han et al., 2008)	Design of a nonlinear PI control for dissolved oxygen tracking at WWTP	DO concentration.	Fuzzy PI controller.	A softy switched nonlinear Takagi-Sugeno fuzzy PI control. Predictive control algorithm.	No	No	Software plant simulation.	PI controllers and DO plant.	The methods show a good tracking performance in the simulation results.	The control system results are validated by simulation only.
(Li and Zeng., 2008)	Design method for solving nonlinear equation systems.	Plant name is not specified, but it is a system of nonlinear equations.	Adaptive controller.	Neural network algorithm, adaptive algorithm. Broyden's methods.	No	No	Simulation	The results show that the approach proposed (adaptive) has much higher accuracy than the neural network method and Broyden's method.	Adaptive algorithm show that is able to compute exactly nonlinear equation systems.	Broyden's method requires a good initial guesses. Adaptive can produce desirable results from

										any initial approximation.
(Prakash and Srinivasan, 2009)	Design of nonlinear PID controller and nonlinear model predictive controller for a continuous stirred tank reactor (CSTR)	Continuous Stirred Tank Reactor. Takagi-Sugeno fuzzy model.	Nonlinear PID (NLPID) design using local linear Nonlinear model predictive controller using local linear models (F-NMPC) and nonlinear model predictive controller using first principle (analytical) model (A-NMPC).	Nonlinear Model Predictive Controller using local linear model.	No	No	Lab Simulation	3 controllers (NLPID, F-NMPC & A-NMPC) and 1 process (CSTR). Through general simulation study, it can be concluded that the proposed F-NMPC helps to reduce the number of computations needed, compared to the analytical model based NMPC.	The methods has displays a significant variation in the damping factor and undamped natural frequency.	The A-NMPC has shows a large computation time than others.
(Zhenhong <i>et al.</i> , 2009)	Modeling DO effects on Biological Nutrient Removal in a Sequencing Batch Reactor.	Activated Sludge Model 2d			No	No	Simulation is carried out in C++ Build language.		The simulated results showed that low DO concentration <1mg/L could seriously influence the activation and growth of microbes, especially nitrifying organisms.	In addition, the removal of COD and phosphorus would be also affected.
(Shuhua and Wei, 2009)	To design a feed-forward NLPID control for a Smart Car	Model of the Motor system.	LPID, NLPID and Nonlinear feed-forward PID controllers.	NLPID algorithm for optimization. Feed-forward control system algorithm.	No	No	Only simulation through MATLAB/Simulink	NLPID and Feed-forward PID where applied to control a Motor system.	Nonlinear feed-forward control has enhanced the dynamic performance and stability of the system.	No real-time control implementation shown.
(Kang, <i>et al.</i> , 2009)	Control of the PH in an Anaerobic Wastewater Treatment system, using Fuzzy PID control.	pH control of the anaerobic WWTP.	Traditional PID, Fuzzy control and Fuzzy PID.	PID control algorithm and Fuzzy PID algorithm.	No	No	Matlab simulations.	3 controllers (PID, Fuzzy control and Fuzzy PID) and 1 Plant. Comparison with the methods of traditional PID, fuzzy control and fuzzy PID, the results show that fuzzy PID has the optimal performance such as responsibility, stability and antisturbance.	Results show that Fuzzy PID control has the optimal performance such as responsibility, stability & anti-disturbance.	Results show much bigger delay time in a process response.
(Ye <i>et al.</i> , 2010)	Design of nonlinear controllers for nonlinear DO wastewater	Dissolved Oxygen	PI, Generic Model Control (GMC) based on Radial Basis Function (RBF)	GMC algorithm based Onimmune Optimization - LS-SVM.	No	No	Simulation software not specified, but appears as Matlab.	2 controller (PI and GMC) methods tested on 1 plant. GMC based on LS-SVM has higher	This method has higher control accuracy in comparison with the PI controller performance.	No indication of software used.

	treatment process based on immune optimization.		GMC based on Least Squares-Support Vector Machine (LS-SVM).					control accuracy compared with PI control and GMC based on RBF.		
(Zaidner et al., 2010)	Design of nonlinear PID control for Stability and control of noisy model.	Stability and control of noisy model. Model type not stated.	LPID and NLPID	Trial and error parameter optimization of NLPID. Nonlinear PID that suggests an optional tuning rules and Gain-scheduling.	Yes	No	Matlab/Simulink simulation.	Linear and nonlinear PID controller used to control 1 Plant. Results show that NLPID work much well than the LPID.	NLPID have unlimited robustness to uncertainties and delay.	Trial error method is time consuming
(Ren et al., 2010)	New nonlinear PID controller and its Parameter design.	An inverted pendulum system.	LPID and NLPID	Lyapunov stability theorem. Popov criterion. Absolute stability theorem. Pole placement control scheme.	No	No	Simulated but, software not mentioned.	2 types of controllers (LPID and NLPID) tested on 1 plant.	The use of nonlinear function (NLPID) is very important when controlling any nonlinear system.	Finding of the optimal set of gains based on many empirical tests is time consuming.
(Ostace et al.,2010)	Challenging of WWTP from the modeling and control point of view.	Benchmark Simulation Model No.1 (BSM1)	Conventional PI and PID controllers. Model Predictive Control (MPC).	Artificial Neural Networks algorithms. MPC controllers	No	No	Lab/ Real-time simulation	2 Controller (MPC and Neural Networks) are tested on 1 Plant.	Controllers proved that they are ready to undertake the challenge of controlling this complex process. MPC have shown the performance above others.	Problematic nonlinear to control which need good control strategies.
(Rayma t et al., 2011)	Is to investigate various strategies implemented to wastewater treatment plants.	Dissolved Oxygen.	Model predictive control. LPID controller.	Artificial neural networks for modeling & prediction purposes.	No	No	No implementation shown but, discussions on different control strategies like PID, MPC for BSM1.	Different control strategies (Model predictive & LPID controller) for BSM1.	Paper addressed control objectives on effluent quality standard and reduction of plant cost operation.	Is the complex nonlinear system wich has difficults in controlling it.
(Xu et al., 2012)	PID Controller Design Based on Neural Network.	MP neuron model. Nonlinear interactions function of neurons.	BP Neural Network PID control and Classic PID control.	BP Neural Network algorithm. Levenber-Marquardt algorithm	No	No	Simulation	2 Controlles (BP NN PID and classic PID). In comparison BP neural network PID is more adaptive, robustness, high control accuracy, a significant improvement in quality control than ordinary PID control quality.	Then neural networks have great capability in solving complex mathematical problems. The advantage of LM is that when the network weight number is insufficient, the convergence rate is very high.	Name of the software use not stated.

[Selvabalan, et al., 2012]	Prediction based controller is required to reproduce accurate hydrograph using PID and Fuzzy controller. Application of knowledge based engineering techniques in water resources development	River discharge and Water processing system.	Linear PID and Fuzzy logic control.	Fuzzy logic controlled analysis method	No	Yes on LAB VIEW	Tried for a river discharge, on a real-time simulation system.	2 controllers and 1 plant.	Of the Fuzzy logic are the reduction of overshoot and stricter regulation of steam temperature. It has a very good result for nonlinear process.	Operation cost in the activated sludge process.
(Yang et al., 2013)	Fuzzy Modeling of Activated Sludge WWTP and Predictive Control of Dissolved Oxygen	ASM1	Fuzzy Model-Based Predictive Controller Design. Model predictive control, parameter identification using the method of least squares.	Structure identification algorithm. Fuzzy c-means cluster algorithm.	No	No	Simulation.	Fuzzy control is used to control the ASM1. Compared with the traditional PID control, the proposed fuzzy model based predictive control paradigm achieves satisfactory benefits in terms of both transient and steady performance.	The recommended controller is able to control uncertainties and time-delays.	Uncertainties and time-delays make the system to be more difficult.
(Luo & Si., 2013)	Stability of Direct Heuristic Dynamic Programming for Nonlinear Tracking Control Using PID Neural Network.	Nonlinear control problem is formulated under a general condition that system nonlinearity is unknown	Lyapunov stability construct, provide new results of uniform boundedness (UUB) for PIDNN-based direct Heuristic Dynamic Programming (HDP) controller.	Direct HDP design algorithm. PIDNN-based direct HDP control design approach to the general discrete-time nonlinear MIMO system tracking control problem	No	No	No simulation.	Direct HDP design algorithm is firstly derived by incorporating the PID control rule into neural networks (NNs).	Mathematics show new results of UUB for the proposed PIDNN-based direct HDP controller via the Lyapunov stability method.	No simulation results shown, results shown are mathematical proven.

(Macnab, 2014)	Design a Stable Neural-Adaptive Control of Activated Sludge Bioreactors.	Activated sludge bioreactor used for WWTP.	PI controller. Feedback linearizing controller. Adaptive neural network control	Adaptive design using Cerebellar Model Arithmetic Computer (CMAC) neural networks algorithm.	No	No	Simulation	3 controllers (Adaptive, Feedback linearizing & PI controller) used to control 1 plant model. The Adaptive method outperforms the other methods, and steady state errors are produced entirely by the observer error. This algorithm takes advantage of the nature of the CMAC local basis functions	The proposed method (Adaptive) self-evaluates the effect of weight updates upon the average error in a local domain, and stops updating the weights when updates are believed to have no beneficial, or insignificant, effect on the error	The LPI performance has degraded significantly away from the setpoint as the system dynamics contain major nonlinearities.
----------------	--	--	---	--	----	----	------------	--	--	--

2.6 Discussion on the findings from the literature review

The review considered the time period between 1942 and 2014 presenting different control algorithms designed for various nonlinear processes.

The literature review shows clearly that the control of the Dissolved Oxygen (DO) concentration is the most significant one for proper control of the activated sludge process, because its control has a potential to reduce the production cost while keeping the oxygen concentration within the standards. This is in support of the motivation of choosing DO concentration in the ASP as a case study for this thesis. A number of strategies for control of the DO concentration, select constant DO set points (usually 2mg/l) while others employ a varying DO set point. There are various approaches used to control nonlinear plants similar to DO in the ASP. These methods are shown in Table 2.2. Most of the controllers implemented perform well, but the disadvantage in some is their slow adaptation towards disturbances.

The majority of the control strategies found in the literature is based on simulation. Very few of those strategies are tested in real-time. This is an indication of how much ground still needs to be covered for real-time implementation of these strategies on full scale plants.

Some linear controller design methods are presented in the literature. Panagopoulos *et al.*, (2002), presented a linear PID controller based on optimization of load disturbance rejection with constraints on robustness to model uncertainties. The design also delivers parameters to deal with measurement noise and set point response. The drawbacks of using this type of controller are that it can only work successfully with linear processes. When it comes to be used in nonlinear processes, any tuning method is needed to be used to calm down the nonlinear system under control, which can lead to much time consuming.

The good thing about using nonlinear control when controlling nonlinear system is that, nonlinear controllers have nonlinear functions that are used to handle unstable conditions in the nonlinear systems.

As stated by Wright, (2001) and Copeland, (2008) large percent of the applied control technique among industrial processes is related to the PID controllers and is that reason that mostly motivated the choice of designing NLPID controllers for the industrial

nonlinear processes, because improvement of LPID technique may result to a big impact on all related industrial processes.

The Ziegler-Nichols (Z-N) method remains a popular technique for tuning controllers that use proportional, integral, and derivative (PID) movements. This method is used because, it is easy to experiment, mostly the need for modification is based on P and I actions on the controller, the D action is a small value in most cases. The Z-N method also includes dynamics of the whole process, which gives a more accurate picture of how the system is behaving. But with this method it is noted that the tuning experiment can be time consuming. Capabilities of the Z-N method to tune the NLPID controllers are investigated in the thesis.

Pole placement method is a special method chosen to be used in this thesis. Pole placement problems are especially important for disturbance rejection and stabilization of dynamical systems. Pole placement method is one of the classic control theories and has an advantage in system control to achieve given desired performance. As may be stated before, the pole placement theories state that Pole placement is to set the desired pole location and to move the pole location of the system to the desired pole location - to get the desired system response. This pole placement control method results in the desired system response and it is easy to fine the controller gains mathematically, but the accuracy of the system transfer function is significantly important and is expensive to implement the method for high order systems.

2.7 New International Electro-technical Commission (IEC) 61499 standard and PLC controller implementation

According to literature evaluation, the *International Electro-technical Commission* IEC 61131-3 standard and the Programmable Logic Controllers (PLC's) are still the mainstream re-programmable electronic devices based on the corresponding programming standard in industrial automation systems. For PLC applications the conventional system verification process is relatively intuitive.

To defeat the shortcomings of *PLC*, the *International Electro-technical Commission* (IEC), developed the new international standard *IEC 61499* (Pang, *et al.*, 2011), which takes over the function block concept from *IEC 61131-3* and founds an open, modularized, and implementation-independent software development structure to fulfill the current industrial needs.

This new IEC standard has been developed as an addition to IEC 61131-3. Its main focus is based on the method for modeling distributed industrial process, measurement, and control systems to obtain vendor independent system architecture (Lastra *et al.*, 2005) and (Dai and Vyatkin, 2012). As IEC 61131-3, the standard IEC 61499 defines concepts and models to summarize the control software in Function Blocks (FB) environment that can be assembled and be newly distributed to several devices. The major difference between IEC 61131- 3 and IEC 61499 is the performance model. IEC 61131-3 has an understood sequential execution model with a cyclic activation of execution tasks. This has drawbacks for distributed applications where the cyclic execution model makes it hard to harmonize distributed applications and gives little control over the execution order of the function blocks in a control application. IEC 61499 was introduced to overcome these limitations by a special events control (Basile *et al.* 2010). The events control the activation of the application parts in a control application. Furthermore, events are intended to actively control the execution sequence of the control application components (Hametner and Georg, 2011).

The challenges and requirements for automation systems have risen extremely during the last years. As based on the operation of the activated sludge, these days the corresponding models are getting larger and more complex, due to the fact that in the course of time more components like engines and control components were considered to get new and better features. Additionally, the new components are necessary to implement new concepts for control methods, which are faster and more efficient than the older ones. The complex plants like WWTP have also effected the software development. (Byrak *et al.*, 2012) state that the development of software such as controller models and operational software for the plants is also getting more complex and more difficult.

The application of the IEC 61850 standard for implementation of these complex control strategies is very promising. Implementation of the designed in the thesis closed loop control system is based on the IEC 61499 standard-based Beckhoff PLC CX5020.

2.8 Conclusion

This chapter reviews the activated sludge wastewater treatment plant and the dissolved oxygen concentration process as a main part and the existing methods for design of controllers for the wastewater and other industrial processes. It concludes that proper and appropriate design of the controller is still the emerging issues in the wastewater plant and hence this thesis focuses on improving the nonlinear controller's designs for efficient operation of the DO concentration process.

The next chapter (Chapter 3) is focusing on developing the mathematical model and the Simulation of the DO process.

CHAPTER THREE

DISSOLVED OXYGEN CONCENTRATION MODELING AND SIMULATION

3.1 Introduction

Wastewater is the water disposal from our homes, offices and industrial activities or any other activity that leads to degradation to its original state. It is water that is not appropriate for human or animal consumption. Wastewater Treatment Plant (WWTP) is a plant that speeds up the natural process whereby water purifies itself. In this thesis only the Activated Sludge Process (ASP) for wastewater treatment is considered. Activated sludge process is the most common type of modern wastewater treatment (Han et al., 2008). In a wastewater treatment plants the wastewater is generally processed in several steps before it is released to the recipient. Lindberg, (1997) gives a survey of the common practices. The wastewater treatment is made to reduce the quantities of nitrogen, phosphorus, organic matter and solid matters in the suspension (Vanrolleghem, 2003). This process is a very important component of the environmental quality. The strict environmental and health regulations together with a demand for cost effective ways of wastewater treatment have made control technology in Wastewater Treatment Plants (WWTP) an important priority. In Chapter 2 (literature review) several models are described, these models try to capture as close as possible the development and advancement of the wastewater treatment processes based on utilization of the activated sludge.

Number of models to define the biological process taking place in the activated sludge process exists, but the International Water Association (IWA) models such as Activated Sludge Model No.1 (ASM1), ASM2, ASM2d and ASM3 are the internationally recognized models. Copp, (2000) states that the plan to create a standardized '*simulation benchmark*' was first planned and advanced by the first International Association of Water Quality (IAWQ) Task Group on Respirometry-Based control of the activate sludge process. This earliest benchmark was then adapted by the European Cooperation in the field of Science and Technology, better known as COST action 624 and 682 in collaboration with the second IWA Respirometry research group (Copp, 2000; Sanchez *et al*, 2003; Wahab *et al*, 2012). In an attempt to standardize the simulation practice and the valuation of the categories of control strategies, these groups have together developed a reliable simulation procedure.

The COST *Simulation Benchmark: Description and Simulator Manual* is a complete report of a standardized simulation and valuation process as well as plant layout, models and parameters, a complete description of disturbances to be applied throughout analysis and valuation conditions for testing the comparative efficiency of simulated strategies (Copp, 2000). The COST simulation benchmark is intended to provide a balanced foundation for comparing past, present and future control strategies without reference to a specific facility. All of these models help as a guide for research, and valuable tools for better understanding of the natural processes and interactions. Many researches considered ASM1 as a reference model, and practical application and have been used for developing the simulator platform in this thesis.

The following are the points that are covered under this chapter:

- Description of Benchmark Layout Structure, part 3.2
- Dissolved Oxygen (DO) Process Model, part 3.3
- Models of the oxygen transfer coefficient, part 3.4
- Dissolved Oxygen model simulation results, part 3.5
- Matlab software, part 3.6

3.2 Description of the Benchmark Process based on the ASM1 biological model

The Benchmark Simulation Model (BSM1) has five biological reactors linked together in series, from which the first two are anoxic and the final three are aerated reactors, Figure 3.1. These reactors are modeled according to the Activated Sludge Model (ASM) proposed by (Ostace *et. al*, 2010). The ASM has thirteen state variables and eight forceful processes and is presented by a set of normal differential equations that define the dynamic variations of the state variables. Each anoxic reactor has a volume of 1000 m³ and each aerated reactor has a volume of 1333 m³, therefore the total biological volume is of 5999 m³. The secondary settler has a depth of 4 m and the area of 1500 m², and is placed at the end of the five reactors (Copp, 2000; Ostace *et. al*, 2010).

Benchmark model is well-defined as a protocol to find a measure of performance of control strategies for activated sludge plant based on numerical or realistic simulations of the controlled plant. The following diagram (Figure 3.1) shows a representation of the simulation benchmark configuration with tanks 1 and 2 mixed and unaerated, and tanks 3, 4 and 5 aerated.

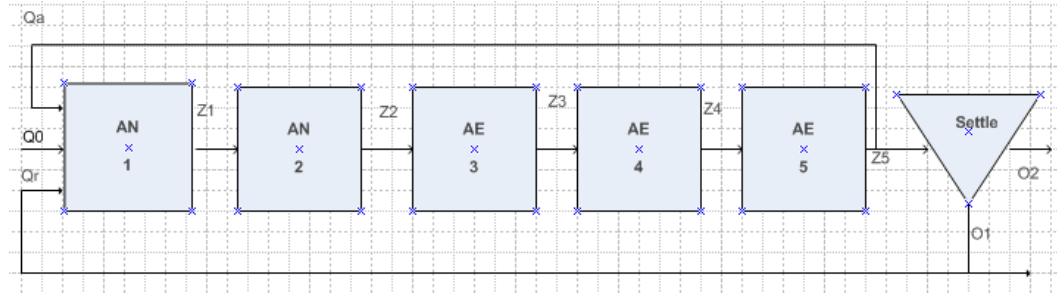


Figure 3.1: Benchmark activated sludge process (Henze et al., 2002)

3.3 Dissolved Oxygen Mathematical Model

The most significant factor in the activated sludge systems is the control of the dissolved oxygen concentration as stated by (Lindberg and Carlsson, 1996). If the associated aeration is done in an optimal way it will lead to substantial reduction in the process energy consumption. The process of aeration AE occurs in the aerobic reactors, but practically, the DO concentration s_o in the activated sludge process is sustained by managing the aeration airflow Q_{air} through the control input $u(t)$. The mathematical model of the biological wastewater treatment processes is used to simulate the dynamic characteristics of various organic nutrients and micro-organisms in the treatment process. The whole process mainly includes biochemical reaction tank modeling. The following equation describes the Dissolved Oxygen (DO) mathematical model: Lindberg, (1997).

$$\frac{ds_{o,n}}{dt} = \frac{1}{V_n} [Q_n (s_{o,n-1} - s_{o,n})] + r_{s_{o,n}} + K_{La,n} (s_{o,sat} - s_{o,n}) \quad (3.1)$$

Where:

- $s_{o,n}$ - the Dissolved Oxygen concentration in the nth tank (in mg/l)
- K_{La} - the Oxygen Transfer Function
- $s_{o,sat}$ - the DO concentration at saturation point in (mg/l)
- $r_{s_{o,n}}$ - the Oxygen Uptake Rate in (d^{-1})
- V - Tank volume in (m^3)
- Q - the wastewater flow rate in m^3/d
- n - Number of the tanks in the process

Equation (3.1) shows the DO concentration dynamics in the tanks with $n = 3,4,5$. Since the benchmark structure tanks are identical, it can remain accepted that the following are equal:

$$s_{o,n} = s_o, Q_n = Q, V_n = V, s_{o,n-1} = s_{o,in}$$

These notations are used further in the thesis

3.3.1 Oxygen Transfer Function and Uptake rate

There are several models of the Oxygen Transfer Functions (OTF). In the dissolved oxygen concentration dynamics, the OTF K_{La} describes the dissolving of oxygen on the basis of the flow rate of air into the water (Vanrolleghem, 2003). It describes the rate at which oxygen is being transferred to the wastewater by the system for the aeration, as a function of airflow rate. The oxygen transfer function can be related to the changes in the intensity of aeration, which is considered as a control input $u(t)$. The transfer function K_{La} as a function of its parameters varies slowly in a matter of hours or even days as proposed by (Lindberg, 1997). The transfer function depends on the aerator type, water depth, basin shape and the airflow rate. The oxygen respiration rate is determined in both, the primary respiration of the microorganisms in the activated sludge, used in mixture and in the endogenous respiration, during their decay. The respiration rate changes significantly in a number of hours; while K_{La} while differing slightly from day to day (Nketoane, 2009). The following Table 3.1 is the summary of the different models of K_{La} proposed in the existing literature of oxygen transfer function models and is given below in Table 3.1. (Lindberg, 1997)

Table 3.1: Different models for oxygen transfer function

Model	Equation
Step	$K_{La} = (0, k_1)$
Square root	$K_{La} = k_1 \cdot \sqrt{u}$
Linear A	$K_{La} = k_1 \cdot u$
Linear B	$K_{La} = k_1 \cdot u + k_2$
Exponential	$K_{La} = k_1 \cdot (1 - e^{-k_2 u})$
Power	$K_{La} = k_1 \cdot u^{k_2}$

Arctan	$K_{La} = k_1 \cdot \tan^{-1}(k_2 \cdot u)$
Cubic spline	$K_{La} = f(u)$
Second order model	$K_{La} = k_2 u^2 + k_1 u$
Polynomial	$K_{La} = k_1 \cdot u + k_2 \cdot \sqrt{u + k_3}$
Piecewise linear	$K_{La} = (k_1 + k_2 \cdot t) \cdot u$

3.3.2 An exponential model of K_{La}

An exponential K_{La} model may be a suitable choice of the oxygen transfer function because it can give a similar shape of the K_{La} function as in Figure 3.2, which is natural in a physical sense as proposed by (Lindberg, 1997). The oxygen transfer function K_{La} is assumed to depend nonlinearly on the airflow rate. It can also be noted from Figure 3.2 that the slope of K_{La} (gain) changes when the airflow rate changes.

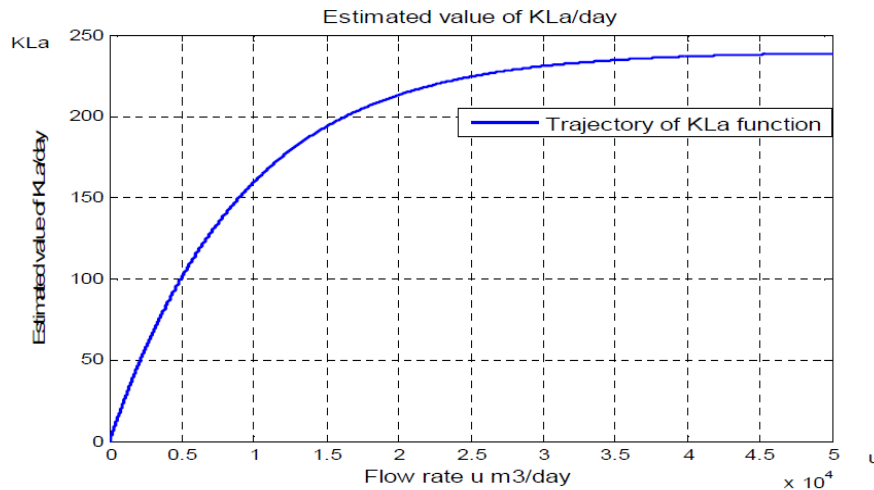


Figure 3.2: Typical shape of the oxygen transfer function ($K_{La}(u)$) as a function of the airflow rate (u).

Equation (3.2) gives mathematical presentation of the oxygen transfer function, represented as a mathematical expression of the air-flow rate; this expression also includes the process control input.

$$K_{La}(t) = K_1 \left[1 - e^{-K_2 u(t)} \right] \quad (3.2)$$

Where:

- $u(t)$ - is the air flow rate,
- K_1 and K_2 - are model parameters associated with the tanks.

Oxygen utilization rate r_{so} is given by the following equation taken from the ASM1 biological model (Copp *et al.*, 1998), (Henze *et al.*, 2002), (Tzoneva, 2007)

$$r_{so}(t) = -\hat{\mu}_H \left(\frac{1-Y_H}{Y_H} \right) \left(\frac{s_{S,n}(t)}{K_S + s_{S,n}(t)} \right) \left(\frac{s_{O,n}(t)}{K_{OH} + s_{O,n}(t)} \right) x_{BH}(t) - \hat{\mu}_A \left(\frac{4.57-Y_A}{Y_A} \right) \left(\frac{s_{NH,n}(t)}{K_{NH} + s_{NH,n}(t)} \right) \left(\frac{s_{O,n}(t)}{K_{OA} + s_{O,n}(t)} \right) x_{BA}(t) \quad (3.3)$$

Where:

- μ_H - is the maximum heterotrophic growth rate,
- Y_H - is the heterotrophic yield,
- μ_A - is the maximum autotrophic growth rate,
- Y_A - is the autotrophic yield,
- $s_{S,n}(t)$ - is the readily biodegradable substrate,
- $s_{NH,n}(t)$ - is the $\text{NH}_4^+ + \text{NH}_3$ nitrogen,
- x_{BA} is the autotrophic biomass
- x_{BH} is the heterotrophic biomass.

K_{NH} , K_{OA} , K_{OH} , K_S are the half-saturation coefficients for heterotrophic growth rate, autotrophic growth, and autotrophic decay respectively. An approximation of respiration (oxygen uptake rate) is very much essential given the fact that respiration seems to be the most critical disturbance signal during the control of the DO concentration and therefore may perhaps be used in the development of control efficiency, (Gerksic *et. al.*, 2006); the whole process can be achieved through on-line approximation of respiration from the present values of the DO concentration and airflow signals. Substituting Equation (3.2) to Equation (3.1) the following equation is obtained:

$$\frac{ds_o}{dt} = \frac{1}{V} [Q(s_{o,in} - s_o)] + r_s + (K_1 [1 - e^{-K_2 u(t)}]) (s_{o,sat} - s_o) \quad (3.4)$$

The Equations (3.3) and (3.4) symbolize the process of the dissolved oxygen model to be controlled. The control of this process is the airflow rate, the controlled output is the concentration of the dissolved oxygen and uncontrolled disturbance is the oxygen

utilization rate. Tzoneva (2007) states that; the disturbance in the system depends upon the input flow characteristics and will make an alteration based on the requirements of the microorganisms for oxygen. It is also stated that; the result of these alterations makes it essential to recalculate the set point and the controller parameters of the closed loop system in order to meet the requirements of the system.

3.4 Dissolved Oxygen simulation model

3.4.1 Description

The equation of the process representing the dissolved oxygen concentration dynamics as illustrated in Equation (3.4) is used to develop an open loop block of the model in Matlab/Simulink software environment. The objective of simulating the DO concentration model is to obtain:

- The solution of the model differential equation for the given step input of the air flow rate and steady state values of the process variables describing the oxygen uptake rate.
- The influence of the internal $s_{o,in}$ and external r_{so} disturbances over the dynamics of the DO concentration.

The investigations and simulations are all done in the software environment of Matlab/Simulink.

3.4.2 Matrix Laboratory and Simulink

Matrix Laboratory (MATLAB) and Simulink are the very powerful technical language and interactive environments for numerical computation, visualization, and programming. The simulation is performed in MATLAB, where all the data's are analyzed, and algorithms are developed. Simulink is used for the creation of models and its applications. The Simulink environment software is made-up of the block diagram for multi-domain simulation and model-based diagrams. The Simulink environment supports automatic code generation, continuous test and verification of the quality for an architectural specification or any embedded systems, (www.mathworks.com). It provides an adapted building block libraries, graphical editor and solvers for model configurations.

Simulink is incorporated with MATLAB, enable the uses to include MATLAB algorithms into models and export simulation results to MATLAB for additional analysis when it's required.

3.4.3 Simulation Input data and Biological Process Model Parameters

The file named “DO_last.m” is introduced in MATLAB workspace; this program file has all the parameters for the simulation of the Dissolved Oxygen Concentration. The program for the input data is given in the Appendix 1 of this thesis. The corresponding block diagram Simulink model file called “DO.mdl” is given in Figure 3.3.

The Equations (3.3) and (3.4) are used for simulation of the DO concentration. The input variables are the disturbances $s_{o,in}$, and r_{so} , the control signal $u(t)$, and the model parameters are μ_H , μ_A , Y_H , Y_A , $s_{S,n}$, $s_{NH,n}$, $K_S, K_{OH}, K_{NH}, K_{OA}$. The output variable is the dissolved oxygen concentration s_o . The parameter values are taken from the ASM1 biological model and some are stated in Table 3.2 (Copp, 1998). The values of K_1 and K_2 are calculated from the value $K_{La} = 240 \text{ day}^{-1}$ by a curve fitting for a given value of the airflow rate, $u = 50000 \text{ m}^3/\text{day}$, as proposed by Holenda *et al.*, (2008).

The values of the parameters for constructing the model of the DO concentration process in Simulink are taken from the benchmark structure at steady state as illustrated in Tables 3.2 below. These parameter values are taken to the Matlab workspace. From there they are used by the Matlab/Simulink DO block diagram.

Table 3.2: Process parameters of benchmark structure

Symbol	Values	Symbol	Values
$s_{o,sat}$	8	s_o	0.491 - 0.05
K_1	240	K_2	$1.961e^{-04}$
K_{OA}	0.3 or 0.4	$s_{o,in}$	0.01
V	1333	t	0:1:8
Q_a	55338	x_{BHS}	2559.4
s_{NHS}	1.733	$s_{S,SS}$	0.889
Q_r	18446	Q_o	18446
μ_{uH}	6.0	μ_{uA}	0.9
y_H	0.67	y_A	0.24
K_{oH}	0.20	K_{NH}	0.2 or 1.0

K_S	10	x_{BAS}	149.8
-------	----	-----------	-------

The Simulink diagram of the dissolved oxygen concentration model is shown below in Figure 3.3. This model can be used for simulation of the behavior of the dissolved oxygen concentration for different steady state values of variables given in Tables 3.2 and parameters in Matlab workspace (with a file: DO_last.m which contains all parameters used for the open-loop DO simulation). The amplitude of the step signal sent to the model is $u = 50000 \text{ m}^3/\text{day}$. The initial condition for the simulation is 0.05 mg/l .

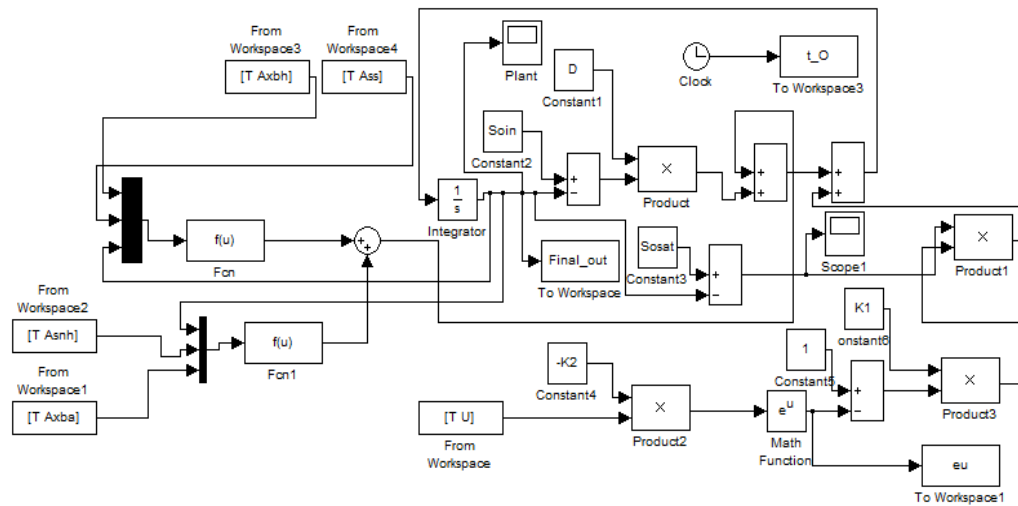


Figure 3.3: Dissolved Oxygen Simulink model diagram

3.4.4 Dissolved Oxygen Simulation Results

The dynamic behavior of the DO concentration for steady state values of the variables obtained from the Benchmark process with ASM1 biological model is shown in Figure 3.4. The dynamic behavior of the DO concentration for different cases of disturbances $s_{o,in}$ and r_{so} can also be determined, by using different values of both x_{BA} (autotrophic biomass) and x_{BH} (heterotrophic biomass). These values are varied as follows: first take the reference values of: $x_{BA} = 149.8$ and $x_{BH} = 2559.4$, then from the reference value add $\pm 5\%$, $\pm 10\%$ and $\pm 50\%$, in order to receive new values of the biomasses, which by Equation 3.3 are used to calculate different values of r_{so} . The aim of the investigation by simulation is to determine the sensitivity of the process dynamic behavior towards the process disturbances $s_{o,in}$ and r_{so} . The value of the oxygen uptake rate depends on the concentration of the microorganisms x_{BA} (autotrophic biomass) and x_{BH} (heterotrophic

biomass). When their concentration is growing the oxygen rate is also growing. In order to investigate the influence of the disturbance r_{so} over the DO process behavior various variations in the concentrations of the microorganisms are made and the corresponding value of the oxygen uptake rate are calculated, as shown in Table 3.3. The values of $s_{o,in}$ and r_{so} are used further in the next chapters to evaluate the influence of the disturbances to the closed loop DO process behavior under the nonlinear PID controllers.

Table 3.3: Changes of the disturbances in the process

$s_{o,in}$	x_{BA}		x_{BH}		r_{so}
0.01	x_{BA}	149.8	x_{BH}	2559.4	-294.8954
	x_{BA} +5%	157.29	x_{BH} +5%	2687.37	-309.6402
	x_{BA} -5%	142.31	x_{BH} -5%	2431.43	-280.1506
	x_{BA} +10%	164.78	x_{BH} +10%	2815.34	-324.3849
	x_{BA} -10%	134.82	x_{BH} -10%%	2303.46	-265.4059
	x_{BA} +50%	224.7	x_{BH} +50%	3839.1	-442.3431
	x_{BA} -50%	74.9	x_{BH} -50%	1279.7	-147.4477
0.8	x_{BA} +5%	157.29	x_{BH} +5%	2687.37	-309.6402
	x_{BA} -5%	142.31	x_{BH} -5%	2431.43	-280.1506
	x_{BA} +10%	164.78	x_{BH} +10%	2815.34	-324.3849
	x_{BA} -10%	134.82	x_{BH} -10%%	2303.46	-265.4059
	x_{BA} +50%	224.7	x_{BH} +50%	3839.1	-442.3431
	x_{BA} -50%	74.9	x_{BH} -50%	1279.7	-147.4477
2	x_{BA} +5%	157.29	x_{BH} +5%	2687.37	-309.6402
	x_{BA} -5%	142.31	x_{BH} -5%	2431.43	-280.1506
	x_{BA} +10%	164.78	x_{BH} +10%	2815.34	-324.3849
	x_{BA} -10%	134.82	x_{BH} -10%%	2303.46	-265.4059
	x_{BA} +50%	224.7	x_{BH} +50%	3839.1	-442.3431
	x_{BA} -50%	74.9	x_{BH} -50%	1279.7	-147.4477

The following diagrams present the DO open loop responses.

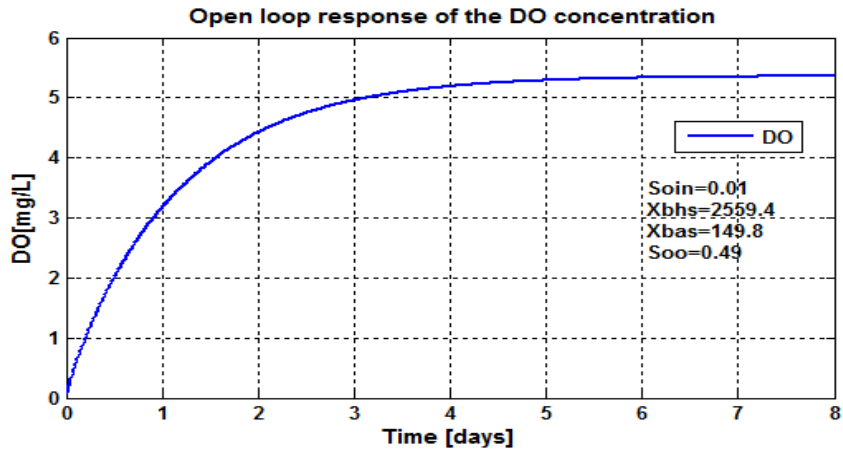


Figure 3.4a: DO concentration open loop response using $s_{o,in}=0.01\text{mg/L}$ and $r_{so}=-294.8954\text{mg/L/day}$

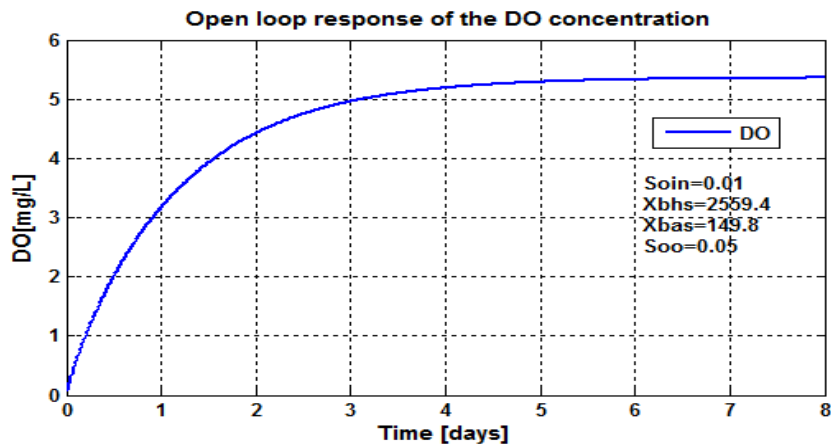


Figure 3.4b: DO concentration open loop response using $s_{o,in}=0.01\text{mg/L}$ and $r_{so}=-294.8954\text{mg/L/day}$

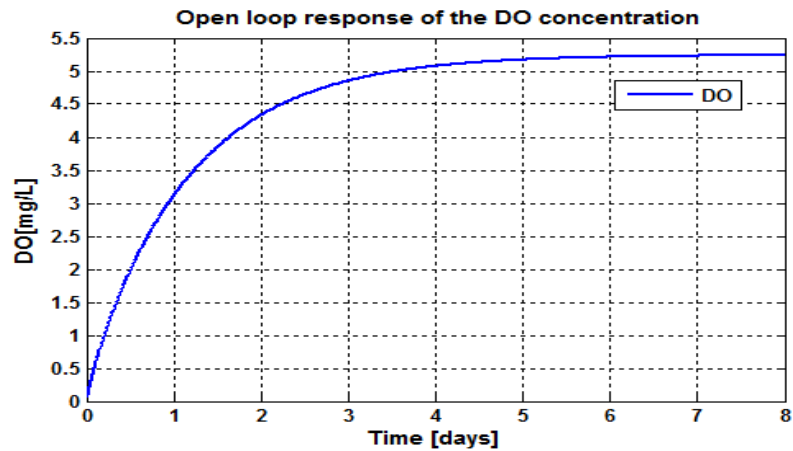


Figure 3.5: DO concentration open loop response using $s_{o,in}=0.01\text{mg/L}$ and $r_{so}=-309.6402\text{mg/L/day}$

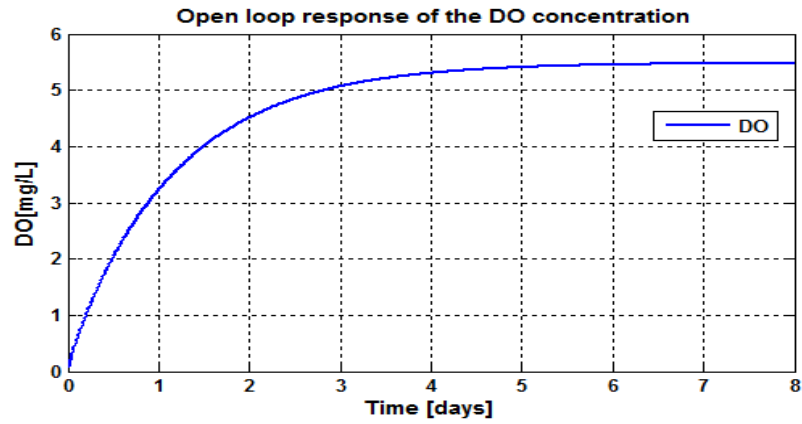


Figure 3.6: DO concentration open loop response using $s_{o,in} = 0.01 \text{ mg/L}$,
 $r_{so} = -280.1506 \text{ mg/L/day}$

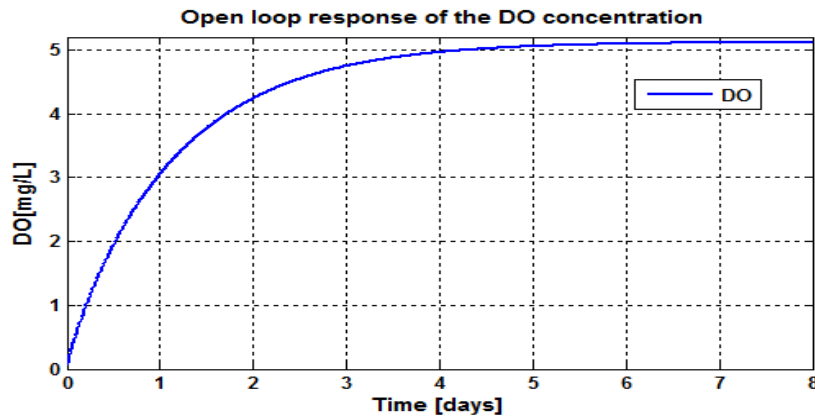


Figure 3.7: DO concentration open loop response using $s_{o,in} = 0.01 \text{ mg/L}$ and
 $r_{so} = -324.3849 \text{ mg/L/day}$

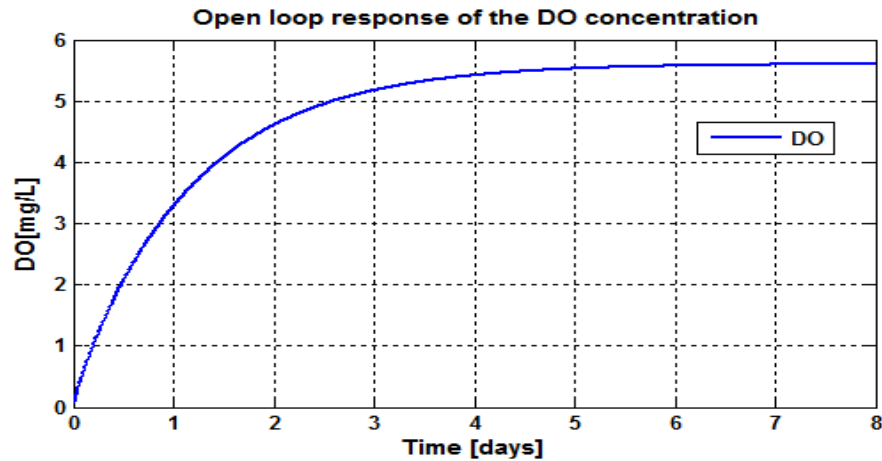


Figure 3.8: DO concentration open loop response using $s_{o,in} = 0.01 \text{ mg/L}$ and
 $r_{so} = -264.4059 \text{ mg/L/day}$

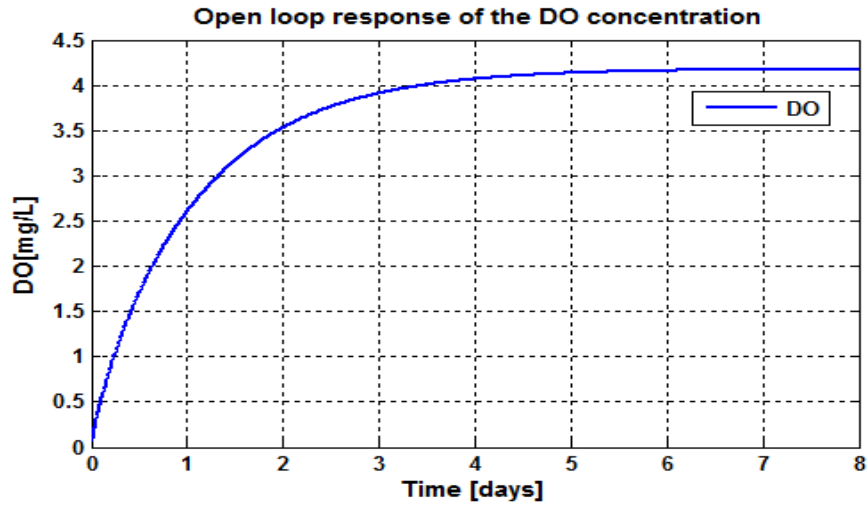


Figure 3.9: DO concentration open loop response using $s_{o,in}=0.01\text{ mg/L}$ and $r_{so}=-442.3431\text{ mg/L/day}$

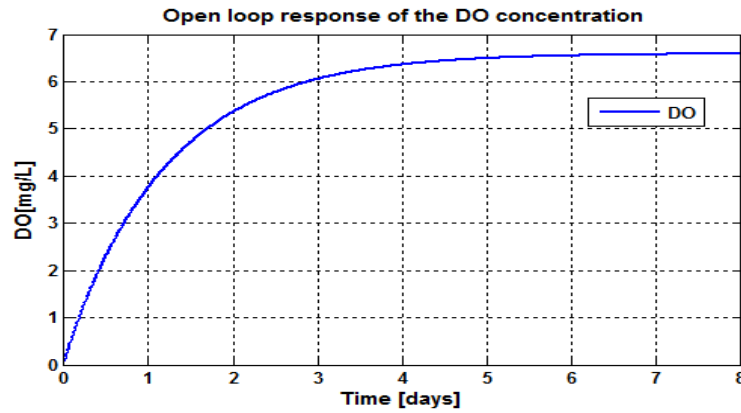


Figure 3.10: DO concentration open loop response using $s_{o,in}=0.01\text{ mg/L}$ and $r_{so}=-147.4477\text{ mg/L/day}$

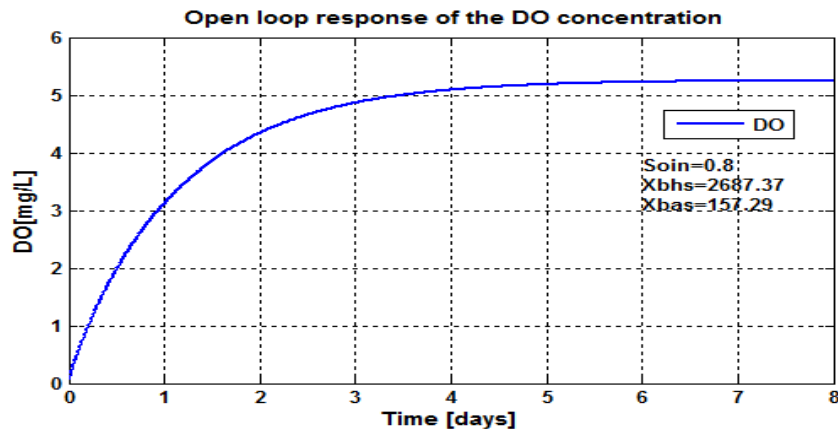


Figure 3.11: DO concentration open loop response using $s_{o,in}=0.8\text{ mg/L}$ and $r_{so}=-309.6402\text{ mg/L/day}$

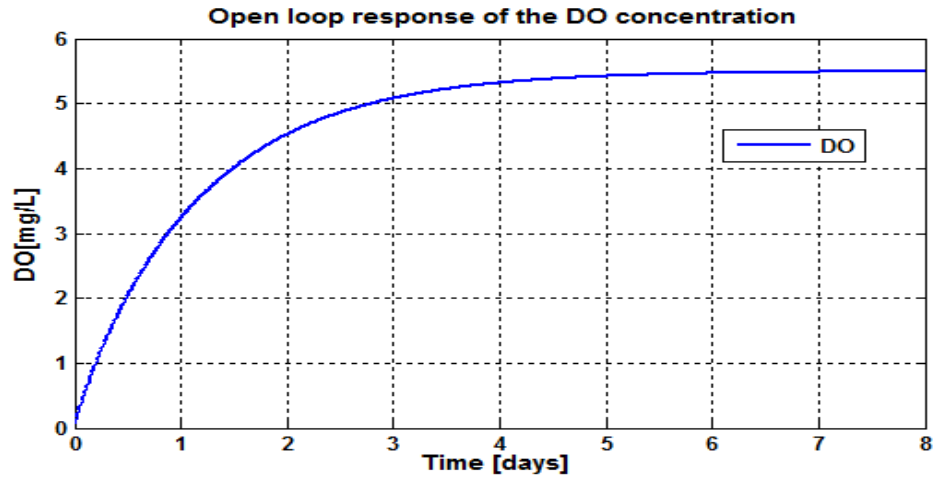


Figure 3.12: DO concentration open loop response using $s_{o,in}=0.8\text{mg/L}$ and $r_{so}=-280.1506\text{mg/L/day}$

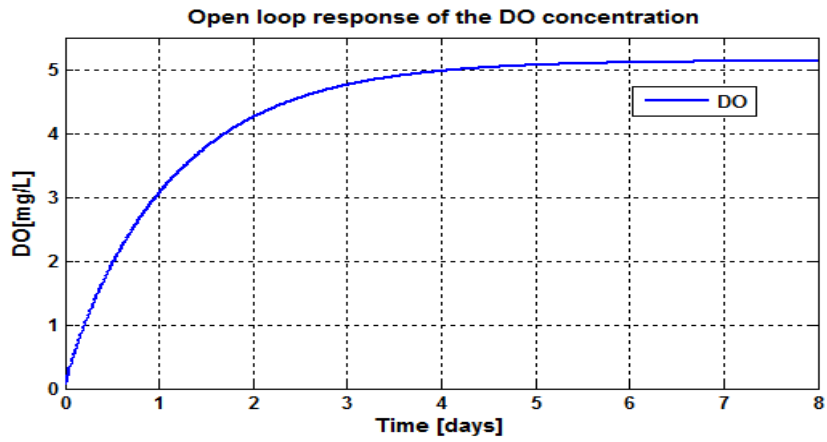


Figure 3.13: DO concentration open loop response using $s_{o,in}=0.8\text{mg/L}$ and $r_{so}=-324.3849\text{mg/L/day}$

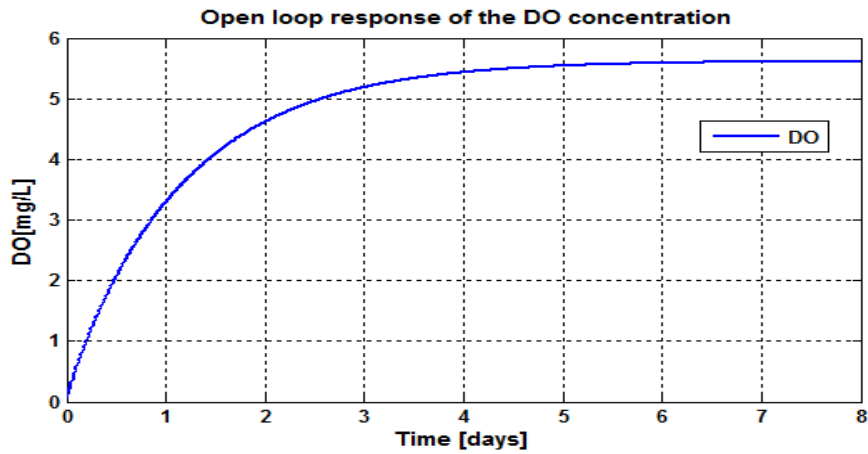


Figure 3.14: DO concentration open loop response using $s_{o,in}=0.8\text{mg/L}$ and $r_{so}=-264.4059\text{mg/L/day}$

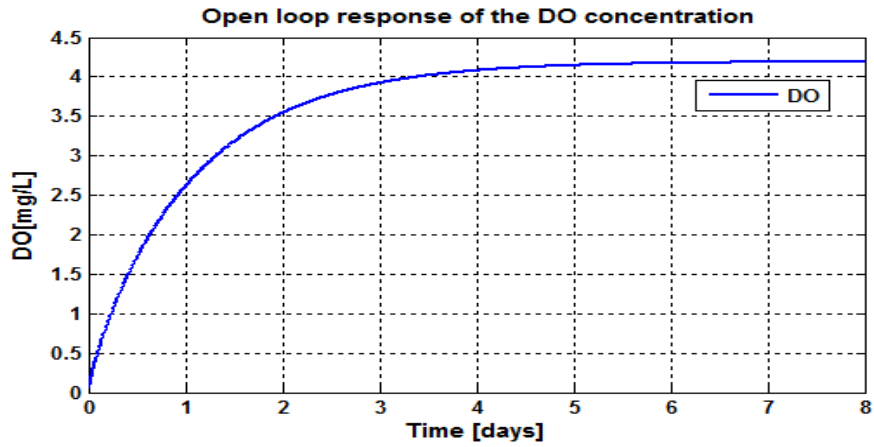


Figure 3.15: DO concentration open loop response using $s_{o,in} = 0.8 \text{ mg/L}$ and $r_{so} = -442.3431 \text{ mg/L/day}$

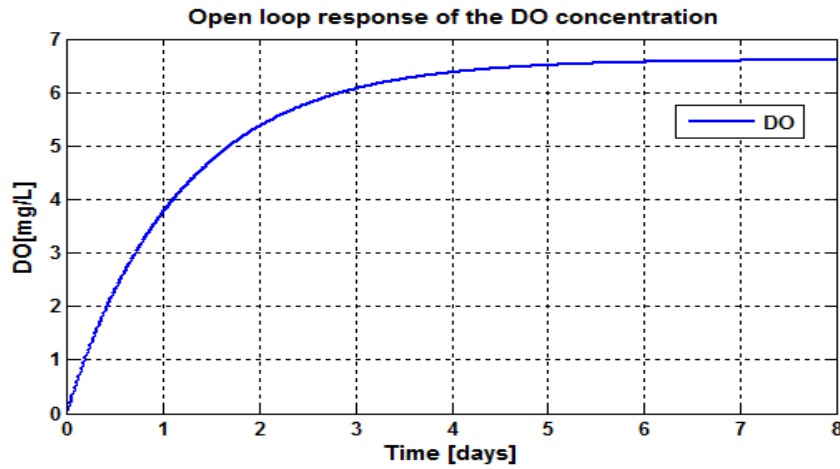


Figure 3.16: DO concentration open loop response using $s_{o,in} = 0.8 \text{ mg/L}$ and $r_{so} = -147.4477 \text{ mg/L/day}$

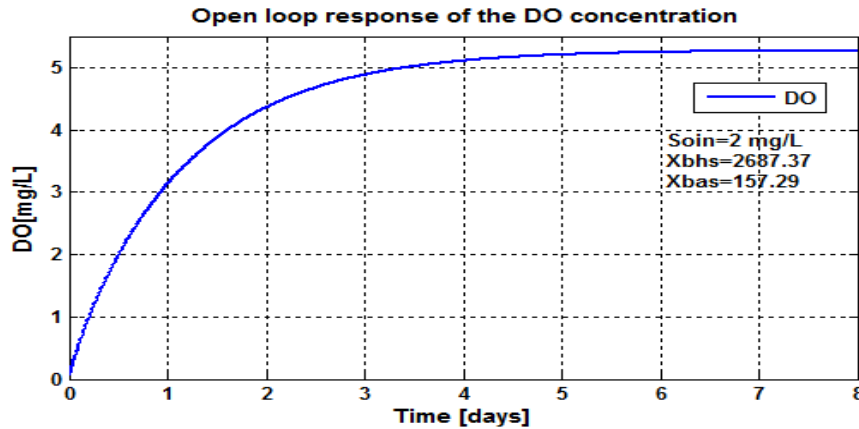


Figure 3.17: DO concentration open loop response using $s_{o,in} = 2 \text{ mg/L}$ and $r_{so} = -309.6402 \text{ mg/L/day}$

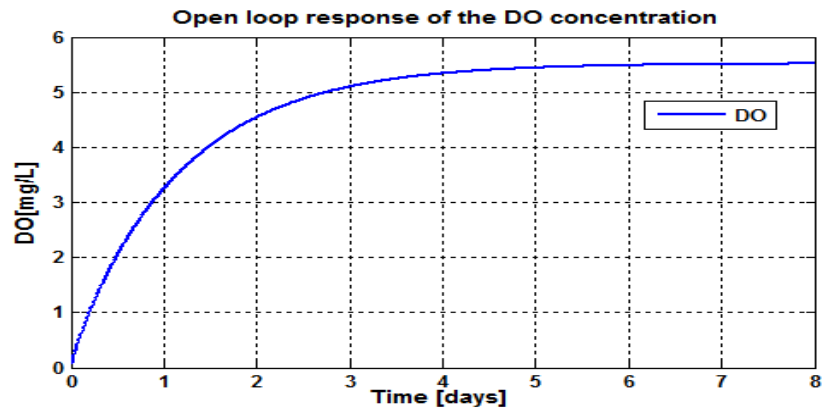


Figure 3.18: DO concentration open loop response using $s_{o,in} = 2\text{ mg/L}$ and $r_{so} = -280.1506\text{ mg/L/day}$

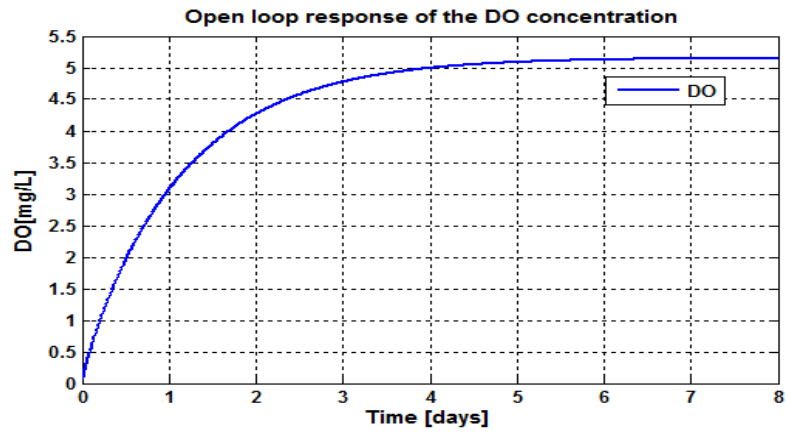


Figure 3.19: DO concentration open loop response using $s_{o,in} = 2\text{ mg/L}$ and $r_{so} = -324.3849\text{ mg/L/day}$

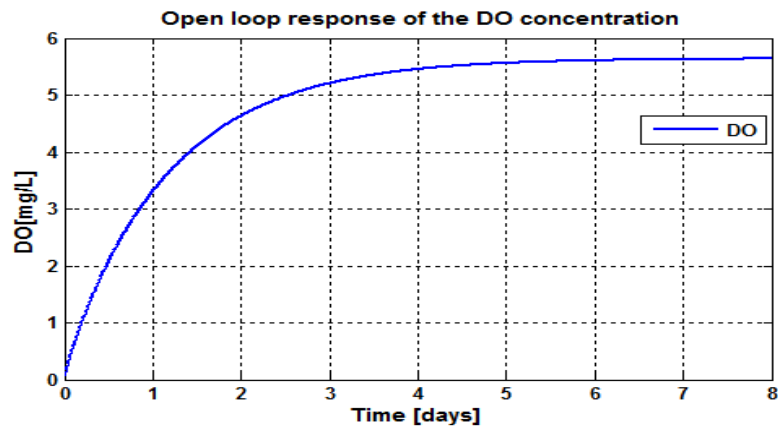


Figure 3.20: DO concentration open loop response using $s_{o,in} = 2\text{ mg/L}$ and $r_{so} = -264.4059\text{ mg/L/day}$

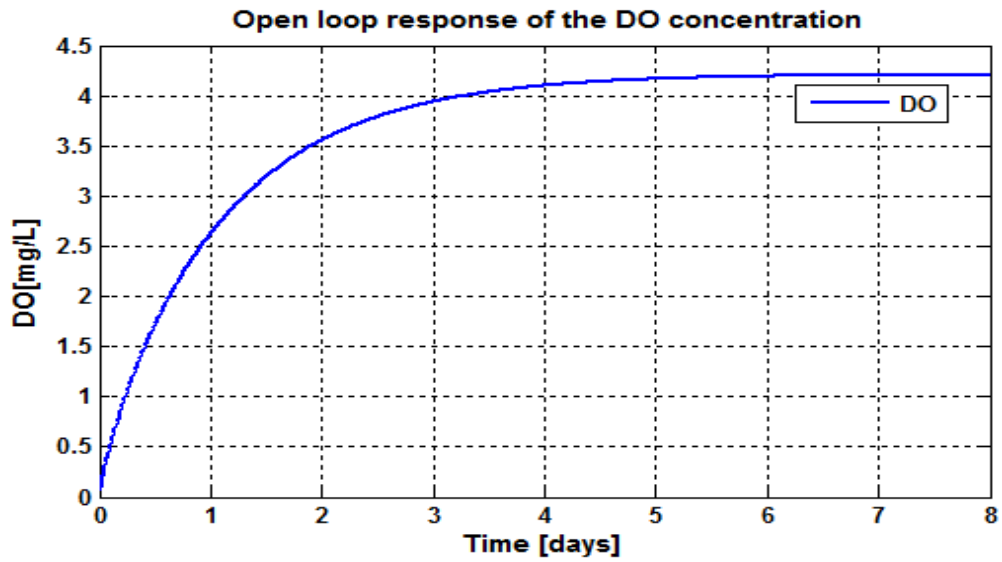


Figure 3.21: DO concentration open loop response using $s_{o,in} = 2 \text{ mg/L}$ and $r_{so} = -442.3431 \text{ mg/L/day}$

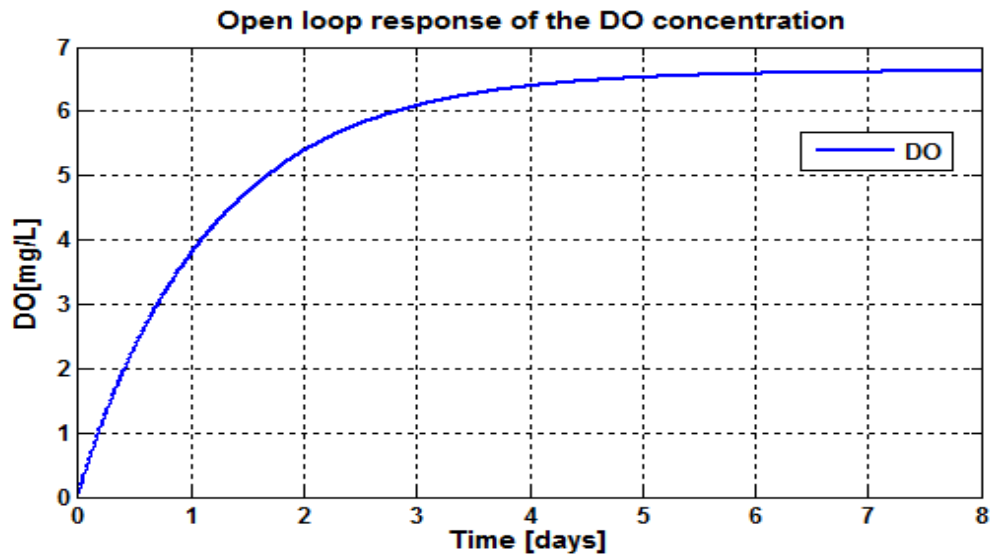


Figure 3.22: DO concentration open loop response using $s_{o,in} = 2 \text{ mg/L}$ and $r_{so} = -147.4477 \text{ mg/L/day}$

3.5 Analysis and Discussion of the results

The behavior of the DO process under the influences of the disturbance $s_{o,in}$ and r_{so} is evaluated and analyzed on the basis of their transition behavior characteristics: settling time, rise time, time delay and steady state value. The characteristics are calculated and shown in Table 3.4:

Table 3.4: DO open loop characteristics behavior

s_{oin}	r_{so}	Time delay[day]	Steady state value[mg/L]	Rise time[day]	Settling time[day]
0.01	-294.8954	0.01	5.4	1.4	4.6
0.01	-309.6402	0.01	5.2	1.4	5
0.01	-280.1506	0.01	5.5	1.4	4.6
0.01	-324.3849	0.01	5.2	1.5	5
0.01	-265.4059	0.01	5.6	1.3	4.5
0.01	-442.3431	0.01	4.2	1.4	4.2
0.01	-147.4477	0.01	6.6	1.4	5
0.8	-309.6402	0.01	5.3	1.4	4.5
0.8	-280.1506	0.01	5.5	1.4	4.2
0.8	-324.3849	0.01	5.2	1.4	5
0.8	-265.4059	0.01	5.6	1.2	5
0.8	-442.3431	0.01	4.2	1.5	4
0.8	-147.4477	0.01	6.6	1.4	5
2	-309.6402	0.01	5.25	1.4	4.5
2	-280.1506	0.01	5.7	1.5	4.5
2	-324.3849	0.01	5.2	1.5	4.6
2	-265.4059	0.01	5.8	1.4	4.8
2	-442.3431	0.01	4.25	1.2	5
2	-147.4477	0.01	6.7	1.3	5

The DO process behavior sensitivity towards the disturbances is done for everyone disturbance separately in such a way that one is kept constant and the other is changed. As Table 3.4 shows the behavior of the DO process under these experiments, when the value of r_{so} being bigger the response of the system in term of the steady state value decreases, but when is small the system has a large steady state value. Different value of r_{so} are calculated using different values of both x_{BA} (autotrophic biomass) and x_{BH} (heterotrophic biomass) values.

3.5.1 Conclusion of the discussion

Comparisons for different disturbances has been done and the results show that as active autotrophic biomass (x_{BA}) increases and active heterotrophic biomass (x_{BH}) decreases, the response of the DO is coming very close to the expected, desired value of 2mg/L and if $s_{o,in}$ increases the system behavior also increases (see Figure 3.4 - Figure 3.19). As the system response shows a behavior which is bigger than the accepted level of this process desired response which is 2mg/L the controller is needed to be designed in order to keep the system behavior close to the reference value and still to stabilize the whole system, even if the disturbances change.

3.6 Conclusion

The process of dissolved oxygen concentration and its model of the oxygen transfer coefficient have been described in this Chapter. Explanation of the benchmark structure process based on ASM1 biological model is also provided. Based on the simulation results of the open loop DO process model, it can be noted that controller design is required to control the system to a better steady state value. Controller design is done in the later Chapter 5, 6 and 7.

The next Chapter (Chapter 4) focuses on the overview of the control theory developments.

CHAPTER FOUR

APPLIED LINEAR AND NONLINEAR CONTROL THEORY

4.1 Introduction

In order to succeed in any process control as a designer it is important to first establish an understanding of the process to be controlled. As specified in Chapter 3, the thesis is not deeply involved in chemical or process engineering, but concerned about how to simplify the representation of the plant needed to be controlled and how to go about controlling it. Most systems have the same fundamental characteristics in common. If the identification of these features is done, designing an appropriate controller can be made easily to follow a well-proven and reliable path. The problem is to learn how to create a practical and a correct mathematical model for the complex plant and how to use the plant model under test to find the typical control actions that can be brilliant enough to control the process to the desired operating conditions.

The control theory considers two main groups of mathematical models of the process to be controlled: linear and nonlinear. On this basis the controllers to be designed for these models are also divided in two groups: linear and nonlinear controllers. The subject of nonlinear control involves the investigation, analysis and the design of the intended nonlinear control systems, which is, of control systems containing a minimum of one nonlinear component. The thesis concentrates on design of nonlinear PID controllers for control of the nonlinear DO concentration process. For the purpose of design short introduction of the control theory and the mathematical models of the linear and nonlinear PID controllers is described.

This Chapter introduces the control theory background. It provides the mathematical models for the linear and nonlinear proportional-integral-derivative controllers (LPID and NLPID), on the basis of their mathematical expressions. Comparative analysis of the characteristics of the closed loop systems under LPID and NLPID control is given. The control history is described in section 4.2, section 4.3 talks about the closed loop system, in section 4.4 the nonlinear control theory is described shortly; section 4.5 introduces the mathematical model of the differential tracker. Mathematical model of the nonlinear PID controller is discussed in section 4.6 and the section 4.7 is the conclusion of this chapter.

4.2 Control History

The *word control* has two primary implications. Essentially, it is seen as the movement of testing or watching that a physical or scientific appliance has a suitable conduct. Besides, to control is to act, to execute choices that ensure that an appliance acts as fancied. Most fundamental to any controller design is the capacity to gauge the yield of the framework and to make a restorative move if the framework's quality goes incorrect from the required value. There are many books and papers on the history of control engineering, (Bennett, 1979), (Burns, 2001), (Bushnell, 1996) that can also be used for more information on the control history.

In spite of the fact that control frameworks of different sorts go once again for long time past days, a more formal investigation of the field started with a motion examination of the diffusive senator, directed by the physicist James Clerk Maxwell paper in 1868 entitled "*On Governors*", (Burns, 2001). Maxwell thought was to linearize the differential mathematical statement of movement so as to discover the trademark comparison of the framework. He demonstrated that the framework is steady if the bases of the trademark mathematical statement have negative genuine parts, as stated by Bennett, (1979). This generated an outbreak of interest in the topic. At that point the issue of recognizing security criteria for direct frameworks was examined by Edward John Routh (1905) and Adolf Hurwitz (1875). Thereafter, Edward Routh (1831-1907) gave a numerical technique to deciding when a polynomial has negative roots, giving a paper on the security of a given condition of movement (Routh, 1877). Alexander Lyapunov (1857-1918) made the most rich and general hypothesis of solidness. He considered the strength of nonlinear differential equations utilizing a summed up thought of vitality (Lyapunov, 1893). He also introduced some concepts and techniques which are still in use. Further improvements as indicated by Burns, 2001 where that John R. Ragazzini (1912 -1988) introduced advanced control and the z- transform in the 1950s, and the fundamental scientific skeleton for hypothetical investigation was created by Laplace (1749-1827) and Fourier (1758 – 1830. Taking after the thought of Lyapunov, Yakov Tsytkin (1919- 1997) considered the stage plane for stable nonlinear control plan and for nonlinear strength examination, Vasile Mihai Popov (1961) provided the circle criterion.

According to Andrei, (2005); Johann Bernoulli (1667-1748) was the first who communicated the rule of optimality. In 1957 Richard Bellman formed the element programming rule to the ideal control of discrete-time frameworks (Bellman, 1957), and in 1958 Lev Pontryagin created the most extreme standard for tackling nonlinear ideal control issues (Pontryaginet *al.*, 1962).

4.2.1 Control Overview and Theory

Control is a division of engineering and mathematics, which deals with the performance of dynamical processes. As soon as one or more yield variables of the process want to track a positive reference in excess of the period, a controller operates the inputs of the plant to achieve the desired result on the output of the whole process. The outside information of a system is known as the reference. Usually the aim of the control principle is to determine the results for the appropriate corrective action from the controller that result in the whole framework (any system) stability, which means, the framework determination embrace the set point and not oscillate around it.

Inputs and yields of the control framework are by and large related through differential comparisons. The system exchange capacity can now and again be attained by

- Discover a solution of the linear differential equations,
- When it is required to find the Laplace Transform of the resulting linear differential equations.
- Linearizing the nonlinear differential equations at the resultant solution.
- Then resolving for the outputs in terms of the inputs in the Laplace domain.

The transfer function of any system is a mathematical representation of that system, it can be represented as far as spatial or transient recurrence, of the relative enter and yield of a straight time-invariant arrangement of the direct differential mathematical statements that describes the framework.

Control Theory deals with manipulating the performance of an unstable system. It is an integrative subfield of knowledge\skill, which began in designing and math, and developed into utilization by the social sciences, in the same way as brain research, humanism, criminology, and in the money related framework. Control frameworks can be considered having four capacities; Measure, Calculate, Compare, and Correct. These four functions are not complete without adding elements like; Transducer, Detector, Transmitter, Controller, and Final Control Element.

4.2.2 Standard Control Theory

The standard control theory shows that the problems of the open-loop controller can be avoided by the introduction of a feedback. The feedback is used in order to control the states or output of a forceful process. As mentioned by (Astrom and Hagglund, 1995) feedback makes the process to be adjustable nearby the set-point, over the presence of

the disturbances and the process characteristics variation, which is the reason why feedback systems are much noticed. The wastewater treatment control investigation shows that the feedforward control scheme uses the information on future disturbances to advantage the treatment process operation by preparing the process to manage-well with the significant hydraulic disturbances or increased biological loading. In this set-up, the feedforward some piece of the controller focuses to suspect for the impact of measured aggravations, while the input part as notice before revises any deviations that come about because of the insufficiencies in procedure model, control limits and insufficient estimation or expectation of the disturbance(s).

The name closed-loop originates from the material pathway in the system: system inputs (like voltage applied to an electric motor) have a great effect on the system outputs (like a speed or torque of the motor), which is measured with devices (like sensors) and processed by the controller. The result; which means the control indication is used as input to the process, closing the loop.

A good standard control design method has to think through load disturbances, model uncertainty, noise measurement, and set-point reaction, Astrom and Hagglund, (1995). The following are possible advantages of using closed-loop control systems (Astrom and Hagglund, 1995):

- Process distraction rejection.
- Possibilities of balancing unstable processes through feedback control.
- Use parameter variations to decrease plant sensitivity
- Reference tracking performance can be improved.

4.2.3 Controller Specifications

At the point when tackling a control issue, it is important to comprehend what the essential objective of control is. Two normal sorts of issues are: to take over the set-guide and toward rejecting aggravations. It is additionally vital to have an evaluation of the significant confinements, which can be (Slotine and Li, 1991)

- System dynamics
- Nonlinearities
- Disturbances
- Process uncertainty

Classic conditions of a control system may include (Slotine and Li, 1991)

- Decreases of load disturbances

- Sensitivity to measurement noise
- Robustness to model uncertainty
- Set-point following

4.2.4 Control Theory Ending

A general conclusion for control concept is that, at the present, it is an integral area of investigation where many unconventional mathematical concepts, methods and techniques work collected to produce a remarkable body of influential used mathematics. The approaches in control of framework are coming both from mathematical development and from industrial growth. The principle wellspring of strategies and methods for tackling the essential issues in Control Theory is given by the numerical programming hypothesis and the ideal control hypothesis, Liu and Daley (2001)

4.3 Closed-loop System transfer function

A closed-loop transfer function in control theory is a scientific expression (algorithm) describing the net result of the effects of a feedback loop on the input signal to the circuits enclosed by the loop.

4.3.1 PID Control Description

A PID controller is a control circle input component broadly utilized as a part of mechanical control frameworks. A PID controller computes slide esteem as the contrast between a measured methodology variable and a coveted set-point. The controller endeavors to minimize the blunder by modifying the methodology control yields. The PID controller is by far the most common control algorithm (Mhaskar *et al.*, 2004). Most feedback loops are controlled by this algorithm or slight variations of it. It is applied in many different forms, as a standalone controller or as a part of a DDC (Direct Digital Control) package or ordered appropriate control of the process. Huge numbers of instrument and control engineers worldwide are utilizing such controllers as a part of their every day work. The PID calculation can be approached from numerous distinctive directions. It can be seen as an issue that can be worked with a couple of dependable guidelines, it can likewise be approached scientifically (Astrom and Hagglund, 1995).

PID is a short form for Proportional-Integral-Derivative; this term speaks of the three terms functioning on the error signal to produce a control signal. The following section is based on the linear PID controller.

4.3.1.1 Linear PID Controller

The usual Linear PID (LPID) controller expression is described as a variety of techniques. The controllers come in many different forms. The PID controller has a few essential capacities: it gives feedback; it can evacuate determined state balances through necessary activity; it can foresee the future through its subsidiary activity. PID controllers are appropriate for several control difficulties, mostly when the process dynamics are gentle and the performance requests are modest. PID controllers are found in large numbers in all industries. The Figure 4.1 below shows a block diagram of the LPID controller in time domain acting on the error signal $e(t)$. PID Controllers attempt to correct the error between a measured process variable and a desired set point, using calculations and then supplying the correct control response or action that can be adjusted according to what is needed in the process.

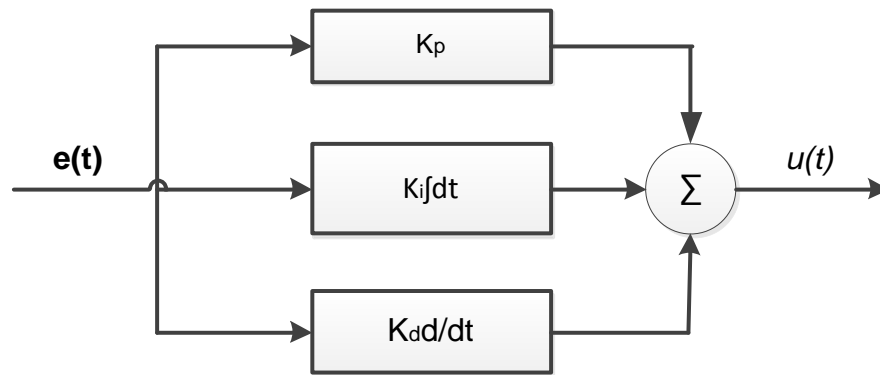


Figure 4.1: Time domain LPID controller structure

If $u(t)$ is the control signal sent to the system, $y(t)$ is the measured output, $r(t)$ is the desired output, and the tracking error is $e(t) = r(t) - y(t)$, the PID controller has the general model, as follows of:

$$u(t) = K_p e(t) + K_i \int e(t) dt + K_d \frac{d}{dt} e(t) \quad (4.1)$$

or

$$u(t) = K_p \left[e(t) + \frac{1}{T_i} \int_0^t e(t) dt + T_d \frac{de(t)}{dt} \right] \quad (4.2)$$

Where: $K_p; K_i = \frac{K_p}{T_i}; K_d = K_p T_d$ are the controller gains, based on a linear combination

between the error, the integral of the error and the derivative of the error,

- T_i - is the integral time constant,
- T_d - is the derivative time constant
- $u(t)$ - is the controller output,
- $y(t)$ - is the output of the process under control and
- $r(t)$ - is the desired reference trajectory.

In the PID controller:

- $e(t)$ - is the current error,
- $\int e(t)dt$ - is the past error
- $\frac{de(t)}{dt}$ - is the future system error.

The linear combinations between these errors are convenient for linear processes only, but approximately all processes in the industry are nonlinear. There are some drawbacks in the operation of the closed loop systems caused by the current, past and future errors:

The input signal to the PID controller $e(t)$ is not a smooth signal; it can be of the type of step inputs, which can lead to overshoot of the dynamic behavior of the output.

The integral part of the control action reduces the steady state error, but at the same time reduces the stability margins because of its phase lag and can make the closed loop system unstable.

The differential part of the control action is very sensitive to noise.

The anticipated closed loop influential is achieved by altering the three parameters K_p, K_i and K_d often prepared by "tuning" process and without particular knowledge of a plant model. Solidness can frequently be guaranteed by utilizing just the corresponding term. The fundamental term allows the dismissal of a step irritation (regularly a significant detail in the procedural control). The subordinate term is utilized to give damping or forming of the reaction. Applying Laplace transformation results in the transformed PID controller equations

$$U(s) = K_p E(s) + K_i \frac{1}{s} E(s) + K_d s E(s) \quad (4.3)$$

$$U(s) = E(s) \left(K_p + \frac{K_i}{s} + K_d s \right)$$

Then the transfer function of the LPID controller in s-domain can be represented as:

$$\frac{U(s)}{E(s)} = G_{PID}(s) = \frac{K_p s + K_i + K_d s^2}{s} \quad (4.4)$$

The most recognized classes of controllers are PID controllers; though, they cannot be used in several more complicated cases without any modification or some additional function, especially in the consideration of MIMO and nonlinear systems (Wahab *et al.*, 2007).

4.4 Nonlinear Control Theory

The linear control topic is a grown-up area under discussion with a long history of successful industrial applications. There are different methods that can be used to design linear or nonlinear controllers. The control theory evaluation shows that, through the use of state space representation of the open-loop scheme and the calculation of a feedback matrix which assigns poles of the process to desired locations, this method (pole placement method) has been applied in various MIMO linear systems. However, in complex systems this needs computer assisted control capabilities, and cannot permanently ensure robustness. This has made an extra interest in the development and applications of nonlinear control theory, especially from wide-ranging areas such as process control, aircraft and spacecraft control, robotics, and biomedical engineering, (Slotine and Lie, 1991).

It is currently very difficult to model and identify general nonlinear systems because of their huge diversity and because of their structural complexity. Once the models are available, it is very significant to explore how they can be used to find an understanding and an effective control of the relevant system. As it is known that there are numerous nonlinear systems which must be controlled in the present industrial world. Thus, it is important to develop methods to model nonlinear systems and to estimate the model parameters. Astrom and Hagglund, (1995), state that another way to overcome this problem is to tune the controller for the worst case and accept degraded performance at another operating condition.

4.4.1 Why Nonlinear control:

There are many reasons that can be mentioned in this interest:

4.4.1.1 Improvement of existing control systems:

The following discussion is comparing the existing control systems with linear or nonlinear control:

The linear control approaches are based on the important assumption of a slight operation range only for the linear model to be valid. The problem for linear method comes when the required range of operation is large, a linear controller will mostly perform poor or the system will be unstable, because the process nonlinearities cannot be properly compensated. On the other hand, nonlinear controllers directly handle the nonlinearities even in large operation range. This may be confirmed in control problems like robot motion, and water treatment. Slotine and Lie, (1991), state that when linear controller is used to control a nonlinear system, it mostly neglects the nonlinear forces associated with the operation process.

4.4.1.2 Investigation analysis of solid nonlinearities:

An additional hypothesis about linear controllers is that the system under control is really linearisable. Despite the fact that, there are several nonlinearities in control systems with irregular nature that do not allow linear estimation; examples of such strong nonlinearities take account of saturation, coulomb friction, dead-zones, hysteresis and backlash, which are found a lot in control engineering (Slotine and Li, 1991). It is not possible to obtain the effects of these nonlinearities from application of methods for linear system analysis. In such instant development of the nonlinear analysis techniques is needed to predict the performance of the system in the presence of the natural nonlinearities. These regularly nonlinearities cause unwanted control system's behavior, such as false limit cycles or system instabilities and for that reason their effects need to be predicted and be appropriately compensated, (Slotine and Li, 1991).

4.4.1.3 Uncertainties of the model:

The investigation of the model control shows the fact that the assumptions of significant known model parameters are generally required when designing linear controllers. However, the involvement of the uncertainties in the system model parameters has been always a problem in many controls. This is most likely due to a slow time modification of parameters, or to an unexpected change/ disturbances in parameters. The linear controllers that are based on inaccurate or outmoded values of the model parameters can exhibit important performance humiliation or even to lead to the closed loop system instability. In the controller system, the nonlinearities can be set-up intentionally so that the model uncertainties are tolerated. Slotine and Li, (1991) suggested two classes of

nonlinear controllers for the purpose of tolerating model uncertainties, which are robust controllers and adaptive controllers.

Robustness is the low sensitivity to effects which are not considered in the design process, such as disturbances, measurement noise, un-modeled dynamics, *etc.* The system should be able to withstand these neglected effects when performing the tasks of interest, Slotine and Li, (1991). In general term the robust control theory deals clearly with the uncertainty in its approach to controller design. The used robust control methods when designing controllers tend to be able to manage with small differences between the true system and the nominal model used for the design, as confirmed through simulation by Su et al., 2005.

Adaptive control is a method used for the control design approach to deal with uncertain systems or time-varying systems. Vanrolleghem, (2003) states that adaptive control use on-line identification of the system parameters, or adjustment of the controller gains, by this means of obtaining strong robustness properties. Keeping up reliable performance of the system in the presence of uncertainty, is the key objective of the adaptive control, this type of control aims to also react positively towards stabilizing the system when unknown variation in the plant parameters occurs, Slotine and Li, (1991).

Optimal control is a control method in which the control signal optimizes a certain cost index. Optimization is one of the outstanding recognized branches of mathematics, that have an aim of finding the values for variables in order to make the most profit or to decrease the costs subject to some constraints, Andrei (2005).

4.4.1.4 Design Simplicity and Nonlinear Control Description

Nonlinear control is the area of control engineering which is specifically involved with the systems that are nonlinear, time-variant, or both. The study of the nonlinear control concept can be used to acquire knowledge on how to design nonlinear controller and additionally apply existing linear methods to more general control systems. Nonlinear control theory is responsible for innovative control methods that cannot be analyzed using Linear Time Invariant (LTI) system theory. If an LTI system theory can be used for investigation and design of a controller, a nonlinear controller can have attractive characteristics (example: simpler implementation, increased speed, or decreased control energy); even though, nonlinear control concept usually requires more careful scientific analysis to justify the conclusion of any situation.

4.5 Mathematical model of the Differential Tracker

The nonlinear systems have much more affluent and more complex performances than linear systems, and their analysis is much harder. Mathematically, this is reflected in two aspects. First, nonlinear equations, unlike linear ones, in general, cannot be solved analytically, and therefore, a complete understanding of the behavior of a nonlinear system is very difficult. Secondly, Slotine and Li (1991) declare that powerful mathematical tools like Laplace and Fourier transforms did not apply to nonlinear systems. Therefore, there are no systematic tools for predicting the behavior of nonlinear systems, or systematic procedures for designing nonlinear control systems. Instead, there is an ironic record of influential analysis and design tools, for each best applicable to particular classes of nonlinear control problems.

Su, et al., (2005), mention that, the most general position sensor used in the industry is the optical encoder because, it has a high resolution, simple discovery circuit, high correctness and relative ease of adaptation in digital control systems when all has to be put into practice. On the other hand, the speed or disturbance measurement, obtained in any nonlinear system, is regularly infected by noise. The nonlinear Differentiator Tracking (DT) can be used for this purpose. The greatest significant role of the DT is to obtain the derivative of a noisy signal with a virtuous signal to noise ratio. The use of the differentiator for the reference input allows a smooth reference to be implemented which can be used with different controllers.

The derivative control error in the PID controller is used very rarely in the industry due to the sensitivity of the noise (Han et al. 1994). The Differential Tracker (DT) is introduced to improve the control quality and can be used as a filter which blocks any part of the signal, when the acceleration exceeds the set reference value. The differential tracker is very often used together with linear on Nonlinear PID (NLPID) controllers, as shown in Figure 4.2 (Su, et al., 2005)

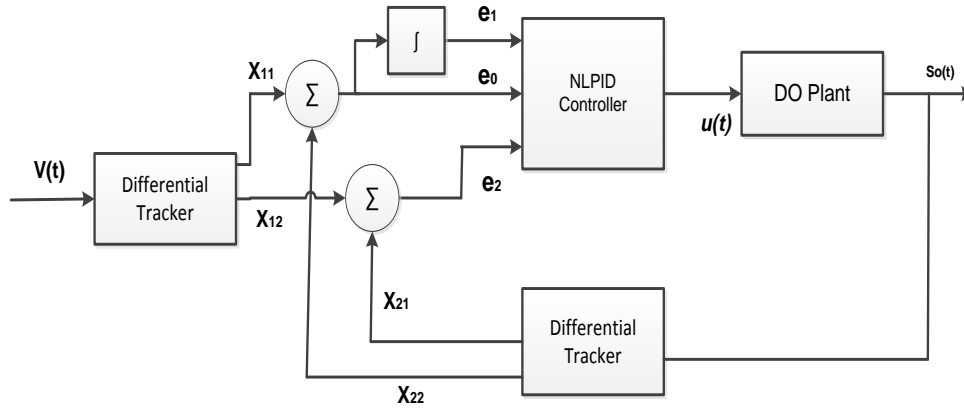


Figure 4.2: Closed-loop NLPID controller with a DT

New dynamic process is introduced to realize the process of differentiation needed for the PID controller implementation and is based on integration in the nonlinear differentiator model proposed by (Wang et al., 1994), as follows:

$$\dot{x}_1(t) = x_2(t) \quad (4.5)$$

$$\dot{x}_2(t) = M \operatorname{sign} \left(x_1(t) - v(t) + \frac{x_2(t)|x_2(t)|}{2M} \right) = -Mf(x_1, x_2) \quad (4.6)$$

Where:

- $v(t)$ - Is the input signal.
- $f(x_1, x_2)$ - Is the differentiator function.
- M - Is the selected/ design parameter

In Equations (4.5) and (4.6) $x_1(t)$ tracks the reference input $v(t)$ in minimum time without overshoot and $x_2(t)$ converges to the derivative of $v(t)$. The variable $x_2(t)$ is obtained by integration and is less sensitive to the noises. The selection of a bigger value of M influences the $\dot{x}_2(t)$ and the acceleration of $x_1(t)$ to be high and leads to fast tracking of $v(t)$. It concludes that the differentiator can be used to track down the unwanted noise signals. DT has two important roles in the theses. They are:

- To filter out the noise in the measurement of the DO process output signal $s_o(t)$
- To determine the $s_o(t)$ and the set-point signal $v(t)$ through integration process.

4.6 Mathematical Model of the nonlinear PID Controller

Numerous modern methodologies are nonlinear and in this way it is entangled to be depicted numerically. On the other hand, it is realized that numerous nonlinear techniques can be palatable controlled utilizing PID controllers giving that control parameters are tuned well. Useful experience demonstrates that this sort of control has a considerable measure of sense since it is straightforward and is focused around 3 essential conduct sorts: corresponding (P), integrative (I) and subordinate (D). As opposed to utilizing a little number of complex controllers, a bigger number of straightforward PID controllers are utilized to control easier forms in a mechanical get together so as to computerize some certain more perplexing techniques. PID controller and its distinctive sorts, for example, P, PI and PD controllers are today essential building squares in control of different methodologies. In resentment their straightforwardness; they can be utilized to take care of even a complex control issue, particularly when joined with diverse utilitarian pieces, channels (compensators or remedy squares), selectors and so on. A nonstop improvement of new control calculations safeguard that the time of PID controller has not past and that this essential calculation will have its part to play in procedure control in unsurprising future. It can be normal that it will be a spine of numerous complex control frameworks.

Nonlinear PID controllers are extension of the conventional well-known LPID by adding specific nonlinear functions to the main linear PID equation. The NLPID controller equations (4.7) to (4.17) are formulated by (Hai-bin et al., 2006), (Han et al., 1994) and (Su at al., 2005) and their typical implementation is shown in Figure 4.2. On the basis of this figure the NLPID controller equation can be written as follows:

$$\varepsilon_0(t) = x_{11}(t) - x_{21}(t) \quad (4.7)$$

$$\varepsilon_1(t) = \int_0^t [x_{11}(t) - x_{21}(t)] dt \quad (4.8)$$

$$\varepsilon_2(t) = x_{12}(t) - x_{22}(t) \quad (4.9)$$

$$\dot{x}_{11}(t) = x_{12}(t) \quad (4.10)$$

$$\dot{x}_{12}(t) = x_{21}(t)$$

$$\dot{x}_{21}(t) = x_{22}(t) \quad (4.11)$$

$$\dot{x}_{22}(t) = -M_2 \text{sign} \left(x_{21}(t) - y(t) + \frac{x_{22}(t)|x_{22}(t)|}{2M_2} \right) \quad (4.12)$$

$$u(t) = K_p |\varepsilon_0(t)|^{ap} \text{sign}(\varepsilon_0(t)) + K_i \left| \int_0^t \varepsilon_0(t) dt \right|^{ai} \text{sign} \left(\int_0^t \varepsilon_0(t) dt \right) + K_d \left| \frac{d\varepsilon_0(t)}{dt} \right|^{ad} \text{sign} \left(\frac{d\varepsilon_0(t)}{dt} \right) \quad (4.13)$$

Where:

$$\int_0^t \varepsilon_0(t) dt = \varepsilon_1(t) \ \& \ \frac{d\varepsilon_0(t)}{dt} = \varepsilon_2(t)$$

Then the Equation (4.13) can be represented in a general form as:

$$u(t) = K_p \text{fal}(\varepsilon_0, a_p, \delta_p) + K_i \text{fal}(\varepsilon_1, a_i, \delta_i) + K_d \text{fal}(\varepsilon_2, a_d, \delta_d) \quad (4.14)$$

Where:

$$\text{fal}(\varepsilon_0, a_p, \delta_p) = \begin{cases} |\varepsilon_0|^{a_p} \text{sign}(\varepsilon_0); |\varepsilon_0| > \delta_p \\ \frac{\varepsilon_0}{\delta_p^{1-a_p}}; |\varepsilon_0| \leq \delta_p \end{cases} \quad (4.15)$$

$$\text{fal}(\varepsilon_1, a_i, \delta_i) = \begin{cases} |\varepsilon_1|^{a_i} \text{sign}(\varepsilon_1); |\varepsilon_1| > \delta_i \\ \frac{\varepsilon_1}{\delta_i^{1-a_i}}; |\varepsilon_1| \leq \delta_i \end{cases} \quad (4.16)$$

$$\text{fal}(\varepsilon_2, a_d, \delta_d) = \begin{cases} |\varepsilon_2|^{a_d} \text{sign}(\varepsilon_2); |\varepsilon_2| > \delta_d \\ \frac{\varepsilon_2}{\delta_d^{1-a_d}}; |\varepsilon_2| \leq \delta_d \end{cases} \quad (4.17)$$

It can be seen from the Equations (4.13) or (4.14) to (4.17) that the nonlinear PID controller has the structure of the linear PID controller but the error between the reference input and the process output is presented by nonlinear functions.

The above mathematical representation of the NLPID controller is used in the thesis to control the process of Dissolved Oxygen concentration.

4.7 Conclusion

In this chapter, an introduction to the PID control theory is given. This provides a theoretical and mathematical basis which is applied in this thesis to solve the research

problem for design of nonlinear control of wastewater treatment process, known as the activated sludge process. In the thesis the design control problem is to find the nonlinear controller parameters that can be the best for control of the dissolved oxygen concentration and that can be implemented on a PLC environment in real-time.

The next Chapter, (Chapter 5) concentrates more on the development of different methods for design and tuning of the NLPID controllers based on Ziegler-Nichols method. The closed loop simulation of the DO closed loop system is performed.

CHAPTER FIVE

DEVELOPMENT OF METHODS FOR DESIGN AND TUNING OF NLPID CONTROLLERS

5.1 Introduction

As may be mentioned before, a control system is a device, or set of devices that manage, command, direct or regulate the behavior of other devices or processes. The controller attempts to minimize the error in the system by adjusting the process control inputs. This section is based on the well-known conventional PID control design.

To develop methods for designing controller's parameters it is necessary to define the main purpose of the process needed to be controlled, which is done in Chapters 2 and 3. The design methods are not the same, due to the knowledge of the process dynamics they require to be capable to produce the required parameter values. This chapter discusses the need for nonlinear controller design in a Section 5.2. The traditional Ziegler-Nichols (ZN) methods are designed in Section 5.3 for linear and nonlinear PID controllers and the subsection 5.3.5 gives the simulation results based on the two nonlinear PID controllers designed for the DO concentration. Section 5.5 provides the conclusion of this chapter.

5.2 The need for designing the Nonlinear PID Controller

The process to be controlled is nonlinear and when controlling the Dissolved Oxygen (DO), the nonlinear characteristics of the oxygen transfer function must be taken into account when designing the controller. The problem in controlling the DO is that the process dynamics are nonlinear. This means that high control performance for all operating conditions of the process may be hard to achieve with a linear controllers, because:

- The linear controllers are designed for the linear process, but the process of the dissolved oxygen in wastewater treatment is non-linear.
- Secondly the parameters of the controller are not determined according to the operating conditions of the process at the moment of control. The set-point is selected according to some normal system requirements, not according to the operating conditions of the process at the instant of control.

A high DO concentration in the internally re-circulated water makes the de-nitrification less efficient. If DO content is too low, the environment is not stable and the activated sludge will not be properly treated. Hence, both for economical and process reasons, it is of interest to properly control the DO (Lindberg, 1997). On the basis of above to control the DO process in a proper manner it is needed to design an appropriate nonlinear controller.

The nonlinear PID controller introduced in Chapter 2 is modified to include continuous dynamic nonlinear functions of the closed loop system error instead of the gain-scheduling approach. Then the nonlinear PID controller model can be presented as a combination of nonlinear error functions in order to achieve a better tracking and better noise rejection system. The NLPID controller used in the thesis is based on an exponential function in the error mathematical formulation as is proposed by (Gao, 2009), (Shuhua et al., 2009) and (Hai-bin et al., 2006). The tuning of the NLPID controller can be considered to be similar to the tuning of the linear PID controller, and it can be implemented on-site to achieve better performance.

5.2.1 Nonlinear PID Controllers

There are different types of nonlinear controllers described in the literature (Chapter 2). The controllers used to control process can have different structures (Pohjola, M, 2006). The choice of the structure determines how well the plant can be controlled. A Linear PID (LPID) controller structure is selected to control the system as it is easy and intuitive to be tuned. It is also used widely in the industry (Astrom *et al*, 1995) and there is a benefit of using a well-known and trusted controller in future applications. LPID controllers make up an important part in industrial control system. Any improvement in LPID controller design and implementation methodology has a serious potential to be used in industrial engineering application. Aydogdu and Korkmaz, (2011), state that the LPID controllers are preferred widely in industrial applications, due to their robust characteristics against changes at the system model.

In most industrial situations the precise nonlinear plant model behavior is not obtained due to too many nonlinear parts and uncertainties. A lot of methods have been developed over the last years for setting the parameters of the NLPID controllers. Some of these methods are based on characterizing the dynamic response of the system to be controlled with a first-order model or second-order model with a time delay (Hagglund, 1991). The plan of the following sections is to use the PID structure, nonlinear functions

of the errors between the set point and the controlled variable and to form the NLPID controller model. Two mathematical models of the NLPID controllers are selected for the purpose of the investigations in the thesis

5.2.1.1 The first selected NLPID controller: (NLPID1)

The algorithm of the NLPID controller is based on introduction of a nonlinear function of the error between the reference and the output signal of the process (Jiang, et al., 2009)

$$u(t) = K_p \left[f(e, \alpha_p, \delta_p) + \frac{1}{T_i} f\left(\int e, \alpha_i, \delta_i\right) + T_d f(\dot{e}, \alpha_d, \delta_d) \right] \quad (5.1)$$

Where:

K_p, T_i, T_d - are the controller gains similar to these of the LPID controller.

$\begin{cases} f(e, \alpha_p, \delta_p) \\ f(e, \alpha_i, \delta_i) \\ f(e, \alpha_d, \delta_d) \end{cases}$ - represent the nonlinear error functions of the NLPID controller.

δ - Constant used to determine the linear range of the error function

α - Nonlinear degree of the error function

$e(t)$ - Is the error signal

The nonlinear function proposed by Jiang *et al.*, (2009) and Zaidner *et al.*, (2010) can be mathematically represented as follows:

$$f(e, \alpha_p, \delta_p) = \begin{cases} \text{sign}(e) \cdot |e|^{\alpha_p}, & \text{when } |e| > \delta \\ \delta^{\alpha-1} \cdot e, & \text{when } |e| \leq \delta \end{cases} \quad (5.2a)$$

$$f(e, \alpha_i, \delta_i) = \begin{cases} \text{sign}\left(\int edt\right) \left|\int edt\right|^{\alpha_i}, & \text{when } \left|\int edt\right| > \delta \\ \delta^{\alpha-1} \cdot \int edt, & \text{when } \left|\int edt\right| \leq \delta \end{cases} \quad (5.2b)$$

$$f(e, \alpha_d, \delta_d) = \begin{cases} \text{sign}\left(\frac{de}{dt}\right) \left|\frac{de}{dt}\right|^{\alpha_d}, & \text{when } \left|\frac{de}{dt}\right| > \delta \\ \delta^{\alpha-1} \cdot \dot{e}, & \text{when } \left|\frac{de}{dt}\right| \leq \delta \end{cases} \quad (5.2c)$$

Where:

e - Input signal of the error function

y - Output signal of the nonlinear error function.

5.2.1.2 The second selected nonlinear PID controller: (NLPID2)

It has been discussed before that, the main algorithm of the NLPID controller is based on the nonlinear function as inherent part of the controller. The usually LPID has been reconstructed using a nonlinear function as follows: proposed by (Hai-bin *et al*, 2006).

$$u = K_p |e|^\lambda \text{sign}(e) + K_i \left| \int_0^t edt \right|^\lambda \text{sign} \left(\int_0^t edt \right) + K_d \left| \frac{de}{dt} \right|^\lambda \text{sign} \left(\frac{de}{dt} \right) \quad (5.3)$$

Where:

- λ - is a constant
- K_p - is the proportional gain,
- K_i - is the integral of the error gain
- K_d - is the derivative of the error gain,
- u - is the combination of error – control signal.

The literature has proposed a nonlinear module (Shuhua and Wei, 2009) whose function is shown in the following equations.

$$\begin{cases} \text{sign}(e) \cdot |e|^\lambda, \text{ when } |e| \geq \delta \\ e / \delta^{1-\lambda}, \text{ when } |e| < \delta \end{cases} \quad (5.4a)$$

$$\begin{cases} \left| \int_0^t edt \right|^\lambda \cdot \text{sign} \left(\int_0^t edt \right), \text{ when } \left| \int_0^t edt \right| \geq \delta \\ e / \delta^{1-\lambda}, \text{ when } \left| \int_0^t edt \right| < \delta \end{cases} \quad (5.4c)$$

$$\begin{cases} \left| \frac{de}{dt} \right|^\lambda \cdot \text{sign} \left(\frac{de}{dt} \right), \text{ when } \left| \frac{de}{dt} \right| \geq \delta \\ e / \delta^{1-\lambda}, \text{ when } \left| \frac{de}{dt} \right| < \delta \end{cases} \quad (5.4d)$$

The two symbols δ and λ are the two parameters of the nonlinear function. The two NLPID controllers (Equations 5.1 – 5.2 and 5.3 - 5.4) are used further in order to achieve the research objective. Equations (5.1 – 5.2) and Equations (5.3 – 5.4) are named as NLPID1 and NLPID2 respectively in the thesis.

The NLPID controller uses nonlinear error functions to replace the linear ones in the conventional PID controller. Comparison between the linear function $e(t)$ and the nonlinear function $f(e, \alpha, \delta)$ shows that the nonlinear one produces high gain for small error ($e(t)$), and small gain for large value of $e(t)$, Zaidner *et al.*, (2010), Hai-bin *et al.*,

(2006). The nonlinear function used in this thesis $f(e, \alpha, \delta)$ is an exponential function. In industry, the linear proportional, integral and derivative control is usually scheduled according to the Process Value (PV) and the magnitude of the error and is used to overcome the nonlinearity of the plant. The considered two nonlinear PID controllers are used with differential trackers, Figure 4.2 placed after the reference signal and after the output signal measurement.

The Differential Tracker (DT) is used to improve the control quality; it is introduced to track the reference and output positions and their differentials. Most of existing controllers are designed for linear systems using the methods of the linear control theory. A nonlinear controller has interesting characteristics such as increased speed, or decreased control energy and it requires more accurate mathematical analysis and modeling to justify its design and prototype. There are not proposed methods for design of the NLPID controllers. Nonlinear control is the area of control engineering which is involved with the systems that are nonlinear, time-variant, or both. Nonlinear control theory studies explain how to apply the existing linear methods to the control systems. It also provides novel control methods which cannot be analyzed using Linear Time Invariant (LTI) system theory.

The thesis investigates the applicability of the methods for design of the linear PID controllers to the design of NLPID controllers and proposes new pole placement method for direct design of the parameters of the NLPID controllers. Ziegler-Nichols and Pole placement methods are used in the thesis form the basis for development of methods for the nonlinear PID controller parameters design.

5.3 Ziegler-Nichols Design Methods

There are three unknown parameters of the controller, which are $K_p, T_i,$ and T_d to be determined. This section focuses on designing the controller's parameters using Ziegler-Nichols method. The closed loop systems based on the linear and nonlinear PID controllers are simulated using the designed parameters.

In generally there are two classical methods for determining the parameters of PID controllers presented by Ziegler and Nichols (1942). These methods are still widely used, either in their original form or in some modification. They often form the basis for tuning procedures used by controller manufacturers and process industry. The methods are based on determination of some features of process dynamics. The controller

parameters are then expressed in terms of these features by straightforward formulas (Astrom and Hugglund, 1995). Both techniques make a priori assumptions on the system model, but do not require the model to be specifically known.

Ziegler-Nichols formulas for specifying the controller's parameters are based on plant step responses. This section is based on designing of the parameters for LPID and NLPID controllers using Ziegler-Nichols (Z-N) first method as the DO process has exponential type of dynamic behavior. The description of the Ziegler-Nichols method, requirements for design specifications, and application of Z-N method for design of the LPID controller is taken into consideration. The designed parameters through the Z-N method in this section are later applied into the NLPID controller and the closed loop system responses are simulated. Then comparison of the simulation results between the based on the LPID and on the nonlinear PID controller systems is done.

5.3.1 Ziegler-Nichols (Z-N) tuning method for design of the LPID controller and its application to NLPID controllers

The first design method presented by Ziegler and Nichols is based on a registration of the open-loop step response of the process to be controlled (DO in this case) where two parameters have to be determined according to (Astrom, 1995). The parameters are determined from a unit step response of the process, as exposed in Figure 5.1. The point where the slope of the system step response has its maximum is first determined, and the tangent line at this point is drawn. The intersections between the tangent line and the coordinate axes and between it and the steady state value line give the parameters L and T .

Where:

L - is the time delay

T - is the time constant of the transition behavior of the plant

The following Figure (5.1) is the open loop response of the dissolved oxygen (DO) under the model Equation 3.1 unit step input.

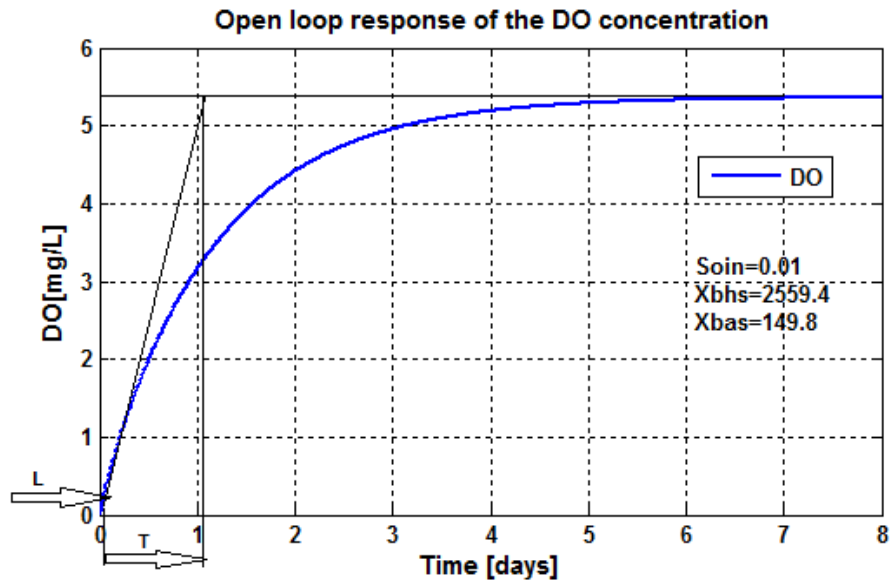


Figure 5.1: DO concentration open loop response using $s_{o,in} = 0.01 \text{ mg/L}$ and $r_{so} = -294.8954 \text{ mg/L/day}$

The algorithm of the first Ziegler-Nichols method is:

- Receive the transition behavior of the DO concentration to step input of the air flow rate.
- Draw the tangent line at the inflection point of the graph, then measure the amplitude of the output, the time constant and the time delay.
- Calculate the PID parameters according to the basic Ziegler-Nichols table shown below.

Table 5.1: Ziegler-Nichols step response method table

Controller type	K_p	$T_i = K_p/K_i$	$T_d = K_d/K_p$
P	T/L	∞	0
PI	0.9 T/L	L/0.3	0
PID	1.2* T/L	2L	0.5L

The measurements on the DO step response give the parameters of the delay and constant time as $L = 0.01$ (days) and $T = 1$ (days) respectively. The controller parameters can now be determined using the Table 5.1 and the following Equations:

$$\begin{cases} K_p = \frac{1.2T}{L} \\ K_i = \frac{1}{2L} \\ K_d = 0.5L \end{cases} \quad (5.5)$$

The results yielded to: $K_p = 120$, $K_i = 50$, and $K_d = 0.005$.

5.3.2 Simulink Block Diagrams

5.3.2.1 Closed loop DO process model under the LPID controller

The model of the DO closed loop system has been built in Simulink with the linear PID controller. The parameters designed in 5.3.1 above using Ziegler-Nichols method are applied on the PID (LPID) controller block to control the process. The diagram of the DO process controlled by the LPID controller is shown in Figure 5.2.

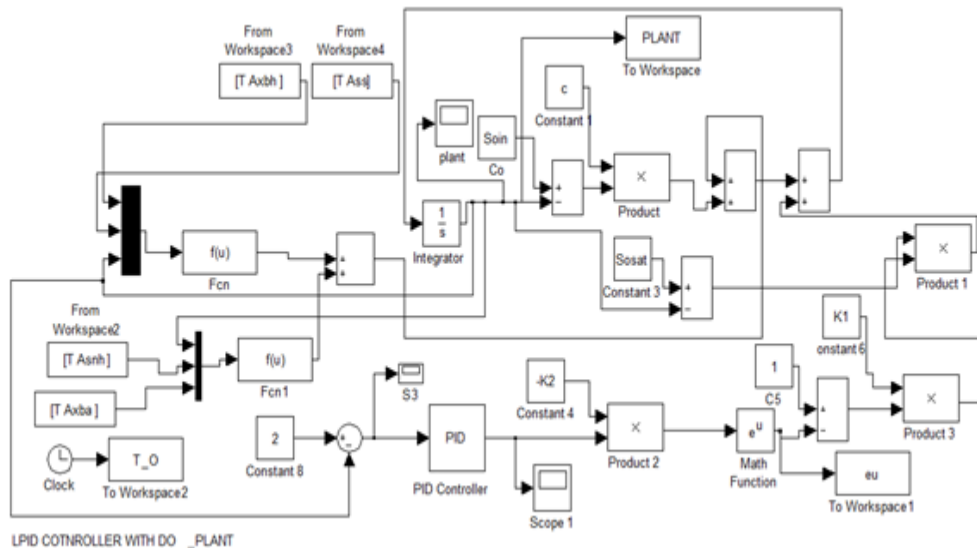


Figure 5.2: Closed Loop diagram of the DO process with the linear PID controller

5.3.2.2 Simulink Block Diagram of the closed loop system based on the NLPID1 controller

Figure 5.3 shows the Simulink block diagram of the closed loop system for the NLPID1 (Equations 5.1 – 5.2) controller and the DO process. The DT is included in the scheme. The behavior of the closed loop system under the NLPID1 controller with Ziegler-Nichols (Z-N) designed parameters based on the LPID controller is shown in Figure 5.6 and Figure 5.7 when the calculated parameters are not tuned. Figure 5.8 to Figure 5.13 display the system output when the controller parameters are tuned in order to achieve

the desired behavior of the plant under the control of the nonlinear PID1, but using the Z-N tuning method as initial step for further tuning.

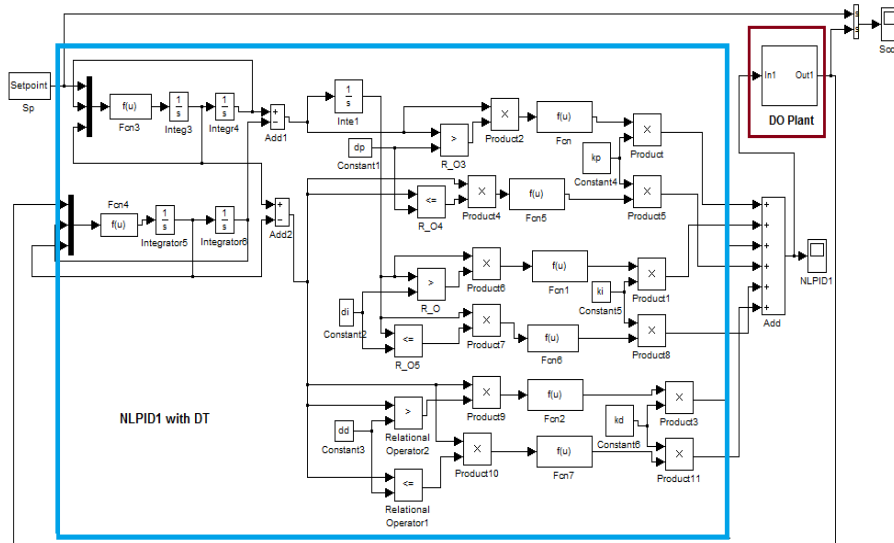


Figure 5.3: Closed loop diagram of the DO process with the NLPID1 controller

5.3.2.3 Simulink model of the closed loop DO process under the NLPID2 controller

Figure 5.4 shows the closed loop Simulink model of the DO process controlled by the second selected nonlinear PID (NLPID2) controller, Equation (5.3 – 5.4) including the Differential Tracker (DT). The behavior of the closed loop DO process model (Figure 5.4) is shown in Figure 5.25 while the calculated parameters are not tuned, Figure 5.26 and Figure 5.27 while the calculated parameter are not tuned enough. Figures 5.28 to 5.43 show the closed loop system output when the controller’s parameters are tuned in order to achieve the desired behavior of the plant and stabilize the system. The corresponding Matlab script file “NLPID2zn_DO.m” Appendix B3 and the Simulink block diagram model shown in Appendix C4 as given in Figure 5.5.

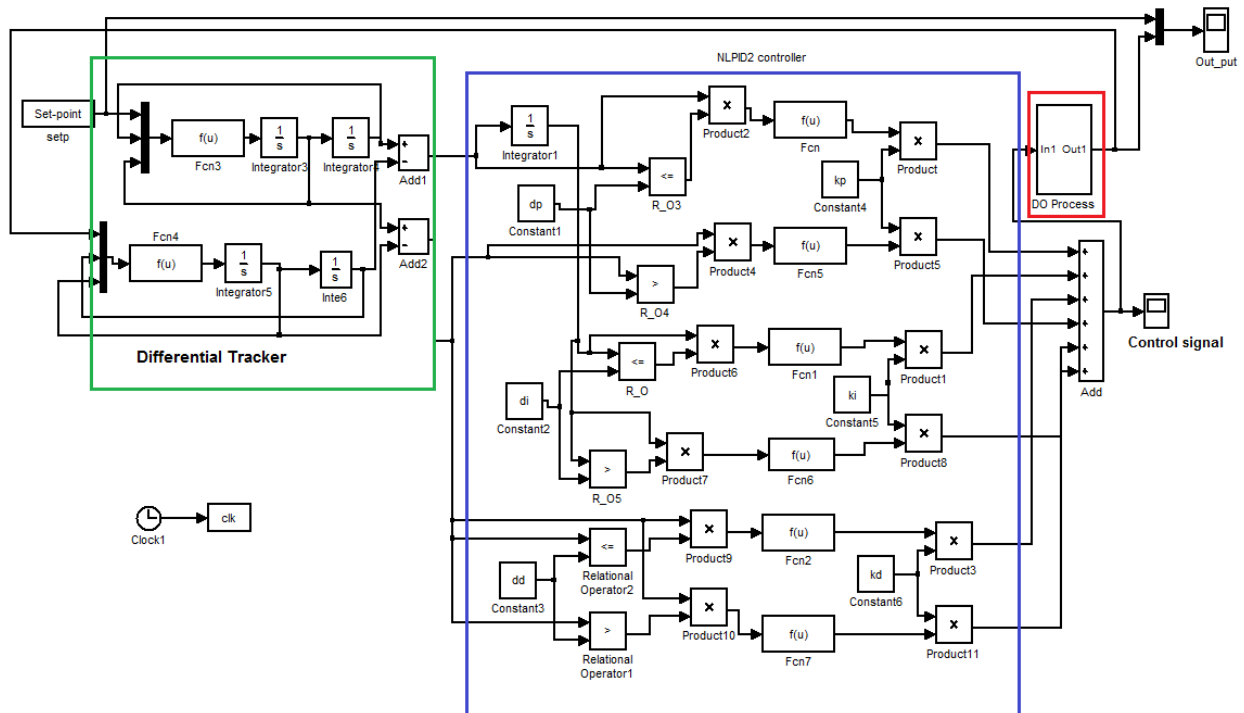


Figure 5.4: Closed loop diagram of the DO process with the NLPID2 controller

5.3.3 Simulation results

Control parameters as designed in section 5.3.1 are applied in the linear and the nonlinear PID controllers modeled above (Figures 5.2, 5.3, 5.4) to control the process of the dissolved oxygen concentration. The designed parameters for K_i , K_p , and K_d are applied first in order to control the DO concentration through the linear PID controller. The same parameters and the corresponding nonlinear functions are used in the nonlinear PID controllers to control the same process. Software is written in Matlab/Simulink environment to introduce the DO process parameters, the nonlinear function parameters and the control parameters in the Matlab workspace. The model parameters are taken from the benchmark structure model No:1 at their steady state at 20°, (Alex, 2008).

5.3.3.1 Simulation results of the closed loop nonlinear DO process under the LPID controller designed by the Ziegler-Nichols Method

The corresponding Matlab mfile “LPID_DO.m” in Appendix B1 and the Simulink block diagram model file “LPIDwithDO.mdl” as given in Figure 5.2 can be seen in Appendix C2. The output of the closed loop system is shown in Figure 5.5.

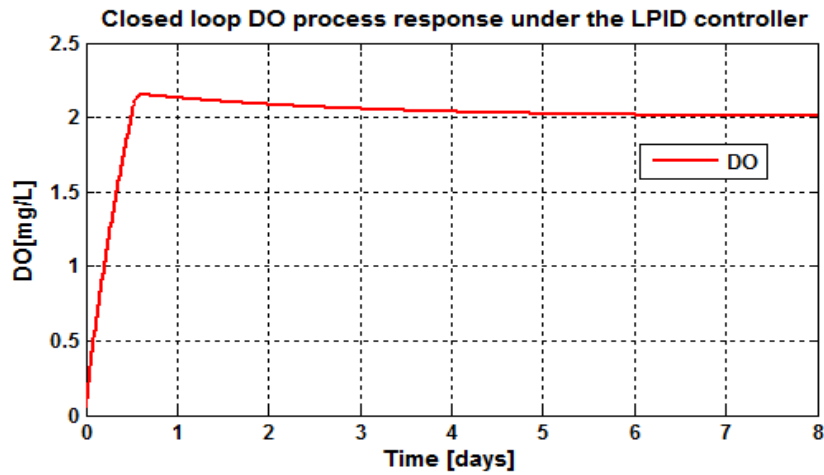


Figure 5.5: DO concentration closed loop behavior using a set-point of 2 mg/L and $r_{so} = -294.8954\text{ mg/L/day}$

The response shows a fast response time with the overshoot of 25%

5.3.3.2 Simulation results of the closed loop DO process under the NLPID1 controller designed by the Ziegler-Nichols Method

The corresponding Matlab mfile “NLPID1withDOzn.m” and the Simulink block diagram model file “NLPID1zn_DOmodel.mdl” as given in Figure 5.3 can be seen in Appendix B and C respectively. The output of the closed loop system is shown from Figure 5.6 and Figure 5.7. The behavior of the DO process is oscillating and this shows that the control parameters designed for the LPID controller cannot directly be used in the NLPID controllers to successfully control the nonlinear DO process. The conclusion is that the tuning of the parameters calculated for the LPID is necessary to be applied when they are used in the NLPID controller in order to improve the system performance. The output results of the closed loop system under the NLPID1 with the tuned LPID controller parameters are shown in Figures 5.8 to Figure 5.24 for different set-points and disturbances.

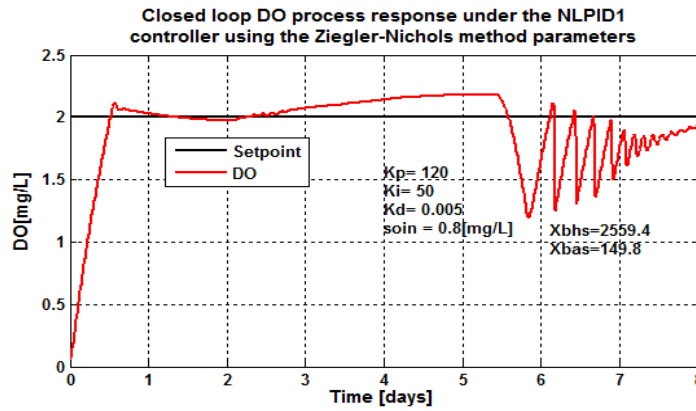


Figure 5.6: Closed loop response of the DO process under the NLPID1 controller using the designed parameters, when the set-point is 2 mg/L , $s_{o,in} = 0.8 \text{ mg/L}$ and $r_{so} = -294.8954 \text{ mg/L/day}$

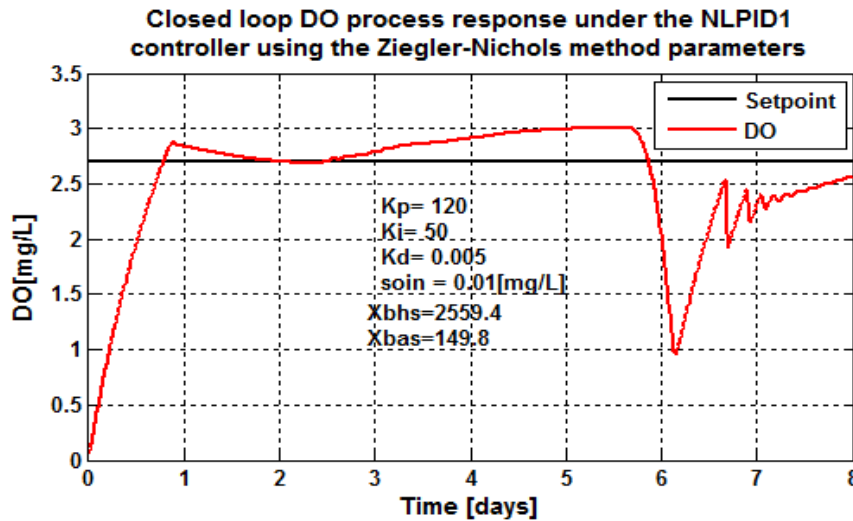


Figure 5.7: Closed loop DO process response under the NLPID1 controller using the designed parameters, when the set-point is 2.7 mg/L and $r_{so} = -294.8954 \text{ mg/L/day}$

Figures 5.6 and Figure 5.7 show that the closed loop system behavior under the designed parameters based on Ziegler-Nichols method for design of the LPID controller and used in the NLPID1 controller to control the DO concentration, is not satisfactory. The internal disturbance ($s_{o,in}$) is changed from a value of 0.8 mg/L to 0.01 mg/L respectively, but changing it did not improve the response of the system. It can be noticed that when the set-point of the system is changed from 2 (Figure 5.6) to 2.7 (Figure 5.7) the oscillations at the final stability point were reduced.

The next Figures show the closed loop results when the fine-tuning of the NLPID1 controller parameters is applied to improve the system behavior.

The following Figures 5.8 to 5.24 show the results when the controller's parameters are adjusted:

- First change is the value of K_i changed from 50 to 5, the values of K_d and K_p are unchanged, Figure 5.8
- Second change - the value of K_i is changed from 5 to 0.5, Figure 5.9

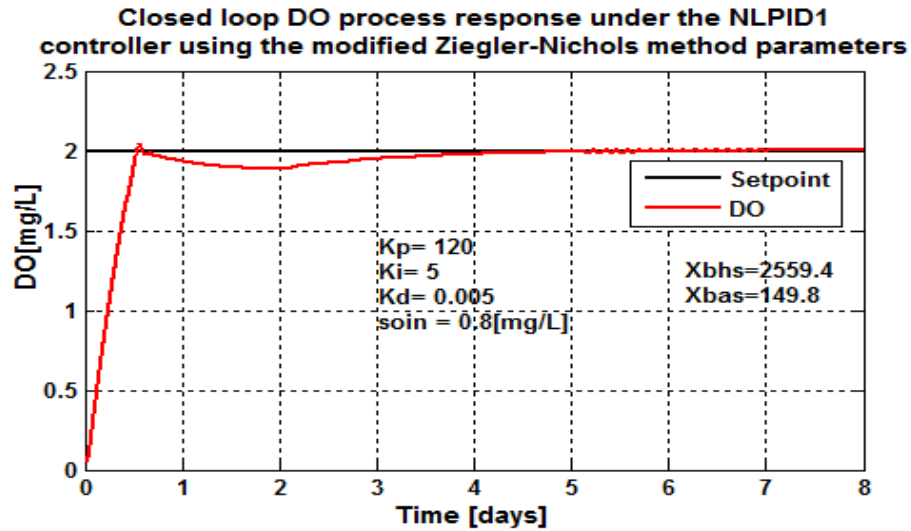


Figure 5.8: Closed loop response of the NLPID1 controller, when the set-point is 2 mg/L and $s_{oin}=0.8 \text{ mg/L}$, $r_{so}=-294.8954 \text{ mg/L/day}$

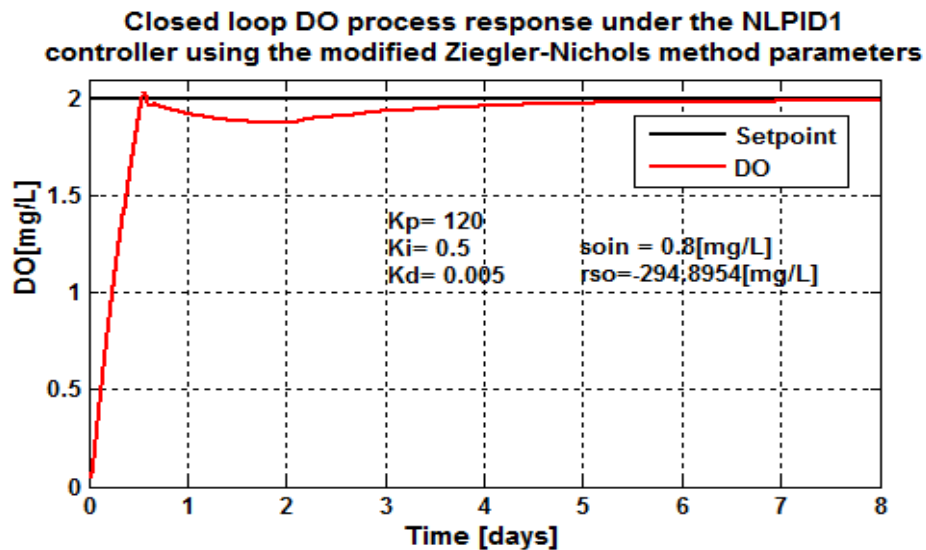


Figure 5.9: Closed loop DO process response under the NLPID1 controller, when the set-point is 2 mg/L , $s_{o,in}=0.8 \text{ mg/L}$ and $r_{so}=-294.8954 \text{ mg/L/day}$

The integral term is decreased to better the system behavior. After the first control parameters modification in Figure 5.8 the system response is much better, but has oscillations at the final equilibrium point. Additional tuning of the controller parameters is

applied and the Figure 5.9 shows that the results of the closed loop system behavior is completely improved through the tuning process.

The controller parameters obtained through the process of tuning are shown in Table 5.2 below:

Table 5.2: NLPID1 Parameters obtained by tuning

Parameters	LPID designed	NLPID1	NLPID1 variant 1	NLPID1 variant 2-selected
K_p	120	120	120	120
K_i	50	50	5	0.5
K_d	0.005	0.005	0.005	0.005
Process characteristic	Fast response time with the overshoot of 25%	System is unstable.	Oscillations are reduced.	System is stable & no oscillations.

On the basis of the results from Table 5.2 the second modification (variant 2) is selected to be used for further investigations in this section of the thesis, to test the system reactions when set-points and disturbances are changed.

In the next figures (Figure 5.10 to Figure 5.24) the disturbances and the set-point variation to different values are performed. This is done in order to make an examination on how well the nonlinear controller (NLPID1) can be able to control the DO system, when uses the tuned control parameters of the Z-N method. Table 5.3 shows the variations of the DO disturbances to be tested.

Table 5.3: Variation for the DO set point and the DO process disturbances

Set-point	S_{oin}	r_{so}
2.7	0.01	-294.8954
2.7	0.01	-309.6402
2.7	0.01	-280.1506
2.7	0.01	-442.3431
2.7	0.01	-147.4477
2	0.8	-294.8954
2	0.8	-309.6402
2	0.8	-280.1506
2	0.8	-442.3431
2	0.8	-147.4477
1.7	0.8	-294.8954
1.7	0.8	-309.6402
1.7	0.8	-280.1506
1.7	0.8	-442.3431
1.7	0.8	-147.4477

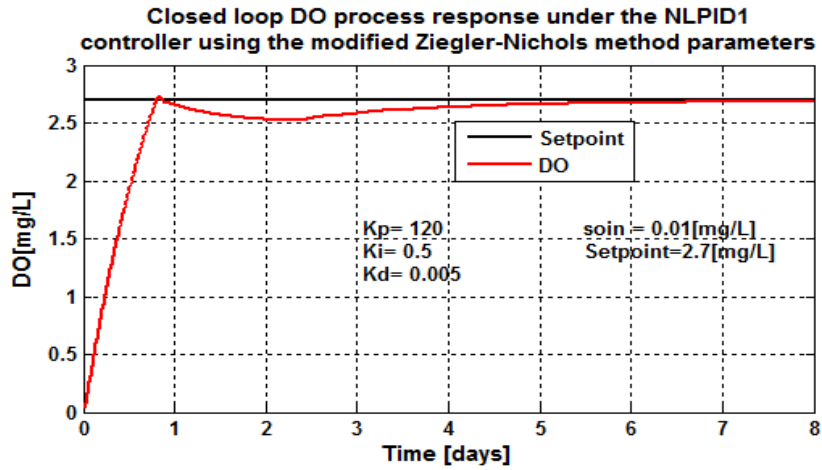


Figure 5.10: Closed loop DO process response under the NLPID1 controller, when the set-point is 2.7 mg/L and $r_{so} = -294.8954 \text{ mg/L/day}$

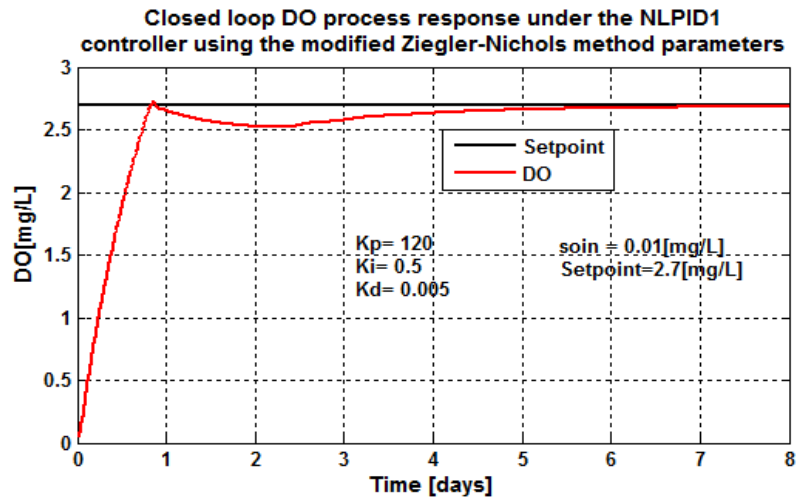


Figure 5.11: Closed loop DO process response under the NLPID1 controller, when the set-point is 2.7 mg/L and $r_{so} = -309.6402 \text{ mg/L/day}$

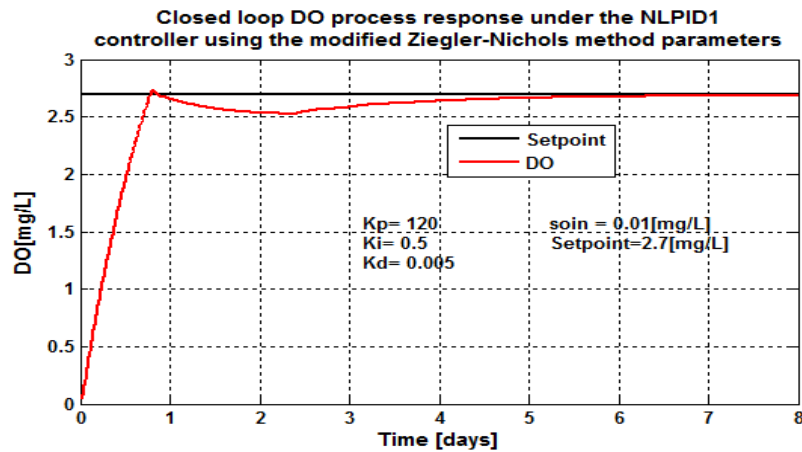


Figure 5.12: Closed loop DO process response under the NLPID1 controller, when the set-point is 2.7 mg/L and $r_{so} = -280.1506 \text{ mg/L/day}$

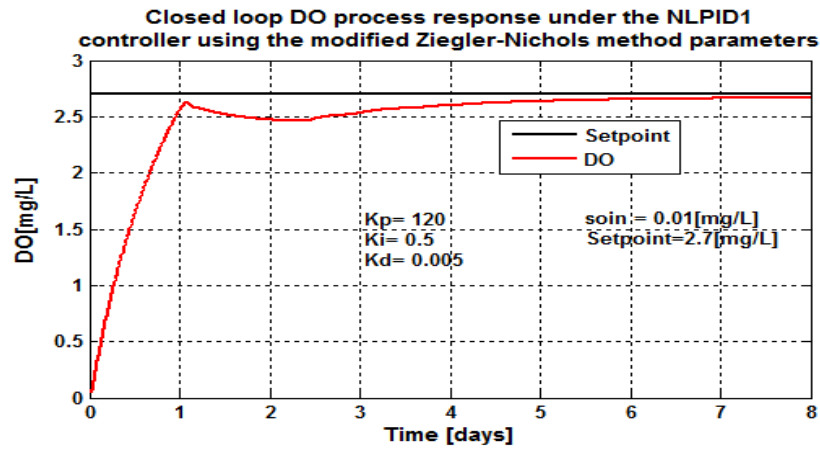


Figure 5.13: Closed loop DO process response under the NLPID1 controller, when the set-point is 2.7 mg/L and $r_{so} = -442.3431 \text{ mg/L/day}$

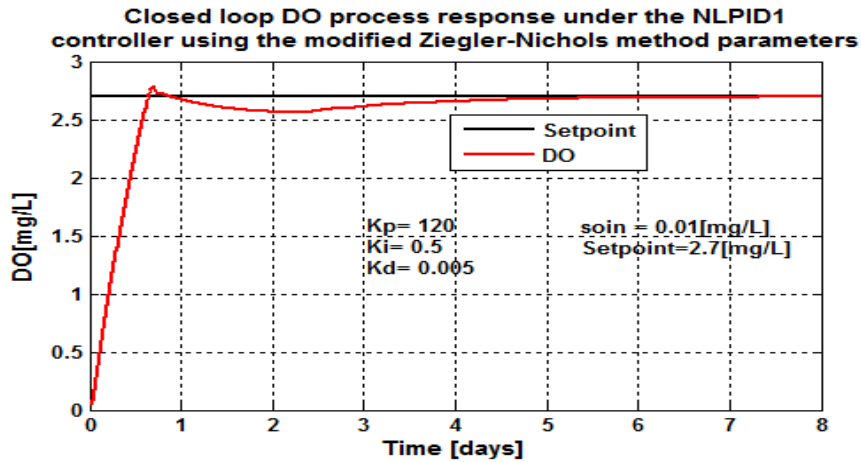


Figure 5.14: Closed loop DO process response under the NLPID1 controller, when the set-point is 2.7 mg/L and $r_{so} = -147.4477 \text{ mg/L/day}$

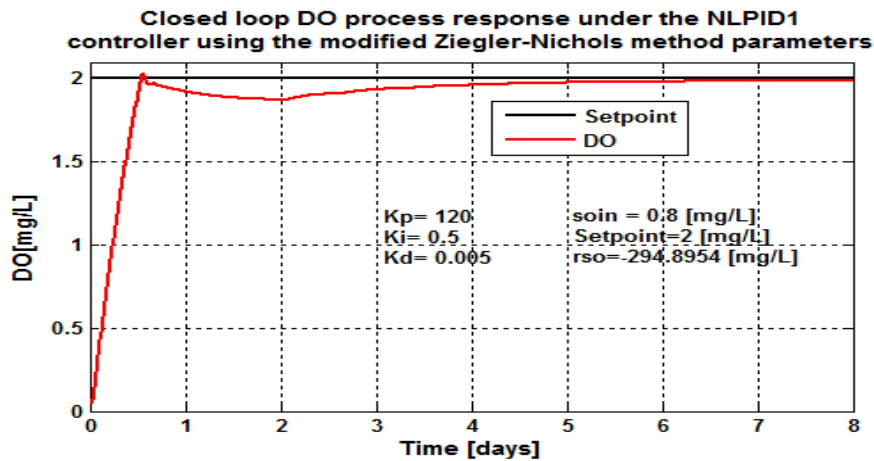


Figure 5.15: Closed loop DO process response under the NLPID1 controller, when the set-point is 2 mg/L and $r_{so} = -294.8954 \text{ mg/L/day}$

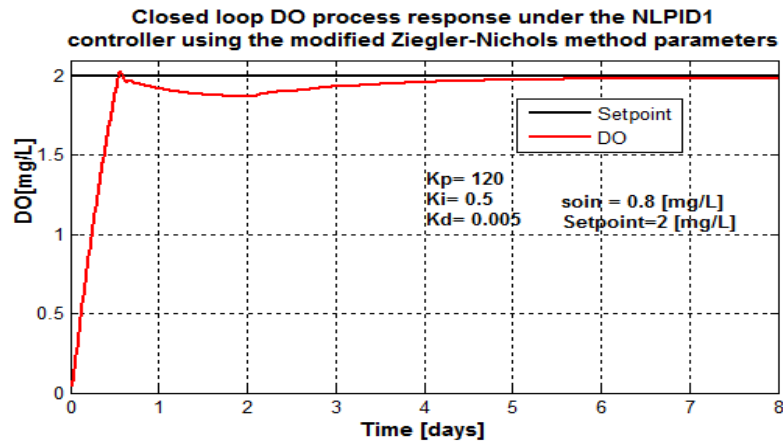


Figure 5.16: Closed loop DO process response under the NLPID1 controller, when the set-point is 2 mg/L and $r_{so} = -309.6402 \text{ mg/L/day}$

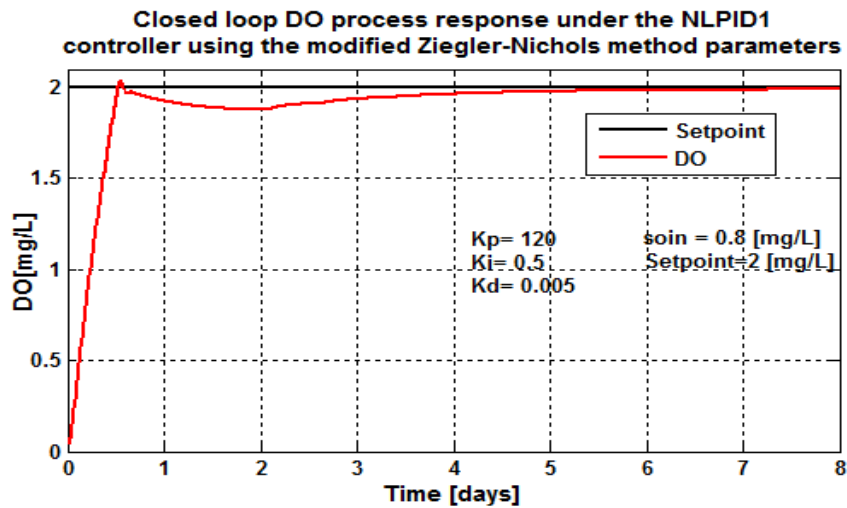


Figure 5.17: Closed loop DO process response under the NLPID1 controller, when the set-point is 2 mg/L and $r_{so} = -280.1506 \text{ mg/L/day}$

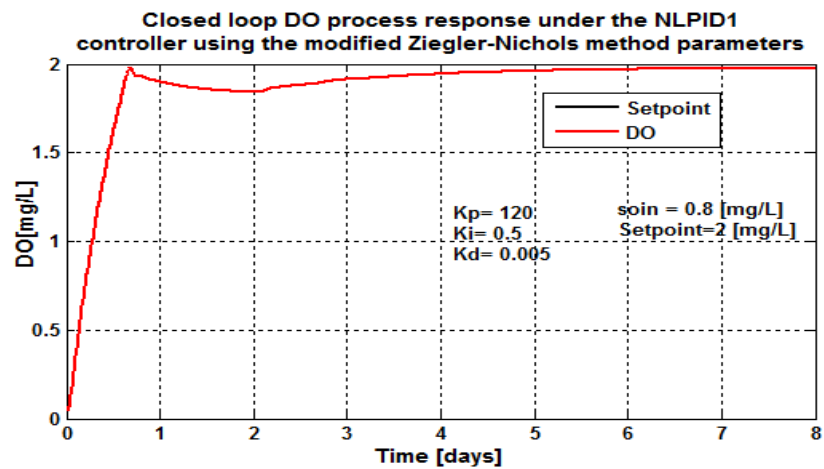


Figure 5.18: Closed loop DO process response under the NLPID1 controller, when the set-point is 2 mg/L and $r_{so} = -442.3431 \text{ mg/L/day}$

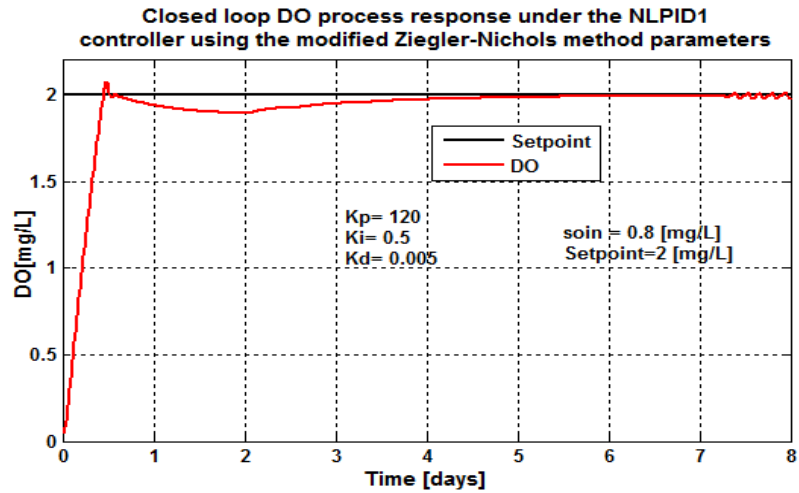


Figure 5.19: Closed loop DO process response under the NLPID1 controller, when the set-point is 2 mg/L and $r_{so} = -147.4477 \text{ mg/L/day}$

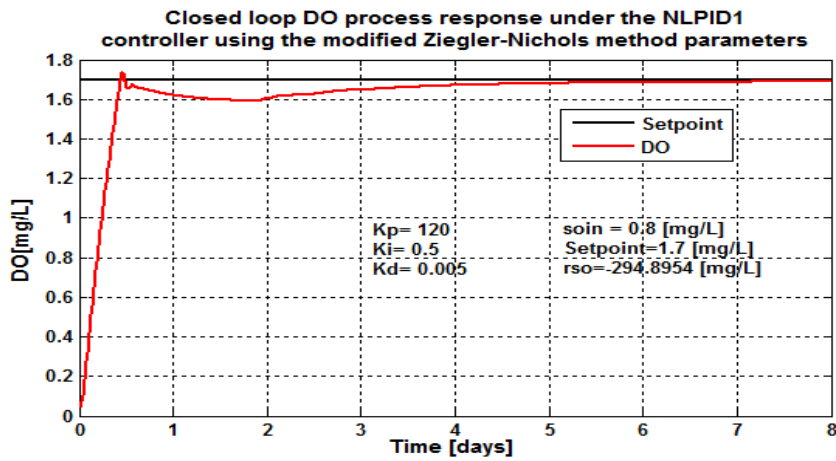


Figure 5.20: Closed loop DO process response under the NLPID1 controller, when the set-point is 1.7 mg/L and $r_{so} = -294.8954 \text{ mg/L/day}$

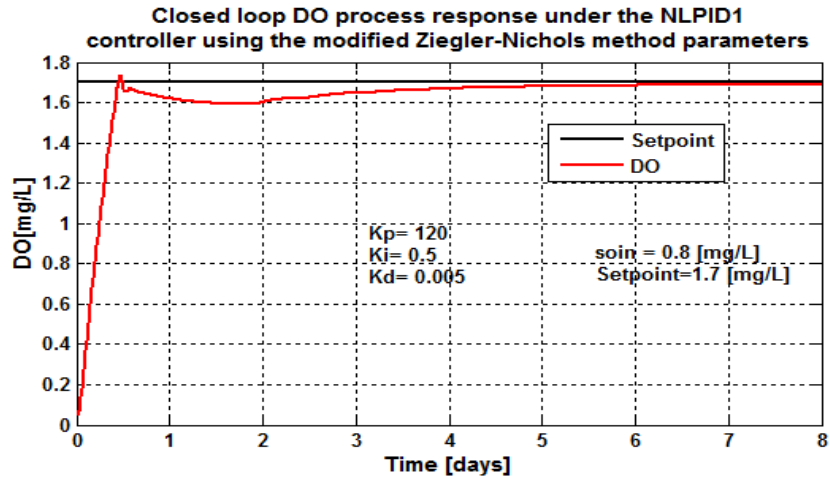


Figure 5.21: Closed loop DO process response under the NLPID1 controller, when the set-point is 1.7 mg/L and $r_{so} = -309.6402 \text{ mg/L/day}$

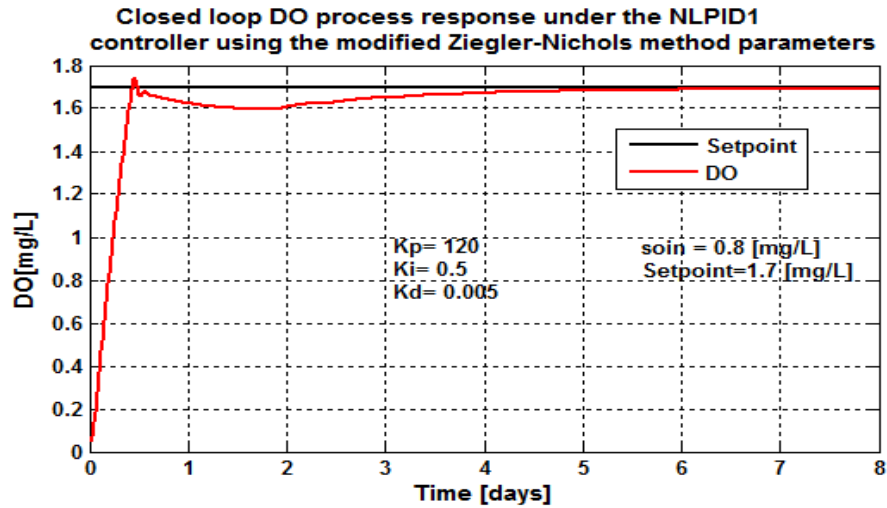


Figure 5.22: Closed loop DO process response under the NLPID1 controller, when the set-point is 1.7 mg/L and $r_{so} = -280.1506 \text{ mg/L/day}$

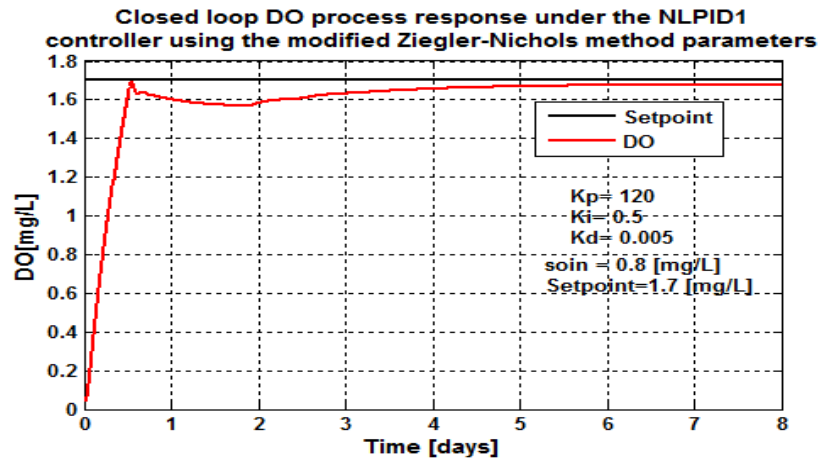


Figure 5.23: Closed loop DO process response under the NLPID1 controller, when the set-point is 1.7 mg/L and $r_{so} = -442.3431 \text{ mg/L/day}$

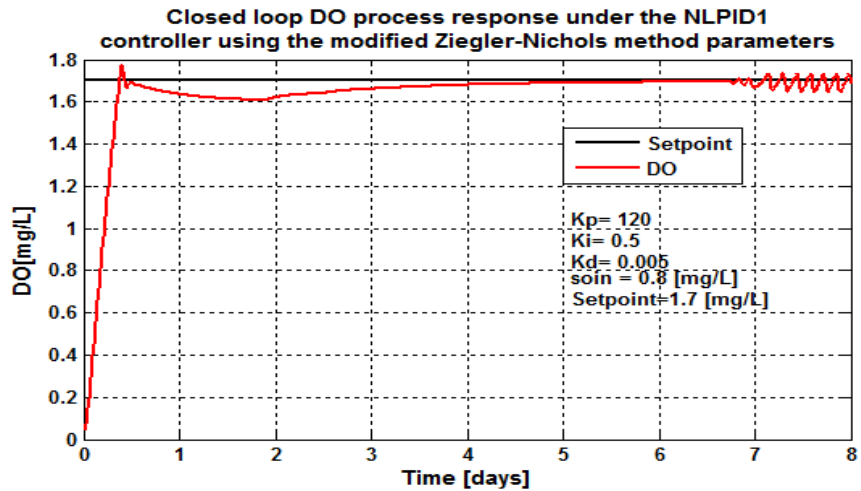


Figure 5.24: Closed loop DO process response under the NLPID1 controller, when the set-point is 1.7 mg/L and $r_{so} = -147.4477 \text{ mg/L/day}$

5.3.3.2.1 Characteristics analysis and discussion

Table 5.4: Closed loop nonlinear DO process characteristics under the NLPID1 controller

Parameters			Characteristics			
Set point	s_{oin} [mg / L]	r_{so} mg / L / day	Time delay [days]	Steady state error [mg / L]	Rise time [days]	Settling time [days]
2.7	0.01	-294.8954	0.05	0.02	0.35	4.2
2.7	0.01	-309.6402	0.05	0.025	0.53	4.3
2.7	0.01	-280.1506	0.05	0.02	0.497	4
2.7	0.01	-442.3431	0.05	0.05	0.43	4.8
2.7	0.01	-147.4477	0.05	0.01	0.463	3.8
2	0.8	-294.8954	0.05	0.02	0.365	3.6
2	0.8	-309.6402	0.05	0.024	0.366	3.8
2	0.8	-280.1506	0.05	0.02	0.36	3.5
2	0.8	-442.3431	0.05	0.05	0.403	4.5
2	0.8	-147.4477	0.05	0.01	0.33	3.5
1.7	0.8	-294.8954	0.05	0.02	0.306	3.6
1.7	0.8	-309.6402	0.05	0.024	0.308	3.8
1.7	0.8	-280.1506	0.05	0.02	0.303	3.6
1.7	0.8	-442.3431	0.05	0.05	0.336	4.5
1.7	0.8	-147.4477	0.05	0.01	0.28	3.6

The closed loop behaviors under different internal disturbances and different set-point values are tested. From Figures 5.10 to Figures 5.14 the process reaction was able to achieve the set-point value and is not affected by the disturbances and set-point changes. The reaction of the DO process under the NLPID1 controller with unchanged parameters for the LPID controller obtained by means of the Ziegler-Nichols method shows a fast response time with no stability (Figures 5.7 & 5.8). In that case a manual tuning of the parameters is done to obtain better result as shows in Figures 5.9 - 5.24, but the settling time is much bigger.

Figure 5.10 to Figure 5.24 show the results of the closed loop system behavior when different internal disturbances ($s_{o,in}$ & r_{so}) and different set-point values are applied. Changes in the values of the disturbances did not show negative effect on the process operation. The process transition curves begin by showing a fast response time, little negative overshoot and long settling time. But the good thing is that the designed controller is able to stabilize the system at any set-point value. It has been noticed that when the disturbance (r_{so}) is low the system is stable with some little oscillations between 7th – 8th days (see Figure 5.24).

The following section applies the control parameter designed through Z-N method into the NLPID2 to control DO process in the ASP.

5.3.3.3 Simulation results of the closed loop nonlinear DO process under the NLPID2

The parameters calculated for the LPID are used in the nonlinear PID controller and simulation of the closed loop behavior is done according to Figure 4.2.

The equivalent Simulink block diagram is given in Figure 5.5, where the parameters designed through Ziegler-Nichols method and applied in sub-section 5.3.3.1 are used.

The first phase of the investigation of the capability of the values of the controller parameters to stabilize the system is done according to the following steps:

- Original designed value for Ziegler-Nichols $K_p = 120$, $K_i = 50$ and $K_d = 0.005$. The system has a big overshoot (see Figure 5.25).
- First change - the value of K_i is changed from 50 to 5. The system result is unstable, Figure 5.26
- Second change - the value of K_i is changed from 5 to 0.5, and K_p from 120 to 200 and K_d remain unchanged, Figure 5.27
- Accepted values for further investigation $K_i = 0.5$, $K_p = 200$ and $K_d = 0.005$. (from Figure 5.28 – Figure 5.42)

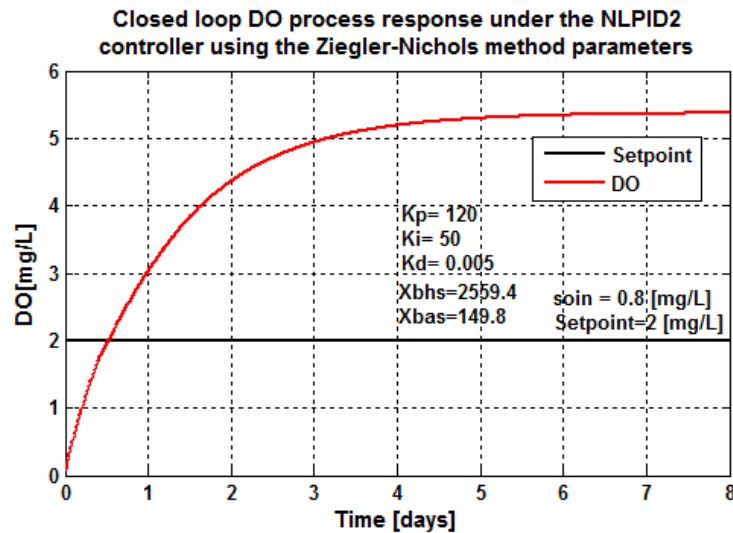


Figure 5.25: Closed loop DO process response under the NLPID2 controller, when the set-point is 2 mg/L and $s_{oin} = 0.8 \text{ mg/L}$

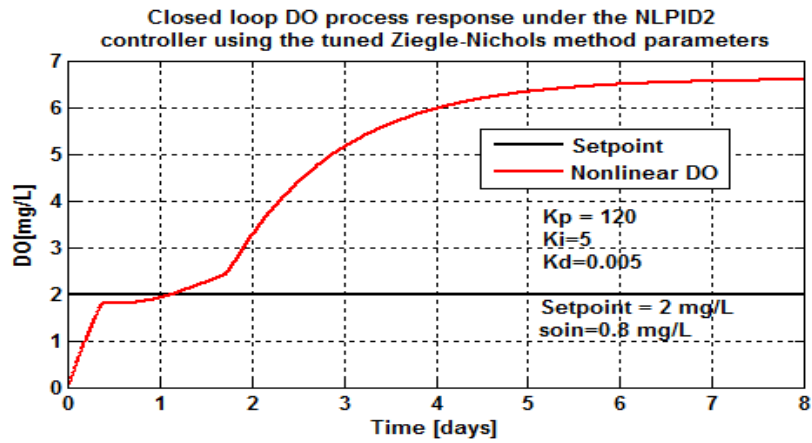


Figure 5.26: Closed loop DO process response under the NLPID1 controller, when the set-point is 2.7 mg/L , $s_{oin}=0.01 \text{ mg/L}$ and $r_{so}=-294.8954 \text{ mg/L}$

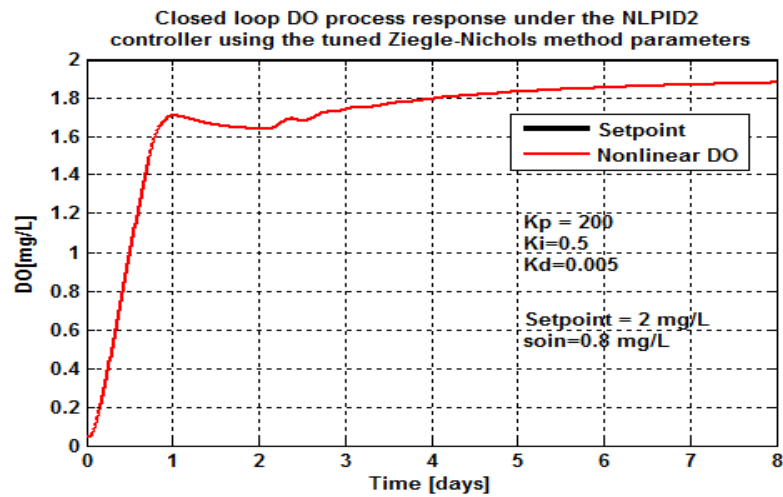


Figure 5.27: Closed loop DO process response under the NLPID1 controller, when the set-point is 2 mg/L , $s_{oin}=0.01 \text{ mg/L}$ and $r_{so}=-294.8954 \text{ mg/L}$

Figures 5.25 and 5.26 show that the nonlinear PID (NLPID2) controller cannot be able to control the nonlinear DO process if it is using un-tuned the designed before controller parameters for the LPID controller based on Ziegler-Nichols (Z-N). Therefore, the second tuned values of controller parameters are applied to the NLPID2 controller (Figure 5.5). The results are shown in Figure 5.27, which shows an improvement in the system behavior; although the trajectories settle below the desired value of 2 mg/L , they show to be the best for the DO process under the NLPID2. They can keep the closed loop system away from overshoots and oscillation during the trial and the error process. The values used in this figure (Figure 5.27) were accepted for further investigation. The obtained values through the process of tuning the parameters and trying to find the best values that can control the system are shown in Table 5.5

Table 5.5: NLPID2 Parameters obtained by tuning

Parameters	LPID designed	NLPID2 original	NLPID2 variant 1	NLPID2 variant 2	NLPID2 variant 2-selected
K_p	120	120	120	200	200
K_i	50	50	5	0.5	0.5
K_d	0.005	0.005	0.005	0.005	0.005
Process characteristics	Fast response time with the overshoot of 25%	System overshoots by 440%.	Unstable, overshoot and settles at a very higher point than the required set point value.	Stable and over-damped.	Good system behavior

On the basis of the results from Table 5.5 the selected values of $K_p = 200$, $K_i = 0.5$ and $K_d = 0.005$ are preferred to be used for further investigations in this section of the thesis to test the system reactions when set-points and disturbances are changed. The different disturbances and set point value that are used to investigate further the performance of the system are shown in Table 5.3

As the variations of the DO disturbances and the set-point changes are applied in the closed loop system, the next figures (Figure 5.28 to Figure 5.41) show the results. This is done in order to make an examination on how well, the nonlinear controller (NLPID2) will work with the DO system, when uses the tuned control parameters, in Table 5.3.

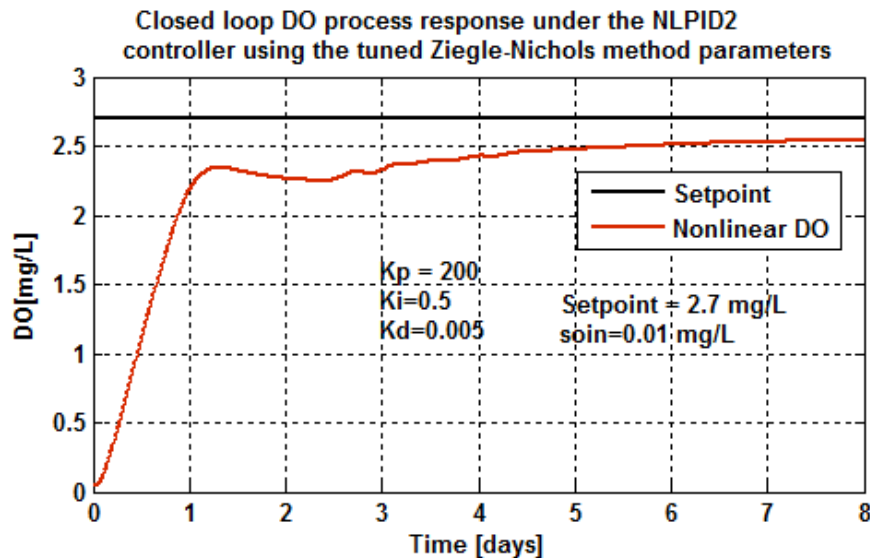


Figure 5.28: Closed loop DO process response under the NLPID2 controller, when the set-point is 2.7 mg/L , $s_{oin} = 0.01 \text{ mg/L}$ and $r_{so} = -294.8954 \text{ mg/L/day}$

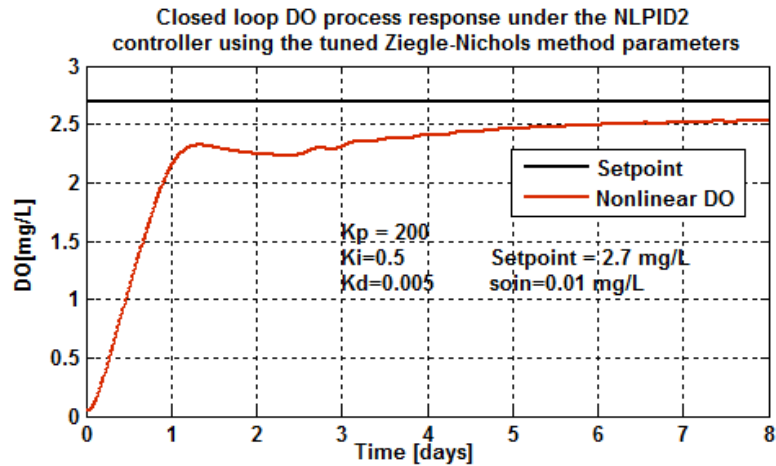


Figure 5.29: Closed loop DO process response under the NLPID2 controller, when the set-point is 2.7 mg/L , $s_{oin} = 0.01 \text{ mg/L}$ and $r_{so} = -309.6402 \text{ mg/L/day}$

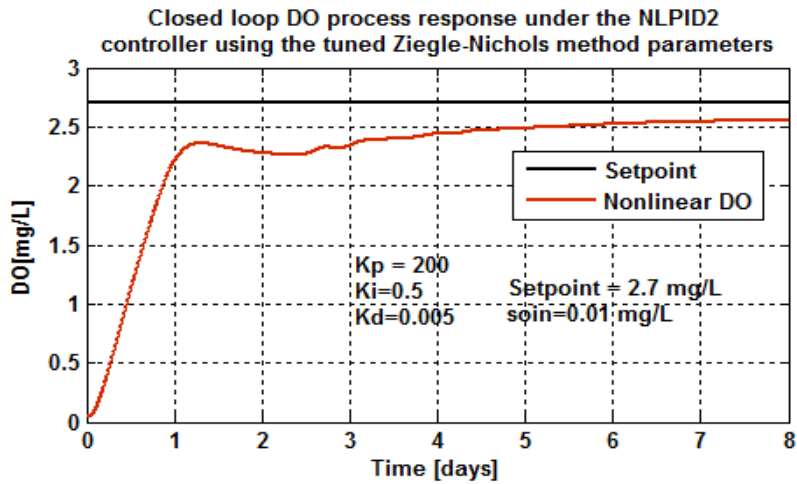


Figure 5.30: Closed loop DO process response under the NLPID2 controller, when the set-point is 2.7 mg/L , $s_{oin} = 0.01 \text{ mg/L}$ and $r_{so} = -280.1506 \text{ mg/L/day}$

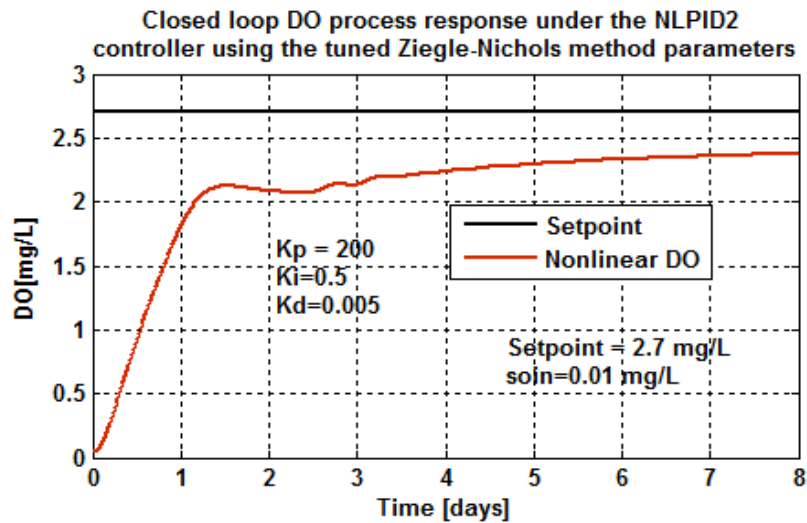


Figure 5.31: Closed loop DO process response under the NLPID2 controller, when the set-point is 2.7 mg/L , $s_{oin} = 0.01 \text{ mg/L}$ and $r_{so} = -442.3431 \text{ mg/L/day}$

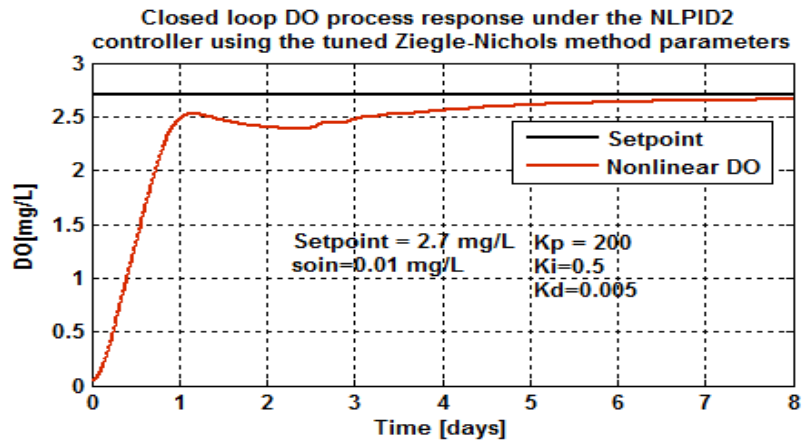


Figure 5.32: Closed loop DO process response under the NLPID2 controller, when the set-point is 2.7 mg/L , $s_{oin} = 0.01 \text{ mg/L}$ and $r_{so} = -147.4477 \text{ mg/L/day}$

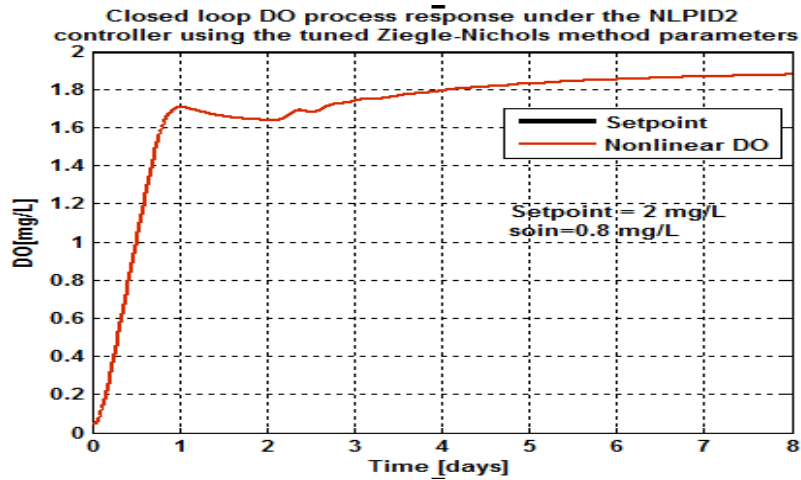


Figure 5.33: Closed loop DO process response under the NLPID2 controller, when the set-point is 2 mg/L , $s_{oin} = 0.8 \text{ mg/L}$ and $r_{so} = -294.8954 \text{ mg/L/day}$

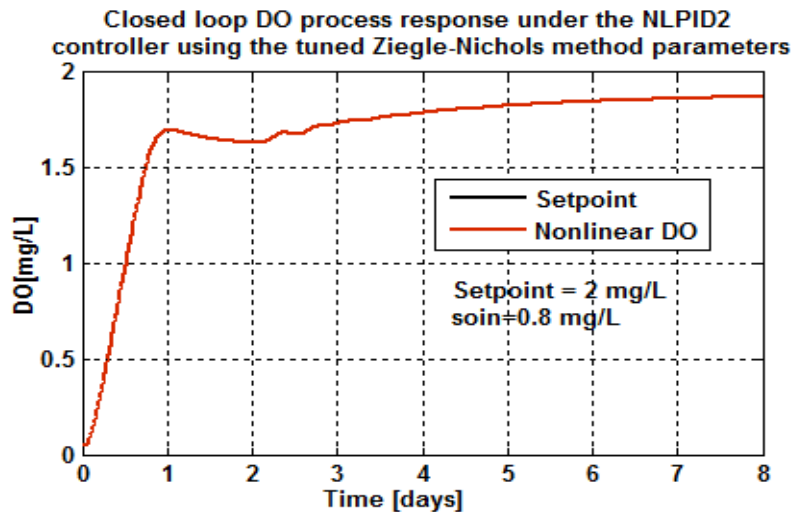


Figure 5.34: Closed loop DO process response under the NLPID2 controller, when the set-point is 2 mg/L , $s_{oin} = 0.8 \text{ mg/L}$ and $r_{so} = -309.6402 \text{ mg/L/day}$

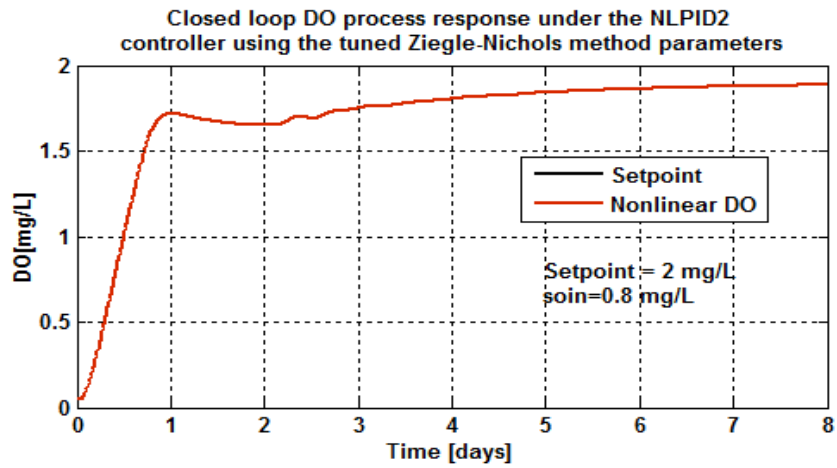


Figure 5.35: Closed loop DO process response under the NLPID2 controller, when the set-point is 2 mg/L , $s_{oin} = 0.8\text{ mg/L}$ and $r_{so} = -280.1506\text{ mg/L/day}$

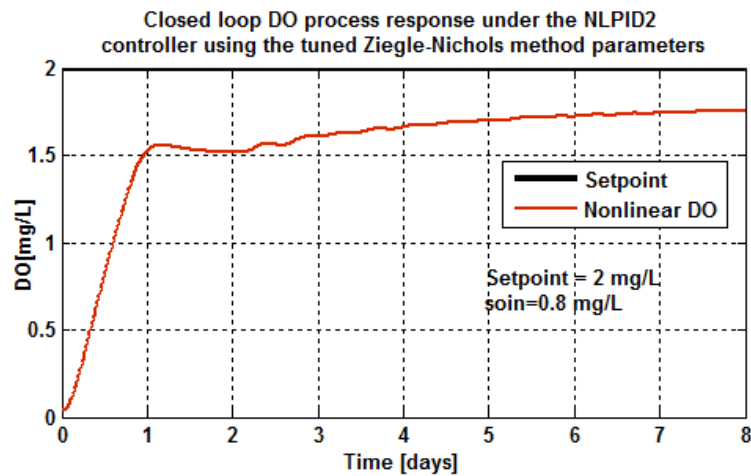


Figure 5.36: Closed loop DO process response under the NLPID2 controller, when the set-point is 2 mg/L , $s_{oin} = 0.8\text{ mg/L}$ and $r_{so} = -442.3431\text{ mg/L/day}$

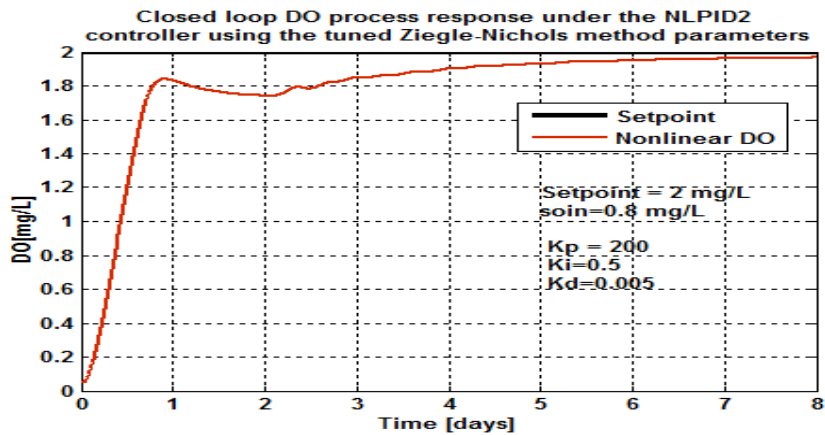


Figure 5.37: Closed loop DO process response under the NLPID2 controller, when the set-point is 2 mg/L , $s_{oin} = 0.8\text{ mg/L}$ and $r_{so} = -147.4477\text{ mg/L/day}$

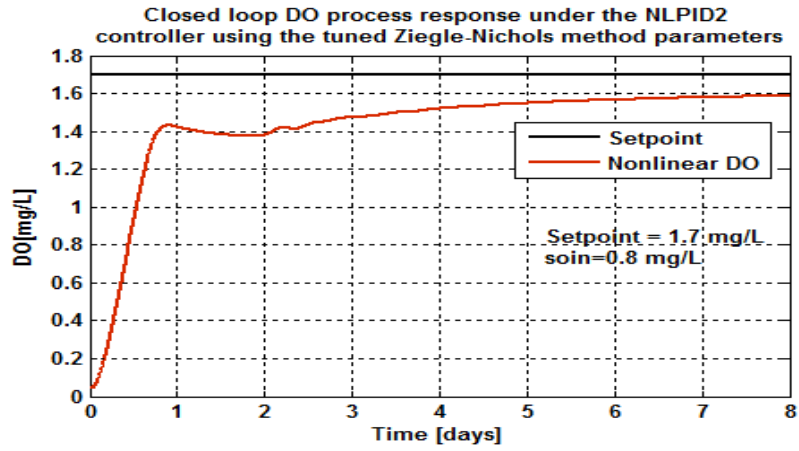


Figure 5.38: Closed loop DO process response under the NLPID2 controller, when the set-point is 1.7 mg/L , $s_{oin} = 0.8 \text{ mg/L}$ and $r_{so} = -294.8954 \text{ mg/L/day}$

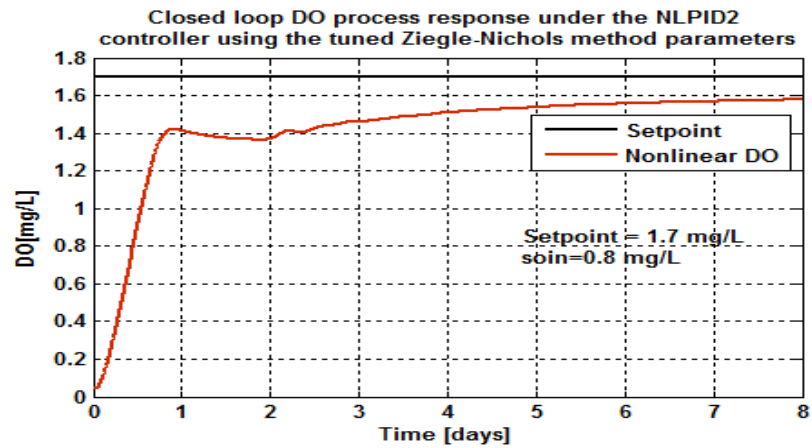


Figure 5.39: Closed loop DO process response under the NLPID2 controller, when the set-point is 1.7 mg/L , $s_{oin} = 0.8 \text{ mg/L}$ and $r_{so} = -309.6402 \text{ mg/L/day}$

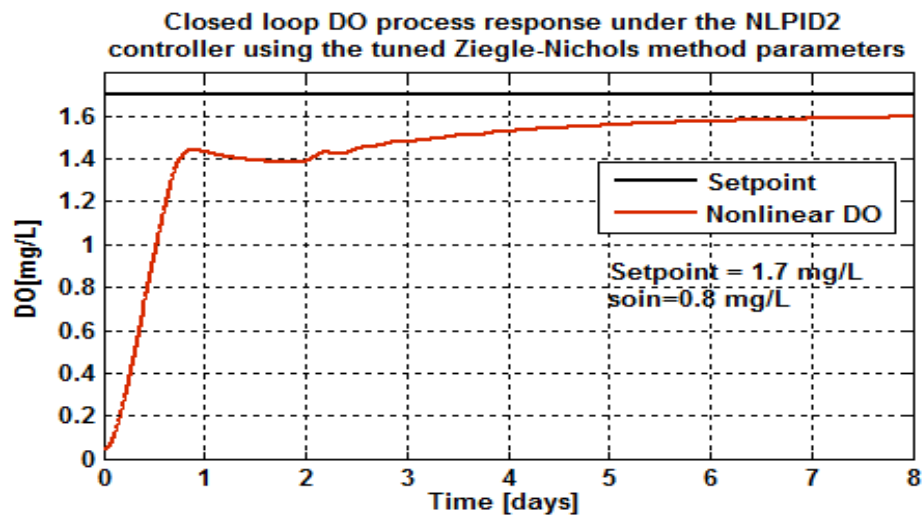


Figure 5.40: Closed loop DO process response under the NLPID2 controller, when the set-point is 1.7 mg/L , $s_{oin} = 0.8 \text{ mg/L}$ and $r_{so} = -280.1506 \text{ mg/L/day}$

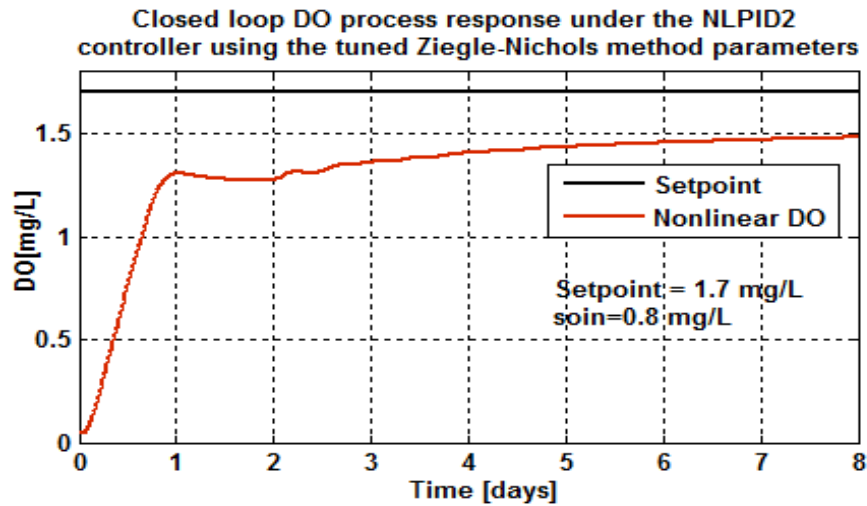


Figure 5.41: Closed loop DO process response under the NLPID2 controller, when the set-point is 1.7 mg/L , $s_{oin} = 0.8 \text{ mg/L}$ and $r_{so} = -442.3431 \text{ mg/L/day}$

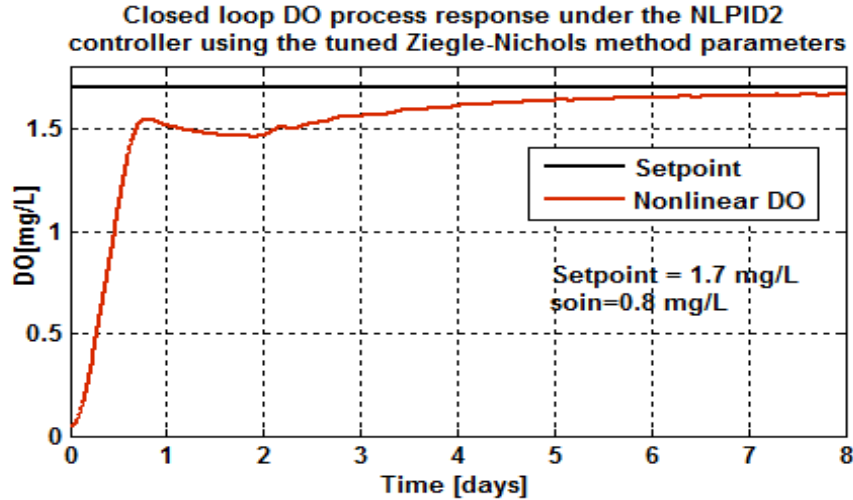


Figure 5.42: Closed loop DO process response under the NLPID2 controller, when the set-point is 1.7 mg/L , $s_{oin} = 0.8 \text{ mg/L}$ and $r_{so} = -147.4477 \text{ mg/L/day}$

The results in Figures 5.33 and 5.37 are based on constant set-point value of 2 mg/L and different internal disturbances shown in Table 5.3. The dissolved oxygen concentration process response has followed a right reaction path and no overshoots, but the problem with these selected control parameters is that with them the controller cannot control the process to the desired set-point value. Extra tuning is needed to solve this issue. Figures 5.38 to 5.42 use the set-point of 1.7 mg/L with different disturbance. Making the observation of the system behavior in the above figures, it can be said that the second designed nonlinear PID (NLPID2) controller through Ziegler-Nichols (Z-N) tuning method for design of the LPID controller was not convenient to control the

dissolved oxygen concentration process, despite the fact that it has followed a right response path, it does not reach the desired value. Table 5.6 shows the characteristics of the DO process under the NLPID2 controller.

Table 5.6: Closed loop DO process characteristics under the NLPID2

Parameters			Characteristics			
Set point	S_{oin}	r_{so}	Time delay [days]	Steady state error [mg/L]	Rise time [days]	Settling time [days]
2.7	0.01	-294.8954	0.06	0.19	0.5	4.5
2.7	0.01	-309.6402	0.06	0.2	0.6	4.85
2.7	0.01	-280.1506	0.06	0.19	0.6	4.5
2.7	0.01	-442.3431	0.06	0.4	0.9	5
2.7	0.01	-147.4477	0.06	0.04	0.5	4
2	0.8	-294.8954	0.06	0.13	0.5	4.5
2	0.8	-309.6402	0.06	0.13	0.6	4.8
2	0.8	-280.1506	0.06	0.114	0.5	4.5
2	0.8	-442.3431	0.06	0.245	0.9	5
2	0.8	-147.4477	0.06	0.035	0.5	4
1.7	0.8	-294.8954	0.06	0.115	0.5	4.5
1.7	0.8	-309.6402	0.06	0.12	0.5	4.7
1.7	0.8	-280.1506	0.06	0.11	0.5	4.4
1.7	0.8	-442.3431	0.06	0.216	0.5	5
1.7	0.8	-147.4477	0.06	0.035	0.5	4

5.3.3.3.1 Discussion

The behavior of the closed loop DO process has been tested using the designed and modified Ziegler-Nichols parameters and the simulation results for linear and the two nonlinear PID controllers have been shown above. The system response using the NLPID controllers with the parameters for the LPID controller obtained by the Ziegler-Nichols method, initially show a good response time, but with NLPID2 the system does not arrive at the set point value. It is observed that when NLPID controller use parameters for the LPID controller designed through Ziegler-Nichols method, it does not achieve good performance of the closed loop nonlinear system. In this case, manual tuning of the parameters is done to obtain better results.

Looking to the results of NLPID1 and NLPID2, the first nonlinear controller (NLPID1) has performed much better; it has a good steady state response, but has a bigger settling time. The second nonlinear controller (NLPID2) has a quicker response time, but it always stabilizes the DO process below the set-point

values. This conclusion has been drawn from the simulation results as captured in the tables (Table 5.4 and Table 5.6).

5.4 Conclusion

Two nonlinear NLPID controllers have been used in this Chapter to control the nonlinear DO process under different operation conditions, different set-point and disturbances. The results have shown that the Ziegler-Nichols control parameters designed for the LPID controller cannot be directly used for the NLPID controllers to control and nonlinear process of the DO concentration. Additional controller parameters tuning is needed to achieve the convenient behavior of the controlled nonlinear system.

The next chapter (Chapter 6) is based on the application of the Pole-Placement method for the design of the LPID and NLPID controller based on the linearized DO model. This is named as Case study 1 (PP1 controller design method based on the linearized DO model).

CHAPTER SIX

APPLICATION OF THE POLE-PLACEMENT METHOD FOR DESIGN OF THE PARAMETERS OF THE LPID AND NLPID CONTROLLERS FOR THE CASE OF THE LINEARIZED MODEL OF THE DO PROCESS

6.1 Introduction

Pole placement is a method employed in feedback control system theory to place the closed-loop poles of a plant in pre-determined positions in the s-plane. Pole placement method is one of the classic control theories and has an advantage in system control to achieve a given desired process performance. Theoretically pole placement is to set the desired pole location and to move the pole position of the system to that desired pole position. Mathematically once the closed loop system transfer function is defined, the desired transfer function should be also defined, and then each coefficient of the same order in the characteristic polynomials of the two systems is compared to be the same. This pole placement control design method results to the desired system response and is easy to find the gains mathematically but the accuracy of the closed loop system transfer function is significantly important and this method is expensive to implement in the high order systems.

The tasks of the control systems used in WWTP can be divided into two main categories:

- Tracking (servomechanisms) and
- Regulation or stabilization.

In the tracking control problems, the objective of the design is to construct a controller, so that the system output tracks the specified time-varying trajectory. In stabilization problems, a control system is designed such that the state of the closed loop system will be stabilized around an equilibrium point (Hai-bin, *et al.*, 2006). Most of the controllers designed to implement these tasks are linear ones. They can be applied successfully for linear systems. Nonlinear control is the area of control engineering involved with systems whose behavior is nonlinear, time-variant, or both. Nonlinear control theory studies describe how to apply the existing linear methods to non-linear control systems. Linear Time Invariant (LTI) system can be used for the analysis and design of a nonlinear controller which can have attractive characteristics such as increased speed, or decreased control energy. However, nonlinear control theory usually requires more rigorous mathematical analysis to justify its conclusions.

This Chapter discusses the application of the Pole-Placement method for the design of the controller parameters in section 6.2, section 6.3 is based on the simulation of the closed loop DO process under LPID controller, section 6.4 gives the closed loop simulations of the DO closed loop process based on the two NLPID controllers (NLPID1 and NLPID2) using the designed tuned the LPID controller parameters. The Conclusion of this Chapter is given in section 6.5.

6.2 Application of the Pole-Placement method for design of a Linear PID controller's parameters

The design of the controller by the pole placement method is based on the desired behavior of the closed loop system. The desired behavior is determined by the values of the poles of the closed loop transfer function. The calculation of the values of the PID controller parameters is through the comparison of the characteristic equation of the closed loop system and the desired characteristic of the closed loop system. The Pole Placement (P-P) method is used in this Chapter for design of the LPID controller parameters for the DO process. Then, the obtained parameters for the LPID controller are used in Matlab/ Simulink to examine the closed loop behavior of the DO process under the NLPID controllers with the obtained parameters for the LPID controller.

The steps of the pole placement algorithm are: Hasaniien *et al.*, (2009)

- I. Make use of the first order linearized equation of the DO process and take the LPID controller equation to form the equation of the closed loop system. The controller parameters are unknown.
- II. Form the characteristic equation of the closed loop system in which the controller parameters are unknown
- III. Specify the desired poles for the behavior of the closed loop DO system and form the desired characteristic equation of the closed loop system
- IV. Compare the two characteristic equations and calculate the value of the unknown parameters.

These steps are described below in detail, as follows:

6.2.1 Linearization of the nonlinear model of the DO Process

The nonlinear model of the DO process is given by Equation (6.1)

$$\dot{s}_o = f(s_o, u) = \frac{Q}{V}(s_{o,in} - s_o) + r_{so} + K_1[1 - e^{-K_2 u}](s_{s,sat} - s_o) = As_o + Bu \quad (6.1)$$

The nonlinear model of the DO process has to be presented as a linear model in the state space as shown by Equation 6.1. The representation can be obtained on the basis of Taylor series calculated around the steady state points $s_{o,ss}$ and u_{ss} , for the state and control variables. The Taylor series is used to represent a function as an infinite sum of the function derivatives and the function variables calculated at a single given point. The nonlinear model $f(s_o, u)$ is differentiated with respect to s_o and u . Then the Taylor series representation of the Equation 6.1 for only the first order derivatives is:

$$\dot{s}_o = f(s_o, u) \Big|_{s_{o,ss}, u_{ss}} + \frac{df(s_o, u)}{ds_o} \Big|_{s_{o,ss}, u_{ss}} (s_o - s_{o,ss}) + \frac{df(s_o, u)}{du} \Big|_{s_{o,ss}, u_{ss}} (u - u_{ss}) = As_o + Bu \quad (6.2)$$

On the basis of the above Equation:

$$A = \frac{df(s_o, u)}{ds_o} \Big|_{s_{o,ss}, u_{ss}} = - \left(\frac{Q}{V} + K_1 [1 - e^{-K_2 u}] \right) \Big|_{s_{o,ss}, u_{ss}} \quad (6.3)$$

$$B = \frac{df(s_o, u)}{du} \Big|_{s_{o,ss}, u_{ss}} = K_1 K_2 [e^{-K_2 u}] * (s_{s,sat} - s_o) \Big|_{s_{o,ss}, u_{ss}} \quad (6.4)$$

And it is accepted that

$$f(s_o, u) \Big|_{s_{o,ss}, u_{ss}} + \frac{df(s_o, u)}{ds_o} \Big|_{s_{o,ss}, u_{ss}} (-s_{o,ss}) + \frac{df(s_o, u)}{du} \Big|_{s_{o,ss}, u_{ss}} (-u_{ss}) = 0 \quad (6.5)$$

The calculated value of the coefficients A and B for the steady state values $s_{o,ss} = 2mg/L$ and $u_{ss} = 50000mg/L/day$ are: $A = -3$, $B = 200$

The linearized DO process model is a state space model of the kind of:

$$\dot{s}_o = As_o + Bu \quad (6.6)$$

$$y = Cs_o \quad (6.7)$$

Where:

- s_o - is the state space variable,
- u - is the control vector for the model,
- A and B - are the state space and control coefficients of the model,
- $C=1$ - is the output coefficient for the dissolved oxygen concentration.

The obtained linearised model (6.6), (6.7) is used to design the PID controller parameters through the pole placement method.

The coefficients A , B and C are obtained through linearization of the nonlinear DO process model for the selected benchmark parameters for the steady state process behavior as given in Table 3.2 of Chapter 3 for the benchmark structure model parameters.

The Laplace transform of Equation (6.6) under zero initial conditions has yielded to the transfer function of the linearized DO process below;

$$G_p(s) = \frac{s_o(s)}{u(s)} = \frac{B}{s - A} \quad (6.8)$$

6.2.2 Characteristic equation of the closed loop system

The transfer function of the usual PID controller in s-domain can be represented as shown below

$$U(s) = E(s) \left(K_p + \frac{K_i}{s} + K_d s \right) \quad (6.9)$$

The transfer function of the PID controller can be represented as:

$$\frac{U(s)}{E(s)} = G_{PID}(s) = \frac{K_p s + K_i + K_d s^2}{s} \quad (6.10)$$

The following block diagram is used to obtain a closed loop DO process transfer function.

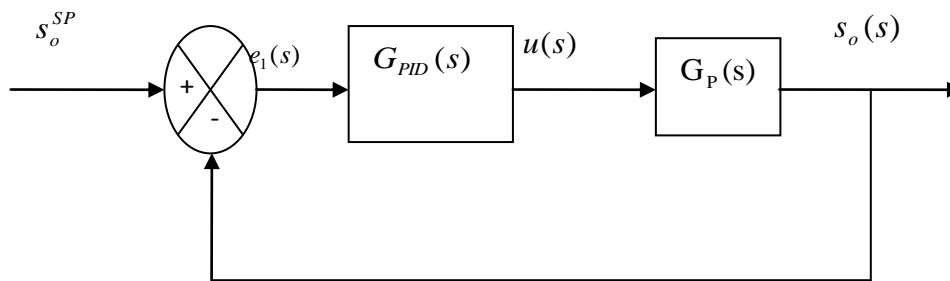


Figure 6.1: Block diagram of the closed loop system

From the block diagram in Figure 6.1 the closed loop transfer function is

$$G_{CL}(s) = \frac{G_{PID}(s) * G_p(s)}{1 + G_{PID}(s) * G_p(s)} \quad (6.11)$$

After substitution of Equation (6.8) and Equation (6.10) in Equation (6.11) the resulting closed loop transfer function is represented by Equation (6.12) below:

$$G_{CL}(s) = \frac{[K_d s^2 + K_p s + K_i]B}{(1 + BK_d)s^2 + (K_p B - A)s + K_i B} \quad (6.12)$$

The corresponding characteristic equation from Equation (6.12) is shown below:

$$\Delta_{DO}(s) = (1 + BK_d)s^2 + (K_p B - A)s + K_i B \quad (6.13)$$

6.2.3 The desired poles and desired characteristic equation

The closed loop characteristic equation (6.13) is of a second order. That is why the desired equation has to be also of order two.

Values of the two desired poles can be selected such that the behavior of the closed loop system can be determined with the following desired characteristics:

- System stability.
- With small or no-overshoot and quick response.

This type of behavior for a second order system can be obtained by selection of complex conjugate poles that guarantees a critical damping frequency of the closed loop system behaviour (Ogata, 2002), as follows:

$$s_{1,2} = -2 \pm j\sqrt{2} \quad (6.14)$$

The corresponding desired characteristic equation from the poles in Equation (6.14) is shown below:

$$\Delta_{DO,des}(s) = s^2 + 4s + 6 \quad (6.15)$$

6.2.4 Calculation of the Linear PID controller's parameters

Using the direct comparison of the closed loop and the desired characteristic equations

$$\begin{aligned} \Delta_{DO}(s) &= \Delta_{DO,des}(s) \\ (1 + BK_d)s^2 + (K_p B - A)s + K_i B &= s^2 + 4s + 6 \end{aligned}$$

Expressions for the linear PID controller co-efficiencies are obtained as shown below:

$$1 + BK_d = 1$$

$$\therefore K_d = 0$$

$$K_p = \frac{4 + A}{B} = \frac{4 + (-3)}{200}$$

$$\therefore K_p = 0.005$$

$$K_i = \frac{6}{B} = \frac{6}{200}$$

$$\therefore K_i = 0.03$$

The designed parameters of the LPID controller for the linearised DO process are

$$K_p = 0.005, K_i = 0.03 \text{ and } K_d = 0.$$

At this point the representations of the Equations for the linear controller parameters (K_p , K_i , and K_d) are known.

The following section is based on the simulation of the closed loop systems (linearized and nonlinear model of DO) under the LPID controller. These simulations are performed in order to investigate the performance of the closed loop linearized DO process model under the LPID controller as well as the performance of the closed loop nonlinear DO process under the LPID controller. When the simulations of the closed loop nonlinear DO process under the LPID controller is completed, changes on the values of the system internal disturbances and the set-point are made in order to investigate how the nonlinear DO process reacts under these changes when it is controlled by the LPID controller.

6.3 Simulation of the linearized and nonlinear closed loop DO process under the LPID controller

The Matlab/Simulink simulation of the linear closed loop system and the nonlinear closed loop system are performed at this point. The Simulink block diagrams of the linearized DO process model under the linear PID and of the nonlinear DO process model under the LPID are shown in Figure 6.2 and Figure 6.3 respectively. The response of each system under control is observed and the results are shown later in Figure 6.4 - Figure 6.5 for the linearised DO, and in Figure 6.6 - Figure 6.20 for the nonlinear DO process respectively.

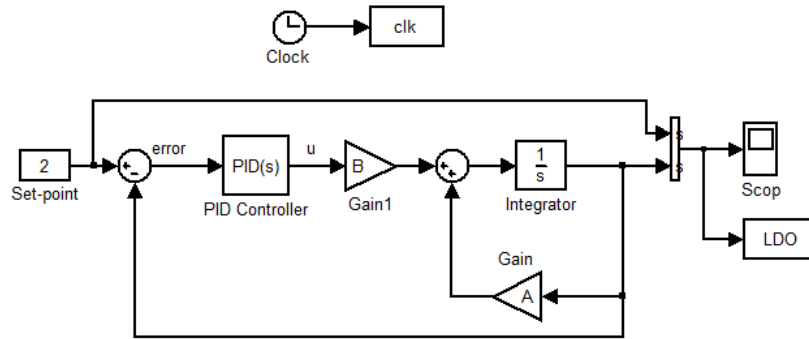


Figure 6.2: Simulink diagram of the linearized closed loop DO process using the Linear PID controller

The controller parameters designed in section 6.2 are used for both closed loop systems, with linearized and nonlinear DO process models.

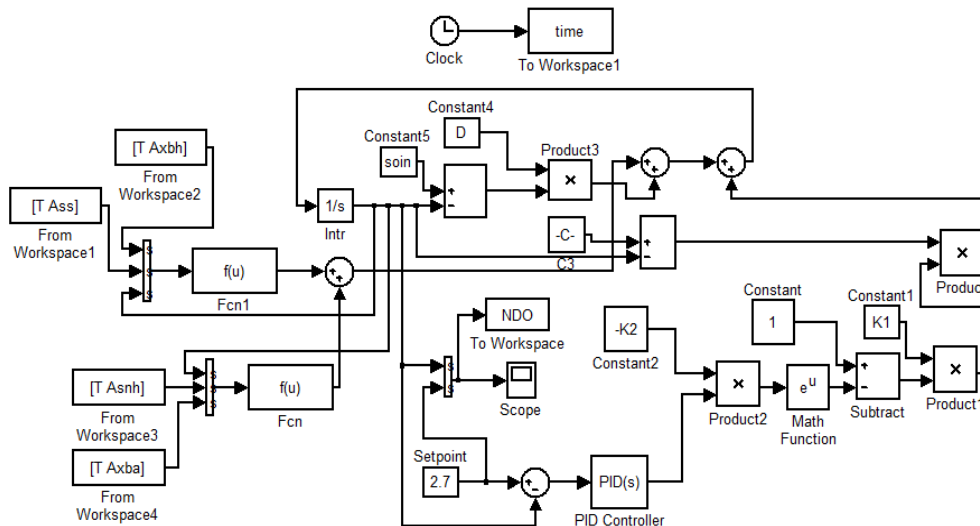


Figure 6.3: Simulink block diagram for the linear PID control of the nonlinear DO process

The nonlinear DO process has its own parameters accepted from Copp *et al.*, (2000). Simulation for the nonlinear DO process model are performed for various values of the disturbances $s_{o,in}$ and r_{so} and for various values of the set-point, as used in Chapter 5. The values are shown in Table 6.1

6.3.1 Simulation results of the closed loop linearised DO process under the linear PID controller

The closed loop system of the linearized DO process model under LPID has been simulated in Matlab/Simulink, and the simulation results are shown in the following figures: (Figure 6.4 – Figure 6.5)

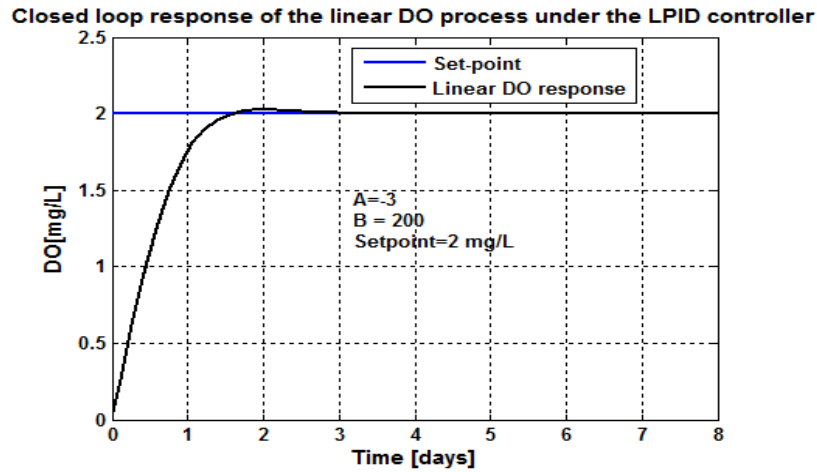


Figure 6.4: Linearized DO process response under the LPID controller, when the set-point is 2 mg / L

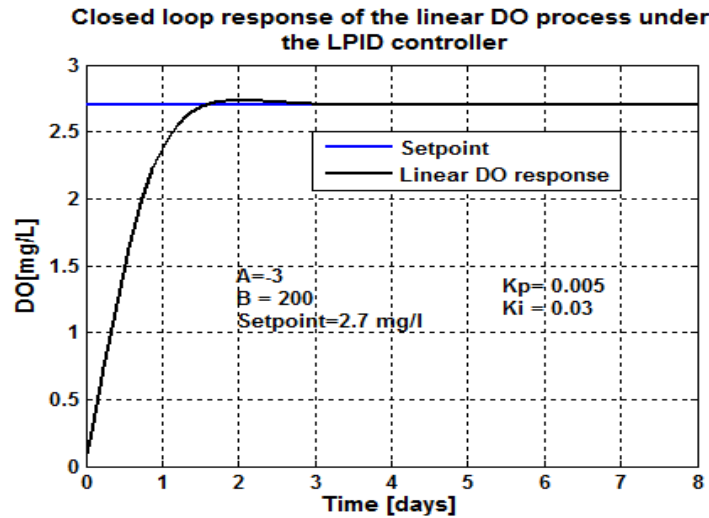


Figure 6.5: Linearized DO process response under the LPID controller, when the set-point is 2.7 mg / L

6.3.2 Simulation results of the closed loop nonlinear DO process behavior under the designed LPID controller

The simulation performed using the designed LPID controller parameters in section 6.2 did not succeed to control the nonlinear DO process during the simulation tests. Therefore, the controller parameters were tuned and the successful parameter values for the LPID controller to control the nonlinear DO process are accepted to be $K_p = 110$ and $K_i = 0.03$ after the trial and error process of tuning was performed. Some of the results obtained during controller parameters tuning are shown in the following figures (Figure 6.6 and Figure 6.7). After the final tuned and accepted values of the LPID controller the results shown in Figure 6.8 to Figure 6.22 were obtained. These results are obtained

under different set-point values and different internal disturbances of s_{oin} and r_{so} shown in Table 6.1

Table 6.1: Variation of the DO set point and the DO process disturbances

Set-point	s_{oin} mg/L	r_{so} mg/L/day
2.7	0.01	-294.8954
2.7	0.01	-309.6402
2.7	0.01	-280.1506
2.7	0.01	-442.3431
2.7	0.01	-147.4477
2	0.8	-294.8954
2	0.8	-309.6402
2	0.8	-280.1506
2	0.8	-442.3431
2	0.8	-147.4477
1.7	0.8	-294.8954
1.7	0.8	-309.6402
1.7	0.8	-280.1506
1.7	0.8	-442.3431
1.7	0.8	-147.4477

The following figures (Figure 6.6 and Figure 6.7) give the nonlinear DO process behaviors under the original designed LPID values.

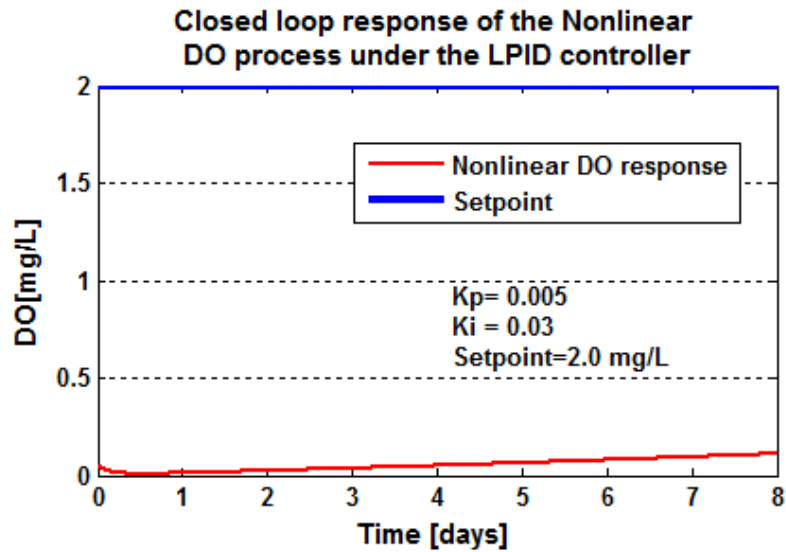


Figure 6.6: Closed loop nonlinear DO process response under the un-tuned LPID controller, when the set-point is 2 mg/L , $s_{oin}=0.01\text{ mg/L}$ and $r_{so} = -294.8954\text{ mg/L/day}$

In Figure 6.6 the LPID controller directly uses the designed by the pole placement method for LPID parameters based on the linearized DO model to control the nonlinear DO process.

In Figure 6.7 below the designed LPID controller parameters were tuned from $K_p = 0.005$ to 30, but the process steady state error is 0.08 which is more than the accepted 5 % error.

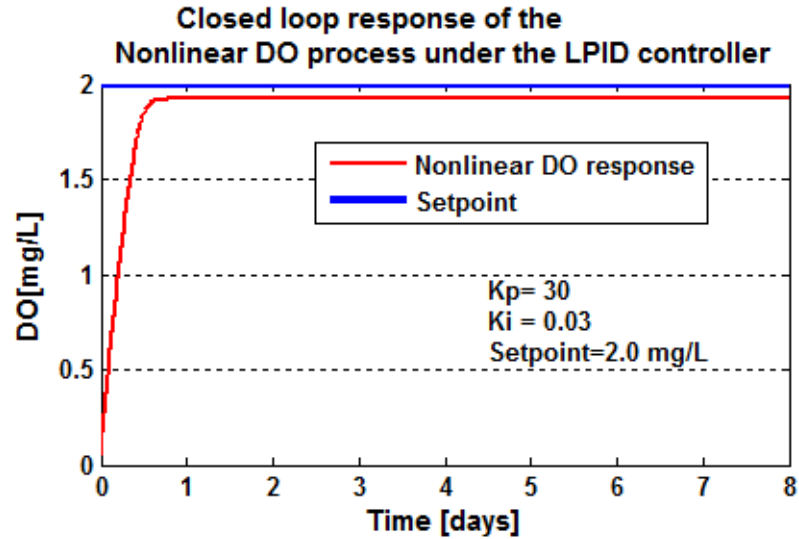


Figure 6.7: Closed loop nonlinear DO process response under the tuned LPID controller, when the set-point is 2.7 mg/L , $s_{oin}=0.01 \text{ mg/L}$ and $r_{so} = -294.8954 \text{ mg/L/day}$

Because the steady state error was big, therefore, K_p is tuned again from 30 to 110. The transition behaviors of the DO process under the tuned LPID controller parameters and different operation conditions (shown in Table 6.1) of the process are given in the following figures (Figure 6.8 and Figure 6.22):

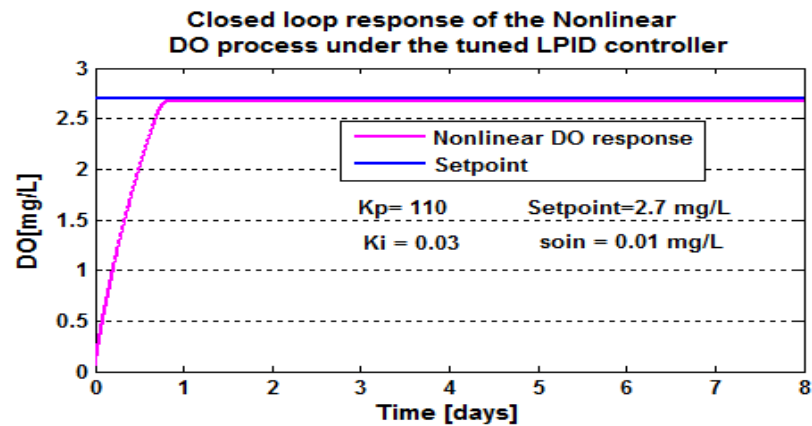


Figure 6.8: Closed loop nonlinear DO process response under the tuned LPID controller, when the set-point is 2.7 mg/L , $s_{oin}=0.01 \text{ mg/L}$ and $r_{so} = -294.8954 \text{ mg/L/day}$

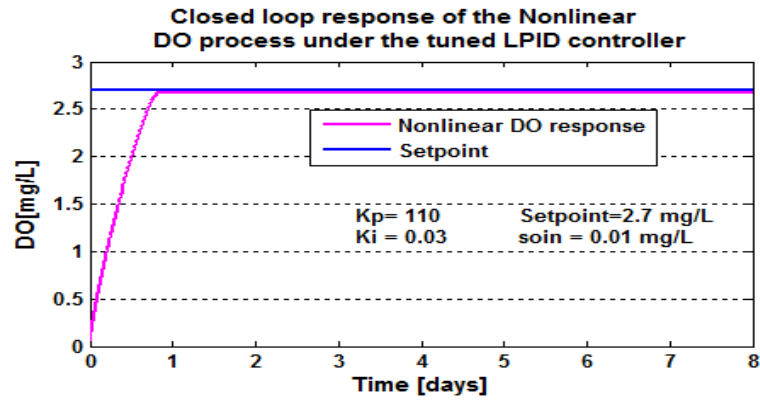


Figure 6.9: Closed loop nonlinear DO process response under the tuned LPID controller, when the set-point is 2.7 mg/L , $s_{oin}=0.01 \text{ mg/L}$ and $r_{so} = -309.6402 \text{ mg/L/day}$

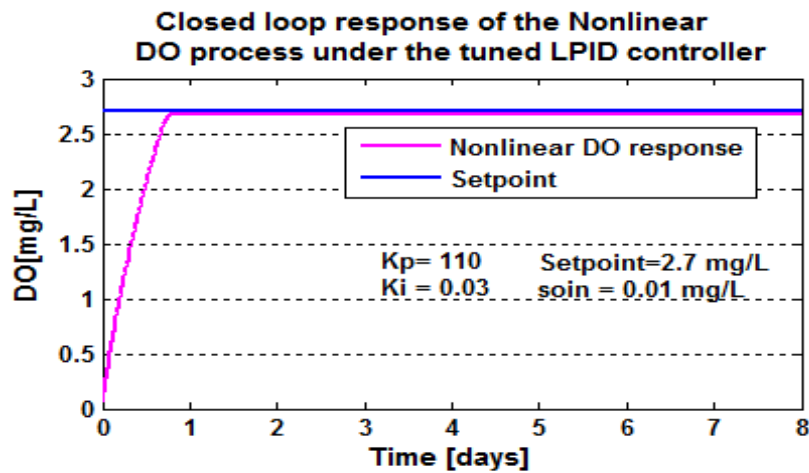


Figure 6.10: Closed loop nonlinear DO process response under the tuned LPID controller, when the set-point is 2.7 mg/L , $s_{oin}=0.01 \text{ mg/L}$ and $r_{so} = -280.1506 \text{ mg/L/day}$

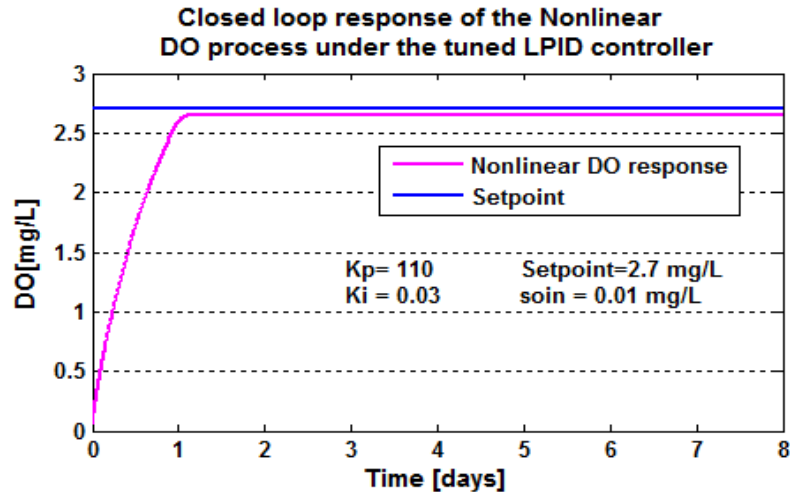


Figure 6.11: Closed loop nonlinear DO process response under the tuned LPID controller, when the set-point is 2.7 mg/L , $s_{oin}=0.01 \text{ mg/L}$ and $r_{so} = -442.3431 \text{ mg/L/day}$

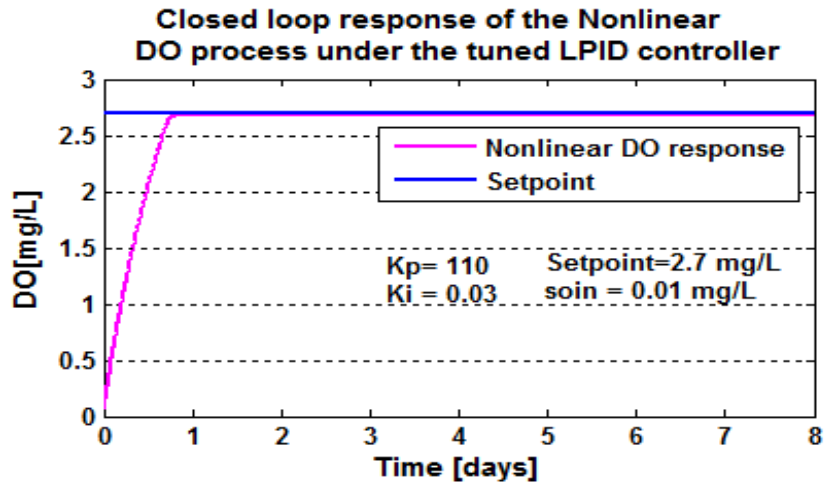


Figure 6.12: Closed loop nonlinear DO process response under the tuned LPID controller, when the set-point is 2.7 mg/L , $s_{oin}=0.01 \text{ mg/L}$ and $r_{so} = -147.4477 \text{ mg/L/day}$

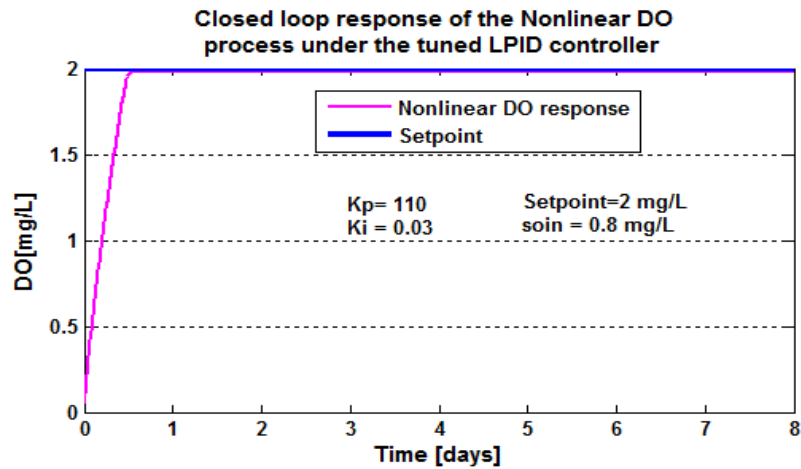


Figure 6.13: Closed loop nonlinear DO process response under the tuned LPID controller, when the set-point is 2 mg/L , $s_{oin}=0.8 \text{ mg/L}$ and $r_{so} = -294.8954 \text{ mg/L}$

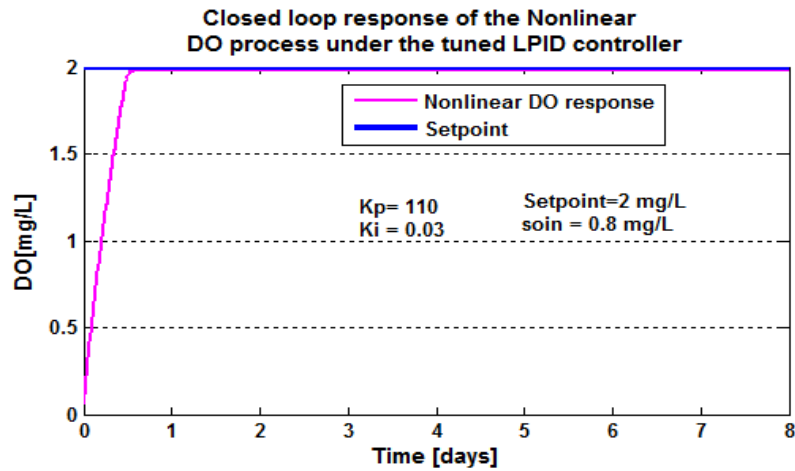


Figure 6.14: Closed loop nonlinear DO process response under the tuned LPID controller, when the set-point is 2 mg/L , $s_{oin}=0.8 \text{ mg/L}$ and $r_{so} = -309.6402 \text{ mg/L/day}$

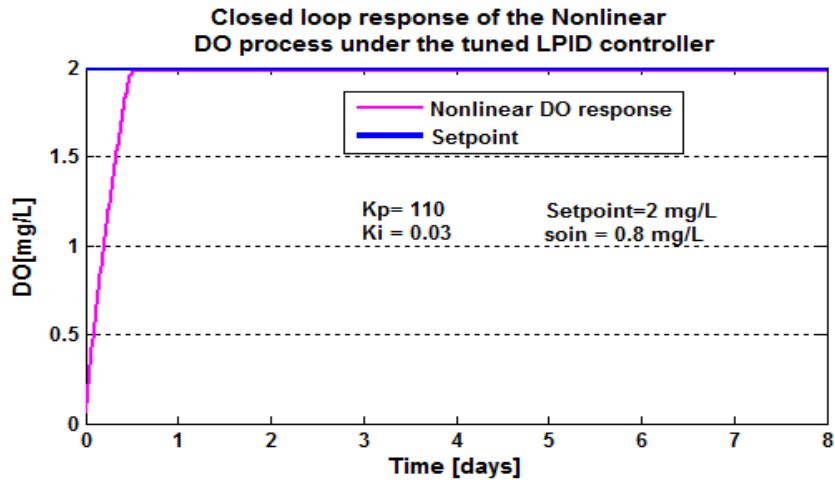


Figure 6.15: Closed loop nonlinear DO process response under the tuned LPID controller, when the set-point is 2 mg/L , $s_{oin}=0.8\text{ mg/L}$ and $r_{so}=-280.1506\text{ mg/L/day}$

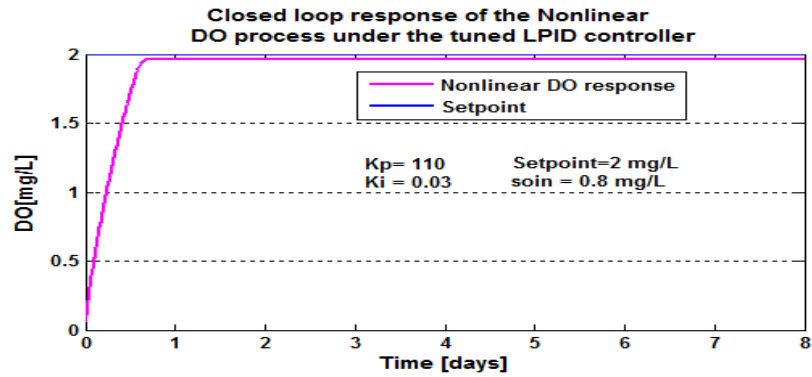


Figure 6.16: Closed loop nonlinear DO process response under the tuned LPID controller, when the set-point is 2 mg/L , $s_{oin}=0.8\text{ mg/L}$ and $r_{so}=-442.3431\text{ mg/L/day}$

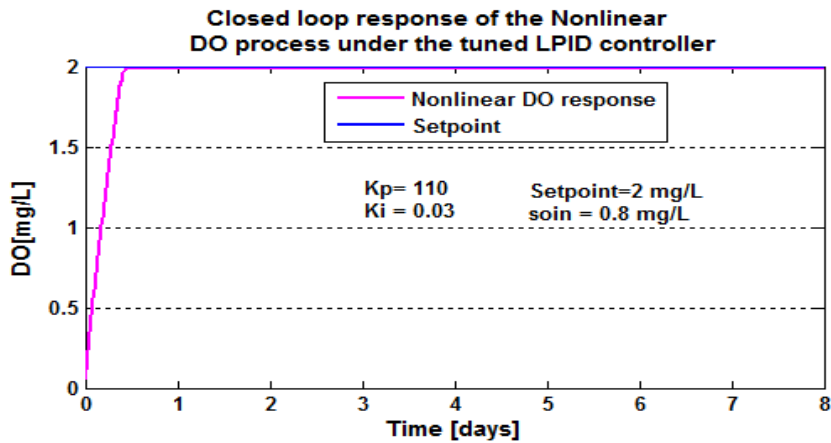


Figure 6.17: Closed loop nonlinear DO process response under the tuned LPID controller, when the set-point is 2 mg/L , $s_{oin}=0.8\text{ mg/L}$ and $r_{so}=-147.4477\text{ mg/L/day}$

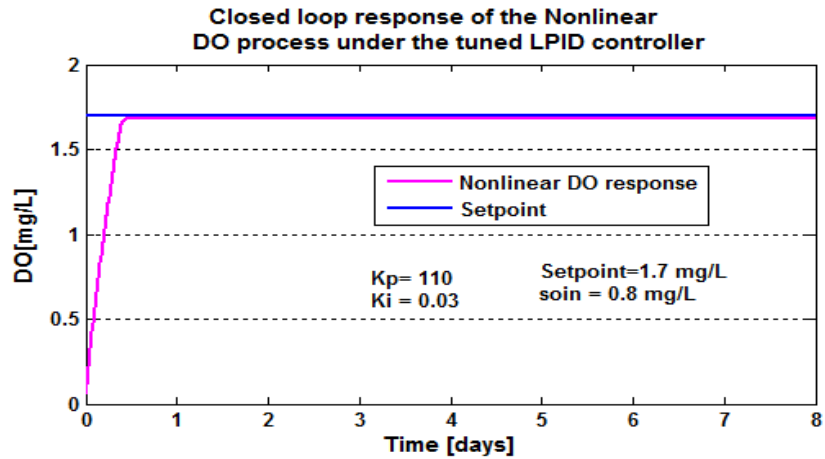


Figure 6.18: Closed loop nonlinear DO process response under the tuned LPID controller, when the set-point is 1.7 mg/L , $s_{oin} = 0.8 \text{ mg/L}$ and $r_{so} = -294.8954 \text{ mg/L/day}$

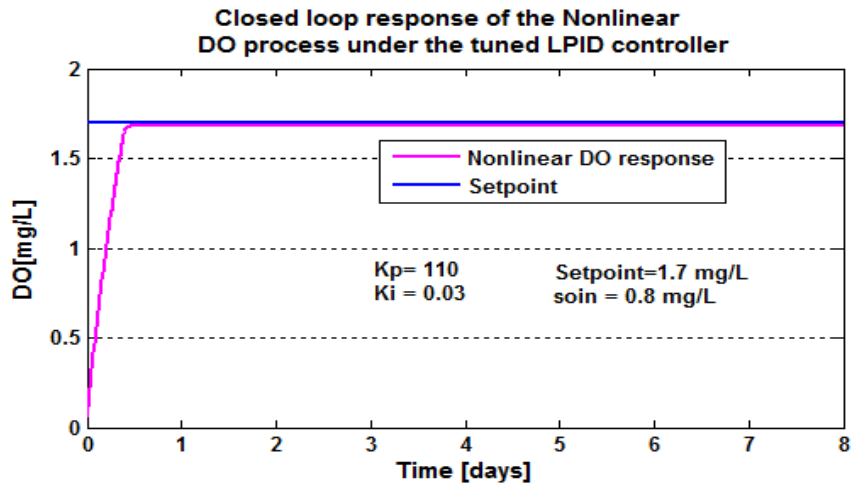


Figure 6.19: Closed loop nonlinear DO process response under the tuned LPID controller, when the set-point is 1.7 mg/L , $s_{oin} = 0.8 \text{ mg/L}$ and $r_{so} = -309.6402 \text{ mg/L/day}$

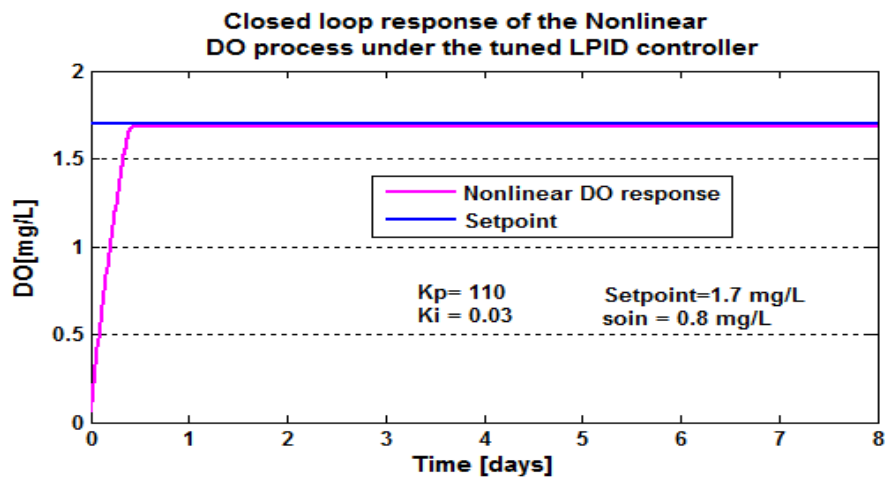


Figure 6.20: Closed loop nonlinear DO process response under the tuned LPID controller, when the set-point is 1.7 mg/L , $s_{oin} = 0.8 \text{ mg/L}$ and $r_{so} = -280.1506 \text{ mg/L/day}$

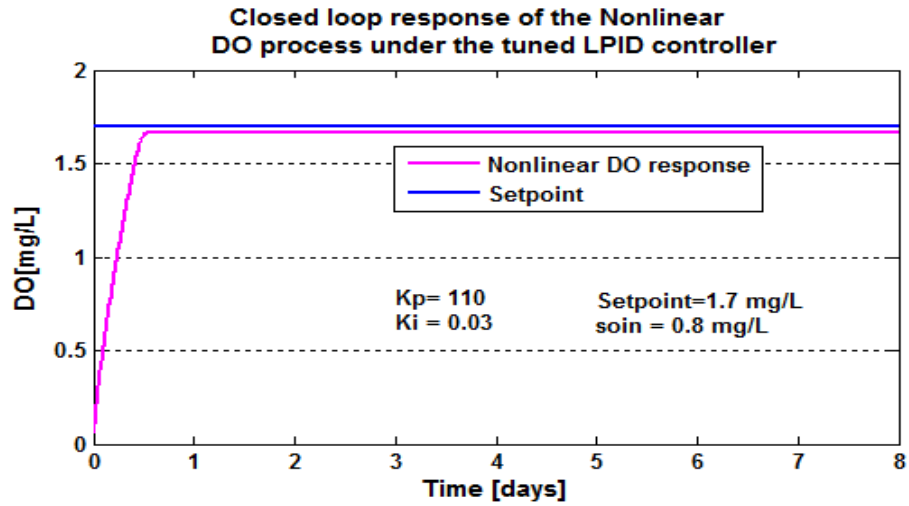


Figure 6.21: Closed loop nonlinear DO process response under the tuned LPID controller, when the set-point is 1.7 mg/L , $s_{oin} = 0.8 \text{ mg/L}$ and $r_{so} = -442.3431 \text{ mg/L/day}$

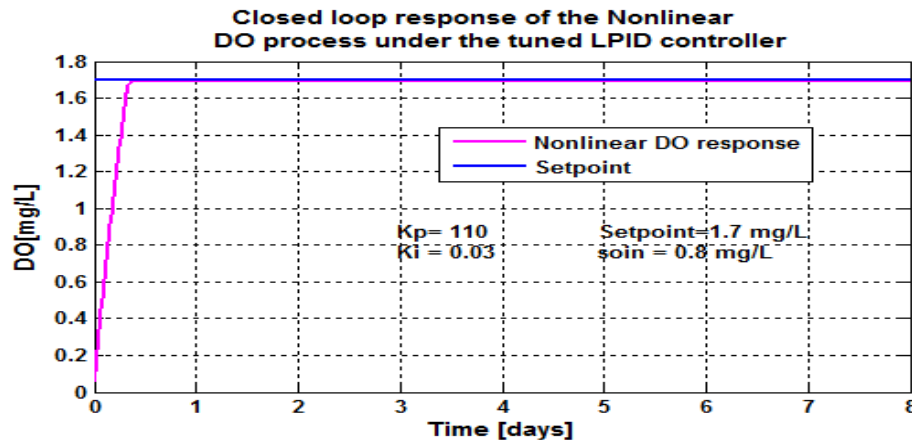


Figure 6.22: Closed loop nonlinear DO process response under the tuned LPID controller, when the set-point is 1.7 mg/L , $s_{oin} = 0.8 \text{ mg/L}$ and $r_{so} = -147.4477 \text{ mg/L/day}$

The closed loop nonlinear DO process behavior characteristics from the Figures 6.8 – 6.22 is measured and shown in Table 6.2.

Table 6.2: Results obtained when the tuned LPID controller parameters are used to control the nonlinear DO process

Parameters			Characteristics			
Set-point	s_{oin} [mg/L]	r_{so} mg/L/day	Time delay [days]	Steady state error [mg/L]	Rise time [days]	Settling time [days]
2.7	0.01	-294.8954	0.001	0.02	0.3	0.5
2.7	0.01	-309.6402	0.001	0.03	0.3	0.5
2.7	0.01	-280.1506	0.001	0.025	0.3	0.5
2.7	0.01	-442.3431	0.001	0.04	0.34	0.5
2.7	0.01	-147.4477	0.001	0.01	0.28	0.5
2	0.8	-294.8954	0.001	0.022	0.3	0.4
2	0.8	-309.6402	0.001	0.03	0.3	0.4

2	0.8	-280.1506	0.001	0.02	0.3	0.4
2	0.8	-332.3431	0.001	0.04	0.35	0.4
2	0.8	-147.4477	0.001	0.01	0.28	0.4
1.7	0.8	-294.8954	0.001	0.02	0.3	0.3
1.7	0.8	-309.6402	0.001	0.02	0.3	0.3
1.7	0.8	-280.1506	0.001	0.02	0.3	0.3
1.7	0.8	-332.3431	0.002	0.04	0.35	0.35
1.7	0.8	-147.4477	0.001	0.01	0.28	0.35

6.3.2.1 Discussion

The parameters designed for the linear PID controller have been used successfully to control the linear DO model; this is shown in Figure 6.4 and Figure 6.5. The same parameters of the LPID controller were applied to control the nonlinear DO process, without success. The tuning of the controller parameters is done and the results for the DO process behavior under the tuned LPID controller is shown in Figure 6.8 – Figure 6.22.

Based on the characteristics given in Table 6.2 the tuned controller parameters have been used successfully to control the nonlinear DO process model. When comparing the same values of the disturbance in a process for different set-point conditions, the settling time is large for the process with conditions that has a large set-point. This can be seen in that data values highlighted light blue in the Table 6.2. In the closed loop DO process model result it can be seen that the value for the steady state error increases when the r_{so} value is larger (see the for comparison green highlights in Table 6.2) and also the rise time increases under the same conditions. The text data typed in red color are the conditions in which the tuned controller performed in the best way under different values of the set point based on one value of r_{so} , but different values of s_{oin} . These disturbances did not affect in the DO operation process, now it can be said that when the r_{so} in small the DO process has a good performance.

6.4 Simulations of the closed loop nonlinear DO process based on the two NLPID controllers

This section focuses on the simulation of the closed loop system in the Matlab/Simulink software environment based on the considered two NLPID controllers. These NLPID controllers are used to control the linearized model and the nonlinear model of the DO concentration. The Pole Placement (PP) method has been used in section 6.2 for design the LPID controller parameters for the linearized DO process model. The parameters of

the LPID controller designed in Matlab are transferred to Simulink for closed loop simulation of the DO process under the NLPID controllers' parameters. The following diagram (Figure 6.23) displays the typical approach used.

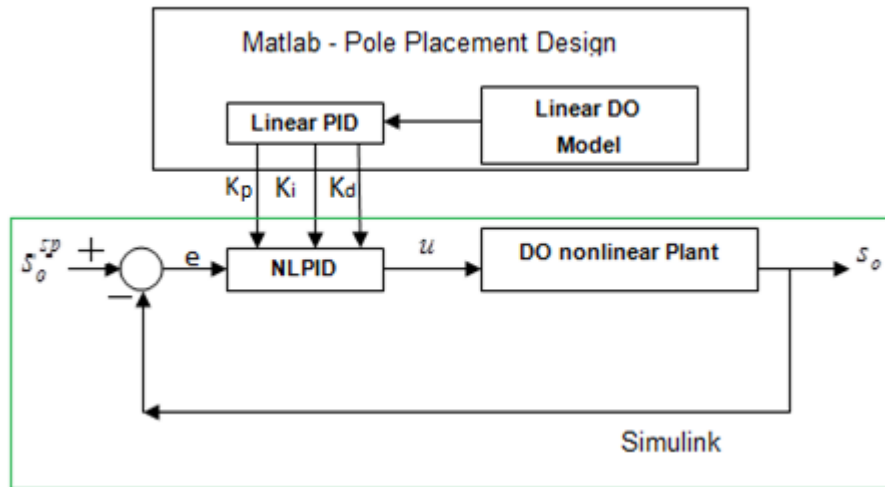


Figure 6.23: Structure for Matlab/Simulink simulation of the closed loop DO process based on the NLPID controllers with parameters designed for the LPID controller and the linearized process model

The investigation of the performance of the closed loop behaviors under the two NLPID controllers is done for the same set-point and disturbance values as in Table 6.1

6.4.1 Closed loop linearized and nonlinear DO process Simulink Block Diagrams based on the NLPID1 and NLPID2 controllers

The simulation of the DO process with NLPID1 using the pole placement designed parameters for the LPID controller based on the linearised DO process as presented in section 6.2 is achieved. The designed values of K_p , K_i , and K_d are applied in the nonlinear controller in order to control and improve the behavior of the DO process concentration. The corresponding block diagram of the Simulink model is given in Figure 6.24 for the linearized DO model under the NLPID1 controller, and Figure 6.25 for the nonlinear DO system under the NLPID1 controller.

Figure 6.26 shows the linearised DO model under the NLPID2 controller and Figure 6.27 shows the Simulink block diagram for the nonlinear model of the DO concentration under the NLPID2 controller. The Matlab calculated parameters are sent to Simulink, and then the response of each closed loop system is observed and the results are shown in the simulation results section later. The controller part of the Figures (6.24 - 6.27) is the same as in Figures (5.3 - 5.4) in Chapter 5. The controller parameters used are those designed for LPID controller based on the linearized DO model, and are tuned to be used in the NLPID controllers to control linear and nonlinear DO process model.

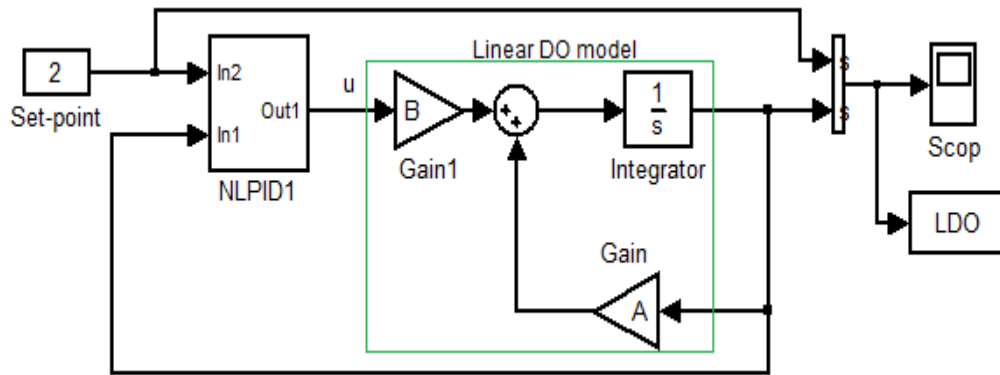


Figure 6.24: Simulink diagram of the closed loop linearized DO process under the NLPID1 controller

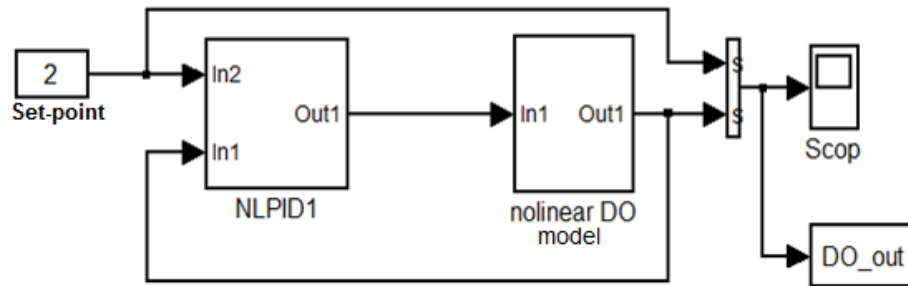


Figure 6.25: Simulink diagram of the closed loop nonlinear DO process under the NLPID1 controller

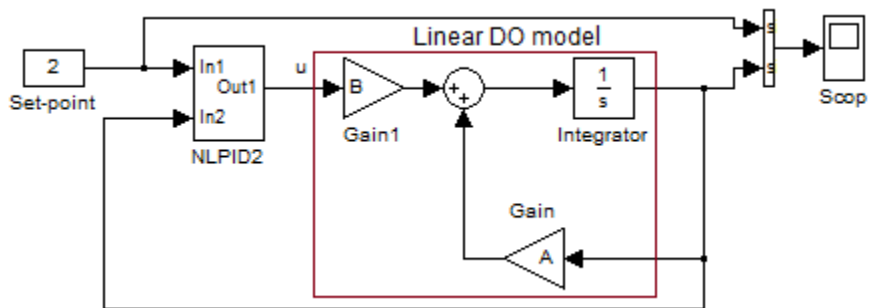


Figure 6.26: Simulink diagram of the closed loop linearized DO process using the NLPID2 controller

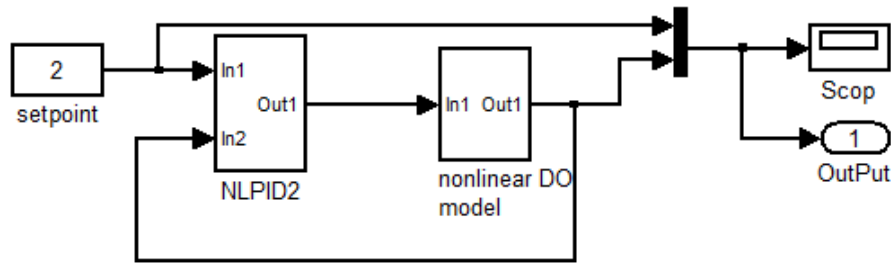


Figure 6.27: Simulink diagram of the closed loop nonlinear DO process under the NLPID2 controller

6.4.2 Simulation results for the closed loop linear and nonlinear DO process based on the NLPID1 and NLPID2 controllers

6.4.2.1 Simulation results for the linearized DO model under the NLPID1 controller

The designed LPID controller parameters through the PP1 method were applied in NLPID1 controller to control the linearised DO process, Figure 6.28 shows the behavior of the closed loop linearized DO model under the NLPID1 controller.

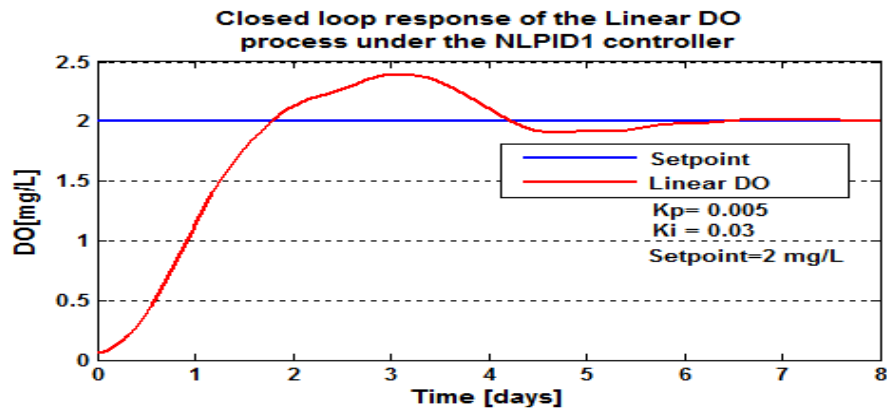


Figure 6.28: Closed loop linear DO process response under the NLPID1 controller, when the set-point is 2 mg/L

Since the output of the system has a big overshoot (40%) as shown in Figure 6.28, the designed LPID controller parameters for the linearized DO process are tuned: K_p from 0.005 to 0.05 and K_i remains the same. Figure 6.29 shows the effect of the first made tuning on the system.

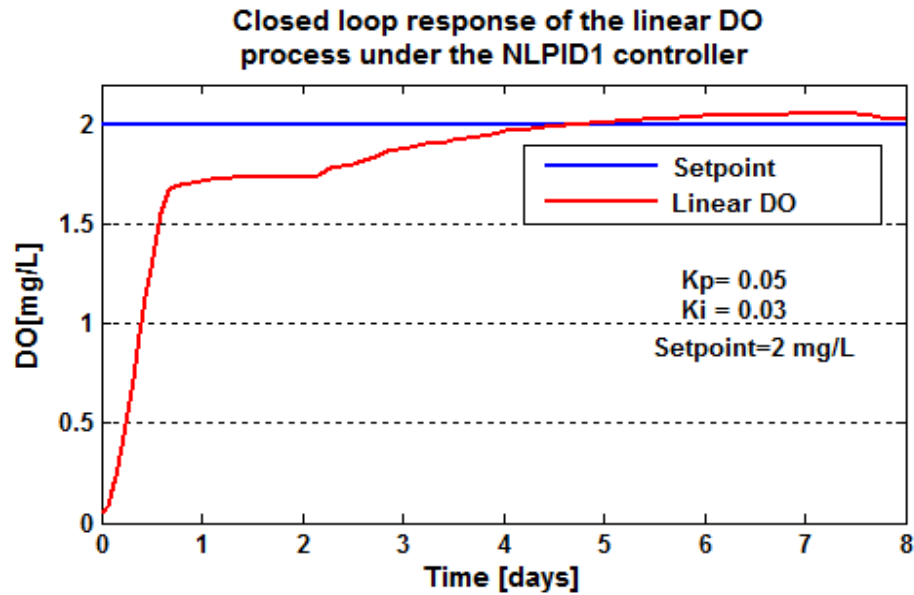


Figure 6.29: Closed loop linear DO process response under the NLPID1 controller, when the set-point is 2 mg/L

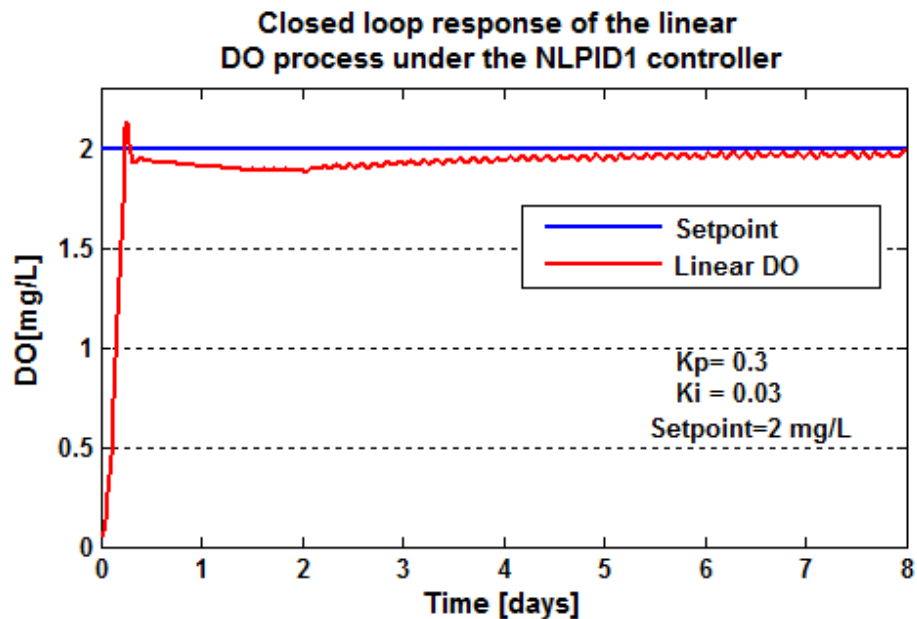


Figure 6.30: Closed loop linear DO process response under the NLPID1 controller, when the set-point is 2 mg/L

For the reason that the system output is not stable and the steady state error is 0.05, the control parameter K_p was additionally tuned to: $K_p = 0.3$, Figure 6.30, and then K_i and K_d are accepted as that of the LPID controller designed values in which: $K_i = 0.03$ and $K_d = 0$. The proportional control parameter value was increased again to $K_p = 0.2$ and that becomes the accepted value of the proportional control. These accepted values were

used for the NLPID1 controller only to control the linear DO process and were tested if they can assure good control to the set-point variations. Some of the results of that simulation are shown in Figure 6.31 and Figure 6.33.

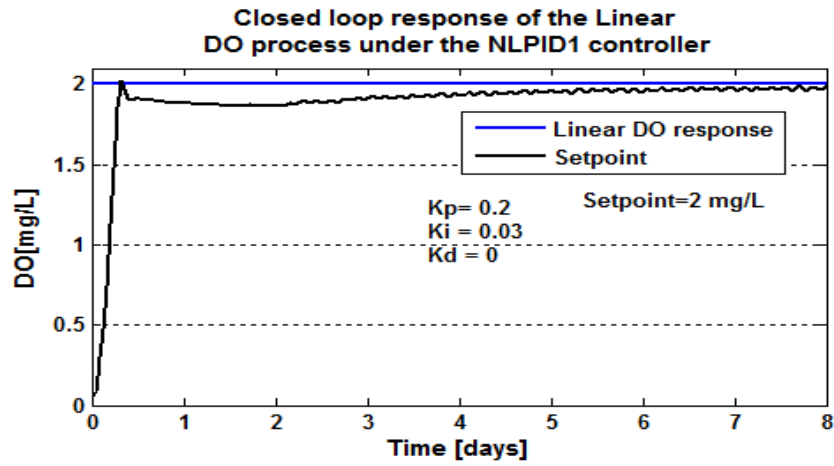


Figure 6.31: Closed loop linear DO process response under the NLPID1 controller, when the set-point is 2 mg/L

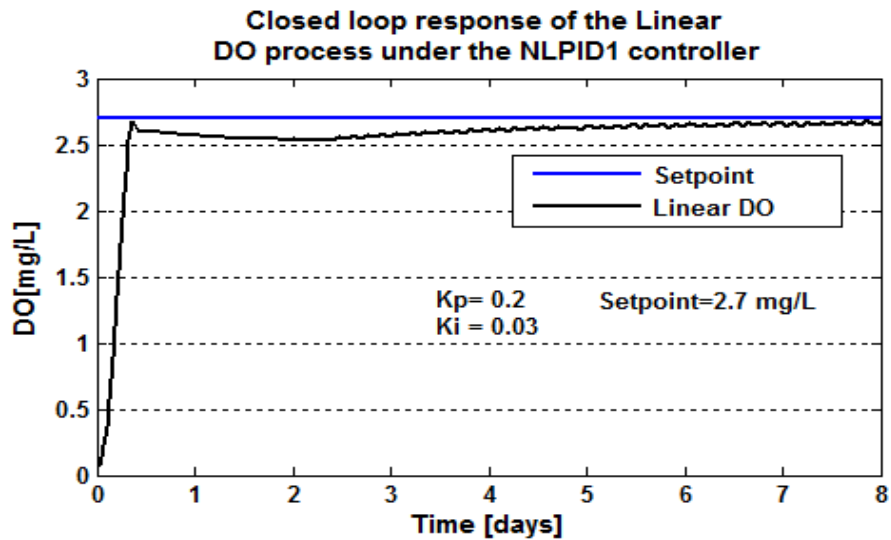


Figure 6.32: Closed loop linear DO process response under the NLPID1 controller, when the set-point is 2.7 mg/L

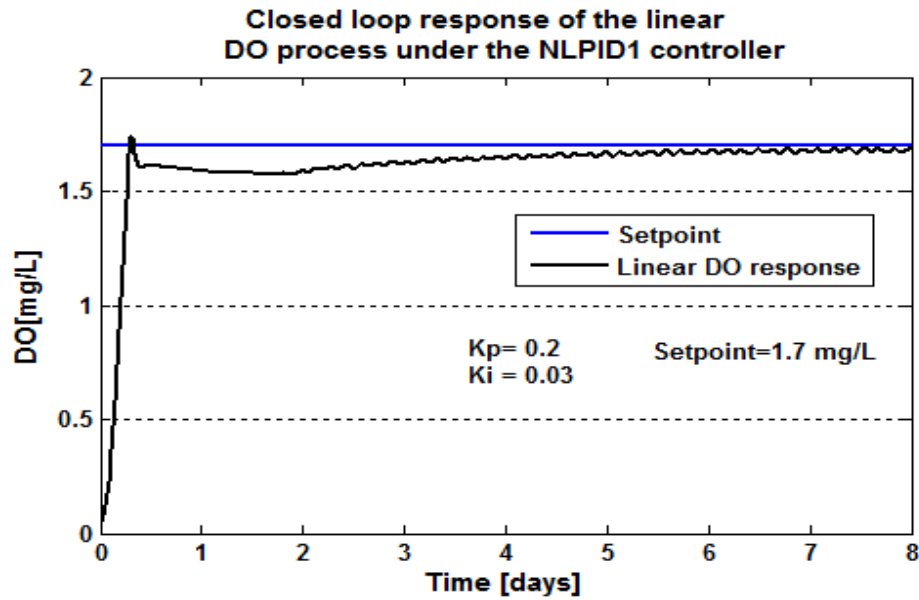


Figure 6.33: Closed loop linear DO process response under the NLPID1 controller, when the set-point is 1.7 mg/L

Table 6.3: Closed loop linearised DO process characteristics under the NLPID1 controller

Set-point	Characteristics			
	Time delay [days]	Steady state error [mg/L]	Rise time [days]	Settling time [days]
2.7	0.05	0.02	0.26	4.2
2	0.05	0.02	0.25	4
1.7	0.05	0.02	0.24	3.8

The simulations in Figure 6.31 to Figure 6.33 are performed in order to investigate how the linearized DO process model under the NLPID1 controller responds in terms of rise time, settling time and steady state error during the set point changes in the closed loop system.

In the results shown in Table 6.3 above the DO process rise time and settling time can be bigger as the process set point changes to a high value. The controller parameters for the NLPID1 controller to control the linearized DO process model have been successfully tuned and they show a good behavior and the steady state error is less than 5%.

6.4.2.2 Simulation results for the nonlinear DO model behavior under the NLPID1 controller

The simulation performed using the designed LPID controller parameters in section 6.2 did not succeed to control the nonlinear DO process during the simulation tests. Therefore, the controller parameters were tuned and the successful parameter values during the try and the error process of tuning are $K_p = 120$ and $K_i = 0.5$. These

parameters are tuned for the NLPID1 controller in order to control the nonlinear DO process.

The controller parameter tuning for the closed loop DO process model under the NLPID1 controller was first performed under one set point value and constant internal disturbance, then after the tuning or selection of the controller parameter values the following results shown in Figure 6.34 to Figure 6.48 were obtained under the different set-point values and different internal disturbances ($s_{o,in}$ and r_{so}) using the variations for the DO set point and the DO process disturbances as given in Table 6.1.

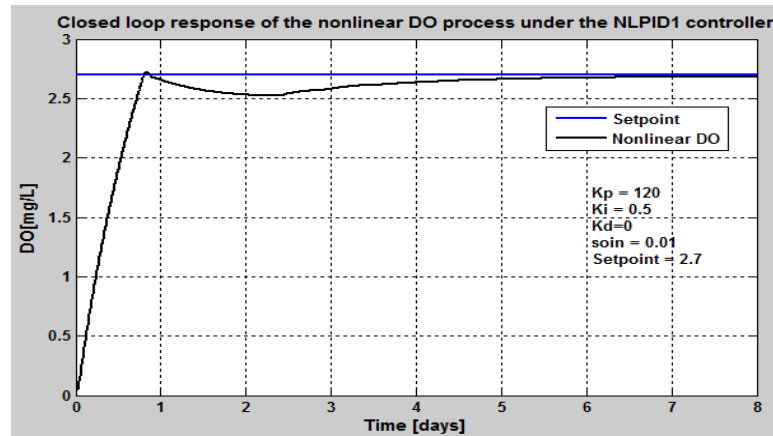


Figure 6.34: Closed loop DO process response under the NLPID1 controller, when the set-point is 2.7 mg/L , $s_{o,in} = 0.01 \text{ mg/L}$ and $r_{so} = -294.8954 \text{ mg/L/day}$

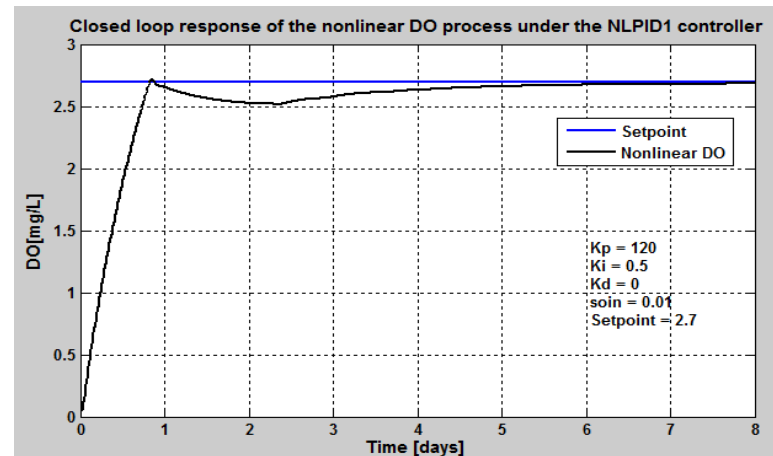


Figure 6.35: Closed loop DO process response under the NLPID1 controller, when the set-point is 2.7 mg/L , $s_{o,in} = 0.01 \text{ mg/L}$ and $r_{so} = 309.6402 \text{ mg/L/day}$

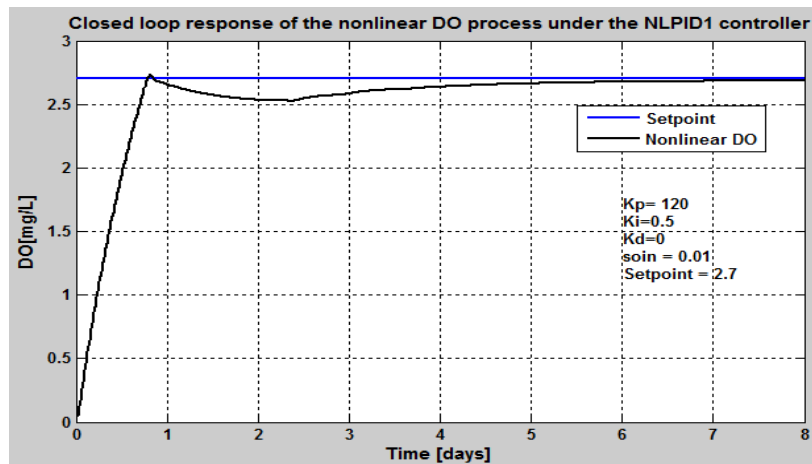


Figure 6.36: Closed loop linear DO process response under the NLPID1 controller, when the set-point is 2.7 mg/L , $s_{o,in} = 0.01 \text{ mg/L}$ and $r_{so} = 280.1506 \text{ mg/L/day}$

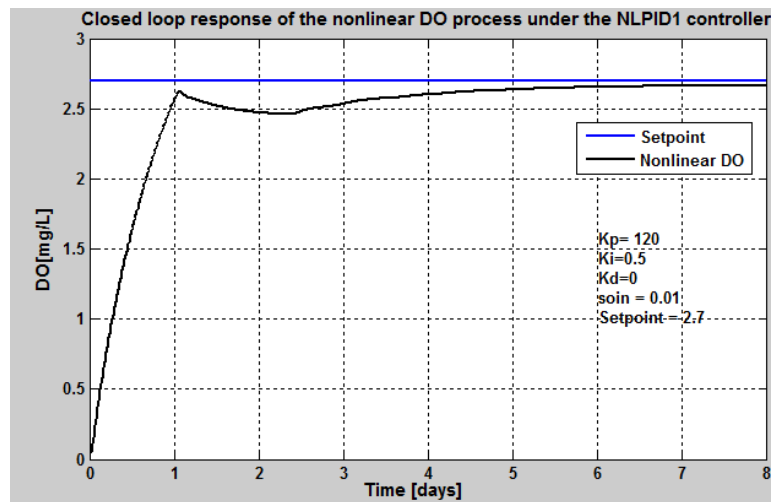


Figure 6.37: Closed loop DO process response under the NLPID1 controller, when the set-point is 2.7 mg/L , $s_{o,in} = 0.01 \text{ mg/L}$ and $r_{so} = -442.3431 \text{ mg/L/day}$

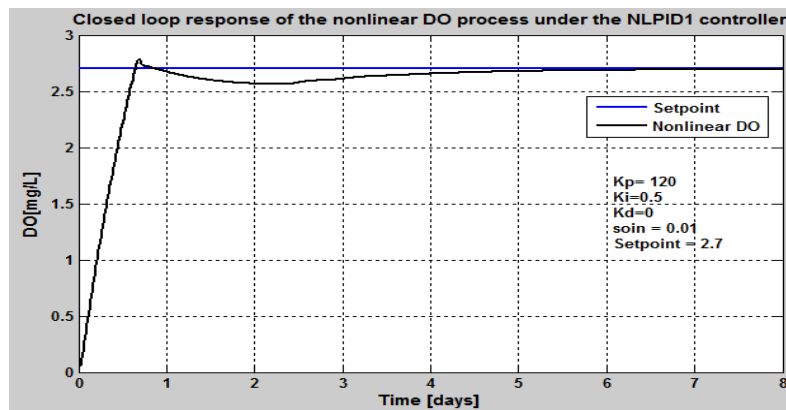


Figure 6.38: Closed loop DO process response under the NLPID1 controller, when the set-point is 2.7 mg/L , $s_{o,in} = 0.01 \text{ mg/L}$ and $r_{so} = -147.4477 \text{ mg/L/day}$

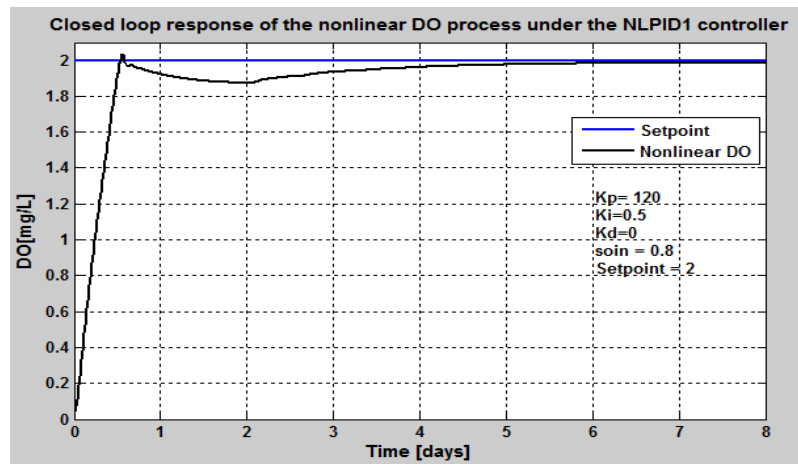


Figure 6.39: Closed loop DO process response under the LPID controller, when the set-point is 2 mg/L , $s_{o,in} = 0.8\text{ mg/L}$ and $r_{so} = -294.8954\text{ mg/L/day}$

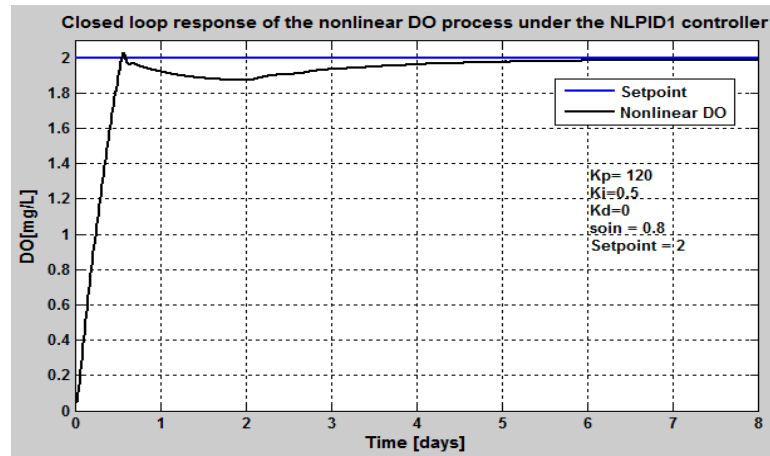


Figure 6.40: Closed loop DO process response under the NLPID1 controller, when the set-point is 2 mg/L , $s_{o,in} = 0.8\text{ mg/L}$ and $r_{so} = -309.6402\text{ mg/L/day}$

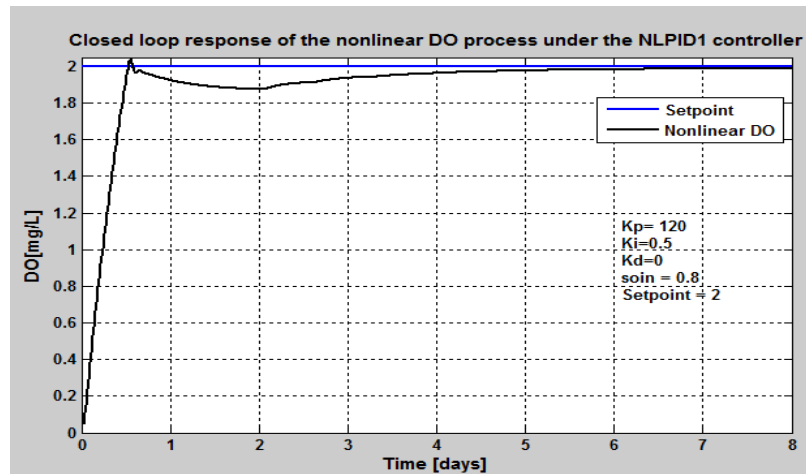


Figure 6.41: Closed loop DO process response under the NLPID1 controller, when the set-point is 2 mg/L , $s_{o,in} = 0.8\text{ mg/L}$ and $r_{so} = -280.1506\text{ mg/L/day}$

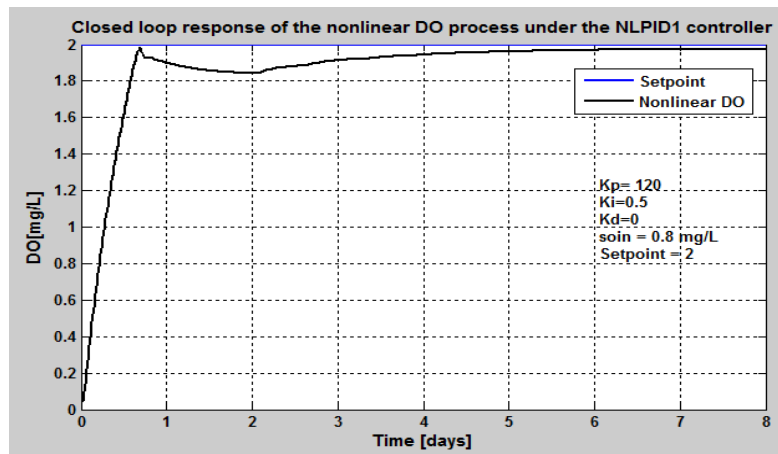


Figure 6.42: Closed loop DO process response under the NLPID1 controller, when the set-point is 2 mg/L , $s_{o,in} = 0.8 \text{ mg/L}$ and $r_{so} = -442.3431 \text{ mg/L/day}$

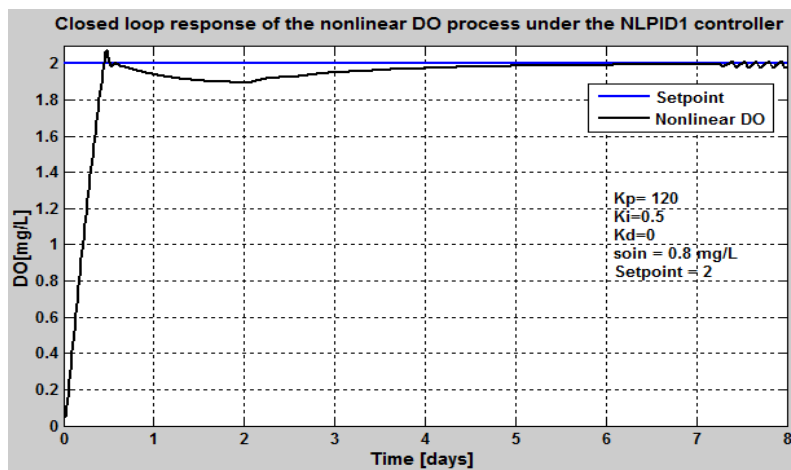


Figure 6.43: Closed loop DO process response under the NLPID1 controller, when the set-point is 2 mg/L , $s_{o,in} = 0.8 \text{ mg/L}$ and $r_{so} = -147.4477 \text{ mg/L/day}$

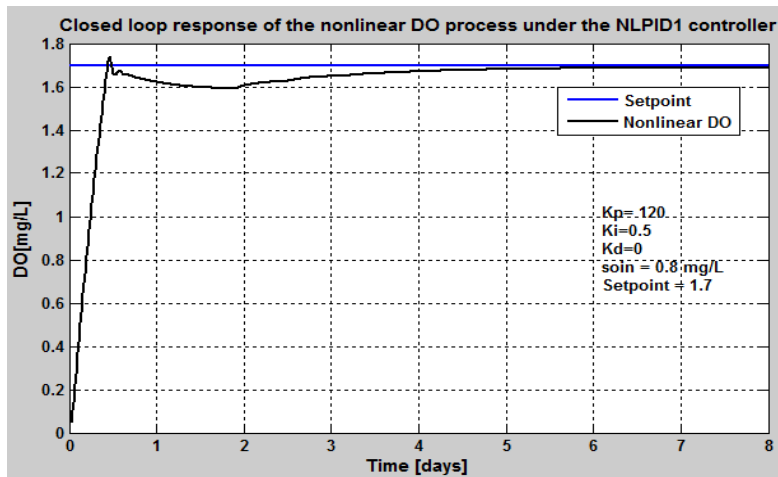


Figure 6.44: Closed loop DO process response under the LPID controller, when the set-point is 1.7 mg/L , $s_{o,in} = 0.8 \text{ mg/L}$ and $r_{so} = -294.8954 \text{ mg/L/day}$,

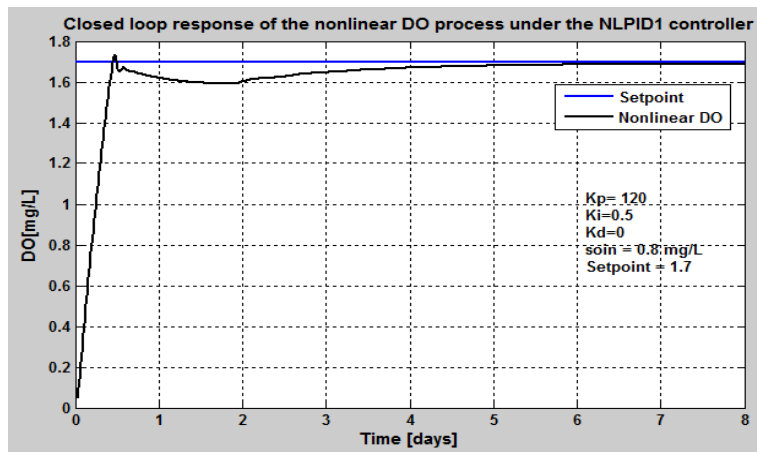


Figure 6.45: Closed loop DO process response under the NLPID1 controller, when the set-point is 1.7 mg/L , $s_{o,in} = 0.8 \text{ mg/L}$ and $r_{so} = -309.6402 \text{ mg/L/day}$

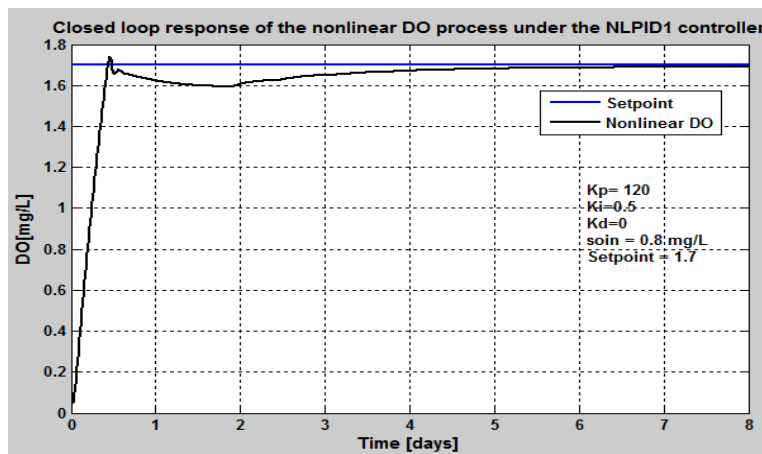


Figure 6.46: Closed loop DO process response under the NLPID1 controller, when the set-point is 1.7 mg/L , $s_{o,in} = 0.8 \text{ mg/L}$ and $r_{so} = 280.1506 \text{ mg/L/day}$

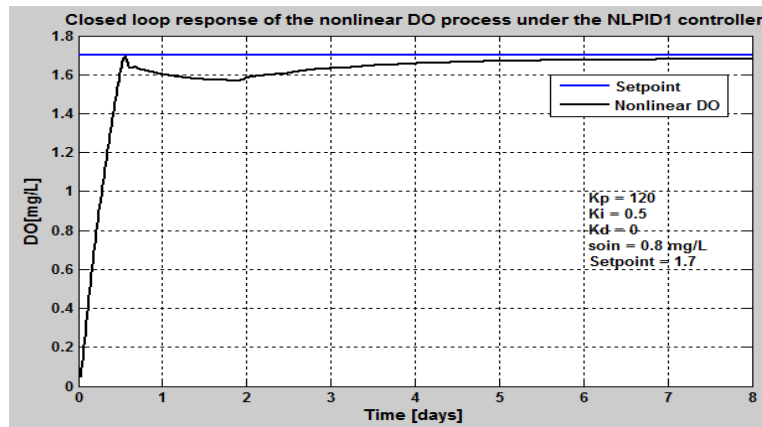


Figure 6.47: Closed loop DO process response under the NLPID1 controller, when the set-point is 1.7 mg/L , $s_{o,in} = 0.8 \text{ mg/L}$ and $r_{so} = 442.3431 \text{ mg/L/day}$

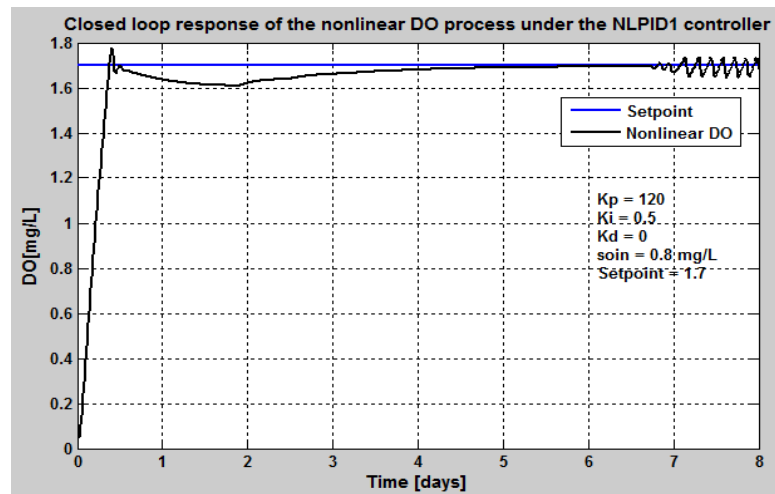


Figure 6.48: Closed loop DO process response under the LPID controller, when the set-point is 1.7 mg/L , $s_{o,in} = 0.8 \text{ mg/L}$ and $r_{so} = 147.4477 \text{ mg/L/day}$

Table 6.4: Closed loop nonlinear DO process characteristics under the NLPID1 controller

Parameters			Characteristics			
Set point	s_{oin} [mg/L]	r_{so} mg/L/day	Time delay [days]	Steady state error [mg/L]	Rise time [days]	Settling time [days]
2.7	0.01	-294.8954	0.05	0.02	0.4	4.4
2.7	0.01	-309.6402	0.05	0.025	0.46	4.8
2.7	0.01	-280.1506	0.05	0.02	0.4	4.5
2.7	0.01	-442.3431	0.05	0.05	0.49	4.9
2.7	0.01	-147.4477	0.05	0.01	0.4	4
2	0.8	-294.8954	0.05	0.02	0.4	3.5
2	0.8	-309.6402	0.05	0.024	0.4	4
2	0.8	-280.1506	0.05	0.02	0.4	3.8
2	0.8	-442.3431	0.05	0.05	0.44	4.2
2	0.8	-147.4477	0.05	0.01	0.4	3.4
1.7	0.8	-294.8954	0.05	0.02	0.38	3.6
1.7	0.8	-309.6402	0.05	0.024	0.35	3.6
1.7	0.8	-280.1506	0.05	0.02	0.33	3.5
1.7	0.8	-442.3431	0.05	0.05	0.4	4
1.7	0.8	-147.4477	0.05	0.01	0.3	3

6.4.2.2.1 Discussion

The closed loop nonlinear DO process behavior under different internal disturbances and different set-point values is tested. The NLPID1 controller with parameters obtained for the LPID controller and the linearised DO process by the pole placement method which is called in short as PP1 method in this thesis failed to control the nonlinear DO process. From Figure 6.34 to Figure 6.48 the process reaction under additionally tuned NLPID1 controller parameters was able to achieve the set-point values and is not strongly affected by the disturbances and set-point changes. Closed loop characteristics of the

nonlinear DO process behavior are given in Table 6.4. When the set point is not changing and the disturbance is changed to a high value, the system settling time increases, and the settling time becomes smaller as the disturbance decrease. The variation of the set point affects both the rise and settling time just like the process disturbance. When the set point is 2.7 mg/L the time that the system takes to settle is more than the settling time when the set point is 2 mg/L or 1.7 mg/L . The analysis shows that the rise time between the set point changes is small when the set point is low: see in Table 6.4 the system response under the set point changing from 2.7 to 1.7 mg/L . The following section applies the designed LPID controller parameters through the PP1 method into the NLPID2 controller to control the linearized DO process.

6.4.2.3 Simulation result for the closed loop linear DO process behavior under the NLPID2 controller

The results shown below are for the closed loop linearized DO model under the NLPID2 controller with the controller parameters equal to those of the designed LPID one based on the PP1 method, which is explained in section 6.2. The results show that the use of the NLPID2 to control the linearised DO process through the parameters designed for the LPID controller can make the system to be unstable and oscillate. The tuning was also applied, but the system taken as a whole did not show good improvement. Figure 6.49 shows the closed loop linear DO process under the NLPID2 controller that uses the designed LPID controller parameters without tuning them. After some try and error controller parameter tests, Figure 6.50 and Figure 6.51 show the closed loop linear DO system under the final accepted new values of the NLPID2 controller parameters for the linearised DO process.

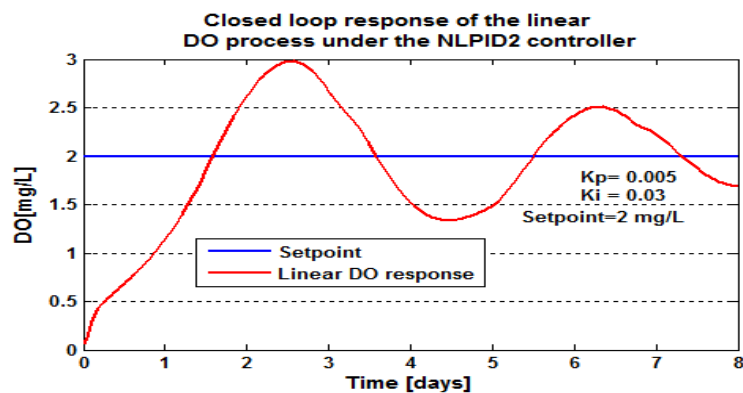


Figure 6.49: Closed loop linearized DO process response under the NLPID2 controller, when the set-point is $2 \text{ mg} / \text{L}$

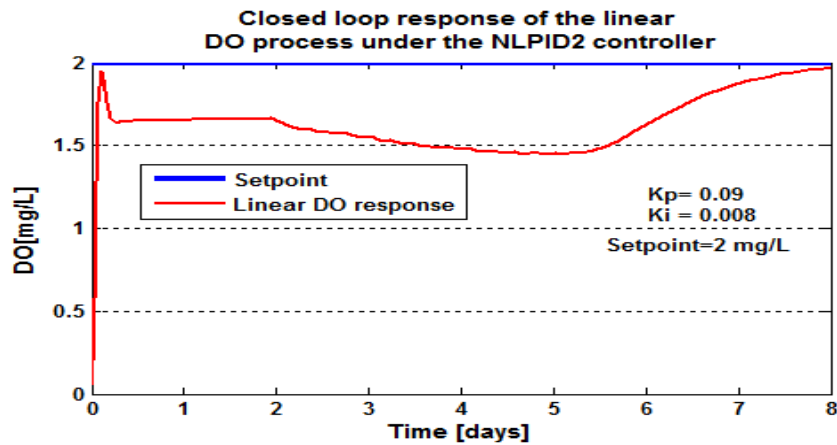


Figure 6.50: Closed loop linearised DO process response under the NLPID2 controller, when the set-point is 2 mg/L

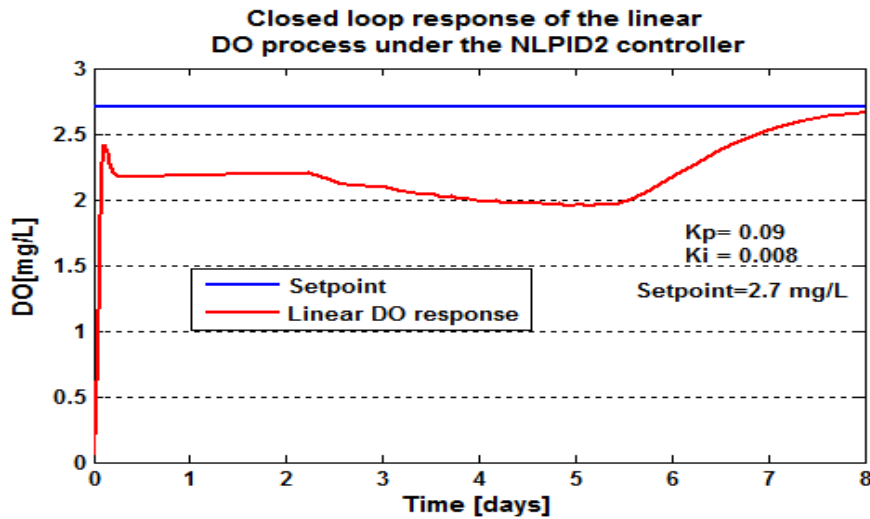


Figure 6.51: Closed loop linearised DO process response under the NLPID2 controller, when the set-point is 2.7 mg/L

Table 6.5: Closed loop linearised DO process characteristics under the NLPID2 controller

Design	Controller parameters		Characteristics	
	Kp	Ki	DO response	Comment
Any set point	0.005	0.03	Unstable & oscillate	The use of NLPID2 to control linear DO process is not recommended.
2	0.09	0.008	Over damped with steady state error of 4% at the final point	
2.7	0.09	0.008	Over damped with steady state error of 4% at the final point	

The simulations in Figure 6.49 to Figure 6.51 show that the NLPID2 controller cannot successfully control the linearized DO process model. Table 6.5 shows the closed loop linear DO process behavior characteristics under the NLPID2 controller with the best tuned parameters that were established after tuning.

6.4.2.4 Simulation results for the closed loop nonlinear DO process behavior under the NLPID2 controller

The closed loop Simulink model used to obtain these results is illustrated in Figure 6.24. First the tuned parameters for the NLPID1 controller for the control of the nonlinear DO process were used to show that they are not convenient for the NLPID2 controller. The try and error tuning process was performed many times in order to find the controller parameters that can be used for the NLPID2 controller to stabilize the DO process and to be no-overshoot. Therefore, as the controller parameters were tuned, the selected parameter values during the trial and the error process of tuning are $K_p = 200$ and $K_i = 0.005$. The simulation results for this section are shown from Figure 6.53 till Figure 6.67 based on different set-point values and different internal disturbances (s_{oin} and r_{so}) using the variations for the DO set point and the DO process disturbances as given in Table 6.1.

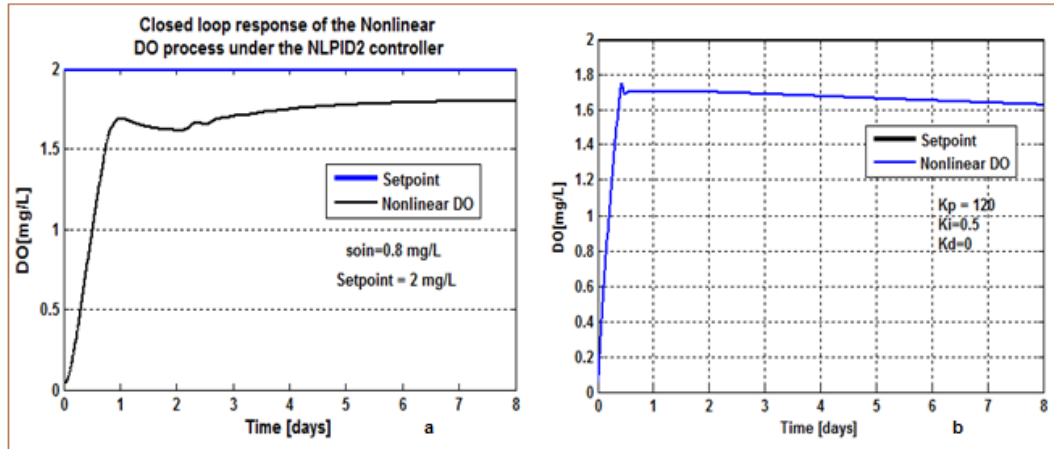


Figure 6.52: Closed loop DO process response under the NLPID2 controller, when the set-point is 2 mg/L , $s_{o,in} = 0.8 \text{ mg/L}$ and $r_{so} = -294.8954 \text{ mg/L/day}$ (Figure 6.52: (a) better tuned controller parameters for NLPID2 and (b) nonlinear DO response under the NLPID2 when the tuned for NLPID1 parameters are used in NLPID2 controller)

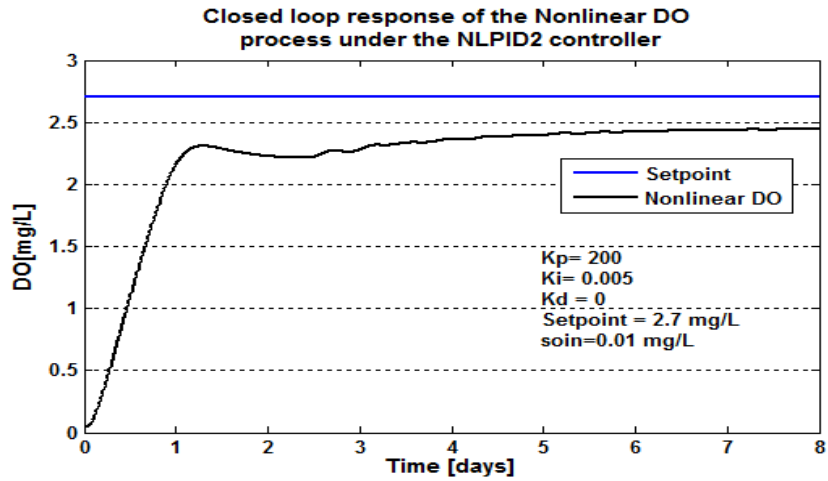


Figure 6.53: Closed loop DO process response under the NLPID2 controller, when the set-point is 2.7 mg/L , $s_{o,in} = 0.01 \text{ mg/L}$ and $r_{so} = -294.8954 \text{ mg/L/day}$

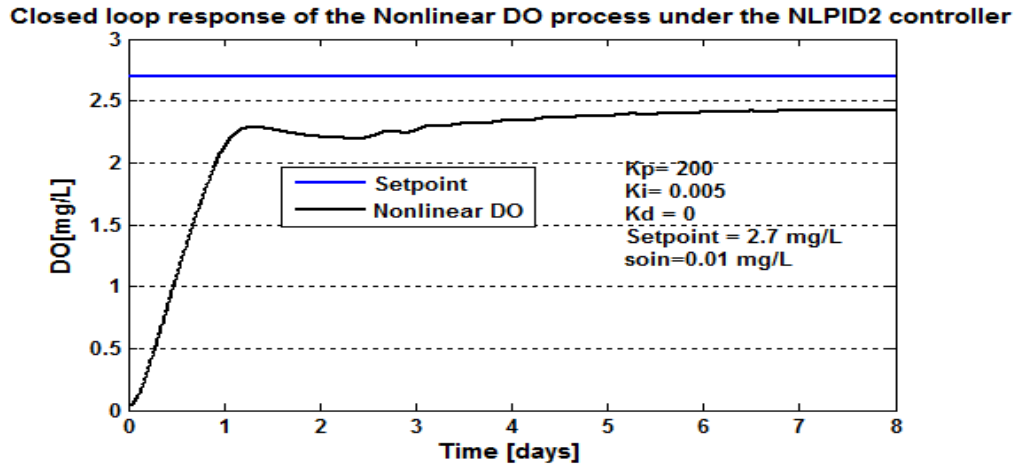


Figure 6.54: Closed loop DO process response under the NLPID2 controller, when the set-point is 2.7 mg/L , $s_{o,in} = 0.01 \text{ mg/L}$ and $r_{so} = -309.6402 \text{ mg/L/day}$

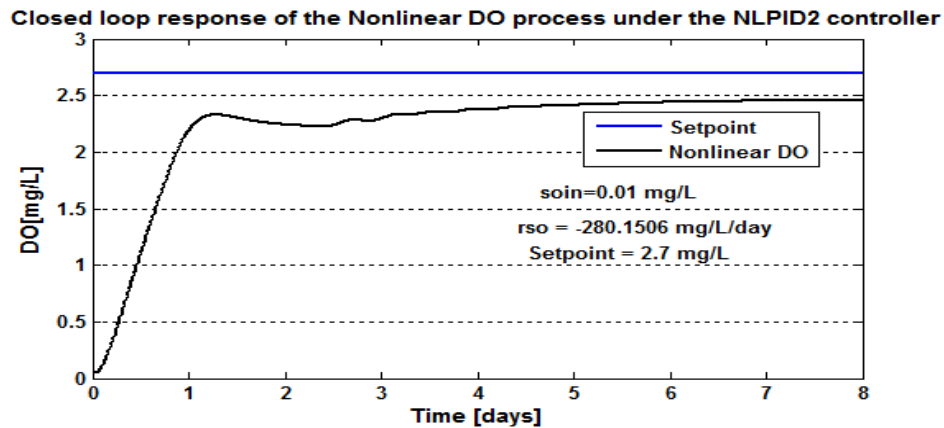


Figure 6.55: Closed loop DO process response under the NLPID2 controller, when the set-point is 2.7 mg/L , $s_{o,in} = 0.01 \text{ mg/L}$ and $r_{so} = -280.1506 \text{ mg/L/day}$

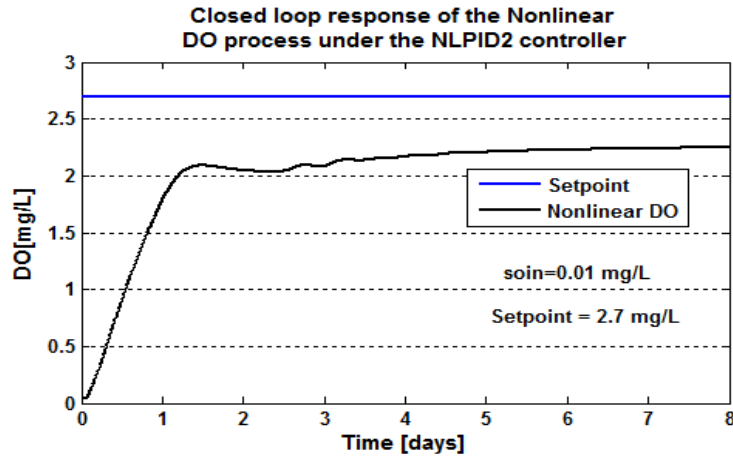


Figure 6.56: Closed loop DO process response under the NLPID2 controller, when the set-point is 2.7 mg/L , $s_{o,in} = 0.01 \text{ mg/L}$ and $r_{so} = -442.3431 \text{ mg/L/day}$

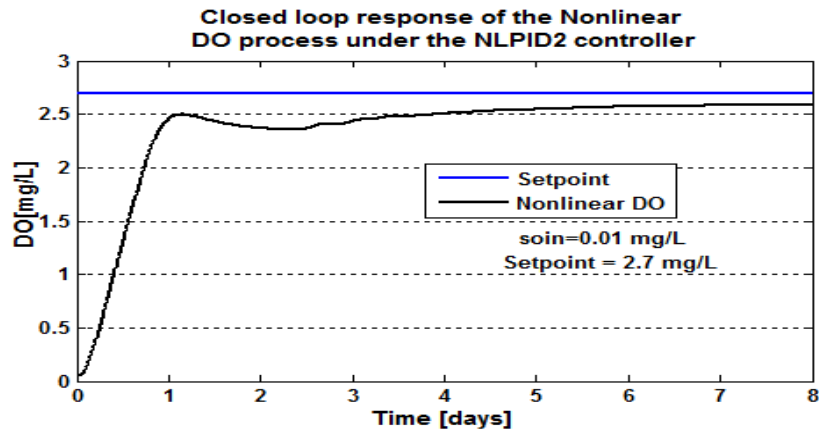


Figure 6.57: Closed loop DO process response under the NLPID2 controller, when the set-point is 2.7 mg/L , $s_{o,in} = 0.01 \text{ mg/L}$ and $r_{so} = -147.4477 \text{ mg/L/day}$

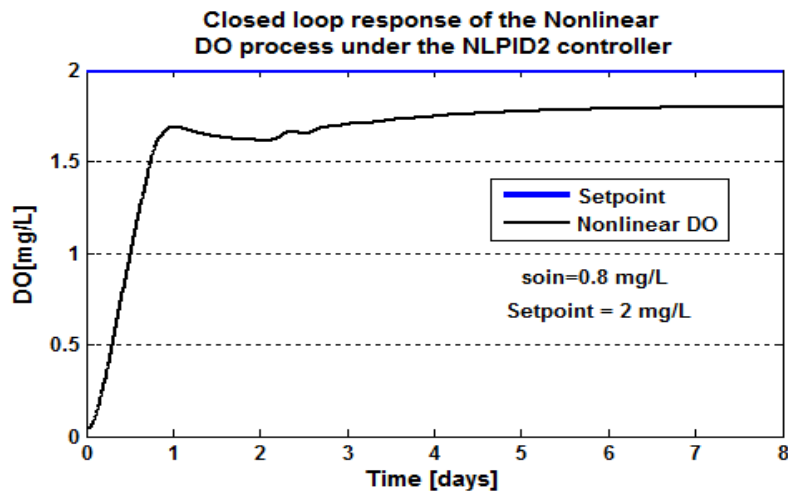


Figure 6.58: Closed loop DO process response under the NLPID2 controller, when the set-point is 2 mg/L , $s_{o,in} = 0.8 \text{ mg/L}$ and $r_{so} = -294.8954 \text{ mg/L/day/day}$

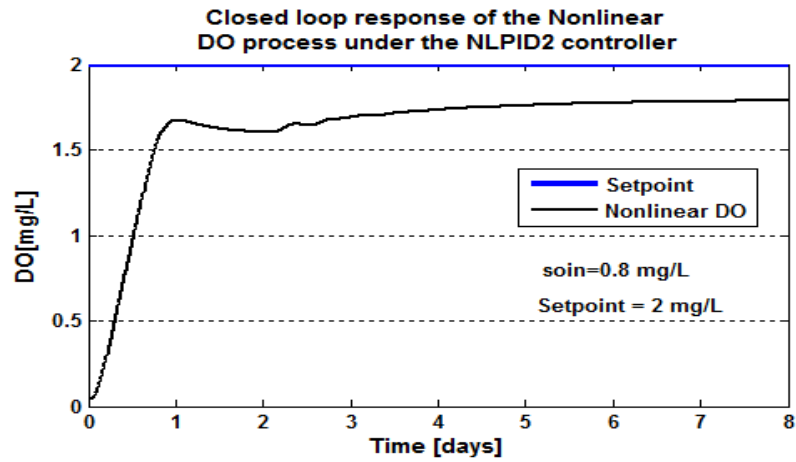


Figure 6.59: Closed loop DO process response under the NLPID2 controller, when the set-point is 2 mg/L , $s_{o,in} = 0.8\text{ mg/L}$ and $r_{so} = -309.6402\text{ mg/L/day}$

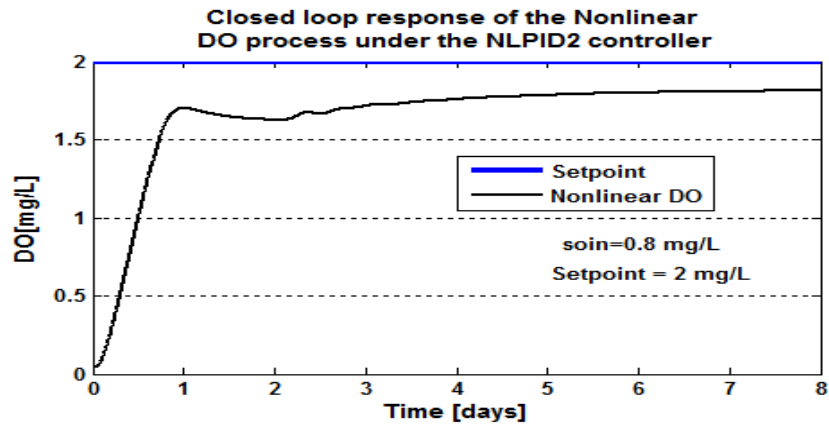


Figure 6.60: Closed loop DO process response under the NLPID2 controller, when the set-point is 2 mg/L , $s_{o,in} = 0.8\text{ mg/L}$ and $r_{so} = -280.1506\text{ mg/L/day}$

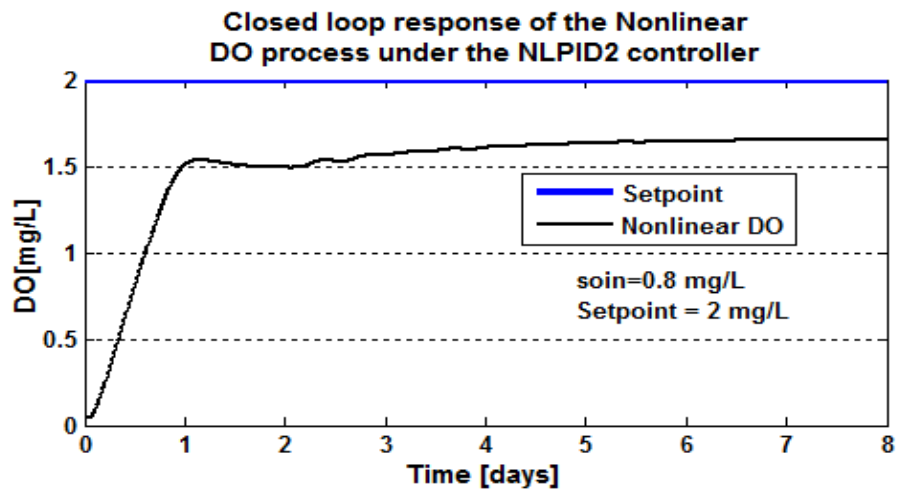


Figure 6.61: Closed loop DO process response under the NLPID2 controller, when the set-point is 2 mg/L , $s_{o,in} = 0.8\text{ mg/L}$ and $r_{so} = -442.3431\text{ mg/L/day}$

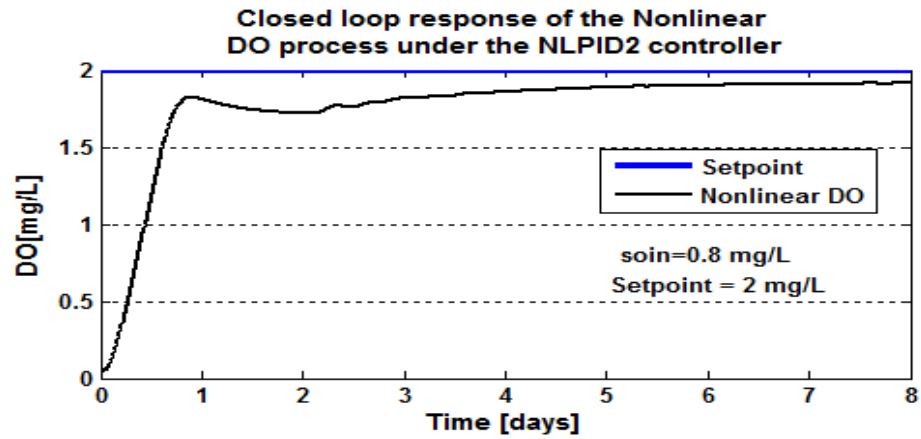


Figure 6.62: Closed loop DO process response under the NLPID2 controller, when the set-point is 2 mg/L , $s_{o,in} = 0.8\text{ mg/L}$ and $r_{so} = -147.4477\text{ mg/L/day}$

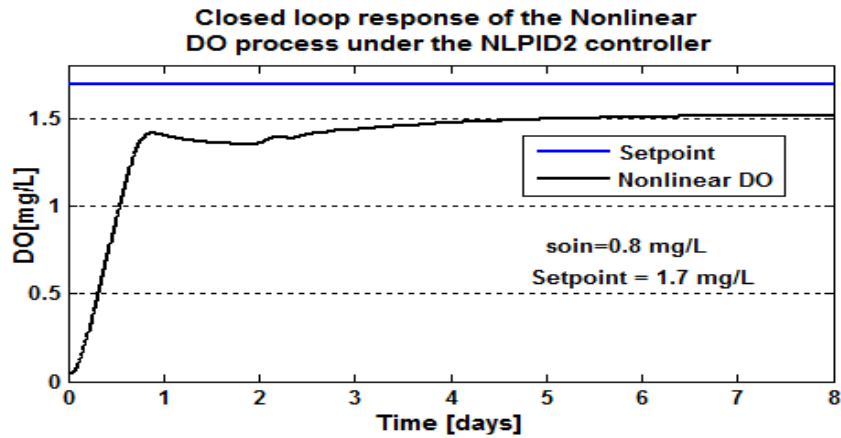


Figure 6.63: Closed loop DO process response under the NLPID2 controller, when the set-point is 1.7 mg/L , $s_{o,in} = 0.8\text{ mg/L}$ and $r_{so} = -294.8954\text{ mg/L/day}$

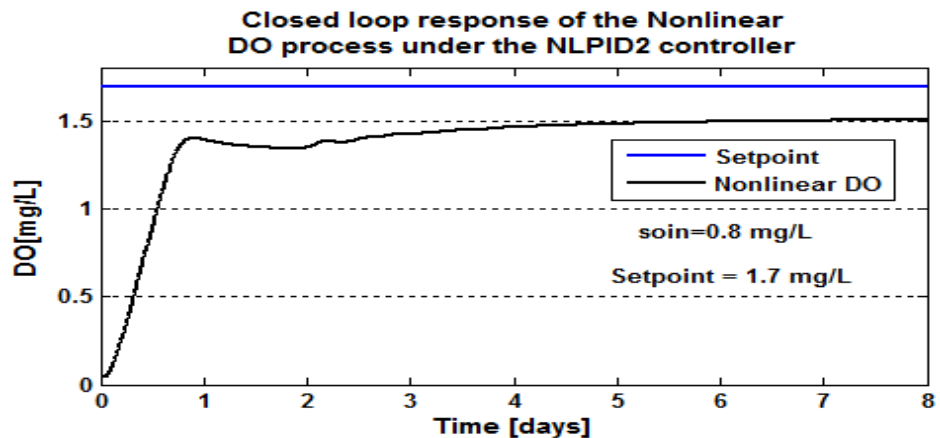


Figure 6.64: Closed loop DO process response under the NLPID2 controller, when the set-point is 1.7 mg/L , $s_{o,in} = 0.8\text{ mg/L}$ and $r_{so} = -309.6402\text{ mg/L/day}$

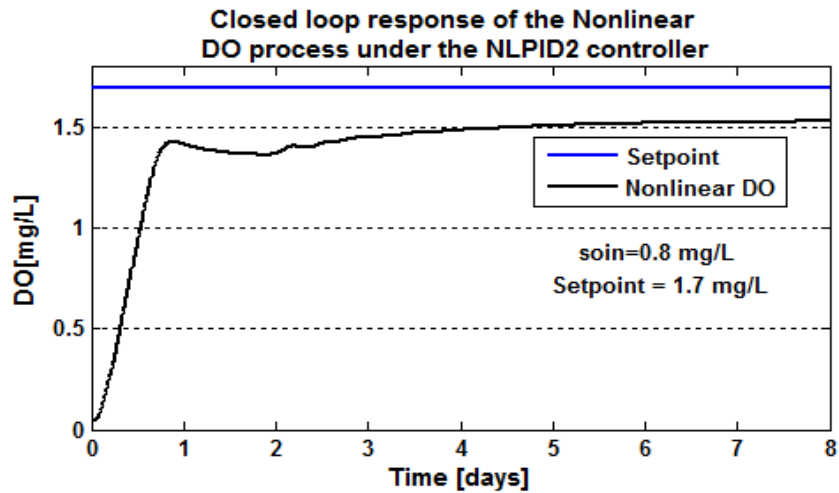


Figure 6.65: Closed loop DO process response under the NLPID2 controller, when the set-point is 1.7 mg/L , $s_{o,in} = 0.8 \text{ mg/L}$ and $r_{so} = -280.1506 \text{ mg/L/day}$

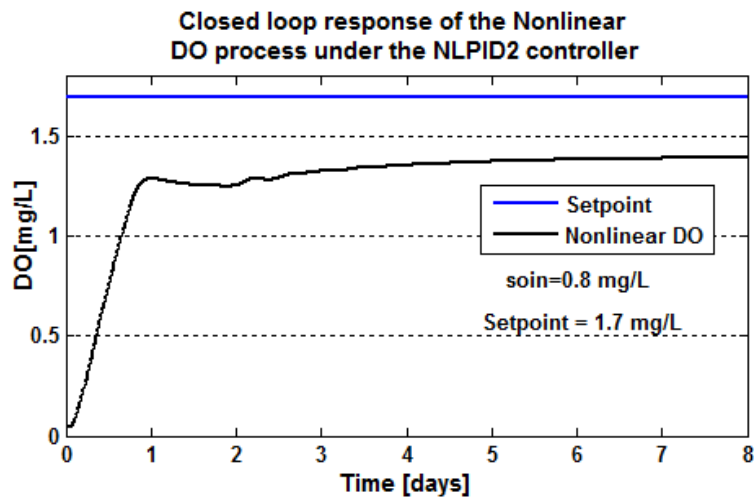


Figure 6.66: Closed loop DO process response under the NLPID2 controller, when the set-point is 1.7 mg/L , $s_{o,in} = 0.8 \text{ mg/L}$ and $r_{so} = -442.3431 \text{ mg/L/day}$

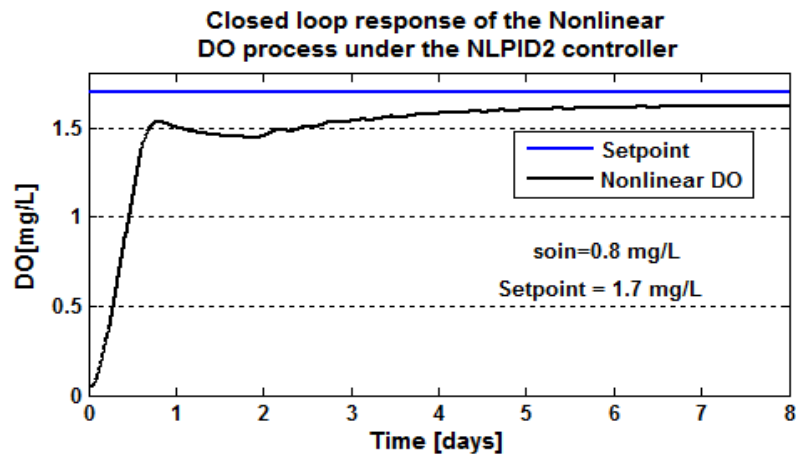


Figure 6.67: Closed loop DO process response under the NLPID2 controller, when the set-point is 1.7 mg/L , $s_{o,in} = 0.8 \text{ mg/L}$ and $r_{so} = -147.4477 \text{ mg/L/day}$

The following Table 6.6 gives the characteristics of the closed loop system behavior.

Table 6.6: Closed loop the nonlinear DO process characteristics under the NLPID2 controller

Parameters			Characteristics			
Set point	S_{oin} [mg / L]	r_{so} mg / L / day	Time delay [days]	Steady state error [mg / L]	Rise time [days]	Settling time [days]
2.7	0.01	-294.8954	0.1	0.25	0.5	4.2
2.7	0.01	-309.6402	0.1	0.27	0.5	4.2
2.7	0.01	-280.1506	0.1	0.25	0.5	4.2
2.7	0.01	-442.3431	0.1	0.45	0.5	4.5
2.7	0.01	-147.4477	0.1	0.1	0.4	4
2	0.8	-294.8954	0.1	0.2	0.5	4.1
2	0.8	-309.6402	0.1	0.21	0.5	4.2
2	0.8	-280.1506	0.1	0.18	0.5	4.1
2	0.8	-442.3431	0.1	0.34	0.5	4.3
2	0.8	-147.4477	0.1	0.1	0.4	4
1.7	0.8	-294.8954	0.1	0.18	0.5	4
1.7	0.8	-309.6402	0.1	0.2	0.5	4
1.7	0.8	-280.1506	0.1	0.18	0.5	4
1.7	0.8	-442.3431	0.1	0.305	0.5	4.2
1.7	0.8	-147.4477	0.1	0.08	0.3	3.7

6.4.2.4.1 Discussion

Simulation results shown in Figures 6.53 till 6.67 are for different set-point value with different $s_{o,in}$ and r_{so} disturbances. Making the observation of the system behavior in the above figures, it can be said that the tuned LPID controller parameters designed based on the PP1 method and applied in the NLPID2 to control the nonlinear DO process are not suitable. In the same way the accepted tuned NLPID1 controller parameters are not suitable enough to be used in the NLPID2 to control the nonlinear DO concentration process (see Figure 6.52(b)). More tuning was applied to find the controller parameter for the NLPID2 controller in order to control the nonlinear DO process model. Although the tuned NLPID2 controller parameters have controlled the nonlinear DO process to the right response path, they fail to make the process to accomplish the designed set point. In the cases like these more tuning is necessary, which is so time consuming and can make the system to oscillate. In this case the closed loop system had overshoots and started oscillations, that's is why more tuning is not the option.

Comparing the same values of the disturbance in a process for different set-point conditions (like 2 and 1.7 mg/L), the settling time is less for the process with conditions that have a smaller set-point value. This can be seen in that data values highlighted light green in the Table 6.6. In the closed loop DO process behavior, it can be seen that the

value for the steady state error increases when the r_{so} value is larger (see the comparison Table 6.7)

Table 6.7: Comparison of the obtained closed loop nonlinear DO process specifications of the designed LPID and NLPID controllers

Set-point	Disturbances	Characteristics	LPID	NLPID1	NLPID2
2.7	$r_{so} = -294.$ $s_{oin} = 0.01$	Rise Time	0.3	0.4	0.5
		Settling time	0.5	4.4	4.2
		Steady state error	0.02	0.02	0.25
		Overshoot	No	No	No
2.7	$r_{so} = -442.3231,$ $s_{oin} = 0.01$	Rise Time	0.34	0.49	0.5
		Settling time	0.5	4.9	4.5
		Steady state error	0.04	0.05	0.45
		Overshoot	No	No	No
2	$r_{so} = -294.$ $s_{oin} = 0.8$	Rise Time	0.3	0.4	0.5
		Settling time	0.4	3.5	4.1
		Steady state error	0.022	0.02	0.2
		Overshoot	No	No	No
2	$r_{so} = -442.3231$ $s_{oin} = 0.8$	Rise Time	0.34	0.44	0.5
		Settling time	0.4	4.2	4.3
		Steady state error	0.04	0.05	0.34
		Overshoot	No	No	No
1.7	$r_{so} = -294.$ $s_{oin} = 0.8$	Rise Time	0.3	0.38	0.5
		Settling time	0.35	3.6	4
		Steady state error	0.02	0.02	0.18
		Overshoot	No	No	No
1.7	$r_{so} = -442.3231$ $s_{oin} = 0.8$	Rise Time	0.34	0.4	0.5
		Settling time	0.35	4	4.2
		Steady state error	0.04	0.05	0.305
		Overshoot	no	No	No

6.5 Conclusion

The linear and two nonlinear PID controllers were designed and tuned to control the linearised and the nonlinear DO process behavior. The closed loop system has been simulated and the responses have been exposed in the related sections. The simulation results show that the use of the designed LPID parameters for the case of the linearised DO model in the NLPID controllers to control the nonlinear DO process is not successful. An additional tuning of the parameters for the NLPID controllers is required. Comparison of the results in Table 6.4 and Table 6.6 shows that the NLPID1 controller performs much better than the NLPID2 one.

The next chapter is based on the design of the LPID and NLPID controllers based on the nonlinear DO process model.

CHAPTER SEVEN

APPLICATION OF THE POLE-PLACEMENT METHOD TO DESIGN LPID AND NLPID CONTROLLERS FOR THE NONLINEAR DO PROCESS MODEL

7.1 Introduction

This Chapter carries the application of the Pole-Placement method to design LPID and NLPID controllers for the nonlinear DO process model. As in this case the DO process is nonlinear, it is not possible to follow the algorithm of the pole placement method used in Chapter 6 for the linear systems. The thesis proposes new procedures for design of the linear and nonlinear PID controllers based on the nonlinear equation of the closed loop system. Section 7.2 describes a novel design procedure based on the Pole-Placement method for design of LPID and NLPID controllers for the nonlinear DO process. Section 7.3 gives the design of the LPID controller parameters for the nonlinear DO process, and its simulation results. The design of the NLPID1 controller parameters for the nonlinear DO process is given in Section 7.4. Section 7.5 discusses the design of the NLPID2 controller parameters for the nonlinear DO process. Section 7.6 gives the conclusion of this Chapter.

7.2 Procedure for Design of the LPID and NLPID Controllers Parameters for the nonlinear DO process based on the Pole-Placement method

The pole placement method is applied to design the controllers' parameters for the LPID and the two NLPID controllers based on the nonlinear model of the DO process.

The following steps are proposed for the design process of the linear and nonlinear PID controllers for the nonlinear DO process model:

- Nonlinear DO model is combined with the PID controller through an exponential model of the Oxygen Transfer Rate (OTR) in order to find the equation of the nonlinear closed loop system.
- The equation of the closed loop system is a function of the PID parameters K_p, T_i, T_d . This equation is a second order equation according the unknown parameters with three unknowns which means its solution can be found only for two of them. On this basis T_d is accepted to be known.
- The Matlab function *fso/ve* is used to find the values of K_p and T_i parameters.

This procedure, called Pole placement2 (PP2) method is described below through

numerical solution of the differential equation of the closed loop system towards K_p and T_i . The nonlinear controllers equations (Equation 5.1 - NLPID1) and (Equation 5.3 - NLPID2) are used to develop the procedure for the controllers design. Design of the controller parameters for the nonlinear DO process in the following sections is divided in three ways: design of the LPID controller parameters based on the nonlinear DO process model, design of the NLPID1 controller parameters based on the nonlinear DO process model, and design of the NLPID2 controller parameters based on the nonlinear DO process model.

7.3 Design of the LPID controller parameters for the nonlinear DO process model

The representation of the time-domain conventional linear PID controller is

$$u = K_p \left[e + \frac{1}{T_i} \int_0^t e dt + T_d \frac{de}{dt} \right] = K_p e + K_i \int_0^t e dt + K_d \frac{de}{dt} \quad (7.1)$$

Where: K_p ; $K_i = \frac{K_p}{T_i}$; $K_d = K_p T_d$ are the controller gains, T_i is the integral time constant, T_d is the derivative time constant and u is the controller output. In general a closed loop system error is $e = r - y$, where y is the output of the process under control and r is the desired reference trajectory.

To design the LPID controller parameters for the nonlinear DO process model; the following steps are followed:

1. The Dissolved Oxygen (DO) concentration process model given by Equation 7.2a is combined with the LPID controller model given by Equation 7.1 through the exponential model of the Oxygen Transfer Rate (OTR), given by Equation (7.2b).

$$\frac{ds_o}{dt} = \frac{1}{V_n} \left[Q_n (s_{o,n-1} - s_o) \right] + r_{s_o} + K_{La} (s_{o,sat} - s_o) \quad (7.2a)$$

Where:

$$K_{La} = K_1 \left[1 - e^{-K_2 u} \right] \quad (7.2b)$$

2. Derivations of the closed loop DO process equation. The equation is written for the error between the set-point and the current value of the dissolved oxygen as follows:

$$e = s^{sp}_o - s_o \quad (7.3)$$

Then the differential equation of the closed loop DO process is:

$$s_o - \frac{Q}{V}(s_{o,in} - s_o) - r_{s_o} - K_1(1 - e^{-K_2 \left\{ K_p \left[e + \frac{1}{T_i} \int e dt + T_d \frac{de}{dt} \right] \right\}})(s_{o,Sat} - s_o) = 0 \quad (7.4)$$

3. Substitute Equation (7.3) in Equation (7.4) to form the final DO process model of the closed loop system expressed as a function of s_o and the LPID controller parameters, as shown in Equation (7.5)

$$s_o - \frac{Q}{V}(s_{o,in} - s_o) - r_{s_o} - K_1(1 - e^{-K_2 \left\{ K_p \left[(s_{o,Sat} - s_o) + \frac{1}{T_i} \int (s_{o,Sat} - s_o) dt + T_d \frac{d(s_{o,Sat} - s_o)}{dt} \right] \right\}})(s_{o,Sat} - s_o) = 0 \quad (7.5)$$

4. If the values of the s_o are known in every moment of time, then the parameters of the LPID controller are the only unknown variables of the Equation (7.5). These parameters can be found by solution of the Equation (7.5) which includes first and second order derivatives of the dissolved oxygen concentration. On this basis, only two controller parameters are considered to be unknown: K_p and T_i . The parameter T_d is considered known and constant. The calculated parameters of the LPID controller depend on the selected value of the DO concentration s_o . The open loop DO process behavior trajectory is selected to be known. Then the parameters K_p and T_i are calculated for every point of this trajectory. As the Equation (7.5) is a nonlinear one it cannot be solved analytically. A numeric method is selected. The Matlab function 'fsolve' is applied. It uses the Leverberg – Marquardt optimization algorithm to calculate the best values of the unknown parameters K_p and T_i . The Equation (7.5) is solved by using some initial guess values of the PID control coefficients K_p and T_i . The LPID parameters are calculated for all values of the open loop trajectory of the dissolved oxygen s_o , found as a reaction of the process to a step input. The following Figure (8.1) shows the flow chart of the calculation procedure.

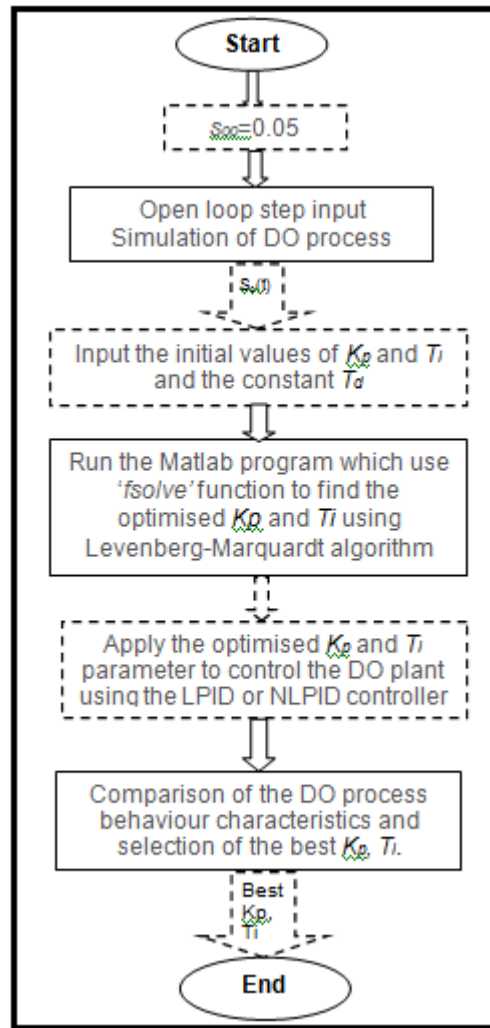


Figure 7.1: Flow diagram to solve the Equation (7.5) according K_p and T_i

A Matlab/Simulink program is developed to calculate the unknown controller parameters in Equation (7.5), Appendix.B7. The obtained parameters K_p and T_i , are shown in Table 7.1.

7.3.1 FSOLVE function based on the Levenberg-Marquardt Algorithm

The Levenberg-Marquardt (LM) algorithm is used to solve the non-linear newly formed equation (in the above case 7.5). It is a standard technique and is used to solve the nonlinear function..

The Levenberg-Marquardt curve-fitting method is actually a combination of two minimization methods:

- i. The *gradient descent* method and
- ii. The *Gauss-Newton* method.

Gavin, (2013) says that in the gradient descent method, the sum of the squared errors is reduced by updating the parameters in the direction of the greatest reduction of the least squares objective. In the Gauss-Newton method, the sum of the squared errors is reduced by assuming the least squares function is locally quadratic, and then the minimum of this quadratic function is found. The Levenberg-Marquardt algorithm acts more like a gradient-descent method when the parameters are far from their optimal value, and act more like the Gauss-Newton method when the parameters are close to their optimal value (Gavin, 2013).

The initial guess values selected for the application for the PP2 procedure for the design of the LPID controller are as follows: K_p initial = 30, T_i initial =10. Based on the given s_o trajectory the following trajectories of the K_p and T_i variables were obtained as shown in Table 7.1.

Table 7.1: Obtained K_p , T_i for the linear PID controller

s_o	K_p	T_i
0.05	29.99	2.99
1.94	29.77	46.34
1.967	29.878	100.27
1.97	29.89	83.8
1.984	29.9	62.27
2.0	29.99	45.89
2.044	30.153	28.054
2.01	30.0	38.33
2.03	30.09	30.9
2.05	30.17	24.6
2.03	30.11	29.2
2.024	30.0760	33.92
2.04	30.5	26.4
2.05	30.175	24.5
2.02	30.08	33.01
2.02	30.0773	33.75
2.02	30.07	33.9

The optimal control parameters shown above in Table 7.1 are calculated under different values of s_o . Matlab function 'fso/ve' is used in a program called "findlpidpar_pp2" to call a function file called "myfun5" and find different final optimal values of K_p and T_i based on the different values of $s_o(t)$, $t_o=0$ to t_f were $t_f=8days$. After these control values were obtained, many tests were performed to determine with which LPID controller parameters the nonlinear DO process behavior is according to the required specifications. The programs developed for this process are given in Appendix B7 and explained in Chapter 9, Table 9.1. The following Table 7.2 gives the best performing

LPID controller parameter for the nonlinear DO process.

Table 7.2: Selected controller parameters for nonlinear DO process under the linear PID controller

Controller	k_i	T_i	K_p
LPID	-1574	26.05	30.1555
LPID	0.8865	33.92	30.0760
LPID	0.8910	33.75	30.0773

From the chosen best performing optimized controller parameters K_p and T_i given in Table 7.2, the best of the best as they are highlighted in green in the above table are used in the LPID controller given in Figure (7.2), to control the closed loop system. Later different disturbance and set point values are changed in the DO process in order to investigate whether these controller parameters can still handle variations in the system. The following section is based on the simulation of the nonlinear DO process under the LPID controller.

7.3.2 Simulink block diagram of the closed loop system under the LPID controller

The model of the DO closed loop system has been built in Simulink based on the linear PID controller as shown in Figure 7.2. The parameters designed for the LPID controller as indicated in Table 7.2 above using the Pole Placement 2 method are applied to the controller block (LPID) to control the process of DO concentration.

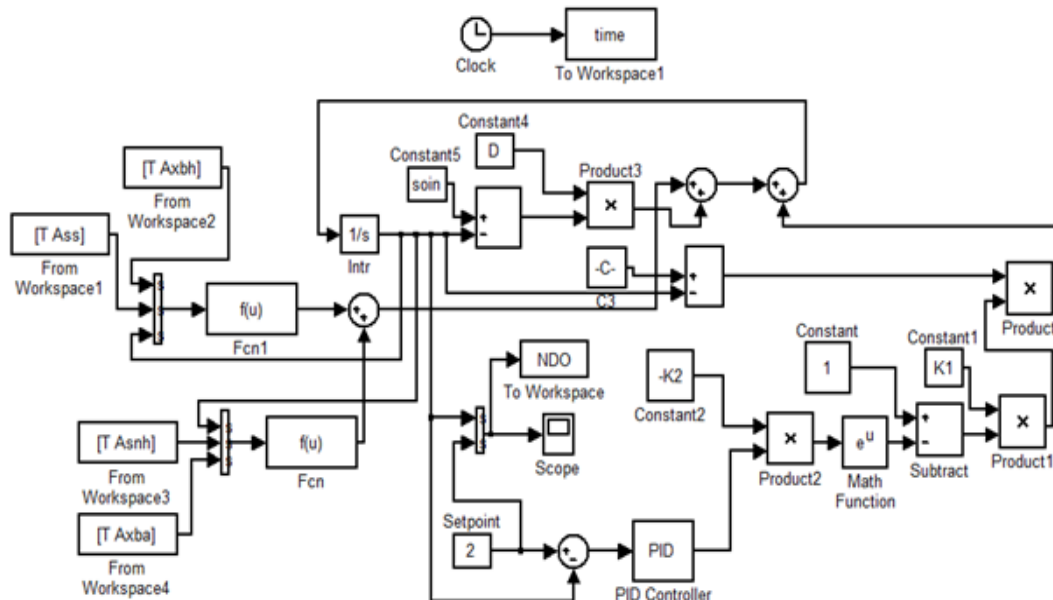


Figure 7.2: Closed Loop diagram of the nonlinear DO process with the linear PID controller

7.3.2.1 Simulation results of the closed loop nonlinear DO process based on the LPID controller

Table 7.3 shows the variations of the DO disturbances that are used to investigate the closed loop system behavior under the LPID controller.

Table 7.3: Variation for the DO set-point and DO process disturbances

Set-point	S_{oin}	r_{so}
2.7	0.01	-294.8954
2.7	0.01	-309.6402
2.7	0.01	-280.1506
2.7	0.01	-442.3431
2.7	0.01	-147.4477
2	0.8	-294.8954
2	0.8	-309.6402
2	0.8	-280.1506
2	0.8	-442.3431
2	0.8	-147.4477
1.7	0.8	-294.8954
1.7	0.8	-309.6402
1.7	0.8	-280.1506
1.7	0.8	-442.3431
1.7	0.8	-147.4477

The values in the above Table 7.3 have been applied in the DO process in order to view the changes that may occur on the system behavior under these conditions. The following results shown in Figure 7.3 – Figure 7.17 were obtained.

Closed loop response of the nonlinear DO process under the LPID controller parameters designed based on the nonlinear DO model

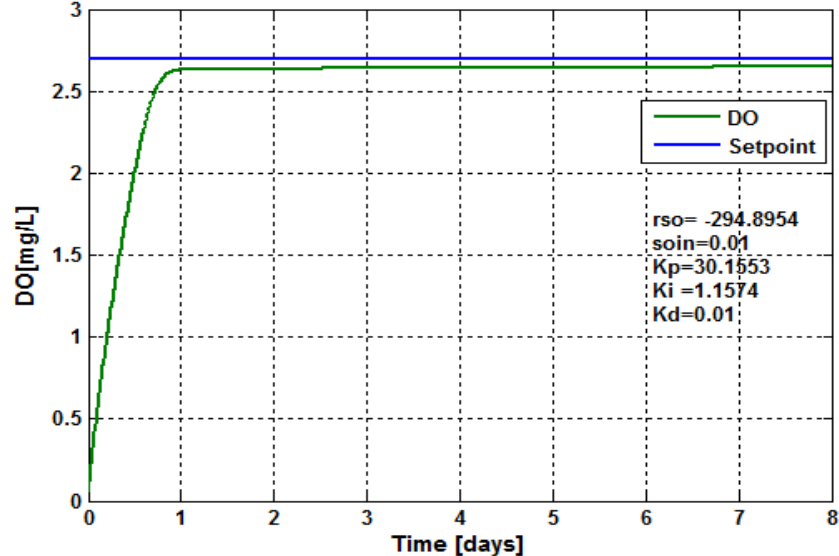


Figure 7.3: Closed loop DO process response under the LPID controller, when the set-point is 2.7 mg/L and $r_{so} = -294.8954 \text{ mg/L/day}$

Closed loop response of the nonlinear DO process under the LPID controller parameters designed based on the nonlinear DO model

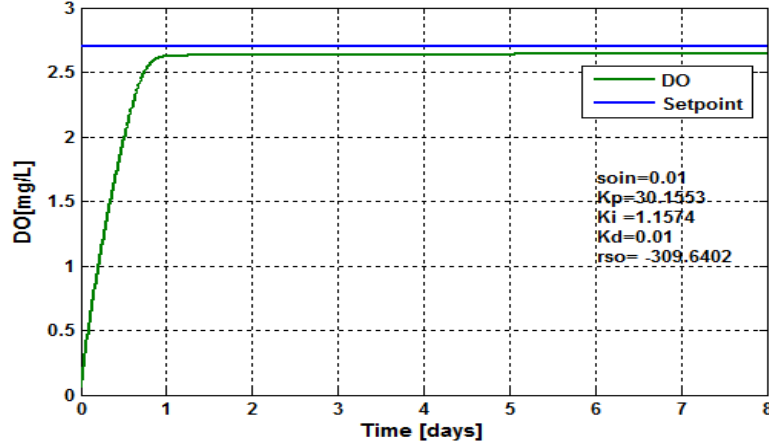


Figure 7.4: Closed loop DO process response under the LPID controller, when the set-point is 2.7 mg/L and $r_{so} = -309.6402 \text{ mg/L/day}$

Closed loop response of the nonlinear DO process under the LPID controller parameters designed based on the nonlinear DO model

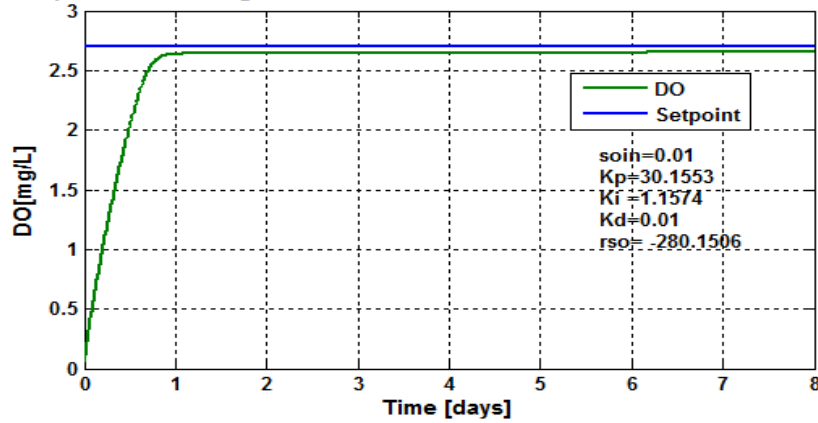


Figure 7.5: Closed loop DO process response under the LPID controller, when the set-point is 2.7 mg/L and $r_{so} = -280.1506 \text{ mg/L/day}$

Closed loop response of the nonlinear DO process under the LPID controller parameters designed based on the nonlinear DO model

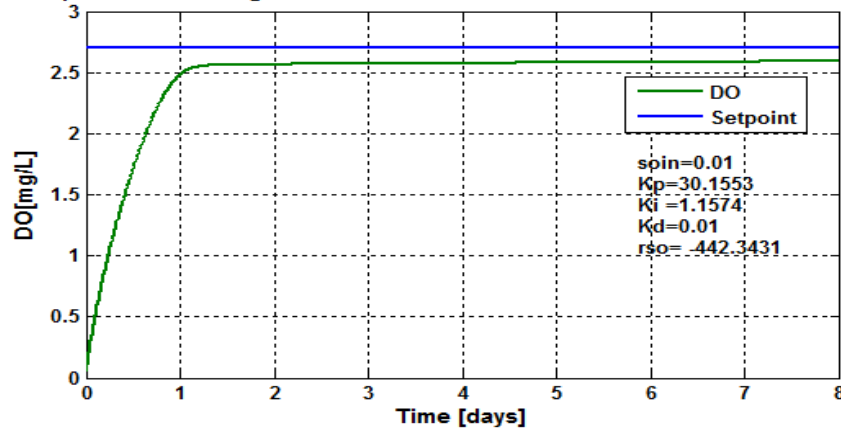


Figure 7.6: Closed loop DO process response under the LPID controller, when the set-point is 2.7 mg/L and $r_{so} = -442.3431 \text{ mg/L/day}$

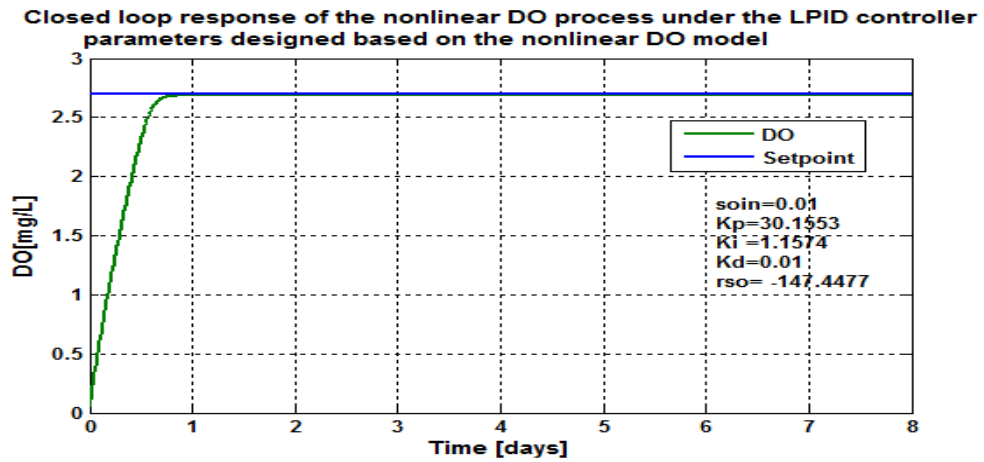


Figure 7.7: Closed loop DO process response under the LPID controller, when the set-point is 2.7 mg/L and $r_{so} = -147.4477 \text{ mg/L/day}$

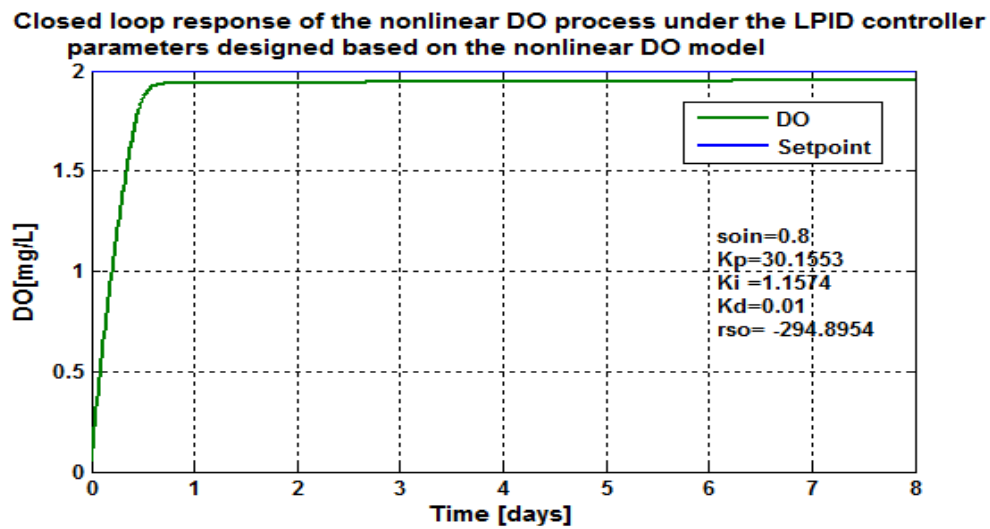


Figure 7.8: Closed loop DO process response under the LPID controller, when the set-point is 2 mg/L and $r_{so} = -294.8954 \text{ mg/L/day}$

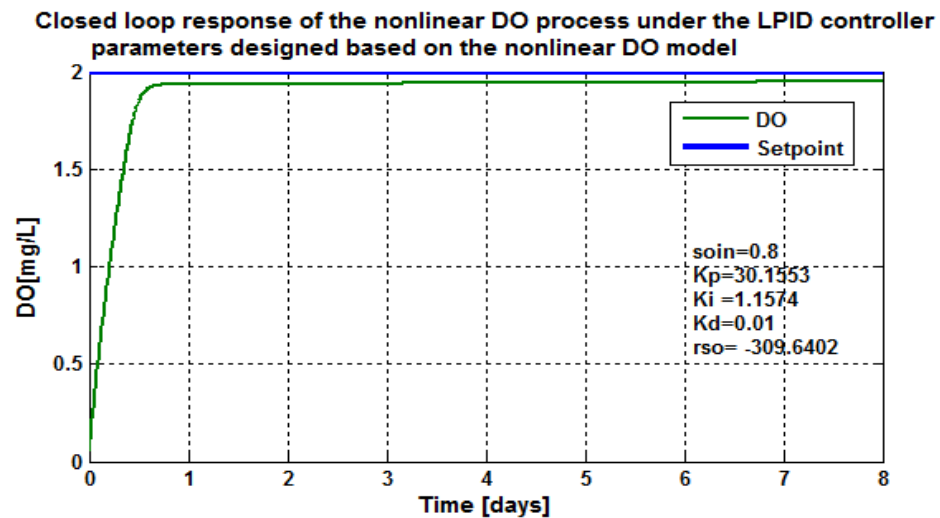


Figure 7.9: Closed loop DO process response under the LPID controller, when the set-point is 2 mg/L and $r_{so} = -309.6402 \text{ mg/L/day}$

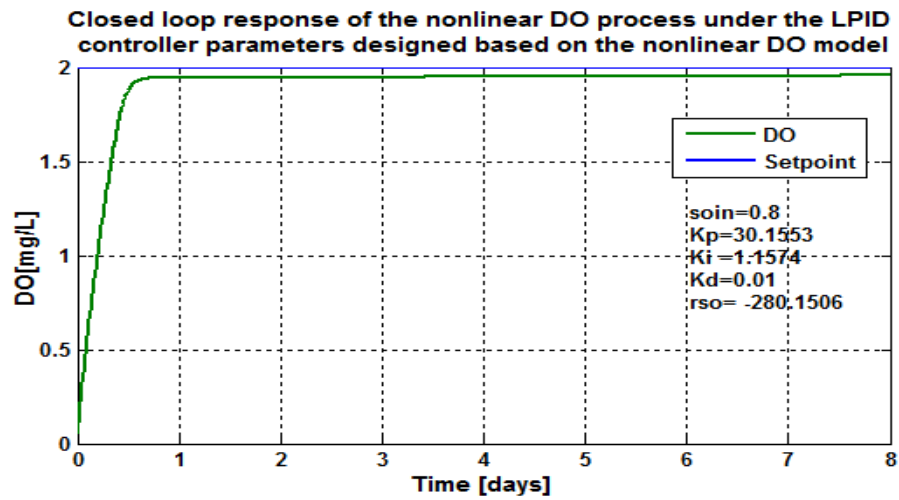


Figure 7.10: Closed loop DO process response under the LPID controller, when the set-point is 2 mg/L and $r_{so} = -280.1506 \text{ mg/L/day}$

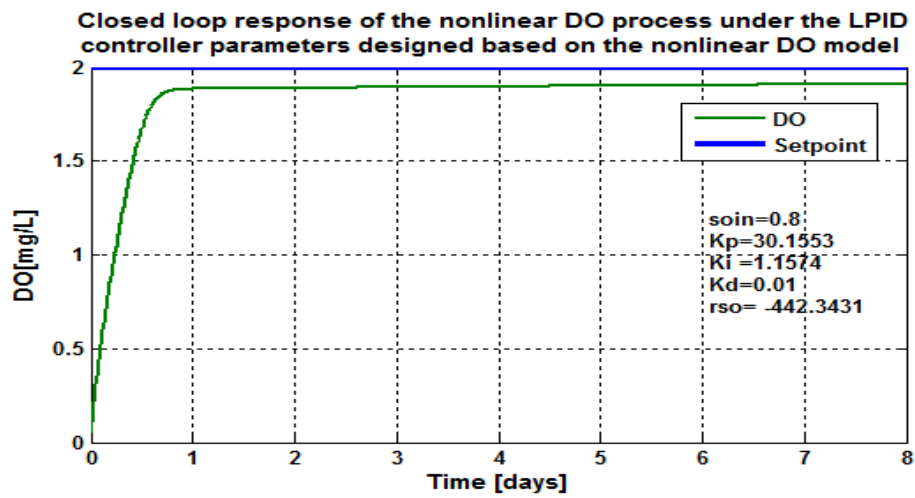


Figure 7.11: Closed loop DO process response under the LPID controller, when the set-point is 2 mg/L and $r_{so} = -442.3431 \text{ mg/L/day}$

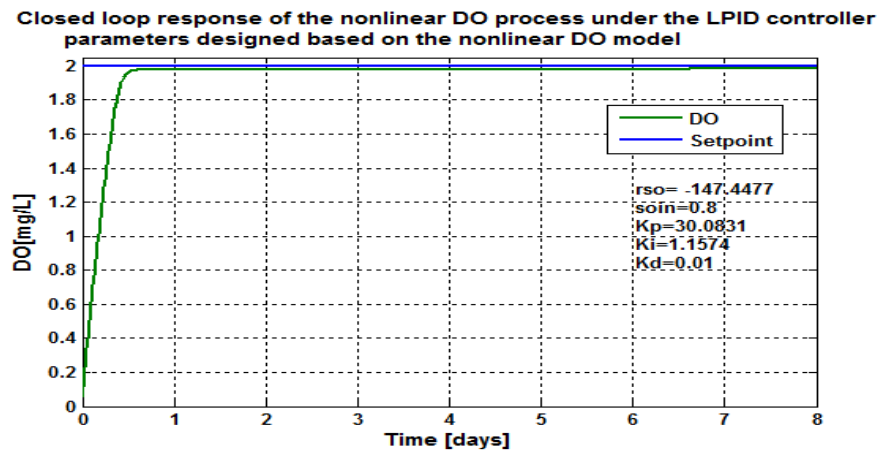


Figure 7.12: Closed loop DO process response under the LPID controller, when the set-point is 2 mg/L and $r_{so} = -147.4477 \text{ mg/L/day}$

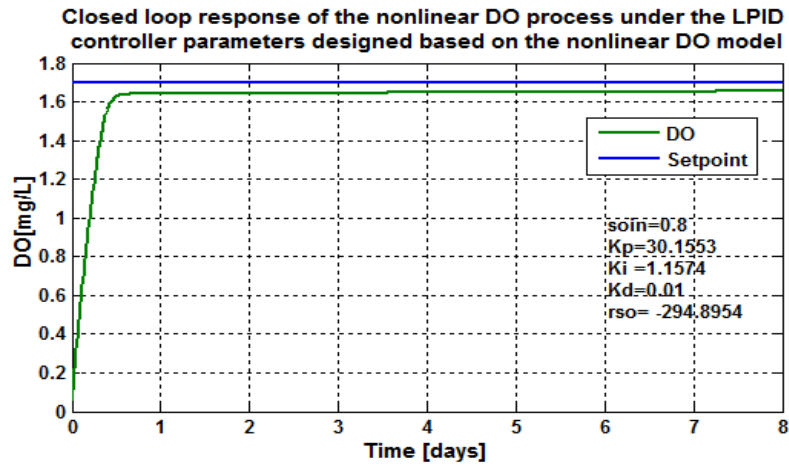


Figure 7.13: Closed loop DO process response under the LPID controller, when the set-point is 1.7 mg/L and $r_{so} = -294.8954 \text{ mg/L/day}$

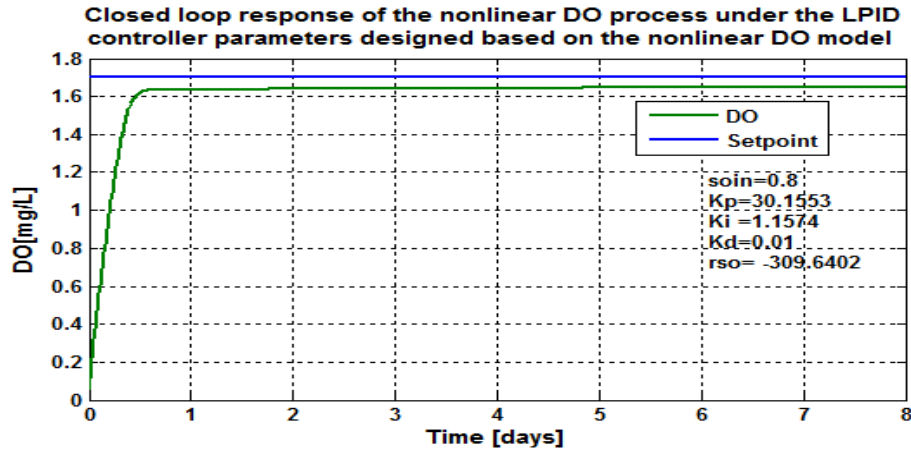


Figure 7.14: Closed loop DO process response under the LPID controller, when the set-point is 1.7 mg/L and $r_{so} = -309.6402 \text{ mg/L/day}$

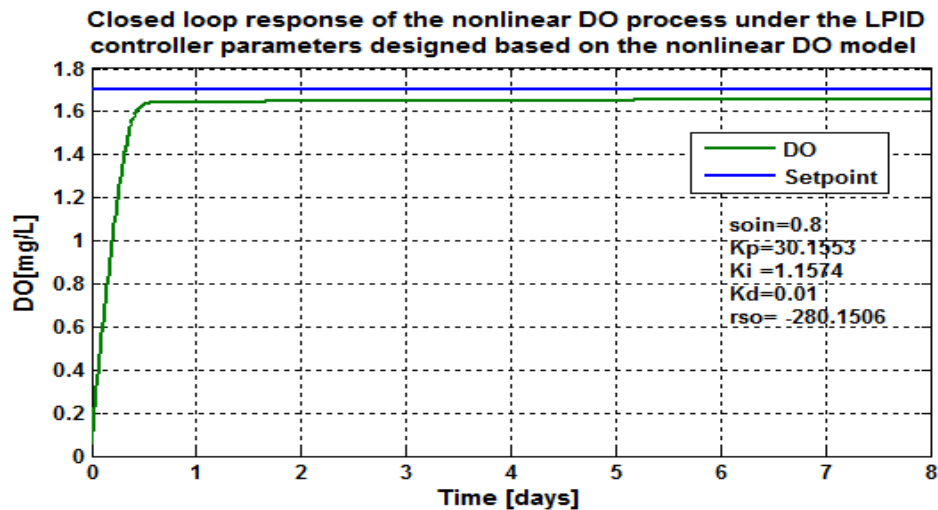


Figure 7.15: Closed loop DO process response under the LPID controller, when the set-point is 1.7 mg/L and $r_{so} = -280.1506 \text{ mg/L/day}$

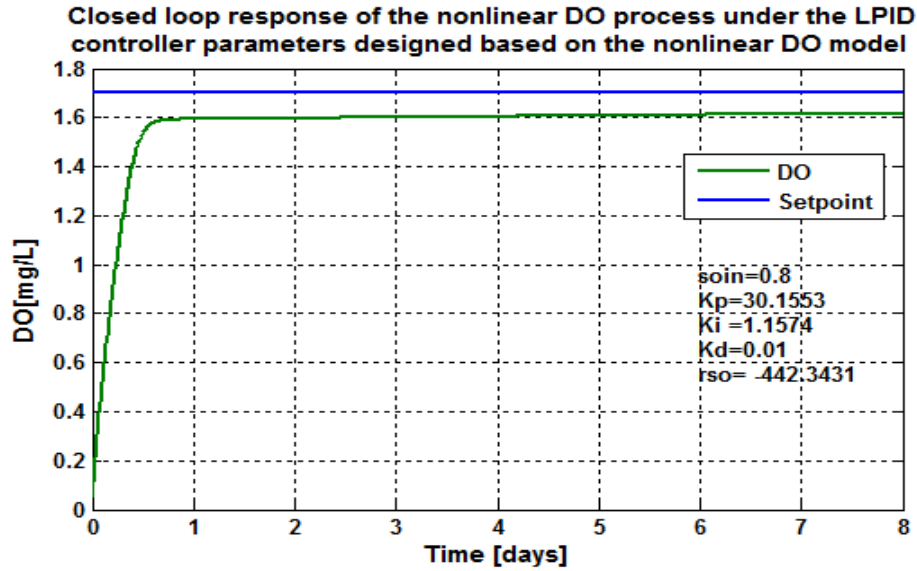


Figure 7.16: Closed loop DO process response under the LPID controller, when the set-point is 1.7 mg/L and $r_{so} = -442.3431 \text{ mg/L/day}$

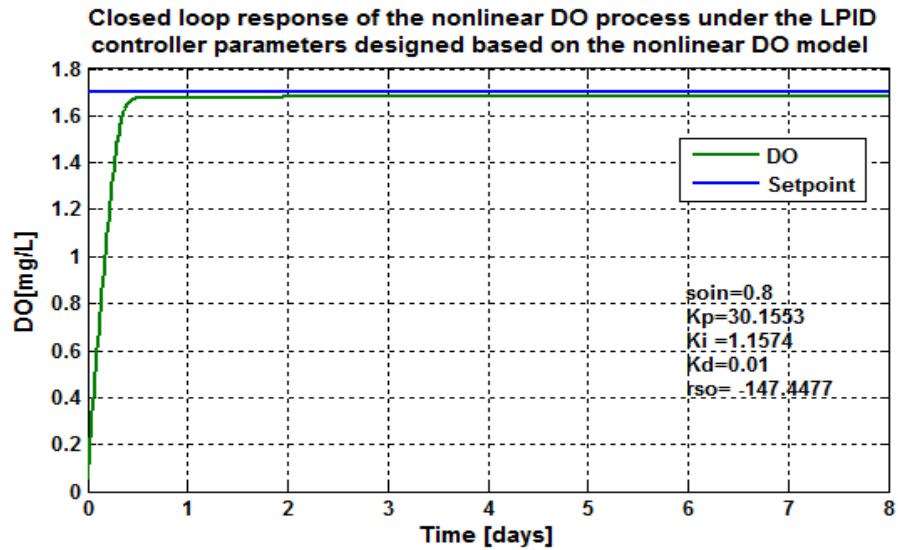


Figure 7.17: Closed loop DO process response under the LPID controller, when the set-point is 1.7 mg/L and $r_{so} = -147.4477 \text{ mg/L/day}$

7.3.2.2 Discussion on the simulation results based on the LPID controller

Table 7.4 shows the characteristics of the behavior of the closed loop DO process controlled by the LPID controller whose parameters are designed based on the nonlinear DO process.

Table 7.4: Nonlinear DO process characteristics under the LPID controller

Parameters			Characteristics			
Set point	s_{oin} [mg / L]	r_{so} mg / L / day	Time delay [days]	Steady state error [mg / L]	Rise time [days]	Settling time [days]
2.7	0.01	-294.8954	0.05	0.05	0.5	1
2.7	0.01	-309.6402	0.05	0.07	0.5	1
2.7	0.01	-280.1506	0.05	0.05	0.5	1
2.7	0.01	-442.343	0.05	0.12	0.7	1.2
2.7	0.01	-147.4477	0.05	0.01	0.5	1
2	0.8	-294.8954	0.05	0.05	0.5	0.75
2	0.8	-309.6402	0.05	0.055	0.5	0.8
2	0.8	-280.1506	0.05	0.05	0.5	0.8
2	0.8	-442.343	0.05	0.12	0.55	1
2	0.8	-147.4477	0.05	0.05	0.4	0.6
1.7	0.8	-294.8954	0.2	0.05	0.3	1
1.7	0.8	-309.6402	0.05	0.07	0.3	0.5
1.7	0.8	-280.1506	0.05	0.05	0.3	0.5
1.7	0.8	-442.343	0.05	0.12	0.4	0.6
1.7	0.8	-147.4477	0.05	0.05	0.3	0.4

Through the characteristics shown in the above (Table 7.4), it is noted that the use of the proposed pole placement procedure can produce the LPID controller parameters capable to lead the DO process to good performance. It can be seen that the steady state error increases if the variation of the internal disturbances is high; this is shown with the green highlight on the table. Considering different set-points conditions high and low (such as 2.7 and 2 mg/L) with the same values of r_{so} and different values of s_{oin} ; it can be seen that the case with the high set-point value of 2.7 has a big rise time and settling time values with the steady state error of 0.1 which is higher than 0.08 in the set point condition of 2 mg/L. When the internal disturbances in the DO process are the same, but the set-points for the process are different; the rise time and settling time are higher in the case of 2.7 mg/L set point.

7.4 Design of the NLPID1 controller parameters for the nonlinear DO process

In order to obtain the nonlinear PID controller parameters, the control design steps shown and explained in section 7.3 must be followed, but now based on the nonlinear PID controller (NLPID1) model:

1. Models of the NLPID1 controller and the plant.

The representation of the nonlinear PID1 controller in time-domain is:

$$u(t) = K_p \left[f(e, \alpha_p, \delta_p) + \frac{1}{T_i} f(\int e, \alpha_i, \delta_i) + T_d f(\dot{e}, \alpha_d, \delta_d) \right] \quad (7.6)$$

The above equation (Equation 7.6) is explained in Chapter 5 (as Equation 5.1.), where: K_p, T_i and T_d are the controller gains similar to these of the LPID controller, δ is the constant used to determine the linear range of the error function, α is the nonlinear degree of the error function (Jiang, 2009), e is the error signal.

The nonlinear function proposed by Jiang *et al.*, (2009) and Zaidner *et al.*, (2010) can be mathematically represented as follows:

$$f(e, \alpha, \delta) = \begin{cases} \text{sign}(e) \cdot |e|^\alpha, & \text{when } |e| > \delta \\ \delta^{\alpha-1} \cdot e, & \text{when } |e| \leq \delta \end{cases} \quad (7.7)$$

Equation (7.8) describes the considered DO process model:

$$\dot{s}_o - \frac{Q}{V}(s_{o,in} - s_o) - r_{s_o} - K_1(1 - e^{-K_2 u})(s_{o,Sat} - s_o) = 0 \quad (7.8)$$

2. Derivation of the equation of the closed loop DO system

The control action in Equation 7.8 must be substituted by Equation 7.6 and Equation 7.7 to form the closed loop equation of the system:

$$\dot{s}_o - \frac{Q}{V}(s_{o,in} - s_o) - r_{s_o} - K_1(1 - e^{-K_2 \left(K_p \left[f(e, \alpha, \delta_p) + \frac{1}{T_i} f(\int e, \alpha_i, \delta_i) + T_d f(\dot{e}, \alpha_d, \delta_d) \right] \right)})(s_{o,Sat} - s_o) = 0 \quad (7.9)$$

3. Solution of the equation (7.9) by a numeric method

The Equation 7.9 is numerically solved by using the Matlab function *fso/ve*. The algorithm for the solution of the Equation (7.9) is the same as this given in Figure 7.1. A Matlab script file named “*Findnlpid1par_PP2.m*” is developed to calculate the control parameters in Equation 7.9 based on the variable of $s_o(t)$, $t = 0:tf$ which is the trajectory of the DO process under unit step input. In order for this program to give the needed solution of Equation (7.9) it works with a function file named as “*myfun1*”, which is called by an iteration loop in the script file to calculate of every point of $s_o(t)$, $t_0 = 0:t_f = 8(\text{days})$, the values of K_p and T_i . These two files are given in Appendix B8. Table 7.5 gives the obtained optimized parameter trajectories.

Table 7.5: Obtained NLPID1 controller parameters designed based on the nonlinear DO process

s_o	Kp	Ti	Ki
0.05	52	10	5.2
0.99	52	10	5.2
1.68	0.9	52	0.017

1.756	1.0	30.04	0.033
1.859	1.409	37.577	0.034
1.940	2.61	69.10	0.03
1.983	5.05	64.032	0.0789
2.00	10.9	65.78	0.165
2.007	24.38	66.66	0.369
2.010	33.64	61.39	0.54
2.014	41.3	51.92	0.79
2.02	48.7	35.38	1.355
2.0322	49.7	28.22	1.72
2.04	51.1	19.23	2.65
2.02	49.75	28.33	1.75
2.020	48.09	35.71	1.34

The performance of the obtained controller parameters was tested to control the nonlinear DO process and the best three selected controller parameters are given in Table 7.6. The best performed K_p and T_i value are used for further tests of the closed loop system behavior under different set-point and disturbance values. The selected controller parameters from the calculated values in Table 7.5 are shown below in Table 7.6.

Table 7.6: The chosen NLPID1 controller parameters for the nonlinear DO process

Controller	s_o	K_p	T_i	K_i
NLPID1	2.04	51.1	19.23	2.65
NLPID1	2.007	24.66	66.66	0.369
NLPID1	2.010	33.64	61.39	0.54
NLPID1	2.014	41.3	51.92	0.79
NLPID1	2.02	48.7	35.38	1.355

7.4.1 Simulink Block Diagram of the DO closed loop system under the NLPID1 controller

Figure 7.18 shows the Simulink block diagram of the closed loop system of the DO process based on the nonlinear PID controller (NLPID1) described and shown in Chapter 5.3.3. In this Chapter, the diagram in Figure 7.18 is simulated using the NLPID1 controller designed based on the nonlinear DO process.

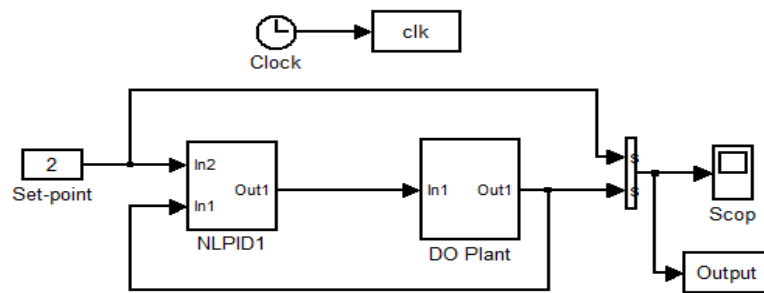


Figure 7.18: Simulink diagram of the closed loop DO process using the NLPID1 controller

NLPID1 controller parameters used for the simulation are the best performing controller parameters that were tested which are highlighted in Table 7.6. The following section gives the simulation results of the closed loop nonlinear DO process under the nonlinear PID1 controller parameters designed based on the PP2 method.

7.4.2 Simulation results of the closed loop nonlinear DO process based on the NLPID1 controller

The simulations are performed according to the various set points and DO process disturbances as given in the Table 7.3. The next figures (Figure 19 to Figure 33) show the results of the closed loop DO system behavior when the disturbance and the set-point variations are performed. This is done in order to make an examination of how well the system will perform under the NLPID1 controller, when using the designed control parameters in Table 7.6.

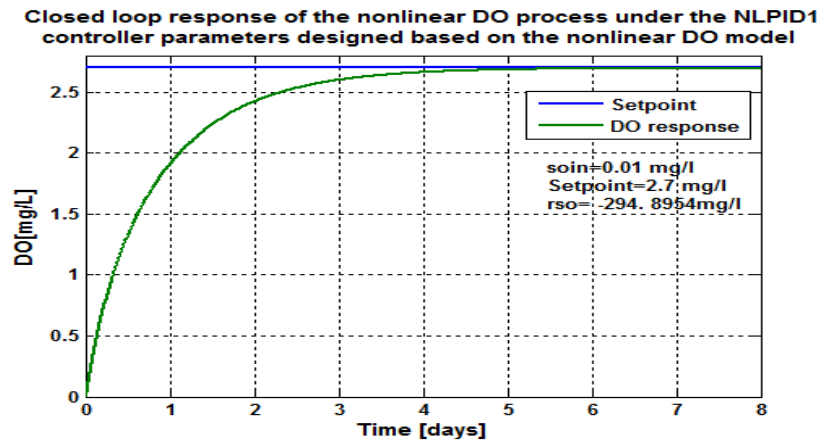


Figure 7.19: Closed loop DO process response under the NLPID1 controller, when the set-point is 2.7 mg/L and $r_{so} = -294.8954 \text{ mg/L/day}$

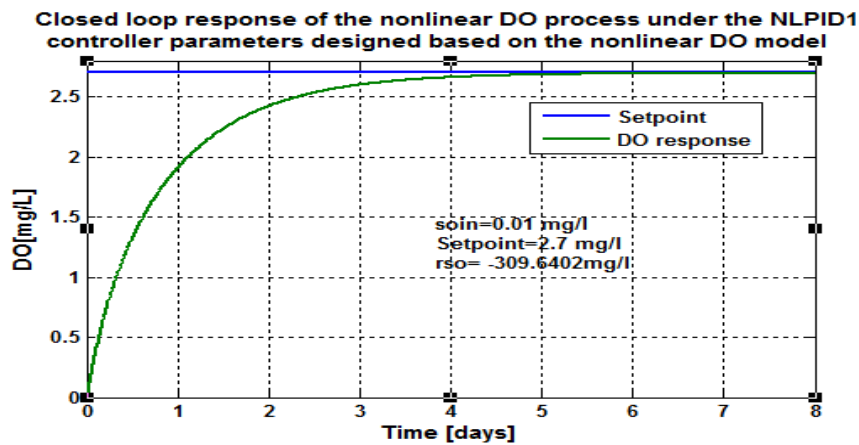


Figure 7.20: Closed loop DO process response under the NLPID1 controller, when the set-point is 2.7 mg/L and $r_{so} = -309.6402 \text{ mg/L/day}$

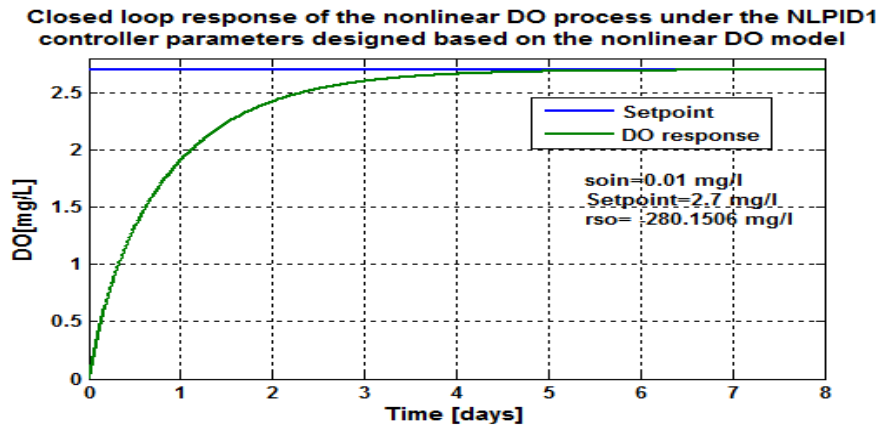


Figure 7.21: Closed loop DO process response under the NLPID1 controller, when the set-point is 2.7 mg/L and $r_{so} = -280.1506 \text{ mg/L/day}$

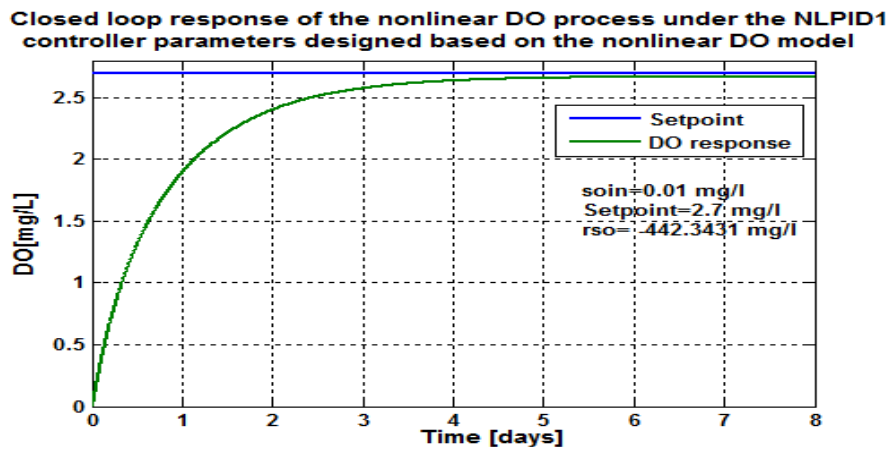


Figure 7.22: Closed loop DO process response under the NLPID1 controller, when the set-point is 2.7 mg/L and $r_{so} = -442.3431 \text{ mg/L/day}$

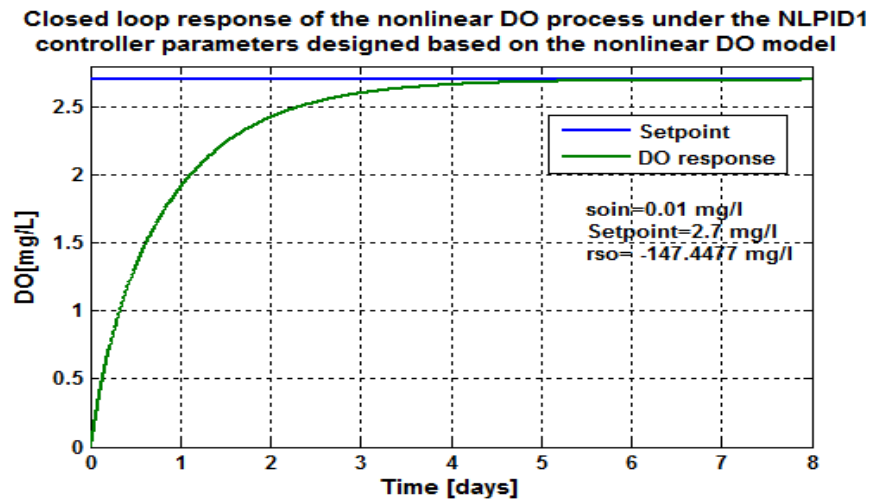


Figure 7.23: Closed loop DO process response under the NLPID1 controller, when the set-point is 2.7 mg/L and $r_{so} = -147.4477 \text{ mg/L/day}$

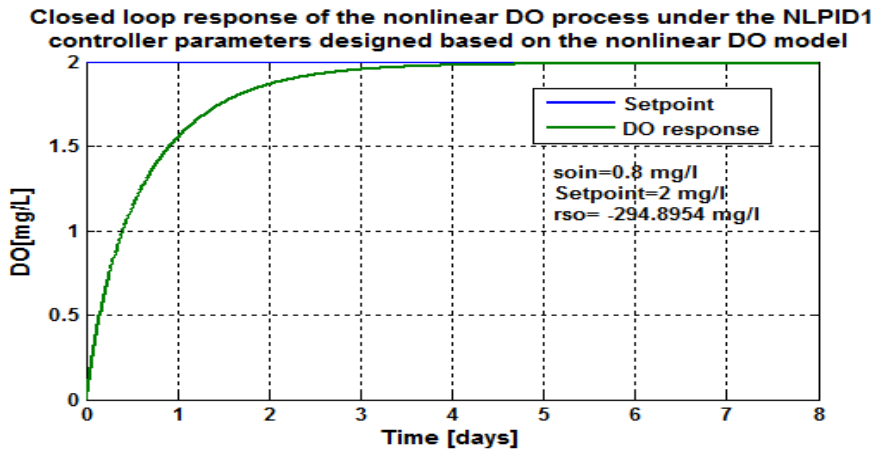


Figure 7.24: Closed loop DO process response under the NLPID1 controller, when the set-point is 2 mg/L and $r_{so} = -294.8954 \text{ mg/L/day}$

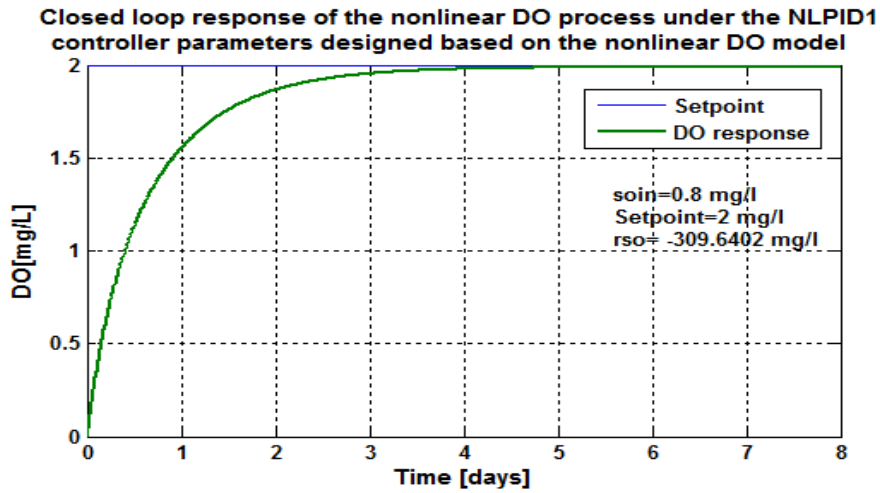


Figure 7.25: Closed loop DO process response under the NLPID1 controller, when the set-point is 2 mg/L and $r_{so} = -309.6402 \text{ mg/L/day}$

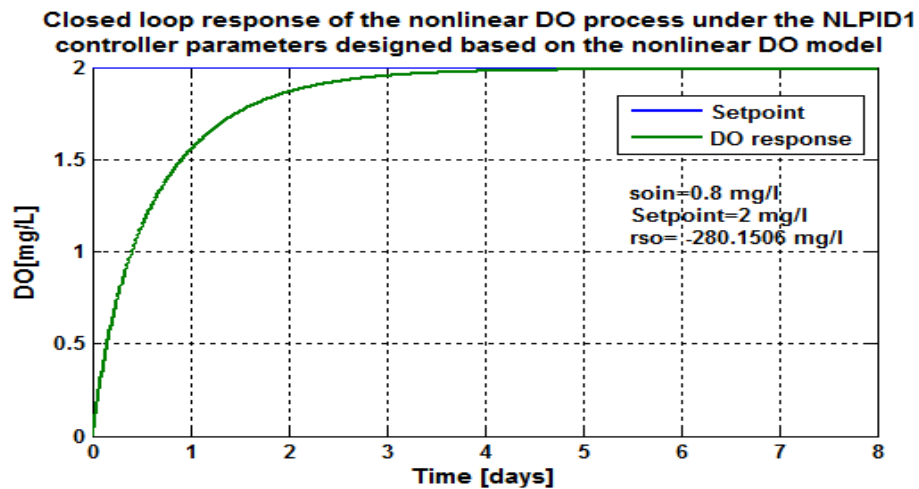


Figure 7.26: Closed loop DO process response under the NLPID1 controller, when the set-point is 2 mg/L and $r_{so} = -280.1506 \text{ mg/L/day}$

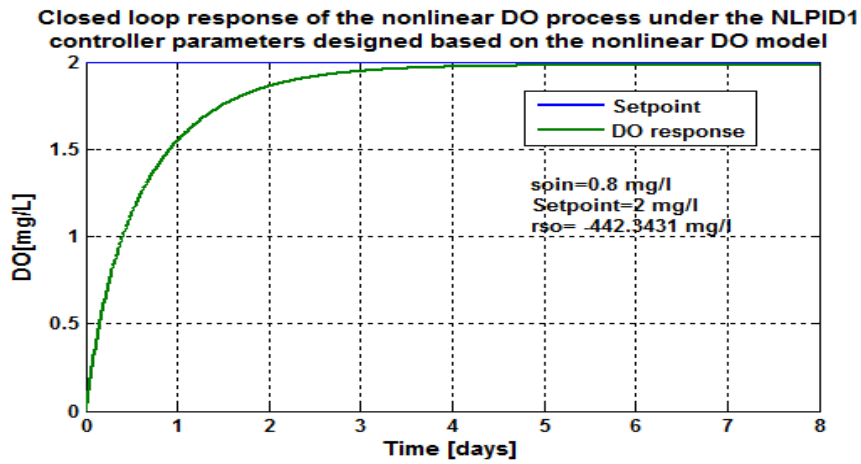


Figure 7.27: Closed loop DO process response under the NLPID1 controller, when the set-point is 2 mg/L and $r_{so} = -442.3431 \text{ mg/L/day}$

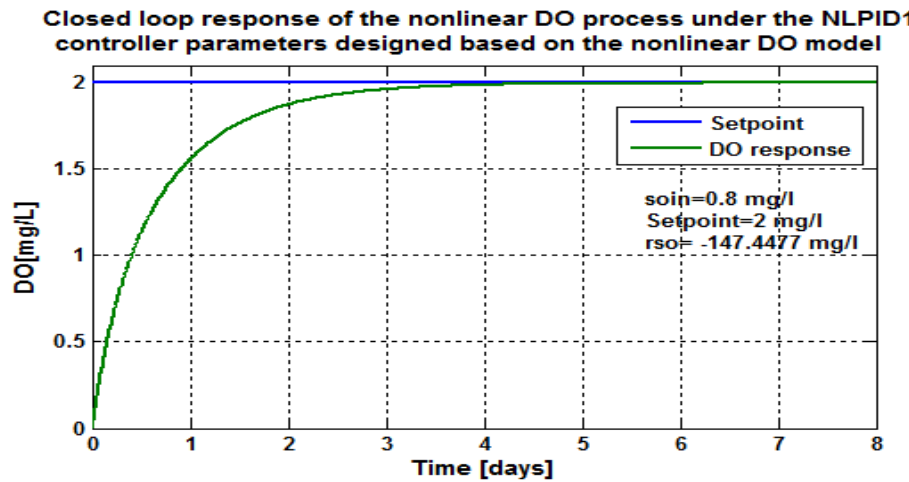


Figure 7.28: Closed loop DO process response under the NLPID1 controller, when the set-point is 2 mg/L and $r_{so} = -147.4477 \text{ mg/L/day}$

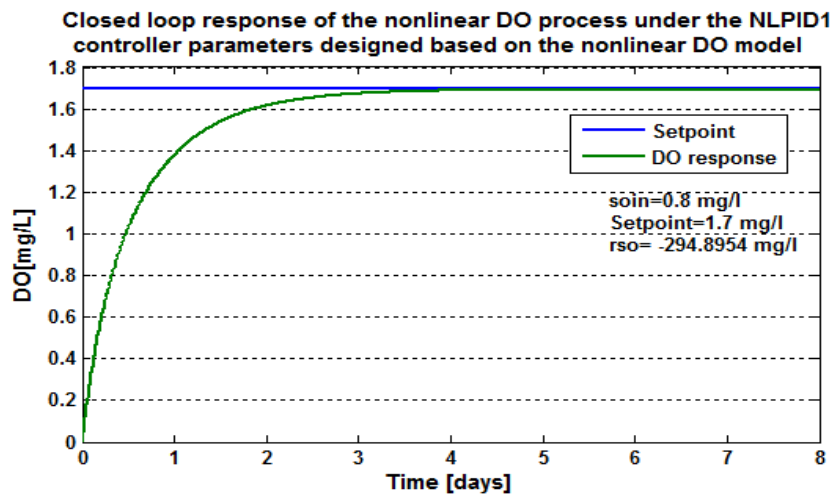


Figure 7.29: Closed loop DO process response under the NLPID1 controller, when the set-point is 1.7 mg/L and $r_{so} = -294.8954 \text{ mg/L/day}$

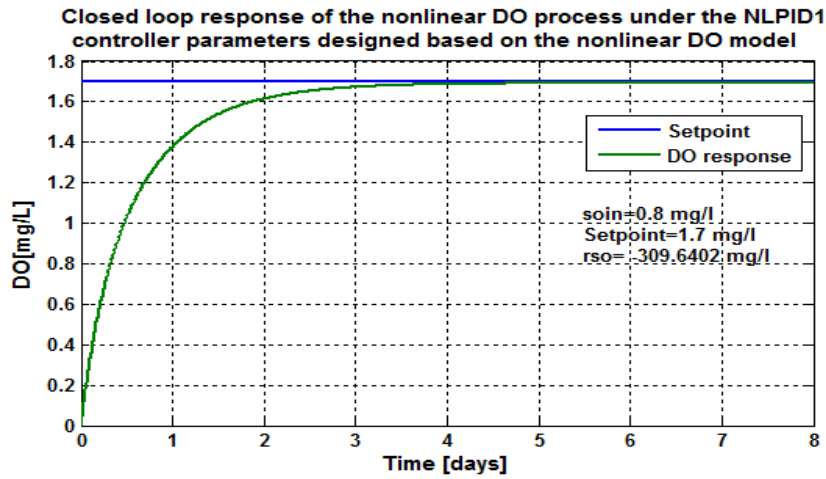


Figure 7.30: Closed loop DO process response under the NLPID1 controller, when the set-point is 1.7 mg/L and $r_{so} = -309.6402 \text{ mg/L/day}$

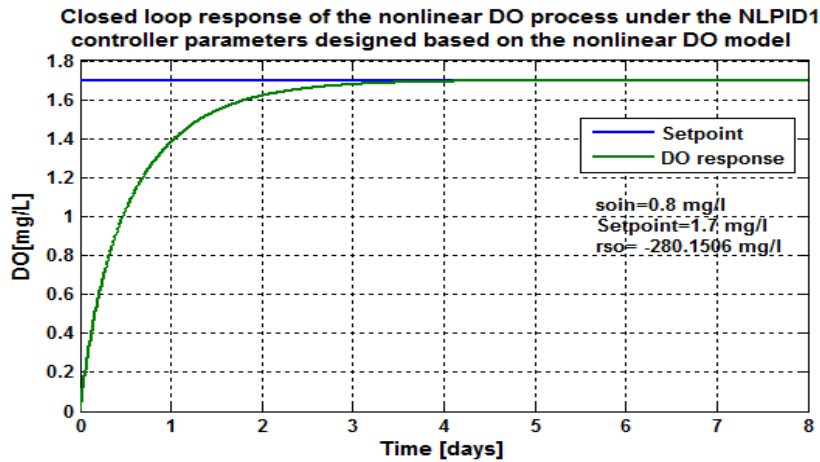


Figure 7.31: Closed loop DO process response under the NLPID1 controller, when the set-point is 1.7 mg/L and $r_{so} = -280.1506 \text{ mg/L/day}$

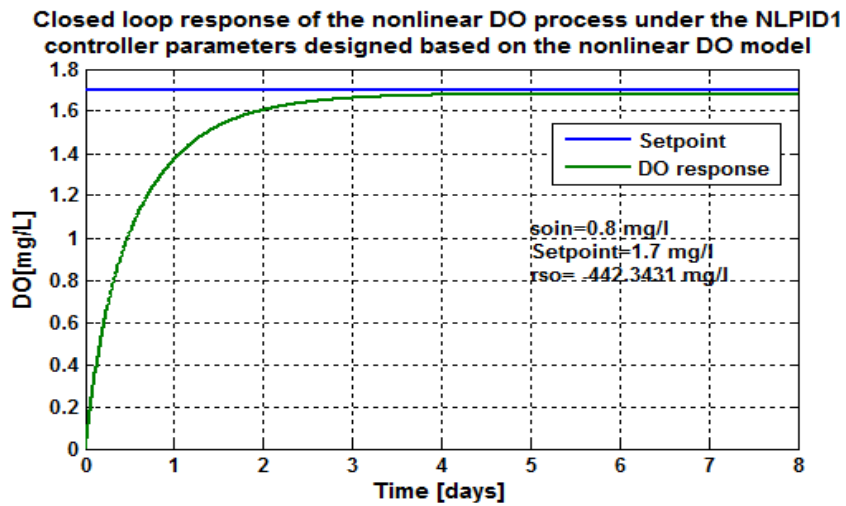


Figure 7.32: Closed loop DO process response under the NLPID1 controller, when the set-point is 1.7 mg/L and $r_{so} = -442.3431 \text{ mg/L/day}$

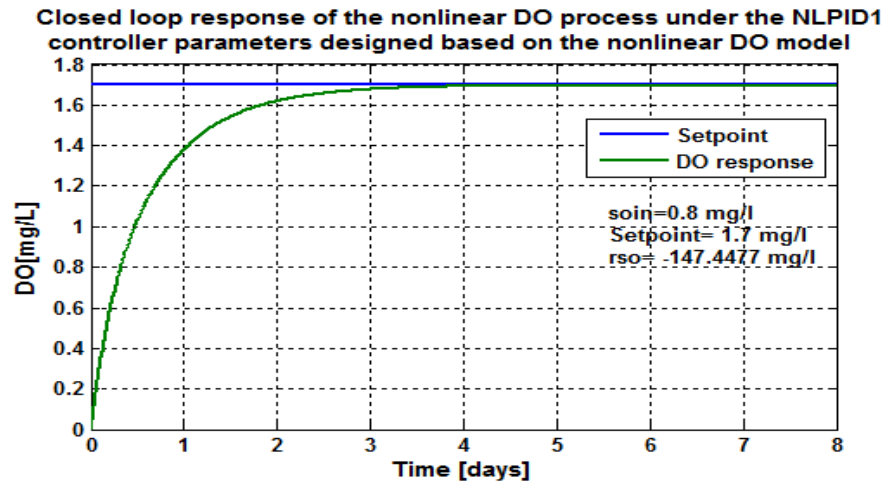


Figure 7.33: Closed loop DO process response under the NLPID1 controller, when the set-point is 1.7 mg/L and $r_{so} = -147.4477 \text{ mg/L/day}$

7.4.3 Discussion on the simulation results based on the NLPID1 controller for different operation conditions

Through the simulations completed in section 7.4.2 for the closed loop system under the NLPID1 controller, the following characteristics of the DO process behavior are calculated in Table 7.7

Table 7.7: Closed loop characteristics obtained when the NLPID1 is used to control the nonlinear DO process

Parameters			Characteristics			
Set point	S_{oin} [mg / L]	r_{so} mg / L / day	Time delay [days]	Steady state error [mg / L]	Rise time [days]	Settling time [days]
2.7	0.01	-294.8954	0.055	0.02	1	3.5
2.7	0.01	-309.6402	0.05	0.02	1	3.5
2.7	0.01	-280.1506	0.05	0.02	1	3.5
2.7	0.01	-442.3431	0.05	0.04	1	4.5
2.7	0.01	-147.4477	0.055	0.02	1	3.4
2	0.8	-294.8954	0.05	0.001	0.9	3
2	0.8	-309.6402	0.05	0.001	0.9	3
2	0.8	-280.1506	0.05	0.001	0.9	3
2	0.8	-442.3431	0.05	0.04	0.9	3
2	0.8	-147.4477	0.05	0	0.9	2.8
1.7	0.8	-294.8954	0.2	0.0005	0.9	2.62
1.7	0.8	-309.6402	0.05	0.0005	0.9	2.5
1.7	0.8	-280.1506	0.05	0.0005	0.9	2.5
1.7	0.8	-442.3431	0.05	0.04	0.9	3
1.7	0.8	-147.4477	0.056	0.0001	0.9	2.6

Figure 7.19 till Figure 7.33 show the result of the closed loop DO process behavior under the NLPID1 controller design based on the Pole-Placement (PP2) method. In the process

the set-point values were changed from 2.7 mg/L , 2 mg/L and 1.7 mg/L . The system response has achieved the desired behavior under the different operating conditions of OUR (r_{so}) and the internal disturbance, which also varies from $s_{o,in} = 0.01 \text{ mg/L}$ to 0.8 mg/L respectively. In Figure 7.19 to Figure 7.23 one set-point has been used, but OUR (r_{so}) is alternating between different values. The reason of keeping the set-point value is to observe how many changes can be seen in the system when there is a disturbance variation every time. It can be noted in the results and in Table 7.7 that the steady state error is larger when the value of r_{so} is high. Figure 7.24 - Figure 7.28 show the results of the closed loop system when the disturbances and the set-point change to a different value. Results show that the process has performed successfully under these conditions (see results graphs and Table 7.7).

In Figure 7.29 to Figure 7.33 the set-point has been changed and set aside to a constant value of 1.7 mg/L and different internal disturbances are used. As it can be seen the process performs well and shows good stability under these conditions.

7.5 Design of the NLPID2 controller parameters for the nonlinear DO process

In Chapter 5 the second nonlinear PID (NLPID2) to be used in this thesis has been discussed. The NLPID2 controller is used in this section firstly for controller parameter design based on the nonlinear DO process model, and secondly to control the closed loop system of DO process. The NLPID is constructed using a nonlinear error function in order to derive the model of the NLPID controller as follows: (Hai-bin *et al*, 2006).

$$u = K_p |e|^\lambda \text{sign}(e) + K_i \left| \int_0^t edt \right|^\lambda \text{sign} \left(\int_0^t edt \right) + K_d \left| \frac{de}{dt} \right|^\lambda \text{sign} \left(\frac{de}{dt} \right) \quad (7.10)$$

Where λ is the constant, K_p is the proportional gain, K_i is the integral gain K_d is the derivative gain, e is the error signal.

The nonlinear error functions are expressed as:

$$\begin{cases} \text{sign}(e) \cdot |e|^\lambda, & \text{when } |e| \geq \delta \\ e / \delta^{1-\lambda}, & \text{when } |e| < \delta \end{cases} \quad \text{for the error} \quad (7.11a)$$

$$\begin{cases} \left| \int edt \right|^\lambda \cdot \text{sign}\left(\int_0^t edt\right), \text{ when } \left| \int edt \right| \geq \delta \\ e / \delta^{1-\lambda}, \text{ when } \left| \int edt \right| < \delta \end{cases} \quad \text{for the integral of the error} \quad (7.11b)$$

$$\begin{cases} \left| \frac{de}{dt} \right|^\lambda \cdot \text{sign}\left(\frac{de}{dt}\right), \text{ when } \left| \frac{de}{dt} \right| \geq \delta \\ e / \delta^{1-\lambda}, \text{ when } \left| \frac{de}{dt} \right| < \delta \end{cases} \quad \text{for the derivative of the error} \quad (7.11c)$$

The two symbols δ and λ are the two parameters of the nonlinear functions.

In order to obtain the nonlinear PID2 controller parameters, the control design steps shown and explained in section 7.3 and the algorithm from Figure 7.1 must be followed, but now based on the nonlinear PID2 controller (NLPID2) model, which yields to the Equation (7.12) of the closed loop system:

$$\begin{aligned} \dot{s}_o - \frac{Q}{V}(s_{o,in} - s_o) - r_{s_o} - \left(K_1(1 - e^{-K_2 \left[K_p |e|^\lambda \text{sign}(e) + K_i \left| \int_0^t edt \right|^\lambda \text{sign}\left(\int_0^t edt\right) + K_d \left| \frac{de}{dt} \right|^\lambda \text{sign}\left(\frac{de}{dt}\right) \right]}) \right) * \\ * (s_{o,Sat} - s_o) = 0 \end{aligned} \quad (7.12)$$

Then, based on the function *fsolve* the Matlab/Simulation scrip file named as “*findnlpid2pa*” is developed for the controller parameter’s calculations and to call a function file called “*myfun2*” as given in Appendix B9. These files are used to determine the unknown controller parameters of the NLPID2 controller. The initial guess values selected for the application for the PP2 procedure for design of the NLPID2 controller are as follows: $K_{p_initial}=30$, $K_{i_initial}=10$. The following Table 7.8 shows the designed controller parameters.

Table 7.8: Controller Parameter designed based on the nonlinear DO process

s_o	K_p	K_i
0.05	30	10
0.54	29.96	9.98
0.58	3.23	-5.9
0.83	11.22	-10.47
0.92	13.98	-10.85
1.8	28.9	-2.33
1.99	29.95	0.04
2.02	30.118	0.522

2.03	30.17	0.76
2.064	30.28	1.151
2.06	30.28	1.14
2.04	30.2	0.86
2.02	30.14	0.6
2.02	30.1	0.57
2.02	30.119	0.52

Obtained controller parameters are tested on the closed DO loop system in order to view and select the best performing controller parameters, which will then be used further to perform the simulations of the closed loop system under different conditions of the system disturbances and set-points. The selected ones are given in Table 7.9.

Table 7.9: Selected NLPID2 controller parameter designed based for the nonlinear DO process

Controller	K_p	K_i
NLPID2	29.95	0.04
NLPID2	30.119	0.522
NLPID2	30.1	0.57

7.5.1 Simulink Block Diagram of the closed loop system under the NLPID2 controller

From Table 7.9 the controller parameters displayed in the second row are selected to be used for further investigation of the DO process behavior under the NLPID2 controller. Figure 7.34 shows the Simulink block diagram of the DO closed loop system with the NLPID2 controller. The Simulink block diagram given in Figure 7.34 and the scrip file named “NLPID2par_DOpp2” are used for the assignment of the NLPID2 controller parameters that are selected from Table 7.9.

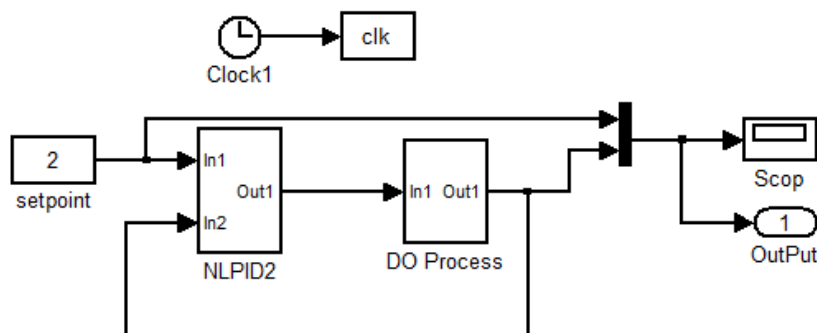


Figure 7.34: Simulink diagram of the DO closed loop system using the NLPID2 controller

7.5.2 Simulation results of the nonlinear DO process under the NLPID2 controller

The simulation results of the closed loop DO process using the NLPID2 controller are

given in Figure 7.35 to Figure 7.49 respectively, for the different set-points and different internal disturbances, as shown in Table 7.3. This is done in order to make an examination of how well the system will perform under the NLPID2 controller, when using the designed controller parameters found and highlighted in section 7.5.

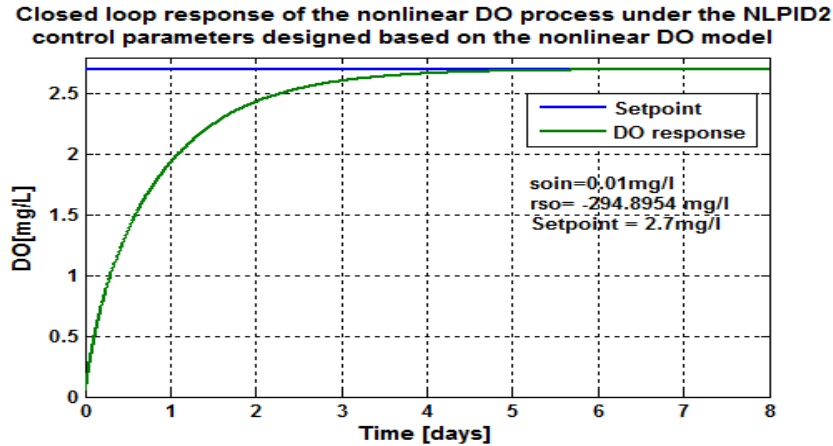


Figure 7.35: Closed loop DO process response under the NLPID2 controller, when the set-point is 2.7 mg/L and $r_{so} = -294.8954 \text{ mg/L/day}$

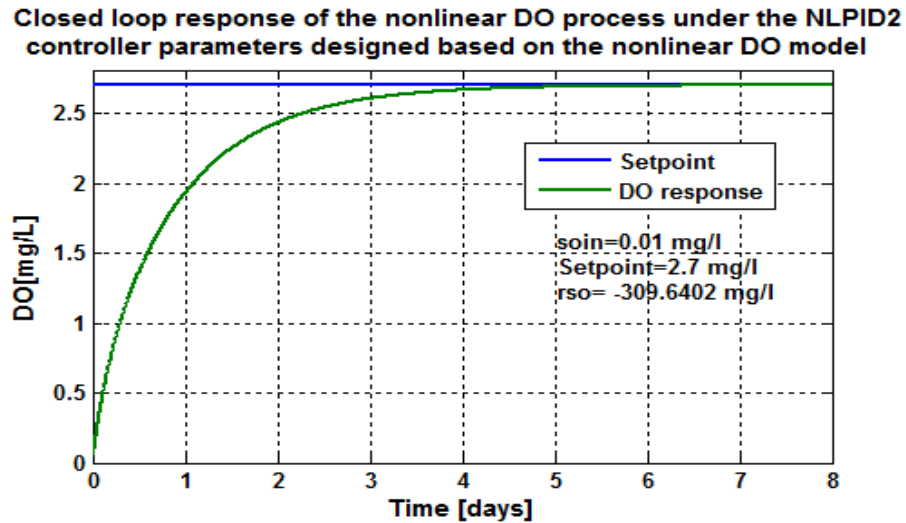


Figure 7.36: Closed loop DO process response under the NLPID2 controller, when the set-point is 2.7 mg/L and $r_{so} = -309.6402 \text{ mg/L/day}$

Closed loop response of the nonlinear DO process under the NLPID2 controller parameters designed based on the nonlinear DO model

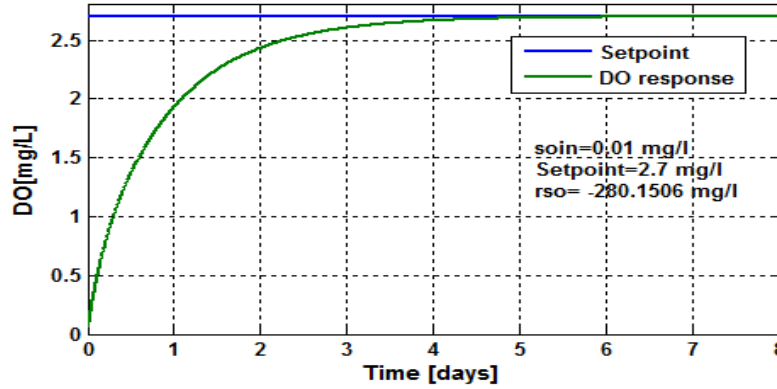


Figure 7.37: Closed loop DO process response under the NLPID2 controller, when the set-point is 2.7 mg/L and $r_{so} = -280.1506 \text{ mg/L/day}$

Closed loop response of the nonlinear DO process under the NLPID2 controller parameters designed based on the nonlinear DO model

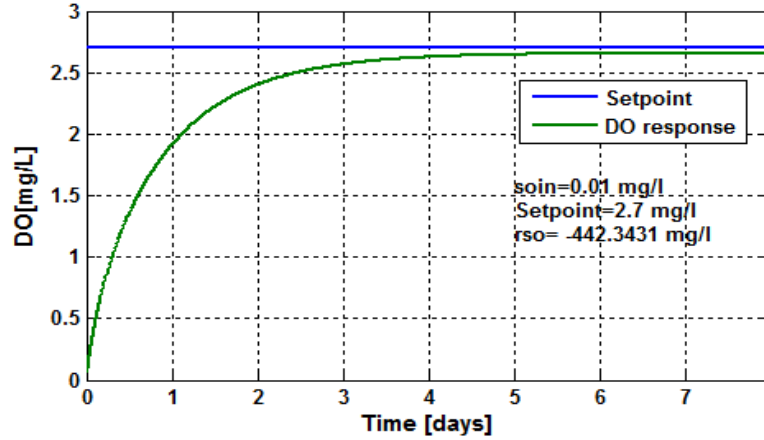


Figure 7.38: Closed loop DO process response under the NLPID2 controller, when the set-point is 2.7 mg/L and $r_{so} = -442.3431 \text{ mg/L/day}$

Closed loop response of the nonlinear DO process under the NLPID2 controller parameters designed based on the nonlinear DO model

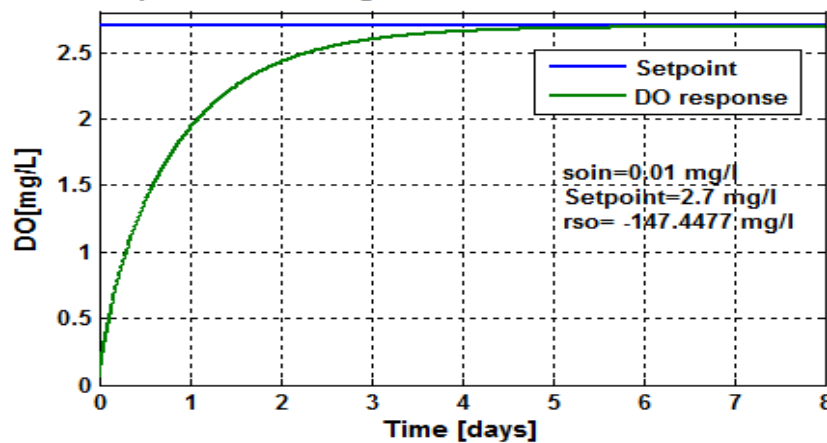


Figure 7.39: Closed loop DO process response under the NLPID2 controller, when the set-point is 2.7 mg/L and $r_{so} = -147.4477 \text{ mg/L/day}$

Closed loop response of the nonlinear DO process under the NLPID2 controller parameters designed based on the nonlinear DO model

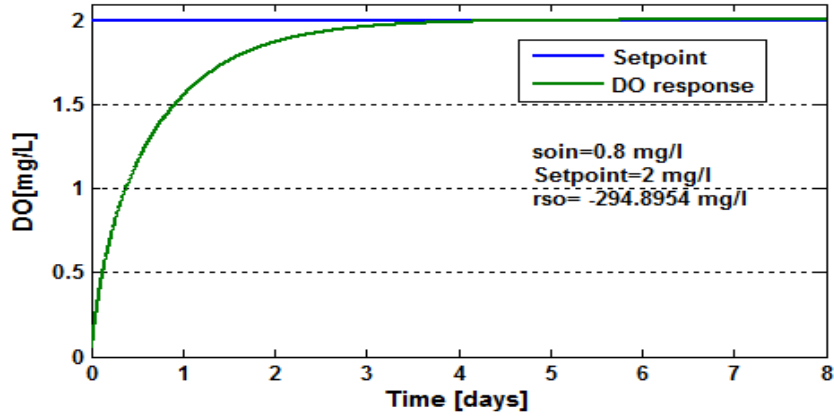


Figure 7.40: Closed loop DO process response under the NLPID2 controller, when the set-point is 2 mg/L and $r_{so} = -294.8954 \text{ mg/L/day}$

Closed loop response of the nonlinear DO process under the NLPID2 controller parameters designed based on the nonlinear DO model

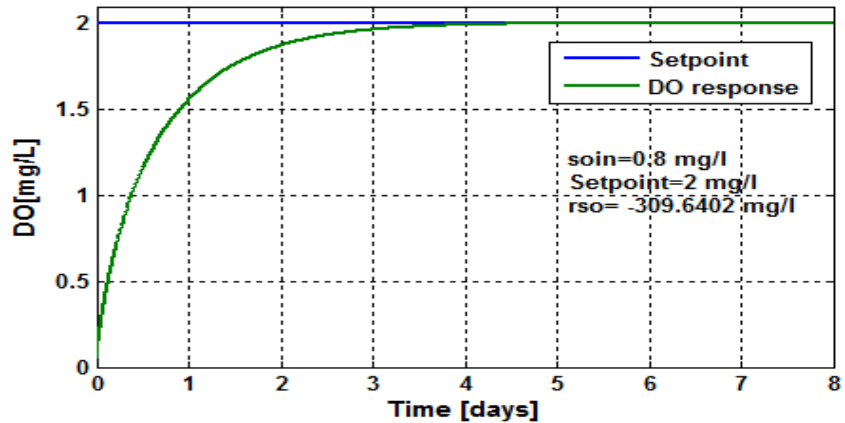


Figure 7.41: Closed loop DO process response under the NLPID2 controller, when the set-point is 2 mg/L and $r_{so} = -309.6402 \text{ mg/L/day}$

Closed loop response of the nonlinear DO process under the NLPID2 controller parameters designed based on the nonlinear DO model

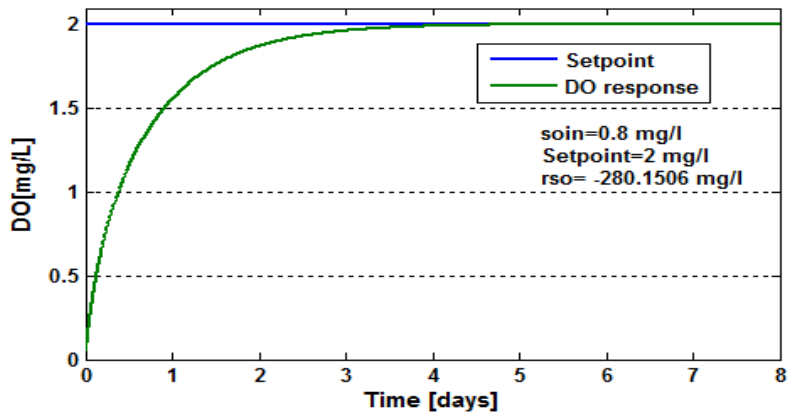


Figure 7.42: Closed loop DO process response under the NLPID2 controller, when the set-point is 2 mg/L and $r_{so} = -280.1506 \text{ mg/L/day}$

Closed loop response of the nonlinear DO process under the NLPID2 controller parameters designed based on the nonlinear DO model

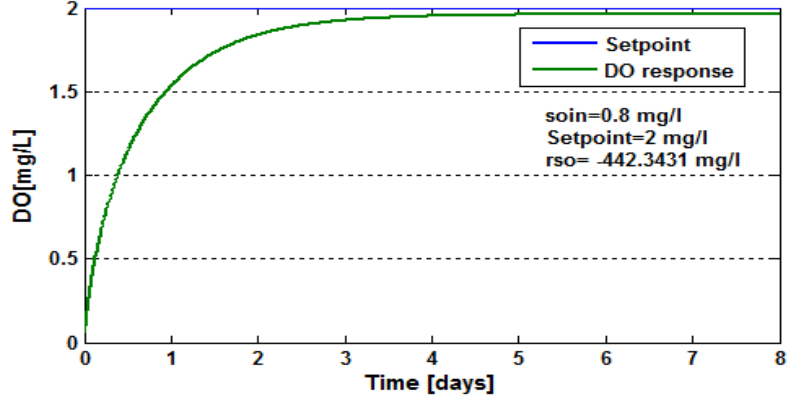


Figure 7.43: Closed loop DO process response under the NLPID2 controller, when the set-point is 2 mg/L and $r_{so} = -442.3431 \text{ mg/L/day}$

Closed loop response of the nonlinear DO process under the NLPID2 controller parameters designed based on the nonlinear DO model

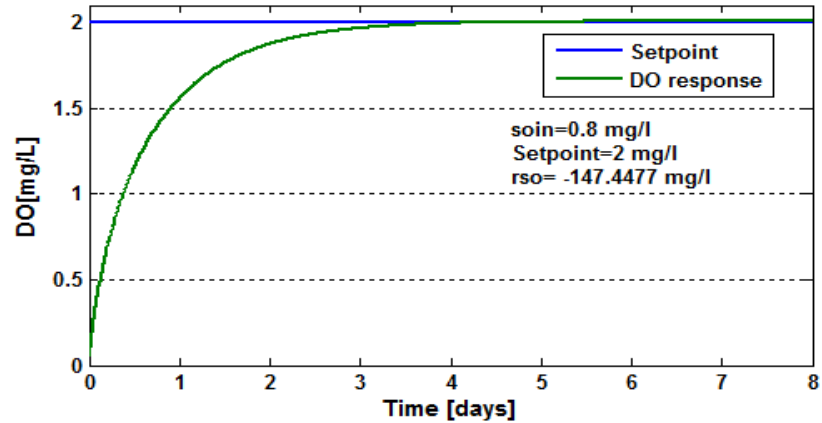


Figure 7.44: Closed loop DO process response under the NLPID2 controller, when the set-point is 2 mg/L and $r_{so} = -147.4477 \text{ mg/L/day}$

Closed loop response of the nonlinear DO process under the NLPID2 controller parameters designed based on the nonlinear DO model

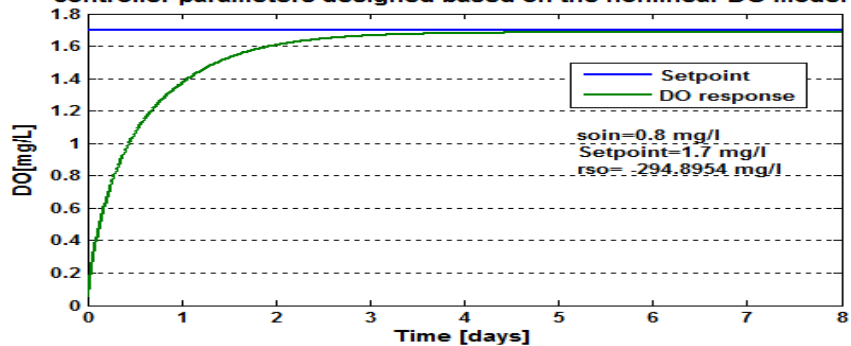


Figure 7.45: Closed loop DO process response under the NLPID2 controller, when the set-point is 1.7 mg/L and $r_{so} = -294.8954 \text{ mg/L/day}$

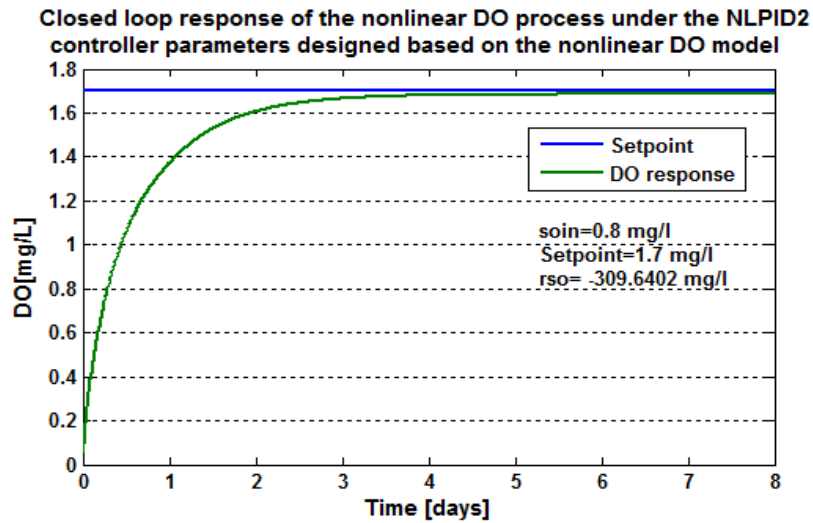


Figure 7.46: Closed loop DO process response under the NLPID2 controller, when the set-point is 1.7 mg/L and $r_{so} = -309.6402 \text{ mg/L/day}$

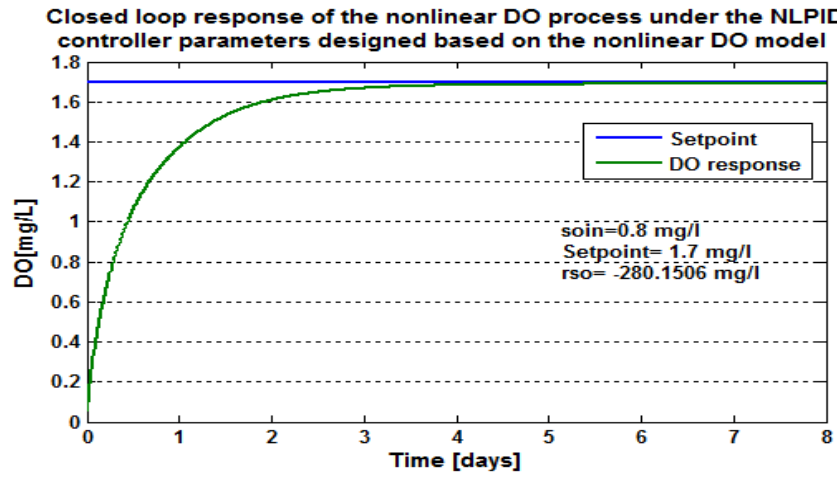


Figure 7.47: Closed loop DO process response under the NLPID2 controller, when the set-point is 1.7 mg/L and $r_{so} = -280.1506 \text{ mg/L/day}$

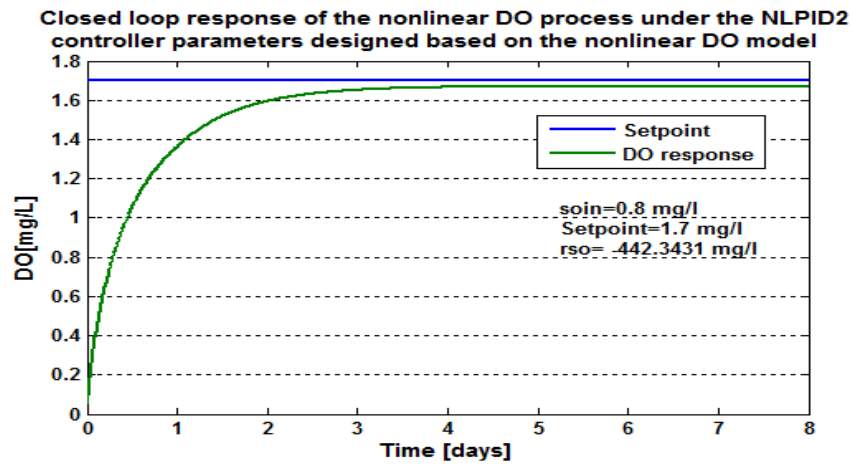


Figure 7.48: Closed loop DO process response under the NLPID2 controller, when the set-point is 1.7 mg/L and $r_{so} = -442.3431 \text{ mg/L/day}$

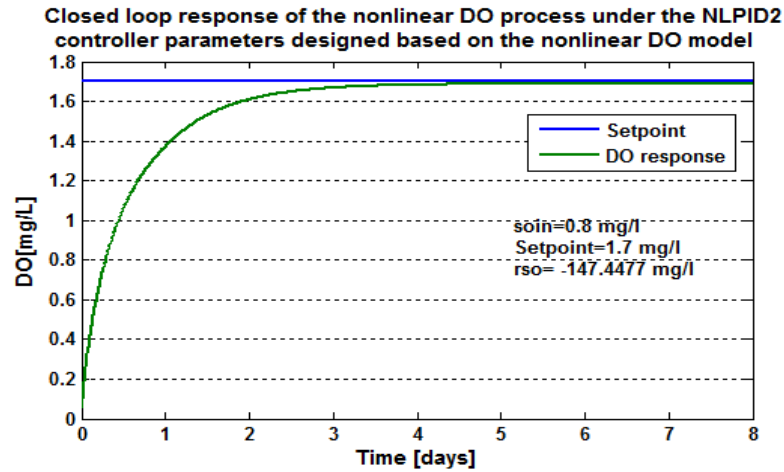


Figure 7.49: Closed loop DO process response under the LPID controller, when the set-point is 1.7 mg/L and $r_{so} = -147.4477 \text{ mg/L/day}$

Table 7.10 shows the characteristics of the closed loop DO process behavior.

Table 7.10: Results obtained when the NLPID2 is used to control the nonlinear DO process

Parameters			Characteristics			
Set point	s_{oin} [mg / L]	r_{so} mg / L / day	Time delay [days]	Steady state error [mg / L]	Rise time [days]	Settling time [days]
2.7	0.01	-294.8954	0.055	0.02	0.6	3.5
2.7	0.01	-309.6402	0.05	0.02	0.6	3.5
2.7	0.01	-280.1506	0.05	0.02	0.6	3.5
2.7	0.01	-442.3431	0.05	0.04	0.6	4.4
2.7	0.01	-147.4477	0.055	0.02	0.6	3.5
2	0.8	-294.8954	0.05	0.001	0.5	3
2	0.8	-309.6402	0.05	0.001	0.5	3
2	0.8	-280.1506	0.05	0.001	0.5	3
2	0.8	-442.3431	0.05	0.04	0.5	3
2	0.8	-147.4477	0.05	0.0005	0.5	2.8
1.7	0.8	-294.8954	0.05	0.001	0.5	2.8
1.7	0.8	-309.6402	0.05	0.001	0.5	2.9
1.7	0.8	-280.1506	0.05	0.001	0.5	2.8
1.7	0.8	-442.3431	0.05	0.04	0.5	3
1.7	0.8	-147.4477	0.05	0.0005	0.5	2.7

7.5.3 Discussion on the simulation results obtained under the NLPID2 controller

The results from Figure 7.35 - Figure 7.49 show some very good closed loop response under different internal disturbances ($s_{o,in}$) and variation of the OUR (r_{so}) in every set-point of the process.

In Figure 7.35 to Figure 7.49 different set-points and different internal disturbances are used in order to test how good the designed controller parameters work to handle the

changes in the systems operation and unexpected variation that may occur. It can be seen that the process works successful under these conditions.

Through these results from the simulations the method used for the design can be recommended to be preferred for the nonlinear controller parameter design.

The following Table 11 shows the comparison of the simulation results based on the LPID and the NLPID controllers considered in this Chapter.

Table7.11: Comparison of the obtained closed loop DO process specifications of the designed LPID and NLPID controllers

Set-point	Disturbances	Characteristics	LPID	NLPID1	NLPID2
2.7	$r_{so} = -294.$ $s_{oin} = 0.01$	Rise Time	0.5	1	0.6
		Settling time	1	3.5	3.5
		Steady state error	0.05	0.02	0.02
		Overshoot	No	No	No
2.7	$r_{so} = -442.3231,$ $soin = 0.01$	Rise Time	0.7	1	0.6
		Settling time	1.2	4.5	4.4
		Steady state error	0.12	0.04	0.04
		Overshoot	No	No	No
2	$r_{so} = -294.$ $s_{oin} = 0.8$	Rise Time	0.5	0.9	0.5
		Settling time	1	3	3
		Steady state error	0.05	0.001	0.001
		Overshoot	No	No	No
2	$r_{so} = -442.3231$ $s_{oin} = 0.8$	Rise Time	0.6	0.9	0.5
		Settling time	1	3	3
		Steady state error	0.12	0.04	0.04
		Overshoot	No	No	No
1.7	$r_{so} = -294.$ $s_{oin} = 0.8$	Rise Time	0.3	0.9	0.5
		Settling time	1	2.62	2.8
		Steady state error	0.05	0	0.
		Overshoot	No	No	No
1.7	$r_{so} = -442.3231$ $s_{oin} = 0.8$	Rise Time	0.4	0.9	0.5
		Settling time	0.6	3	3
		Steady state error	0.1	0.04	0.04
		Overshoot	No	No	No

Through the closed loop DO process specifications shown in Table 7.11, between the LPID and the NLPID controllers, it can be noted that the DO process under the LPID controller has a faster rise time and settling time in comparison with the two NLPID controllers, but it cannot be recommended to be used, because it has a larger steady state error in comparison with the NLPID1 and NLPID2 controllers.

The NLPID controllers achieve a very small steady state error which is very important for

the proper control of the DO concentration. Software developed to design the NLPID controllers produces their parameters in a short time, which allows the design procedure to be done in real-time, as shown in Figure 7.50. This possibility will be considered as a future work.

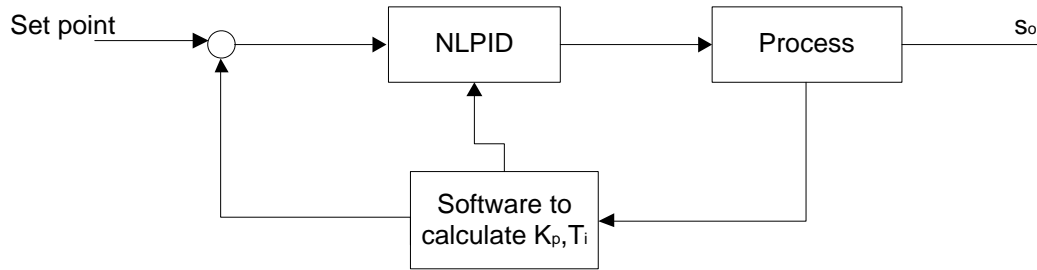


Figure 7.50: Real –time application of the NLPID controller parameters design

7.6 Conclusion

In this Chapter, pole placement based method for design of the LPID controller parameters for the nonlinear DO process, and pole placement based method for design of the two NLPID controllers for the nonlinear DO process are developed. The design idea in development of these pole placement based methods for the nonlinear processes is to substitute the analytical solution of the closed loop system characteristic equation by a numeric solution of the equation of the closed loop system. The Matlab function '*fsolve*' and Levenberg-Marquardt algorithm allow solving of the nonlinear closed loop equations for more than one unknown controller parameter.

Based on the simulation results performed in this chapter for the closed loop DO process under the LPID controller (section 7.3), the NLPID1 controller (section 7.4) and the NLPID2 controller (section 7.5) respectively, the developed methods for application of the Pole-Placement method to design LPID and NLPID controllers for the nonlinear DO process model indicate to be the best performing methods throughout this thesis investigation, compared with the other two methods used in Chapter 5 and Chapter 6.

The simulation phase has been done and the results are shown and have been discussed in Chapter 5, 6 and 7. To achieve this, the next step is to perform real-time simulation of the closed loop DO process environment for real-time simulation as described in the next Chapter (Chapter 8).

CHAPTER 8:

REAL-TIME SIMULATIONS OF THE CLOSED LOOP DO SYSTEM IN PLC A USING MODEL TRANSFORMATION TECHNIQUE

8.1 Introduction

The developed closed loop control system for the nonlinear dissolved oxygen (DO) process under the two nonlinear PID controllers (NLPID1 and NLPID2) revealed in Chapter 6 and Chapter 7 has been transferred to the Beckhoff CX5020 PLC through the Total Windows Control and Automation Technology (TwinCAT) software, based on the new model engineering approach used in this Chapter. This is done by linking MATLAB/Simulink with TwinCAT software based on the Function Block Programming adopted from the IEC61499 standard, and is achieved through a transformation between the two block-diagram languages-Simulink and TwinCAT. The transformation supported by the developed tools sets the foundation of the corroboration and validation framework for IEC61499 standard (Dai, W.W. & Vyatkin, V. 2010) - based Function Blocks and the real-time control of the closed-loop system with the models of the plant. This chapter discusses the following: PLC history in part 8.2, PLC hardware and Software in part 8.3, Beckhoff Cx5020 PLC in part 8.4, TwinCAT 3 software in part 8.5, the model transformation discussion and Implementation for real-time simulation of the closed system in part 8.6, Section 8.7 gives overall results discussion and Section 8.8 is the conclusion of this chapter.

The main aim of this Chapter is to use a PLC to implement the real-time simulation of the closed loop nonlinear DO process under the designed controllers. The designed nonlinear controllers to be used for the real-time simulation are discussed in Chapter 6 and Chapter 7.

8.2 Programmable Logic Controller (PLC) History

Control algorithms for industrial process technology like WWT plants or manufacturing systems are mostly implemented on embedded devices like Programmable Logic Controllers (PLC).

In the 1960's PLC were initially created to substitute relays and relays control frameworks. Relays were extremely helpful in a few applications. The principle issue is the way that they are mechanical devices. This implies that they wear down and must be replaced regularly. A relay likewise takes up a considerable amount of space. These

alongside with different considerations, encouraged the improvement of PLCs. More changes to PLCs happened in the 1970's. In 1973 the capacity to convey between PLCs was included. This additionally made it likely to have the controlling circuit far from the machine it was controlling. In 1990's they was an increased in collection of ways in which a PLC could be programmed adding up to ladder logic, (block diagrams, instruction list, C, etc.) which was similar to schematic of the relay logic. Around then PLCs were possible to be replaced by PC's at times (<http://www.plcs.net/>). All PLCs are still used that much being in different types of commercial ventures, and it is likely that they will stay there for a long while. Shown below in Figure 8.1 is the historical diagram of the PLC invention.

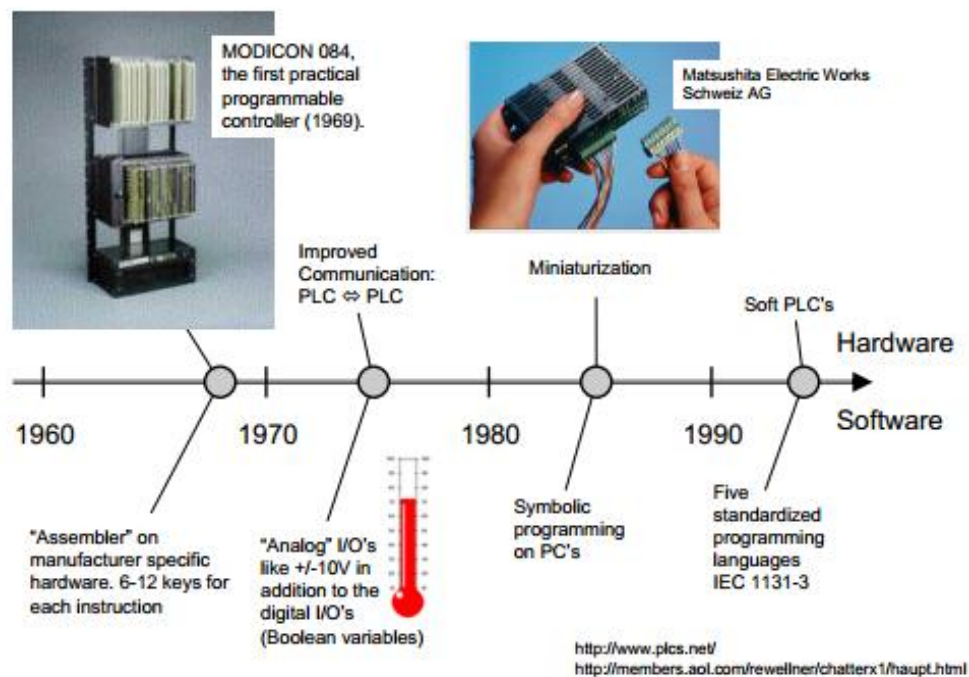


Figure 8.1: Historical diagram of the PLC development

(<http://www.plcs.net/>)

Programmable logic controllers are now the most widely used industrial process control technology. A PLC is a mechanical evaluation machine that is fit for being customized to perform control capacities. It is intended for numerous input and output plans, expanded temperature ranges, assurance to electrical commotion, and imperviousness to vibration and effect. The characteristics of the PLCs include interfaces between inputs and outputs, which is already inside the controller. They are using understandable programming language which primarily deals with logic and switching operations.

8.3 PLC hardware and Software

8.3.1 Advantages and disadvantages of using PLC

As it may have been mentioned before PLC was invented to replace the necessary sequential relay circuits for machine control. PLCs are very much used in many real world applications. Whenever there is an industry present, there is a high chance that a PLC presents. The industrial use of PLC involves machinery, packaging, material handling, automated assembly or countless of other industries were probably already using Programmable controllers. There are many advantages of using this technology, as mentioned by Dai and Vyatkin, (2010) some of them are as follows:

- PLCs are more flexible -It is easier to create and change a program in a PLC than to wire and rewire a circuit.
- They are remarkably robust, and able to stand all sorts of difficult conditions, such as extreme temperatures or dust in the air.
- They do not have contacts that attire out, like relays does.
- Communication ability – A PLC can communicate with other controllers or computer equipment to perform such functions as supervisory control, data gathering, monitoring devices, process parameters, and download and upload of the programs.
- Easier to troubleshoot -PLCs have diagnostics and override functions that allow users to easily trace and correct software and hardware problems.
- Faster Response Time - PLCs are designed for high-speed and real-time applications.
- Cost effectively - PLCs were originally designed to replace relay control logic, and the cost savings have been so significant that relay control is becoming outdated excluding for power applications.
- Improve reliability - Once a program has been written and tested, it can be easily downloaded to other PLCs. The program takes the place of much of the external wiring that would normally be required for control of a process.

The following are disadvantages of PLC:

- PLCs are not very good at handling large amount of data, or complex data.
- PLCs are also not very good with displaying data and portability which consists of making software tools able to accept and properly interpret vendors' libraries elements from different builders.

8.3.2 Programmable Logic Controller Hardware

A classic PLC divided into parts is illustrated in Figure 8.2 (Fall, 2006). It consists of the basic components which are:

- The PLC processor or controller (CPU)
- I/O (Input /Output) modules
- Chassis or backplane
- Power supply
- Programming software that runs in a PC

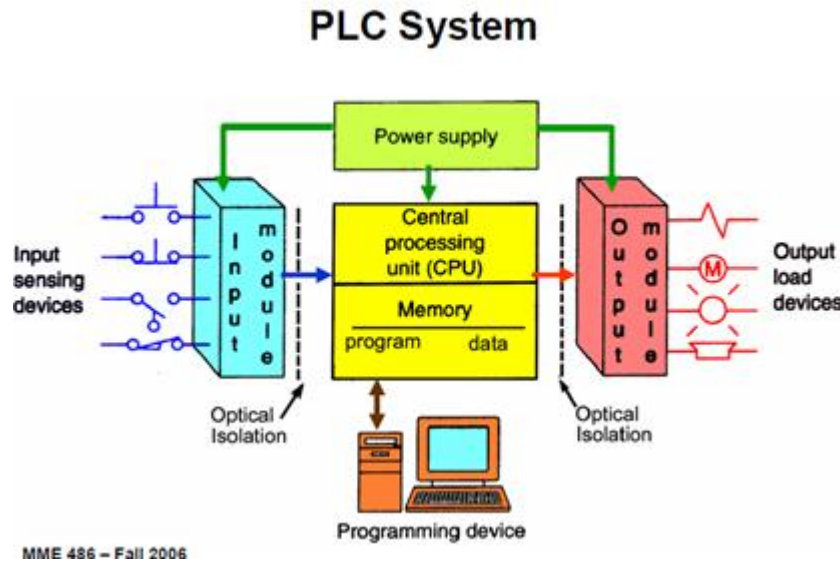


Figure 8.2: Classic part of the PLC
(adapted from MME 486 – Fall 2006)

8.3.2.1 Central Processing Unit (CPU)

The processor (CPU) is the intelligence of the PLC. A classic processor usually consists of a microprocessor for implementing the logic and controlling the communications among the modules. The processor requires memory for storing the results of the logical operations performed by the microprocessor. Memory is also required for the program EPROM (Erasable Programmable Read-Only Memory) or EEPROM (Electrically Erasable Programmable Read-Only Memory) plus Random Access Memory (RAM). The CPU controls all PLC activity and is designed so that the user can enter the desired program in any of the programming language understood by that particular PLC.

The PLC program is executed as part of a repetitive process referred to as a scan, Figure 8.3. A typical PLC scan starts with the CPU reading the internal state of the CPU. Then, the CPU reads the status of inputs. All program logic has to be stored and executed based on the status of the inputs. Once the program execution is completed,

the status of all outputs is updated. This process is repeated continuously as long as the PLC is in the run mode.

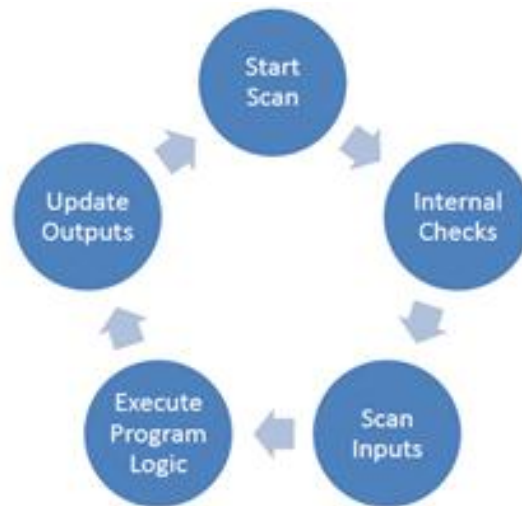


Figure 8.3: Typical PLC scans cycle (Scan based like IEC 61131-3)

8.3.2.2 Input/ Output (I/O) Modules

According to the classic PLC in (Figure 8.2) the I/O modules are linked to the out-side world. The I/O framework structures the interface by which field devices are joined with the controller. The reason for this interface is to condition the different signs got from or sent to outside field devices. Input devices such as limit switches, sensors, and pushbuttons are hardwired to the input terminals. Output devices such as small motors, solenoid valves, and indicator lights are hardwired to the output terminals.

8.3.2.3 Framework or backplane

The Everything PLCs need is some system for conveying between the controller, I/O and correspondences modules. Here are three courses used to perform this correspondence between the different segments that make up the PLC framework (Fall, 2006)

The modules are installed in the *same framework* as the PLC and communicate over the frame backplane.

Modules are designed to *plug* into each other. The interconnecting plugs form a backplane. There is no chassis, Figure 8.4.

Modules are built into the PLC. The modules come together in one physical block.

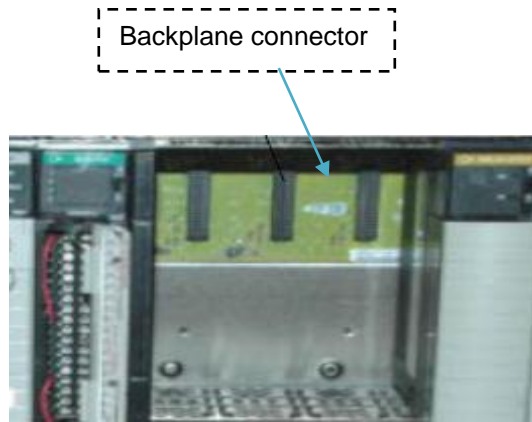


Figure 8.4: Classic PLC framework
(Adapted from MEL – 334: PLC)

8.3.2.4 Power Supply

A power supply is needed to provide power to the PLC and any other modules. The power supply, supplies DC power to the internal circuitry of CPU and other modules that plug into the framework, see Figure 8.2. If a PLC system is large, this power supply does not normally supply power to the field devices. With larger systems, power to field devices is provided by external alternating current (AC) or direct current (DC) supplies.

8.3.2.5 Programming Device

A programming device is used to enter the desired program into the memory of the processor. A personal computer (PC) is the most commonly used programming device. Most brands of PLCs have software available so that a PC can be used as the programming device. This software allows users to create, edit, document, store, and troubleshoot the programs. The PC communicates with the PLC processor via a serial or parallel data communications link.

8.3.3 PLC Software

According to the PLC developers and referring to the historical diagram shown in Figure 8.1, PLC programs can be written using any of the five IEC 61131-3 standardized programming languages, which are (<http://www.plcs.net/>)

- Ladder Diagram (LD),
- Structured Text (ST),
- Function Block Diagram (FBD),
- Instruction List (IL),
- Sequential Function Chart (SFC).

8.4 Beckhoff CX50x0 Programmable Logic Controllers

Beckhoff CX50x0 is an embedded device that can or does play an important role in the field of industrial automation systems. The flexible and powerful PLCs like Beckhoff CX50x0 are needed to cope with the increasing complexity of today's necessities from the automation industry. Figure 8.5 represents several features of the CX50x0

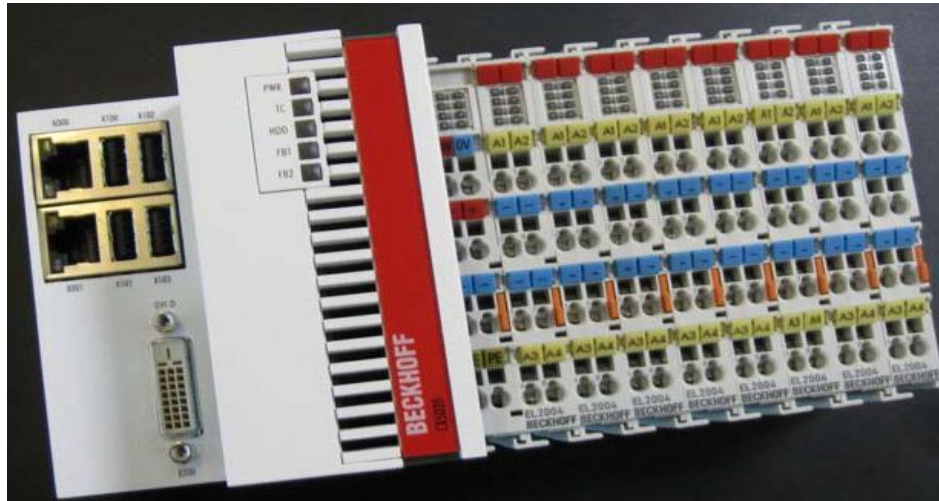


Figure 8.5: General CX50x0 DIN rail Industrial PCs
(www.beckhoff.com/cx5000/)

The CX device series combines the worlds of Industrial PC and hardware PLC and is suitable for medium-performance control tasks.

8.4.1 CX5020 - Embedded PC series

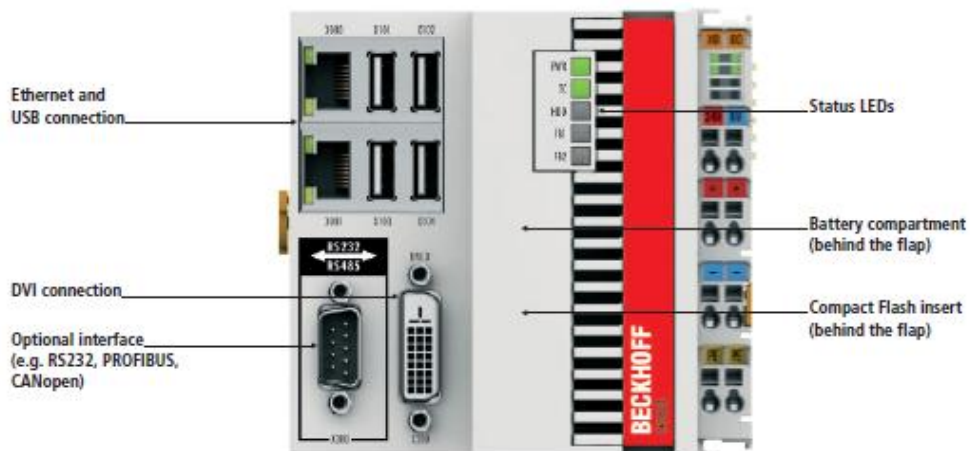


Figure 8.6: Diagram of the CX5020

(Adapted from www.beckhoff.com/english.asp?emdedded_pc/cx5010_cx5020.htm)

The above diagram (Figure 8.6) shows a well-established CX5020 PLC from Beckhoff. The CX5020 is Embedded PC from the CX5000 series based on Intel® Atom™ processors. The CX5020 has a 1.6 GHz Intel® Atom™ Z530 processor. The Z530 features hyper threading technology, i.e. it has two virtual CPU cores for more effective execution of software.

The following Table 8.1 is a technical data sheet of the CX5020 Beckhoff PLC.

Table 8.1: CX5020 technical data sheet from (www.beckhoff.com)

Technical data	CX5010-x1xx	CX5020-x1xx
Processor	Processor Intel®Atom Z510, 1.1 GHz clock frequency	Processor Intel®Atom Z510, 1.6 GHz clock frequency
Internal main memory	512 MB RAM (Internal, not expandable)	512 MB RAM (optionally 1 GB installed ex factory)
Flash memory	64 MB Compact Flash card (optionally extendable)	
Persistent memory	Integrated 1-second UPS (1 MB on Compact Flash card)	
Interfaces	2xRJ 45, 10/100/1000 Mbit/s, DVI-D, 4xUSB 2.0, 1 x optional interface	
Diagnostics LED	1 x power, 1 x TC status, 1 x flash access, 2 x bus status	
Clock	Internal battery-backed clock for time & data (battery exchangeable)	
Operating system	Microsoft Windows CE 6 or Microsoft Windows Embedded Standard 2009	
Control software	TwinCAT 2 PLC runtime or TwinCAT 2 NC PTP runtime	
Power supply	24 V DC (-15%/ +20%)	
Current supply I/O terminals	2 A	
Dielectric strength	500 V (supply/ internal electronics)	
Max. power loss	12 W (including the system interfaces)	12.5 W (including the system interfaces)
Dimensions (W x H x D)	100 mm x 100 mm x 91 mm	
Operating temperature	-25....+60 °C/ -25...+85 °C	
Relative humidity	95 %, no condensation	
Vibration/shock resistance	Conforms to EN 60068-2-6/EN 60068-2-27	
EMC immunity/emission	Conforms to EN 61000-6-2/EN 61000-6-4	

The integration of closed loop control algorithms into industrial control systems represents an important subject in the automation field. Due to its event-based execution model, IEC 61499 standard bears advantages concerning the closed loop control application implementation. This provides flexibility and allows the implementation of various and more complicated feedback algorithms. Beckhoff claims that, regardless of the compatible network/fieldbus that EtherCAT is connected to, data from all the equipment can be passed to the CX5020 master controller with standard Ethernet media.

8.5 TwinCAT development software

The Total Windows Control and Automation Technology also known as TwinCAT is a software platform developed by Beckhoff. TwinCAT 3 automation software transforms a

CX5000 system into a powerful PLC and motion control system that can be used with or without visualization. The greatest motivation behind this software is the integration of PLC, Motion Control (MC) and Human Machine Interface (HMI), in one software and on one CPU. The advantages are: reduced interface complexity, PC based control technology as 'open' control concept, one project storage place for hardware and software, etc. In combination with the TwinCAT automation software, the CX Embedded PC has become a powerful compatible with IEC 61131-3 standard PLC. The following section is based on TwinCAT automation software.

8.5.1 TwinCAT Architecture

TwinCAT consists of run-time systems that execute control programs in real-time and represents development environments for programming, diagnostics and configuration. Any Windows programs, for instance visualization programs or Office programs, can access TwinCAT data via Microsoft interfaces, or can execute commands.

Almost every kind of control application is possible with TwinCAT 3. The user can access different programming languages to realize these applications. In addition to the classic PLC programming languages of the IEC 61131-3 standard, the user can now also program with the high-level languages C and C++ as well as Matlab/Simulink. These and other attributes show why TwinCAT 3 is also called eXtended Automation: Architecture, Engineering and Runtime and this is shown in Figure 8.7 below.

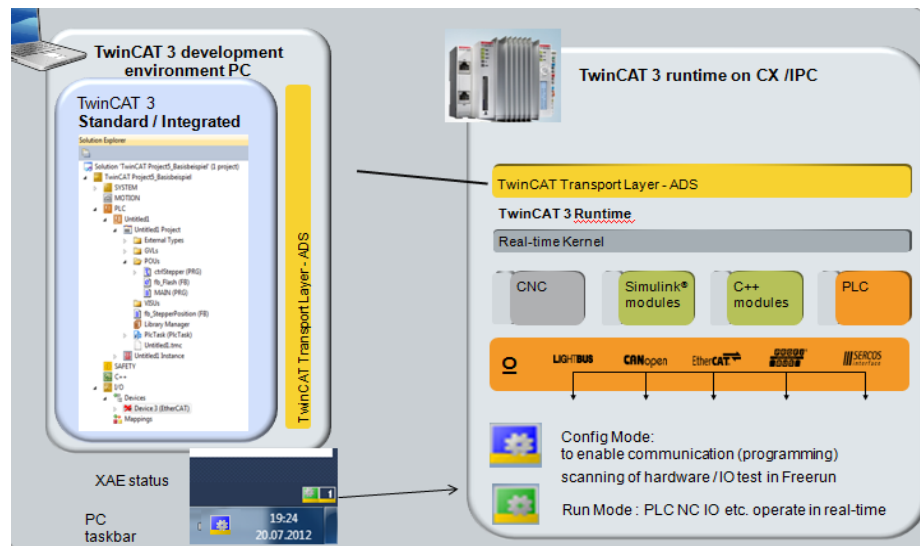


Figure 8.7: eXtended Automation Architecture (XAA)

TwinCAT Architecture has two subdivisions: eXtended Automation Engineering (XAE) and eXtended Automation Runtime (XAR) as illustrated in Figure 8.8. TwinCAT 3 is

divided into two components: eXtended Automation Engineering and eXtended Automation Runtime. The TwinCAT 3 engineering components enable the configuration, programming and debugging of applications.

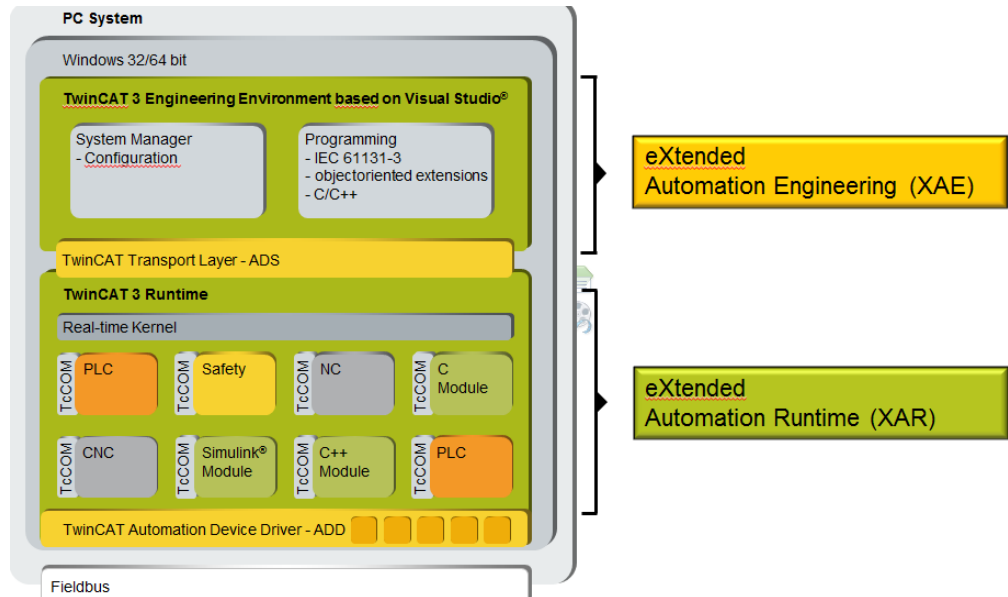


Figure 8.8: eXtended Automation Architecture (XAA)

The TwinCAT 3 runtime consists of further components: basic components and functions. The basic components can be extended by functions. Table 8.2 expresses further information about those divisions.

Table 8.2: XAE and XAR

eXtended Automation Engineering (XAE)	eXtended Automation Runtime (XAR)
Visual Studio 2010 for real-time programming in IEC 61131-3 and C/C++	Execution of the created modules in real-time.
Visual Studio 2010 for system configuration.	Support for 64-bit systems and Support for multi-core CPUs.

8.5.1.1 eXtended Automation Engineering (XAE):

One of the key approaches of TwinCAT 3 is to simplify the software engineering. Instead of developing own stand-alone tools it is obviously worthwhile to integrate into common and existing software development environments. On behalf of TwinCAT 3 the development environment is the Microsoft Visual Studio 2010. By integrating TwinCAT 3 as an extension into the Visual Studio, an expandable and future platform is provided.

The TwinCAT 3 eXtended Automation Engineering has the following attributes:

- TwinCAT 3 Standard, and TwinCAT 3 Integrated
- System Manager,
- PLC, and Motion Control,
- C/C++ programming,
- Matlab/Simulink Integration
- C#/ .NET programming

Figure 8.9 shows the overview layout of XAE

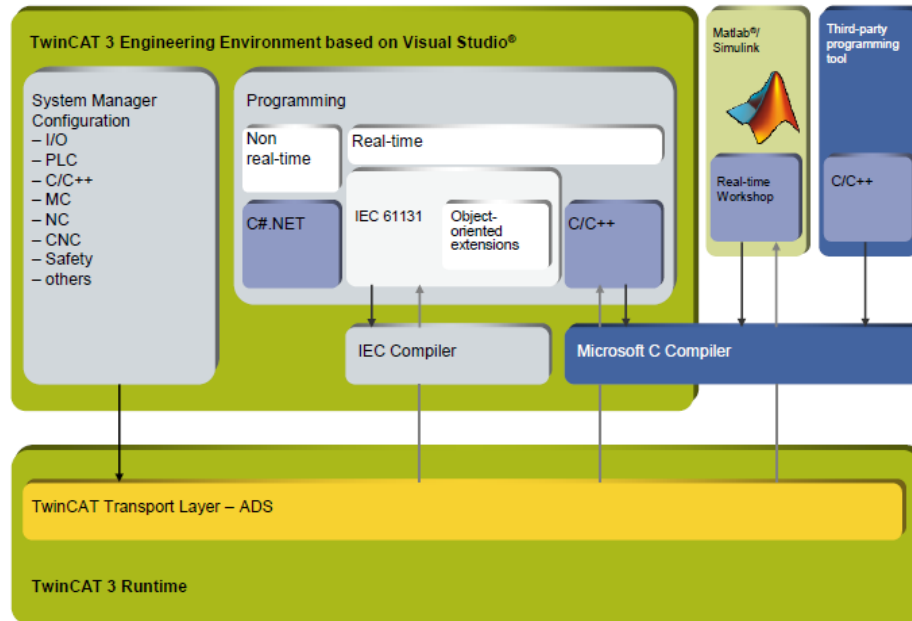


Figure 8.9: eXtended Automation Engineering (XAE)
(www.beckhoff.com)

8.5.1.2 Engineering (XAE) - Matlab/Simulink integration

MATLAB/Simulink is a tool for the computer-assisted simulation of physical or biological systems and has been in widespread use in research and development for many years. The models of the systems to be simulated are usually implemented at graphic level in the form of block diagrams. In addition to the standard library, toolboxes are available for various areas of application, with which the time and effort for modeling can be reduced. One of the strengths of Simulink that should be highlighted in conjunction with automation technology is the design of controllers at simulation level. The functions of the higher-level software environment MATLAB (with appropriate toolboxes) enable the informal design of controllers using calculation methods based on the control theory. Controllers designed in this way can then be simulated and confirmed together with a model of the controlled system in Simulink, (Yang and Vyatkin, 2012). However, entire

production plants can also be modeled and tested in simulation instead of simple controlled systems.

The CX5020 from Beckhoff as described in section 8.4 has been used in this research as a real-time platform to execute the application developed in Simulink to TwinCAT 3. To achieve real-time simulation of the system obtained in TwinCAT 3, the closed loop algorithm is downloaded into the Beckhoff PLC CX5020. Ethernet is used as a communication driver element to link the PC and the PLC via fast duplex communication. Ethernet module scans the PLC continuously for values of the input variables and writes them in an appropriate database in TwinCAT 3.

The integration of Matlab/Simulink with TwinCAT enables execution of TwinCAT modules that were generated as Simulink models in the Matlab simulation environment. The chosen interfacing type between Simulink PC and PLC displays the parameters and variables in the graphic interface of TwinCAT 3 and enables viewing and modification in the real-time environment at runtime. The integrated motion functionalities simplify the engineering as well as the new well-arranged safety applications. These and other attributes has proven why TwinCAT 3 is also a high-minded eXtended Automation.

The advantages of Simulink Integration in TwinCAT 3 are:

- Simulink is well-known in the scientific and measurement environment
- great variety of toolboxes (e.g. Fuzzy)
- creation, simulation and optimization of control circuits
- debug interface between Simulink and TwinCAT

8.5.2 Code generation algorithm

Code generation process is done to transform the Simulink model to a real-time algorithm set up on the PLC. The closed loop simulation models in Chapter 6 and Chapter 7 are transformed from MATLAB/Simulink environment to TwinCAT 3 through model transformation process. This procedure is done to achieve real-time simulation of the closed loop system in PLC. To transfer the closed loop algorithm from Matlab/Simulink program to TwinCAT 3 for each method used in this thesis the following steps are used:

- design of the closed loop system and building its block diagram in Simulink environment
- automatic generation of C/ C++ code by the Simulink Coder
- compilation with Visual Studio C Compiler

- parameterization in the TwinCAT System Manager
- download of the transformed block diagram and its execution in the TwinCAT 3 Runtime environment

Figure 8.10 shows a demonstration process of the code generation from Simulink.

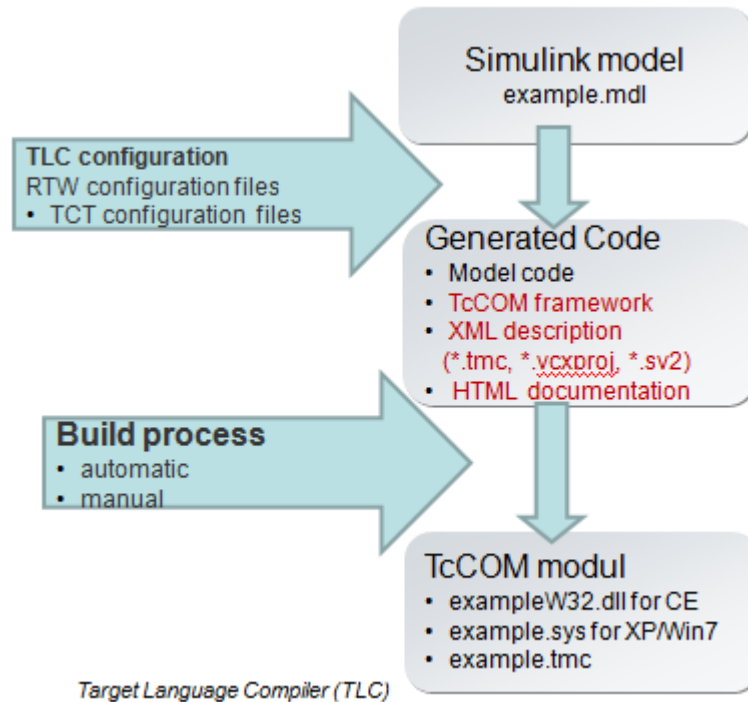


Figure 8.10: Typical Code generation Process

The TE1400 TwinCAT Target for MATLAB/ Simulink enable the user to generate real-time capable modules, which can be executed in the TwinCAT 3 runtime. These modules can be instantiated multiple times, parameterized and debugged in the TwinCAT 3 engineering environment.

The requirements for transformation of the Simulink model to TwinCAT 3 are:

- Matlab/Simulink (> Version 2010a)
- Simulink Coder (Matlab Coder)
- Target for Matlab Simulink - TE1400
- Visual Studio 2010

The following procedure must be followed:

- Select TwinCAT Target
- Simulink Coder generates C or C++ Code
- Microsoft C/C++ Compiler generates Binary Code

- TwinCAT Target generates description file.tmc

Figure 8.11 shows the process link from a Simulink to TwinCAT 3 module.

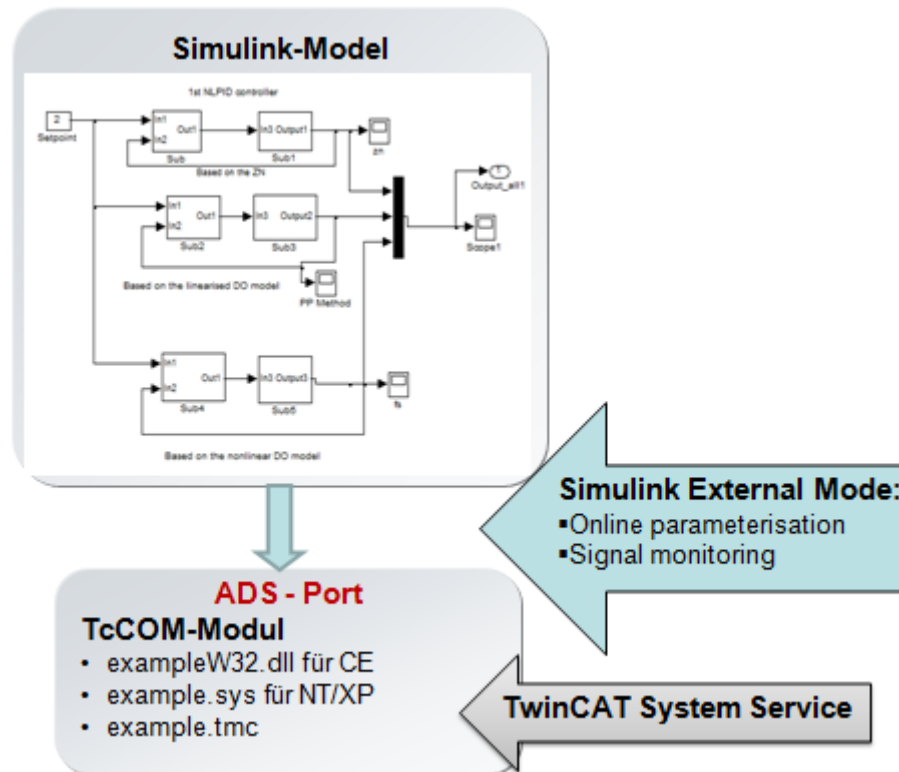


Figure 8.11: From Matlab/Simulink to TwinCAT

The above Figure (8.11) shows the Simulink Coder that generates real-time capable C or C++ code from the block diagrams developed in Simulink. The TwinCAT Target for MATLAB/Simulink uses the Simulink coder to create a TcCOM module (real-time-capable TwinCAT module) with the input and output behavior according to the source Simulink model. Generated modules can be instantiated in TwinCAT 3 projects, where those can be parameterized using the TwinCAT 3 Engineering Environment (XAE), if parameter changes are necessary. After starting the TwinCAT 3 runtime, the module is executed in real-time and can therefore be integrated into a real machine controller such as PLC in this thesis.

The following Figure 8.12 shows how the signal can be monitored online through TwinCAT 3

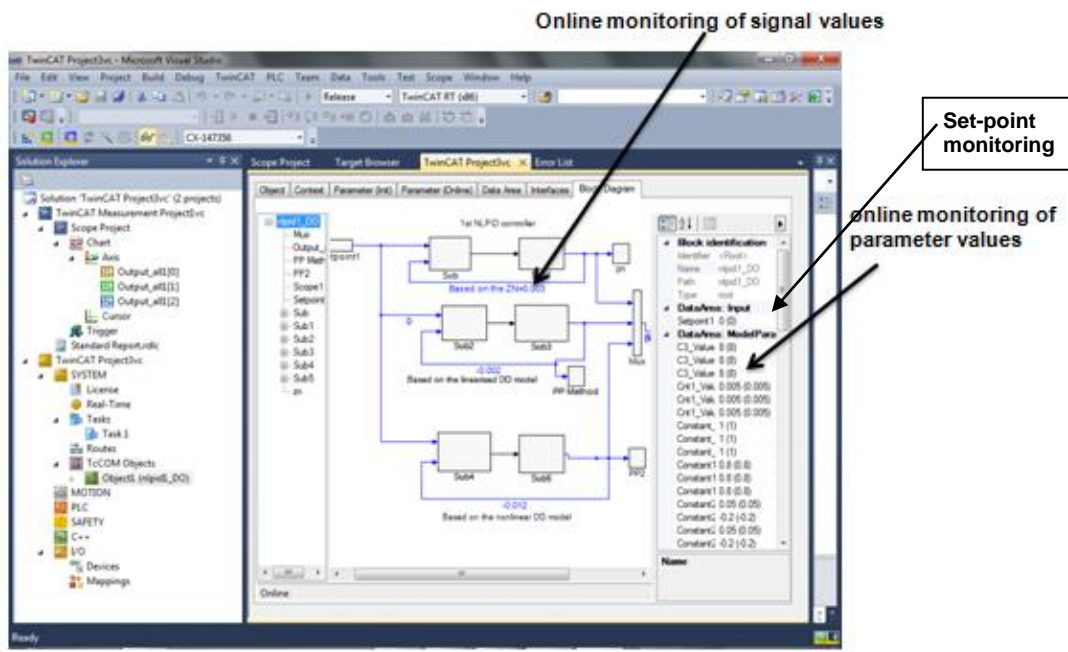


Figure 8.12: Debugging in TwinCAT3

The requirements for TwinCAT 3 XAE (Engineering):

- Windows XP with Service Pack 3 (x86) or Windows 7 (x86 or x64)
- processor running at 1.6 GHz or higher
- 2 GB RAM
- 3 GB free hard disk space
- graphics adapter supporting DirectX9, running at a minimum resolution of 1024x768

8.5.2.1 eXtended Automation Runtime (XAR):

The TwinCAT 3 Runtime offers a real-time environment, where TwinCAT modules can be loaded, executed and managed. The individual modules need not be created with the same compiler and thus can be programmed independently and by different manufacturers or designers. (<http://infosys.beckhoff.com>). Also it is not important if these modules are generated using the PLC, Numerical Control (NC), Computer Numerical Control (CNC). Numerous tasks can run on one control PC, because the different modules (C/C++, MATLAB) can call themselves in the TwinCAT 3 runtime, there are much more possibilities for the software architecture of the application. Therefore it is possible to combine a number of modules, which have their own functionalities, to one complete machine application. The following Figure 8.13 presents the structure of TwinCAT 3 XAR modular runtime system.

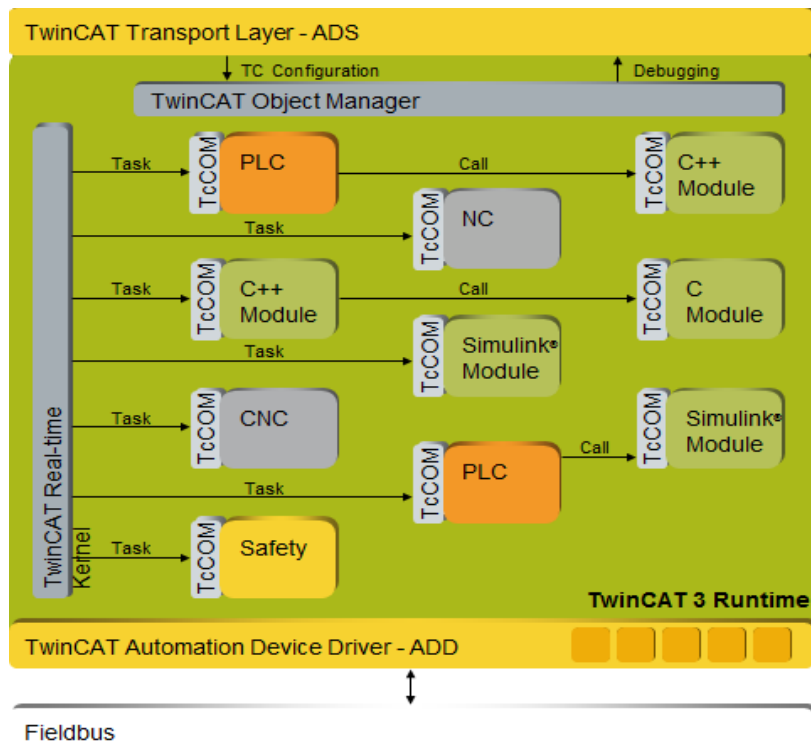


Figure 8.13: Modular structure of the TwinCAT 3 runtime environment
 (<ftp://download.beckhoff.com/>)

8.6 Model Transformation and Real-time Results

The model transformation technique is a new model-based engineering approach, which is based on the IEC61499 functional block programming standard. This standard allows real-time control of complex plants with a new generation of programmable logic controllers (PLCs). In this thesis model transformation is presented by bridging MATLAB/Simulink with TwinCat 3 Function Block models. This is achieved by a transformation between the two block diagram languages. The transformation supported by the developed tools sets the cornerstone of the verification and validation framework for IEC 61499 Function Blocks in closed-loop with the models of the plant (Yang and Vyatkin, 2012). The framework also paves the way to running closed-loop plant-controller systems and building complex models using the efficient object instantiation techniques of IEC 61499.

MATLAB/ Simulink is selected as simulation environment to test the closed loop system because it is a powerful well-known tool in the modeling, simulation domain and it follows the principles of functional block programming, and the model transformation method. Functional blocks offer a higher level of generalization than the conventional PLC based

design language. Model transformation automatically translates each state flow block into customized basic IEC 61499 function blocks with, the same inputs, outputs and parameters as their Simulink counter parts (Bayrak, 2012).

8.6.1 Generating a TwinCAT module from a Simulink model for the DO closed loop system

The following steps show the basics on how the model transformation is done. Figure 8.14 is the closed loop Simulink model of the dissolved oxygen under nonlinear PID control, in which the Simulink subsystem blocks, contains all necessary files to reproduce this model in TwinCat 3 environment. In order to make the Simulink model real-time capable, it is also necessary to configure a Fixed-Step solver.

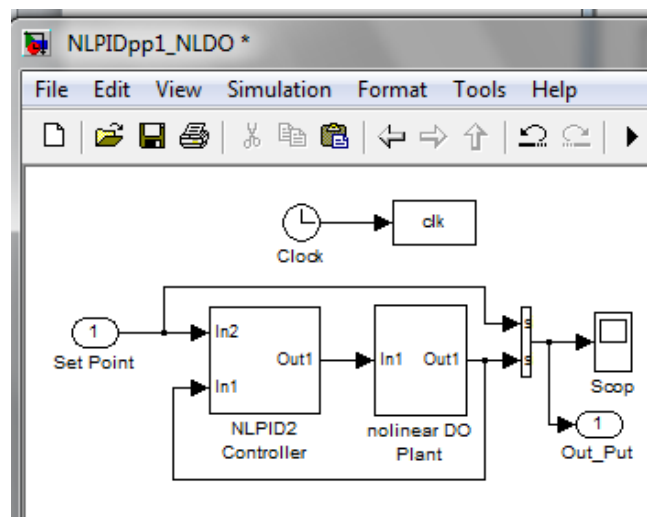


Figure 8.14: Simulink model

8.6.1.1 Generate a TwinCAT module procedure

1. The model file (Figure 8.14) is opened in Simulink and the coder settings are accessed via the *Model Explorer* in the *View* menu in Simulink. Figure 8.15 shows the *Model explorer* where the configuration is done. Expand in the model name “*NLPID_DO*” then select *Configuration*, *Code Generation*, then choose the System target file “*TwinCAT.tlc*”, by using the *Browse* button.

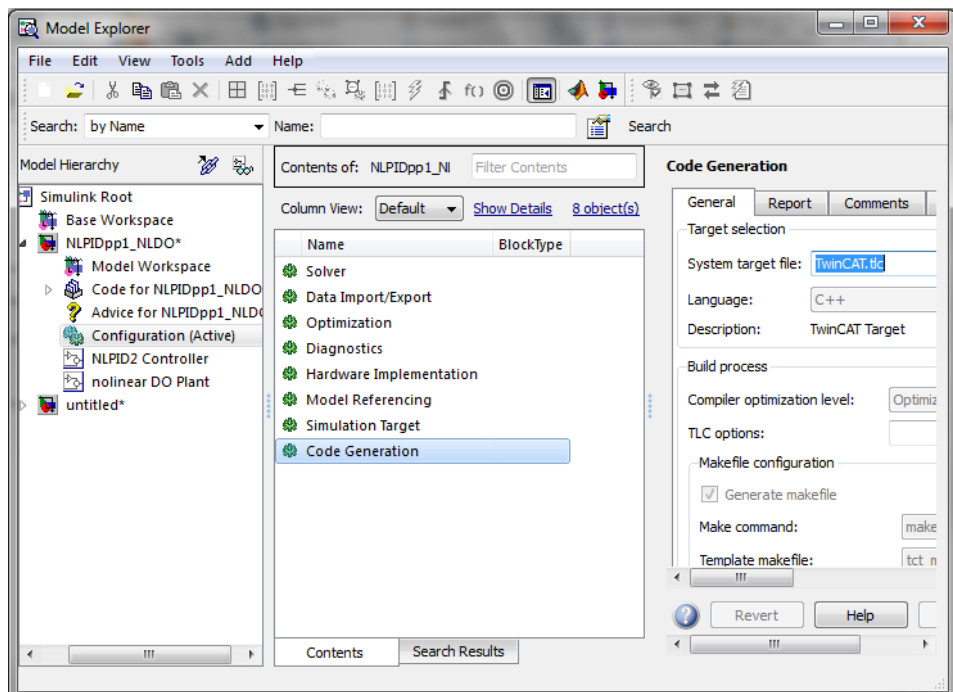


Figure 8.15: Model Explorer browser for System Configuration

2. Then after that, the *Model Explorer* is closed, and the code generation process is started via the Simulink-Menu *Tools->Code Generation->Build Model* in that pattern as highlighted in Figure 8.16.

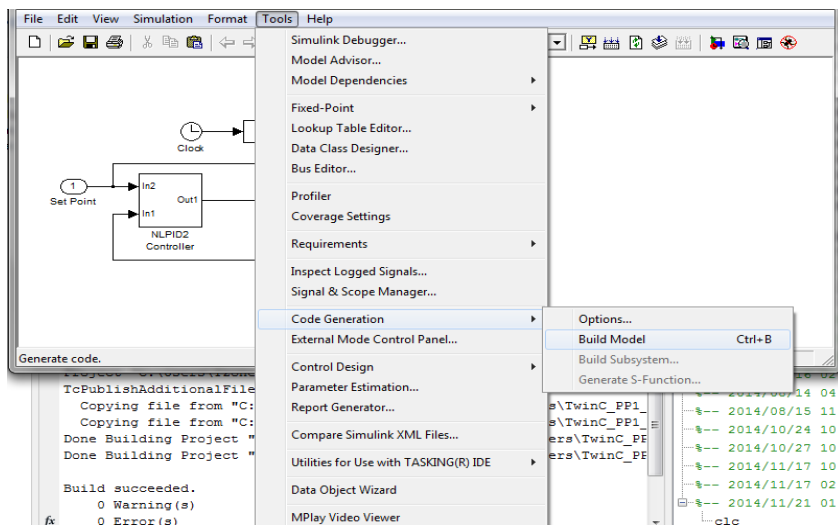


Figure 8.16: Code Generation

The code generation progress is displayed in the MATLAB command window. If the process passes with no error, that indicates the communication between Simulink and TwinCat has been successful achieved

8.6.1.2 The generated TwinCAT module as a TwinCAT project

1. Now create the TwinCAT project by opening the TwinCAT engineering environment. In the environment release the *Solution Explorer*, expand the node *System* and Select *Add new item* in the context menu of the node “*TcCOM Objects*”. After following these steps, the dialog Figure 8.17 is obtained.

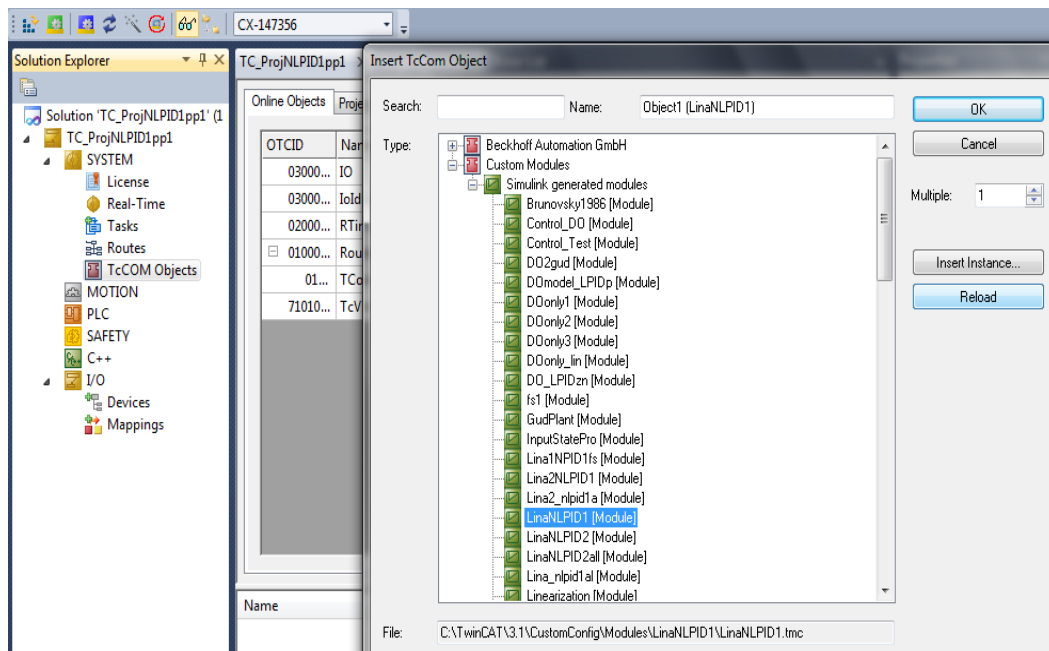


Figure 8.17: Simulink model transformation process to TwinCAT representation

2. In the Figure 8.17, selection of the module is done to upload the Simulink model to TwinCAT. The module (with its default settings) should automatically have been configured to add on to this task. The task must also be arranged to work with module “*NLPID_DO*”. To check this, select the object node *Object1 (NLPID_DO)* and open the tab “*Context*”. The table results contain the object ID and the object name of the task as shown in Figure 8.18, with the priority and cycle time value. Wrong mapping of the data type, cycle time and the use of the same priority level, all of this can make the computation algorithm to behave incorrectly.

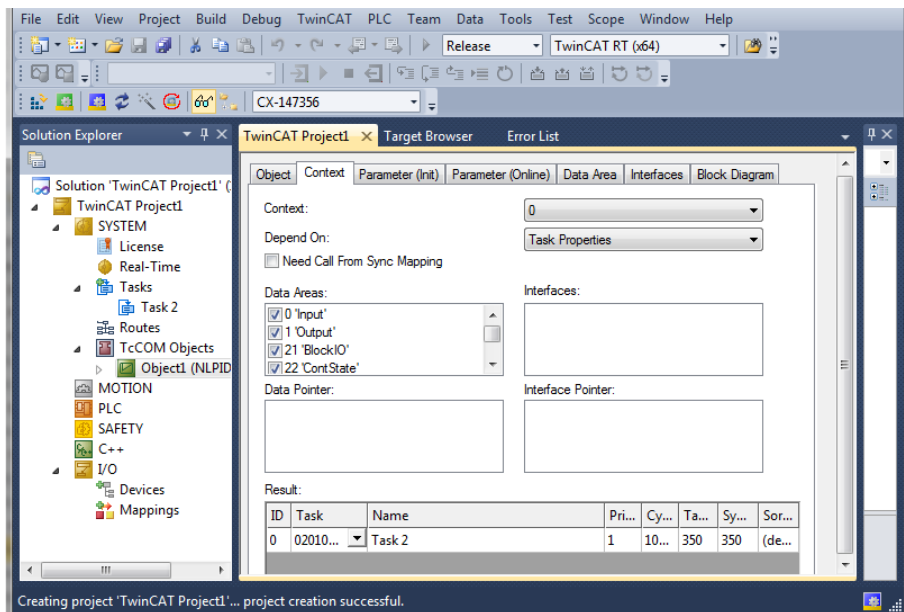


Figure 8.18: Setup the priority and a cycle time for the object “NLPID_DO”

3. At this moment the configuration is completed and can be activated on the target system which is the CX5020 Beckhoff PLC. The procedure is as follows:
 - Choose the target system; the current configuration shall be activated on.
 - Activate the configuration on the targeted system. Confirm the dialogs, asking whether to overwrite the current configuration and start the TwinCAT system.
 - The target status icon changes its color to green (running).
 - If the *Block Diagram* tab is selected, the block diagram status should change to "Online" and its property grid should show some online values (see Figure 8.19).

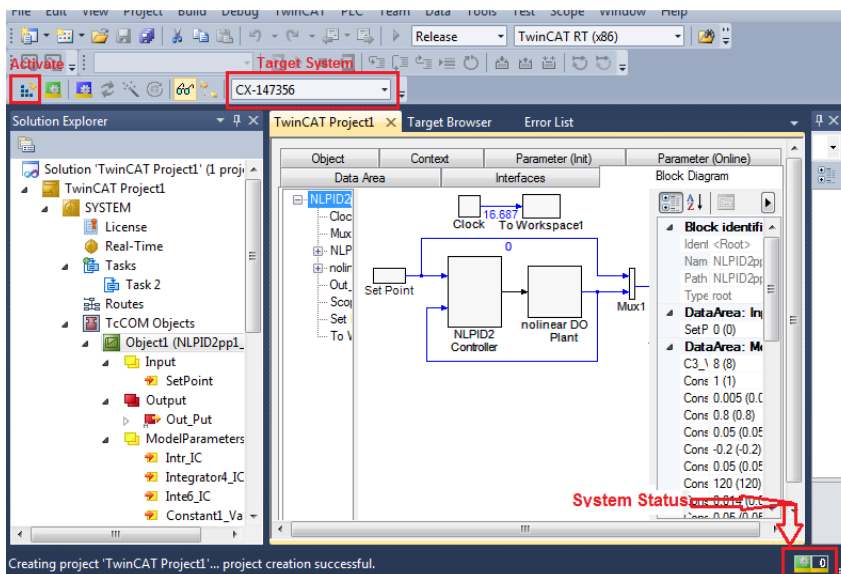


Figure 8.19: Simulink model transformed to TwinCat module actively working in a PLC CX5020

The achievement of the code transformation and evaluation of the structure together with the implementation of the closed loop system in real-time simulation prove that the TwinCat PLC CX5020 environment has the greatest conformity in structure with the simulation model in Simulink.

The following section is based on the real PLC real-time simulation of the closed loop DO system with two NLPID controllers (NLPID1 and NLPID2) considered in the previous chapters (Chapter 6 and Chapter 7).

8.6.2 Simulink Model to TwinCat Transformation of the closed loop DO process system under the NLPID1 controller

Figure 8.20 shows a full transformation of the closed loop system from Simulink to TwinCAT 3. The block labeled NLPID1 has a nonlinear controller in it and the block labeled DO process model has a nonlinear plant in it. The notations in figure 8.20 are:

In1 – input of the set-point value

In2 – feedback input

In3 – is the input into the process

Out1 – is the output of the control signal

Out2 – is the output of the process

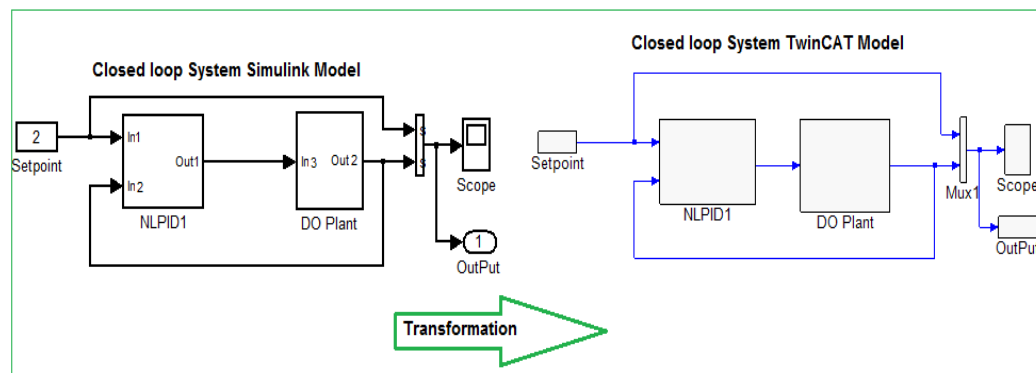


Figure 8.20: Transformed Simulink closed loop model to the TwinCAT closed loop model

Real-time implementation of the control algorithms are tested in a TwinCAT 3 simulation environment and then downloaded into a Beckhoff CX 5020 PLC for implementation. Vyatkin and Yang, (2012), state that the amount of time for performing model transformation depends on the complexity of the model in Simulink. The amount of time used for the transformation of the model in this thesis is 10ms.

Some of the advantages of the TwinCAT 3 solution are:

- Simulink model is hardware independent

- No Beckhoff specific blocks required in Simulink for the module generation
- Changing of the module cycle time in TwinCAT without a new compilation of the Simulink model.
- Graphical representation in the TwinCAT 3 engineering environment
- Online monitoring of parameters and signals in TwinCAT 3 run-time.
- Online editing or change of parameter values
- Powerful debugging mechanisms (breakpoint)
- Generation of a PLC function block capturing the model
- Support of all toolboxes which are supported by the Simulink Coder

8.6.3 Implementation in Real-Time using the NLPID1 controller

The implementation of the real time simulation is done in the TwinCAT environment using the developed control algorithms in the chapters (Chapter 6 and 7). The PLC implementation in real-time simulation environment is performed only for the NLPID controllers with the nonlinear DO process using the two methods shown in the thesis - Chapter 6 and Chapter 7.

8.6.3.1 Real-time results for the DO closed loop system under the NLPID1 controller

The real-time simulation is performed in CX5020 PLC and the set-point and internal disturbance are changed to different values as shown in Table 8.3. These changes are applied to see whether the system can maintain the online stability response or will become unstable. The real-time simulation in CX5020 result of the closed loop DO process under the nonlinear PID1 controller parameters and different disturbance as in Table 8.3 are revealed afterward in Figure 8.21 to Figure 40.

Table 8.3: DO process disturbances and set point values to be applied in real-time

Set-point	s_{oin}	r_{so}
2.7	0.01	-294.8954
2.7	0.01	-442.3431
2.7	0.01	-147.4477
2	0.8	-294.8954
2	0.8	-442.3431
2	0.8	-147.4477
1.7	0.8	-294.8954
1.7	0.8	-442.3431
1.7	0.8	-147.4477

The Real-time simulation results of the closed loop system under the NLPID1 controller using the tuned controller parameters designed based on the Pole Placement method for

the LPID and tuned to be applied in the NLPID1 controller are shown from Figure 8.21 to Figure 8.30. Detailed explanation of this method is given in Chapter 6.

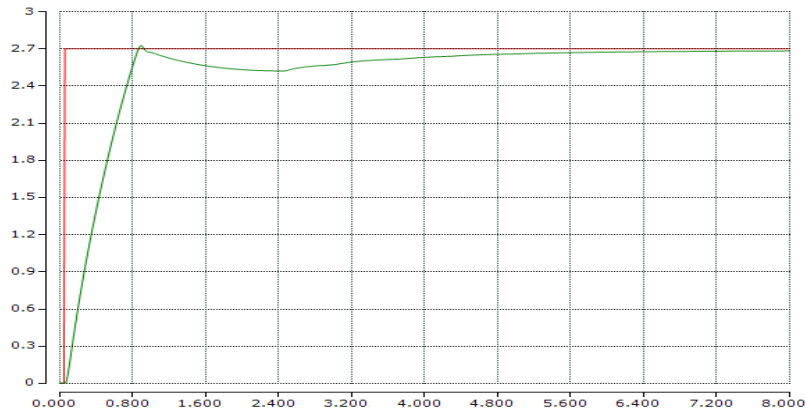


Figure 8.21: Real-time PLC simulation results of the closed loop system with NLPID1 (PP1) controller when the set-point is 2.7 mg/L , $s_{o,in} = 0.01 \text{ mg/L}$ and $r_{so} = -294.8954 \text{ mg/L/day}$

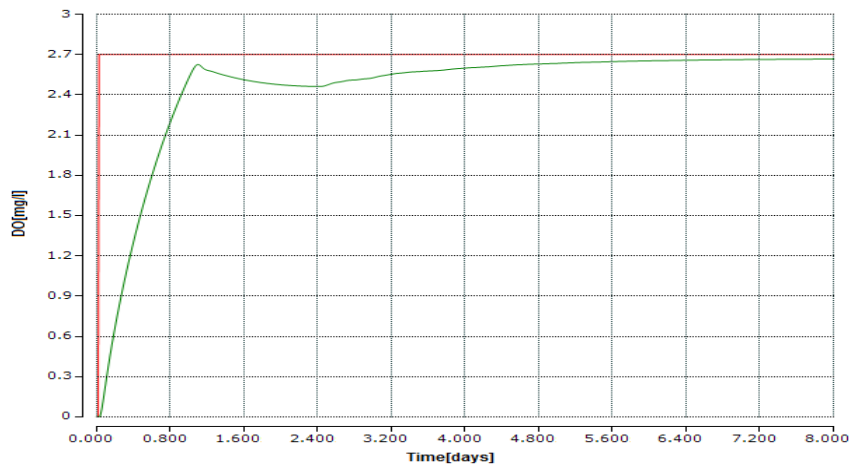


Figure 8.22: Real-time PLC simulation results of the closed loop system with NLPID1 (PP1) controller when the set-point is 2.7 mg/L , $s_{o,in} = 0.01 \text{ mg/L}$ and $r_{so} = -442.3431 \text{ mg/L/day}$

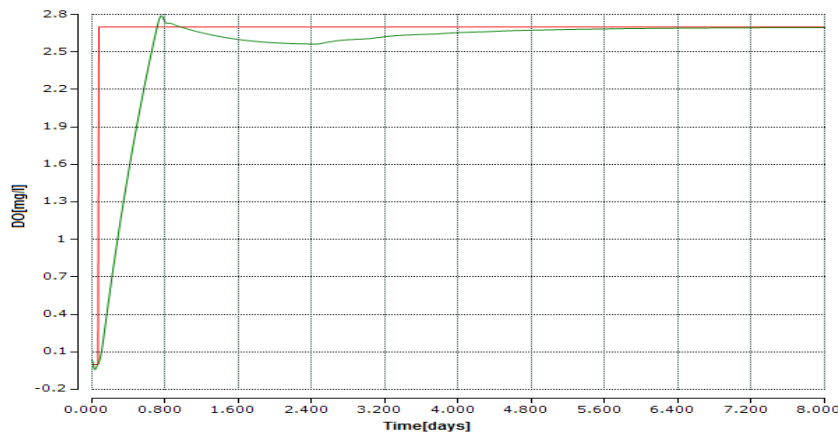


Figure 8.23: Real-time PLC simulation results of the closed loop system with NLPID1 (PP1) controller when the set-point is 2.7 mg/L , $s_{o,in} = 0.1 \text{ mg/L}$ and $r_{so} = -147.4477 \text{ mg/L/day}$

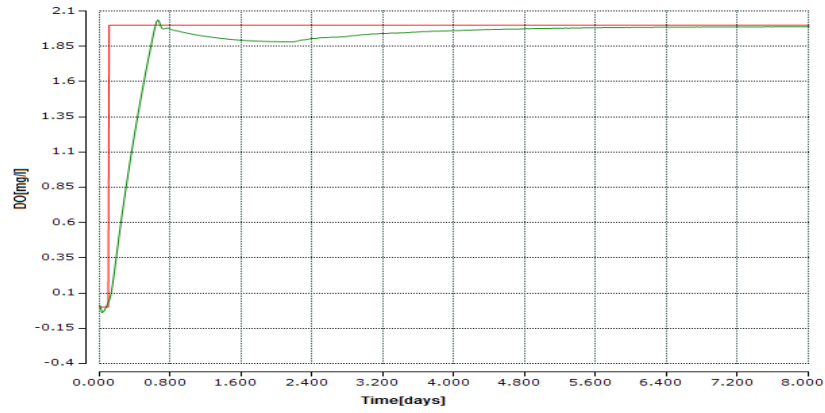


Figure 8.24: Real-time PLC simulation results of the closed loop system with NLPID1 (PP1) controller when the set-point is 2 mg/L , $s_{o,in} = 0.8 \text{ mg/L}$ and $r_{so} = -294.8954 \text{ mg/L/day}$

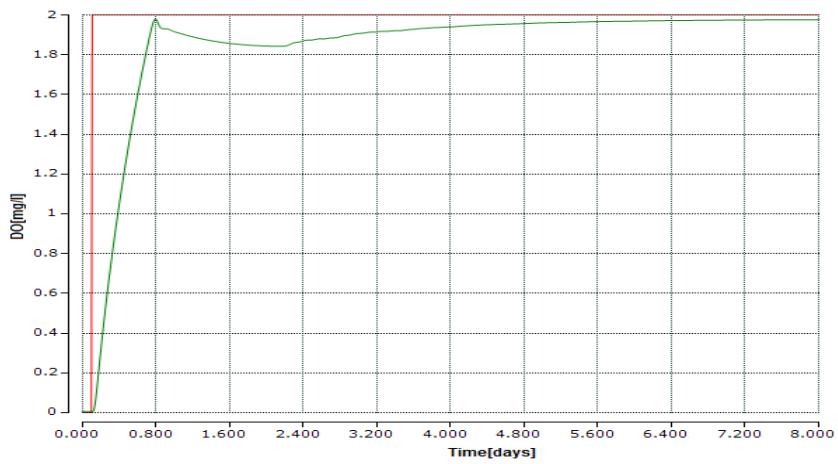


Figure 8.25: Real-time PLC simulation results of the closed loop system with NLPID1 (PP2) controller when the set-point is 2 mg/L , $s_{o,in} = 0.8 \text{ mg/L}$ and $r_{so} = -442.3431 \text{ mg/L/day}$

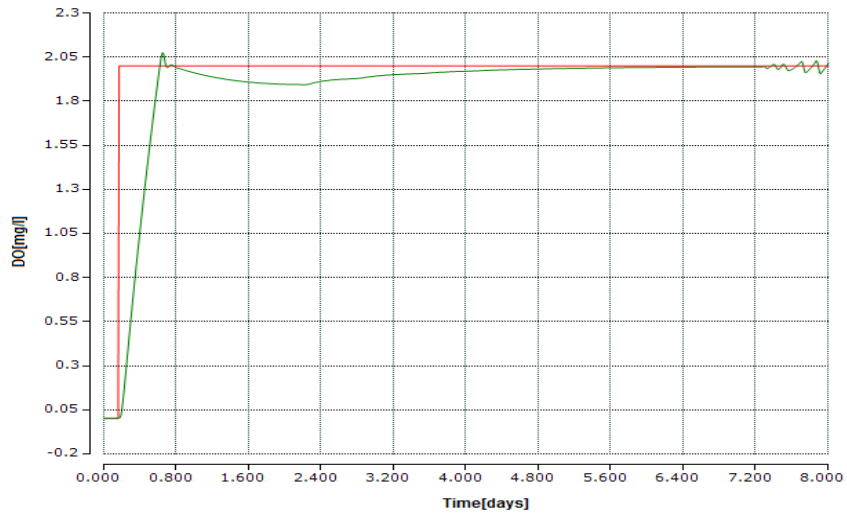


Figure 8.26: Real-time PLC simulation results of the closed loop system with NLPID1 (PP1) controller when the set-point is 2 mg/L , $s_{o,in} = 0.8 \text{ mg/L}$ and $r_{so} = -147.4477 \text{ mg/L/day}$

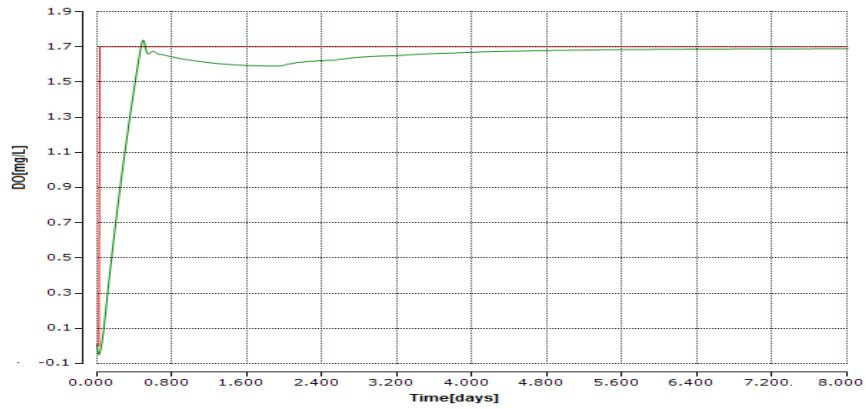


Figure 8.27: Real-time PLC simulation results of the closed loop system with NLPID1 (PP1) controller when the set-point is 1.7 mg/L , $s_{o,in} = 0.8 \text{ mg/L}$ and $r_{so} = -294.8954 \text{ mg/L/day}$

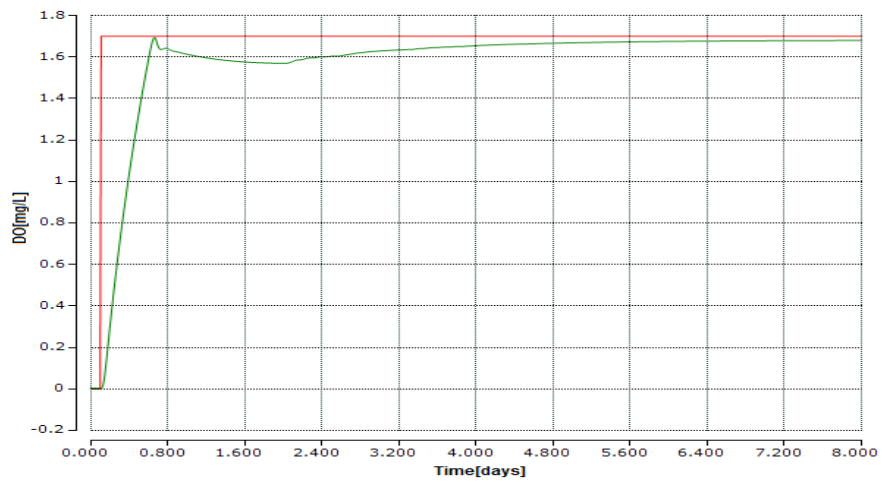


Figure 8.28: Real-time PLC simulation results of the closed loop system with NLPID1 (PP1) controller when the set-point is 1.7 mg/L , $s_{o,in} = 0.8 \text{ mg/L}$ and $r_{so} = -442.3431 \text{ mg/L/day}$

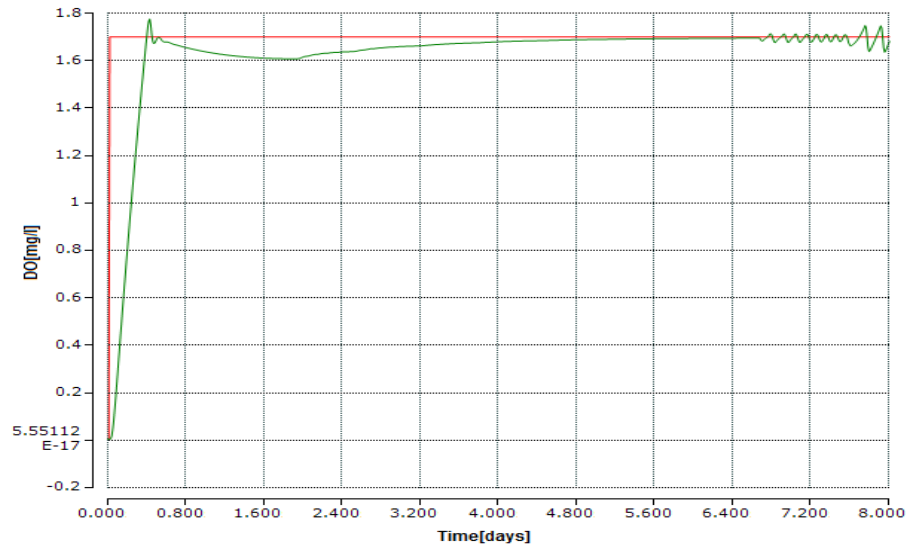


Figure 8.29: Real-time PLC simulation results of the closed loop system with NLPID1 (PP1) controller when the set-point is 1.7 mg/L , $s_{o,in} = 0.8 \text{ mg/L}$ and $r_{so} = -147.4477 \text{ mg/L/day}$

The closed loop DO process behaviors under the different internal disturbances and different set-point values are tested in real-time. Process reaction in real-time seems to be able to accomplish different set-points conditions and is not badly affected by the changes applied in the disturbances. The PLC real-time simulation results are the same as in Matlab/Simulink in Chapter 6; this means the model transformation explained in section 8.6 is successfully completed.

To validate the transformation method the correctness two DO closed loop process trajectories for the same set point and disturbance are shown in the Figure 8.30

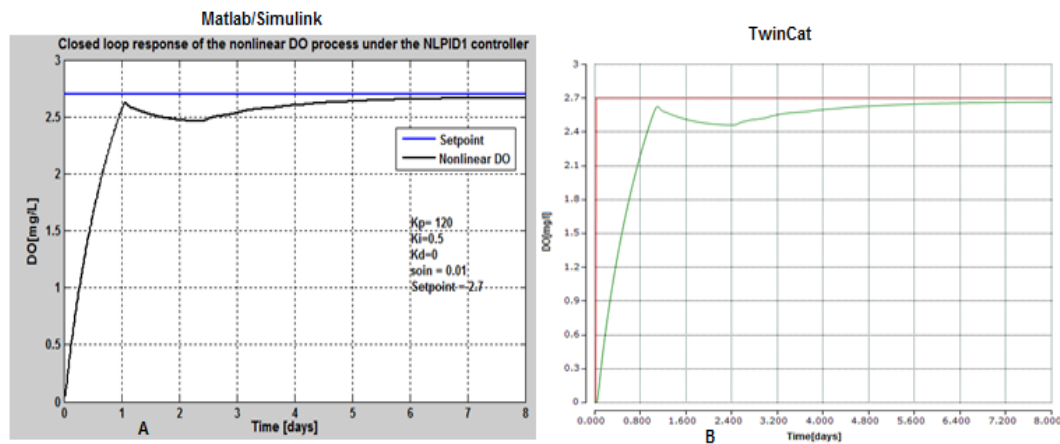


Figure 8.30: Comparison of two trajectories of the closed loop DO process response under the NLPID1 (PP1) controller, when the set-point is 2.7 mg/L , $s_{o,in} = 0.01 \text{ mg/L}$ and $r_{so} = -442.3431 \text{ mg/L/day}$: Figure 8.30A- Simulink results and Figure 8.30B Real-time PLC results

It can be seen from Figure 8.30 that the behavior of the closed DO behavior is the two platforms.

The following TwinCAT 3 real-time results are for the closed loop DO process behavior under the NLPID1 with parameters designed based the nonlinear DO model (PP2 method), Figure 8.31 – Figure 8.40

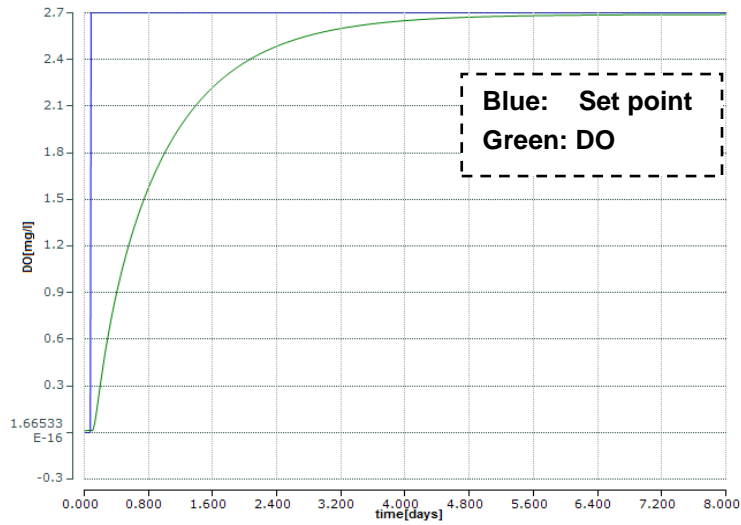


Figure 8.31: Real-time simulation of the closed loop system with NLPID1 (PP2) controller when the set-point is 2.7 mg/L , $s_{o,in} = 0.01 \text{ mg/L}$ and $r_{so} = -294.8954 \text{ mg/L/day}$

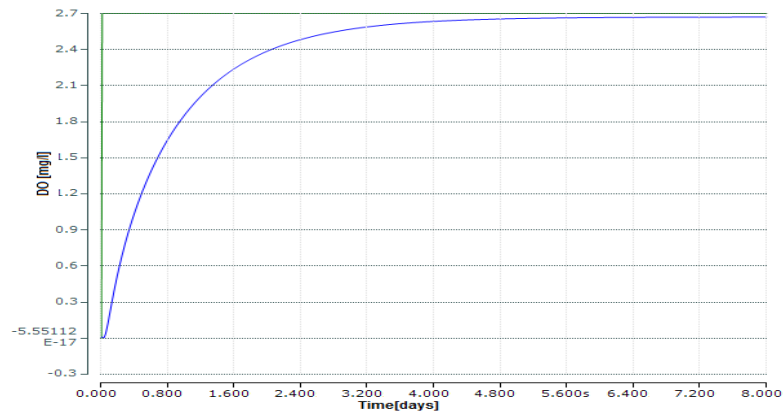


Figure 8.32: Real-time simulation of the closed loop DO process response under the NLPID1 (PP2) controller, when the set-point is 2.7 mg/L and $r_{so} = -442.3431 \text{ mg/L/day}$

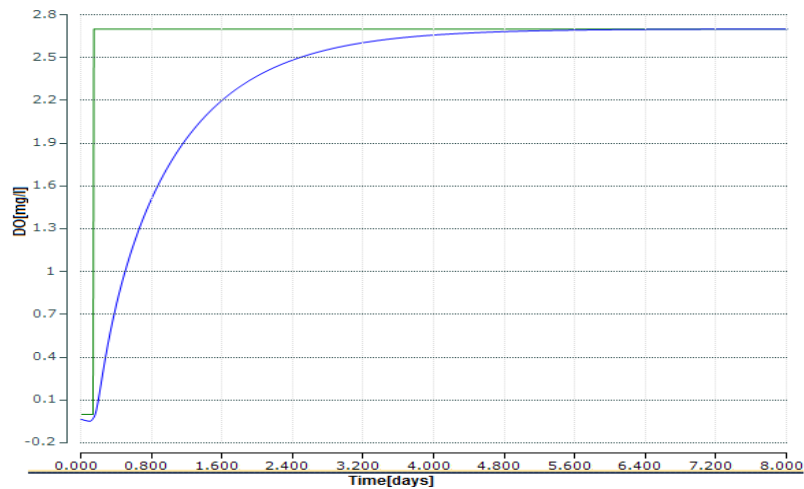


Figure 8.33: Real-time simulation of the closed loop DO process response under the NLPID1 (PP2) controller, when the set-point is 2.7 mg/L , $s_{o,in} = 0.01 \text{ mg/L}$ and $r_{so} = -147.4477 \text{ mg/L/day}$

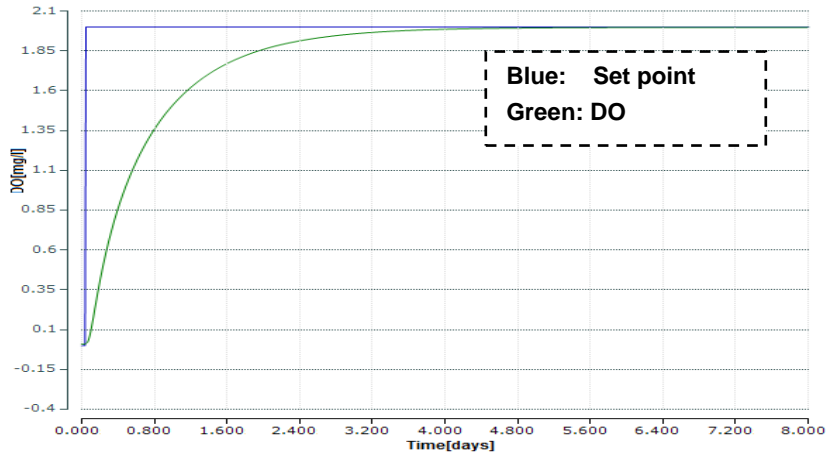


Figure 8.34: Real-time simulation of the closed loop DO process response under the NLPID1 controller, when the set-point is 2 mg/L , $s_{o,in} = 0.8 \text{ mg/L}$ and $r_{so} = -294.8954 \text{ mg/L/day}$

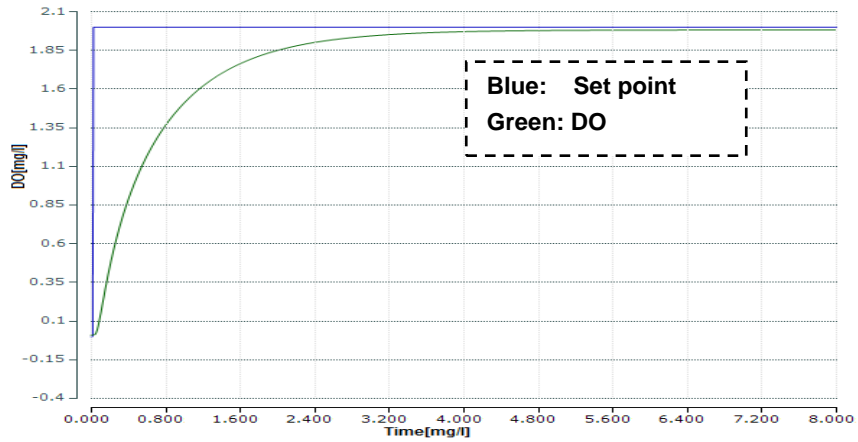


Figure 8.35: Real-time simulation of the closed loop DO process response under the NLPID1 controller, when the set-point is 2 mg/L , $s_{o,in} = 0.8 \text{ mg/L}$ and $r_{so} = -442.3431 \text{ mg/L/day}$

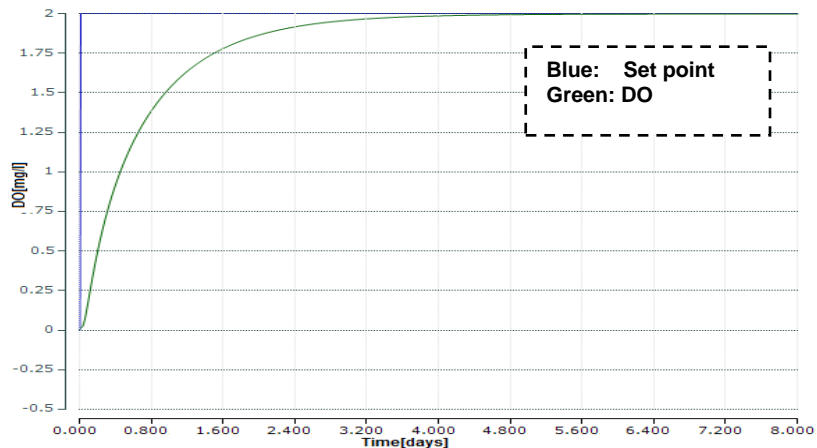


Figure 8.36: Real-time simulation of the closed loop DO process response under the NLPID1 (PP2) controller, when the set-point is 2 mg/L , $s_{o,in} = 0.8 \text{ mg/L}$ and $r_{so} = -147.4477 \text{ mg/L/day}$

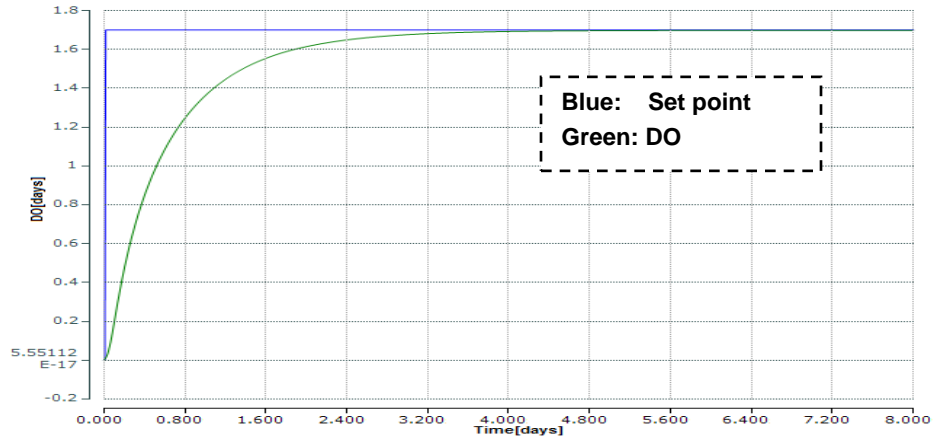


Figure 8.37: Real-time simulation of the closed loop DO process response under the NLPID1 (PP2) controller, when the set-point is 1.7 mg/L , $s_{o,in} = 0.8 \text{ mg/L}$ and $r_{so} = -294.8954 \text{ mg/L/day}$

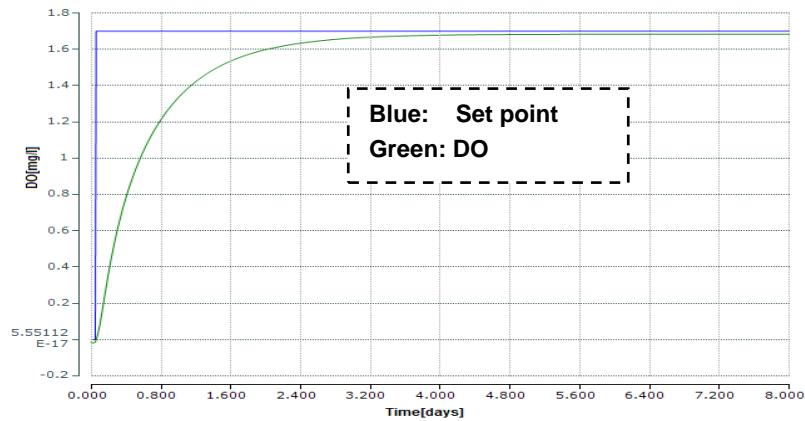


Figure 8.38: Real-time simulation of the closed loop DO process response under the NLPID1 (PP2) controller, when the set-point is 1.7 mg/L , $s_{o,in} = 0.8 \text{ mg/L}$ and $r_{so} = -442.3431 \text{ mg/L/day}$

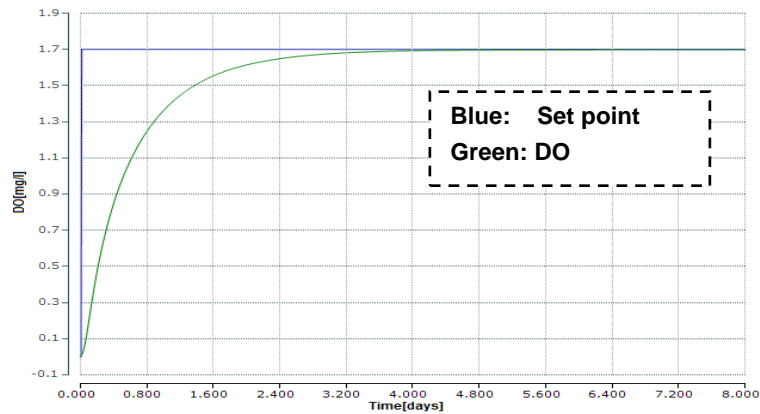


Figure 8.39: Real-time simulation of the closed loop DO process response under the NLPID1 (PP2) controller, when the set-point is 1.7 mg/L , $s_{o,in} = 0.8 \text{ mg/L}$ and $r_{so} = -147.4477 \text{ mg/L/day}$

In order to validate the correctness of the transformation method the closed loop DO process trajectories obtained through simulation in Matlab/Simulink environment and

through real-time simulation in the TwinCAT3 environment are plotted in Figure 8.40 for the same values of set point and disturbances.

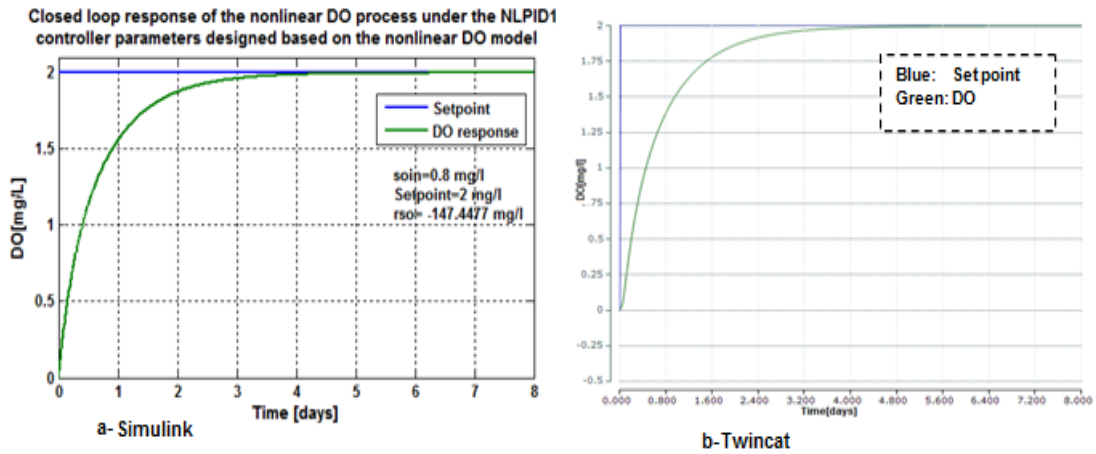


Figure 8.40: Comparison two trajectories of the closed loop DO process response under the NLPID1 (PP2) controller, when the set-point is $2 \text{ mg} / \text{L}$, $s_{o,in} = 0.8 \text{ mg} / \text{L}$ and $r_{so} = -147.4477 \text{ mg} / \text{L} / \text{day}$ (Figure 8.40a- Simulink results and Figure 8.40b Real-time PLC results)

The comparison shows that the PLC real-time simulation results are the same as these in Matlab/Simulink in Chapter 7; this means the model transformation is achieved successfully. Table 8.4 discusses the system characteristics of the closed loop DO process behavior under the NLPID1 controller designed by different methods (PP1 and PP2).

Table 8.4: Comparison between the characteristics behavior of the closed loop DO process behavior under the NLPID1 controller parameters designed by the PP1 and PP2 methods

NLPID1	Set-point	Disturbances		Simulink Results				PLC TwinCat Results			
Method		$S_{o,in}$	r_{so}	Time delay [days]	Rise time [days]	Settling time [days]	Steady state error [mg / L]	Time delay [days]	Rise time [days]	Settling time [days]	Steady state error [mg / L]
PP1	2.7	0.01	-294.8954	0.05	0.4	4.4	0.02	0.05	0.4	4.4	0.01
	2.7	0.01	-442.3431	0.05	0.49	4.9	0.05	0.05	0.49	4.9	0.04
	2.7	0.01	-147.4477	0.05	0.4	4	0.01	0.05	0.4	4	0.01
	2	0.8	-294.8954	0.05	0.4	3.5	0.02	0.05	0.4	3.5	0.01
	2	0.8	-442.3431	0.05	0.44	4.2	0.05	0.05	0.44	4.2	0.04
	2	0.8	-147.4477	0.05	0.4	3.4	0.01	0.05	0.4	3.4	0.005
	1.7	0.8	-294.8954	0.05	0.38	3.6	0.02	0.05	0.38	3.6	0.01
	1.7	0.8	-442.3431	0.05	0.4	4	0.05	0.05	0.4	4	0.04
	1.7	0.8	-147.4477	0.05	0.3	3	0.01	0.05	0.3	3	0
PP2	2.7	0.01	-294.8954	0.05	1	3.5	0.02	0.05	0.4	3.5	0.01
	2.7	0.01	-442.3431	0.05	1	4.5	0.04	0.05	0.49	4.5	0.04
	2.7	0.01	-147.4477	0.05	1	3.4	0.02	0.05	0.4	3.4	0
	2	0.8	-294.8954	0.05	0.9	3	0.001	0.05	0.4	3	0.01
	2	0.8	-442.3431	0.05	0.9	3	0.04	0.05	0.44	3.2	0.04
	2	0.8	-147.4477	0.05	0.9	2.8	0.0001	0.05	0.4	2.8	0
	1.7	0.8	-294.8954	0.05	0.9	2.62	0.0005	0.05	0.38	2.6	0.01
	1.7	0.8	-442.3431	0.05	0.9	3	0.04	0.05	0.4	3.2	0.04
	1.7	0.8	-147.4477	0.05	0.9	2.6	0.001	0.05	0.3	2.6	0

The comparison demonstrates that the best real-time control is achieved when the design of the nonlinear controller is done on the bases of the nonlinear model of the process for both simulation environments.

8.6.3.2 Discussion on the real-time simulation results of the closed loop system with the NLPID1 controller when using different set points

The real-time simulation of the closed loop system is done in the Beckhoff CX5020 PLC physical platform with NLPID1 controller designed by two methods: PP1 (Pole placement method for LPID controller design based on the linearized DO model) and PP2 (Pole placement method for NLPID1 controller design based on the nonlinear DO model). Observing from Figure 8.21 up to Figure 8.40, it can be seen that, the PP2 method shows good behavior in a PLC as it did in Matlab/ Simulink environment. The set-point values altered from 2.7, to 2 and to 1.7, but the system response has successfully achieved all the desired behavior under the different process internal disturbances (r_{so} and $s_{o,in}$) in real-time. Therefore, the model transformation is achieved successfully.

8.6.4 Implementation in Real-Time using the NLPID2 controller

The closed loop control system with the nonlinear PID controller (NLPID2) has been successfully transformed to TwinCAT 3 environment through model transformation method, see Figure 8.41. To achieve model transformation of the closed loop system, it is very important to ensure the correctness of the model developed in Simulink environment. In Figure 8.41 the notations are:

- In1 – input of the set-point value
- In2 – feedback input
- In3 – is the input into the process
- Out1 – is the output of the control signal
- Out2 – is the output of the process

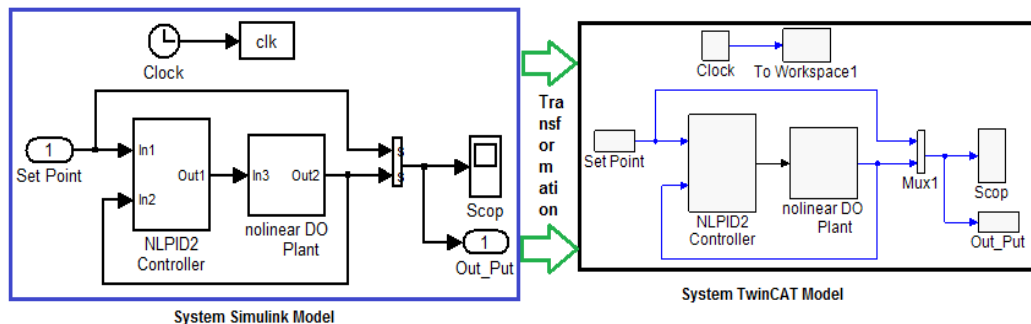


Figure 8.41 Model Transformations for the closed loop system with the NLPID2 controller

The real-time simulation of the closed loop system is performed in CX5020 PLC with different set-point and internal disturbances as shown in Table 8.3.

The real-time simulation results of the closed loop DO process performed in CX5020 PLC under the nonlinear PID2 (NLPID2) designed by different methods are shown in following part.

8.6.4.1 Results from the real-time simulation of the closed loop system with NLPID2 controller

Figure 8.42 to Figure 8.50 show the real-time results of the closed loop DO process behavior under the NLPID2 using the tuned controller parameters obtained by the Pole-Placement (PP1) method for the design of the LPID controller based on the linearized DO model.

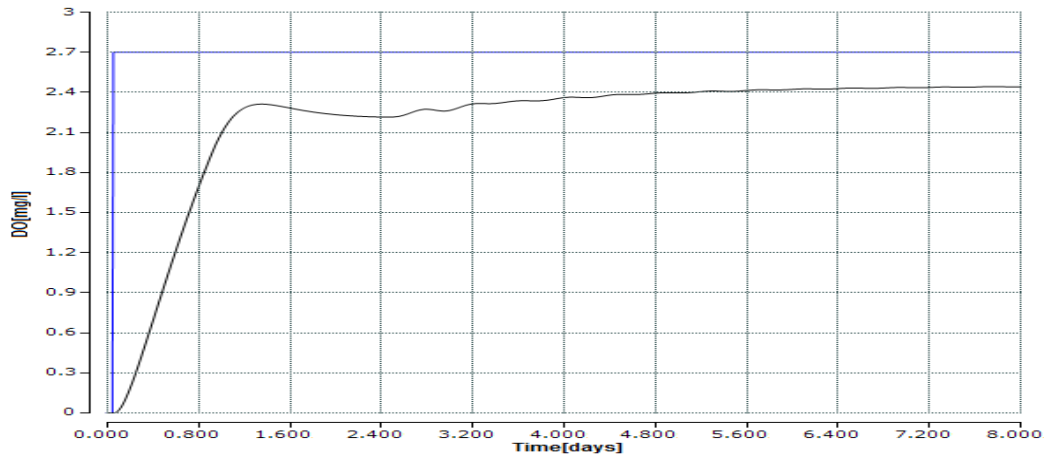


Figure 8.42: PLC Real-time simulation of the closed loop system with the NLPID2 (PP1) controller when the set-point is 2.7 mg/L , $s_{o,in} = 0.01 \text{ mg/L}$ and $r_{so} = -294.8954 \text{ mg/L/day}$

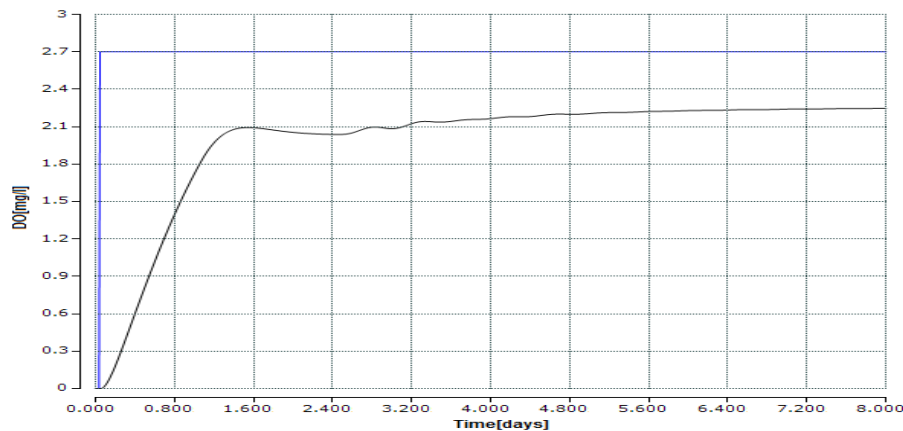


Figure 8.43: PLC Real-time simulation of the closed loop system with the NLPID2 (PP1) controller when the set-point is 2.7 mg/L , $s_{o,in} = 0.01 \text{ mg/L}$ and $r_{so} = -442.3431 \text{ mg/L/day}$

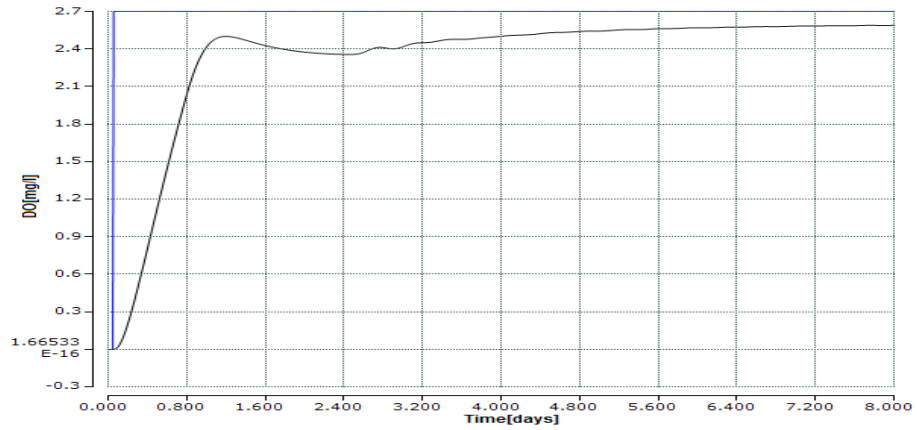


Figure 8.44: PLC Real-time simulation of the closed loop system with the NLPID2 (PP1) controller when the set-point is 2.7 mg/L , $s_{o,in} = 0.1 \text{ mg/L}$ and $r_{so} = -147.4477 \text{ mg/L/day}$

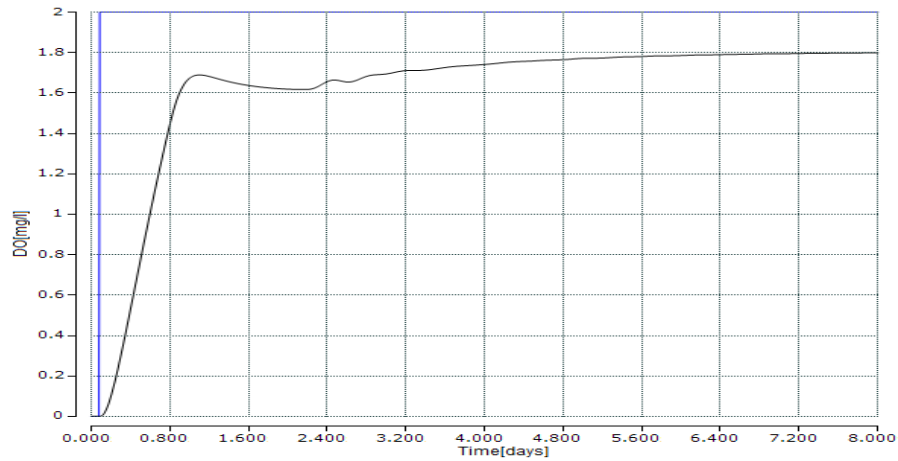


Figure 8.45: PLC Real-time simulation of the closed loop system with the NLPID2 (PP1) controller when the set-point is 2 mg/L , $s_{o,in} = 0.8 \text{ mg/L}$ and $r_{so} = -294.8954 \text{ mg/L/day}$

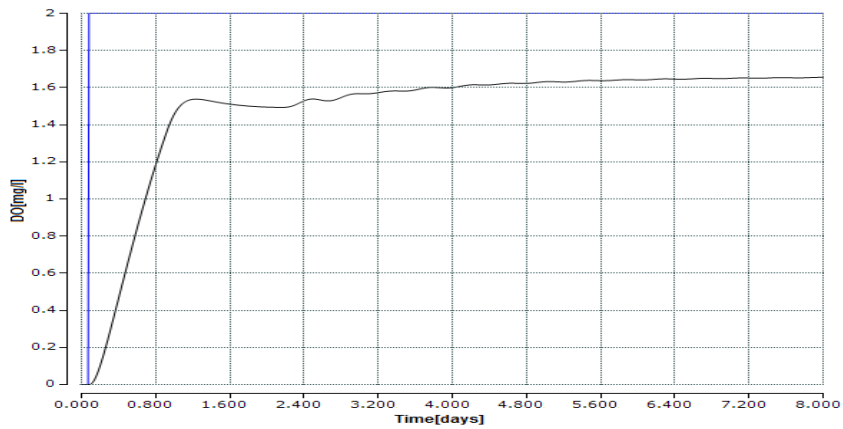


Figure 8.46: PLC Real-time simulation of the closed loop system with the NLPID2 (PP1) controller when the set-point is 2 mg/L , $s_{o,in} = 0.8 \text{ mg/L}$ and $r_{so} = -442.3431 \text{ mg/L/day}$

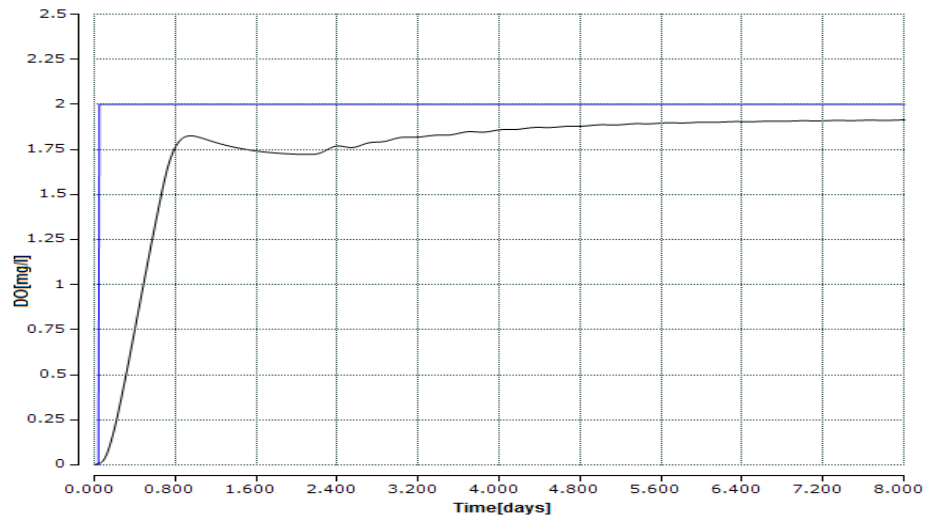


Figure 8.47: PLC Real-time simulation of the closed loop system with the NLPID2 (PP1) controller when the set-point is 2 mg/L , $s_{o,in} = 0.8 \text{ mg/L}$ and $r_{so} = -147.4477 \text{ mg/L/day}$

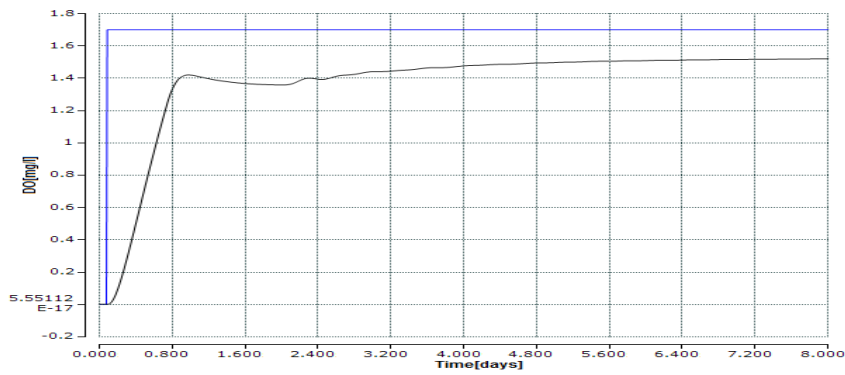


Figure 8.48: PLC Real-time simulation of the closed loop system with the NLPID2 (PP1) controller when the set-point is 1.7 mg/L , $s_{o,in} = 0.8 \text{ mg/L}$ and $r_{so} = -294.8954 \text{ mg/L/day}$

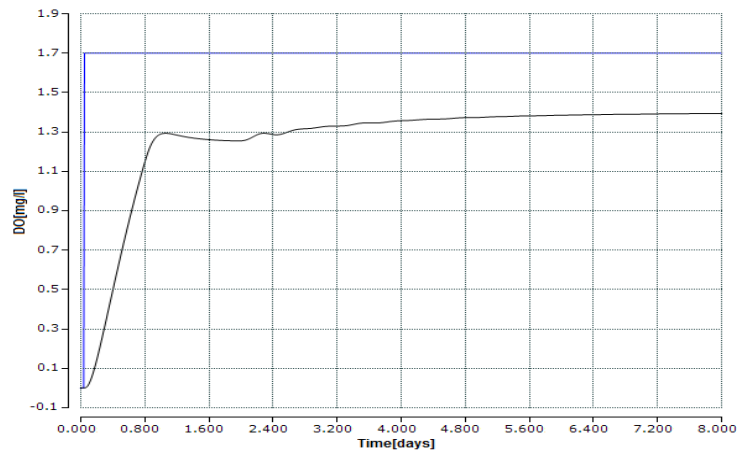


Figure 8.49: PLC Real-time simulation of the closed loop system with the NLPID2 (PP1) controller when the set-point is 1.7 mg/L , $s_{o,in} = 0.8 \text{ mg/L}$ and $r_{so} = -442.3431 \text{ mg/L/day}$

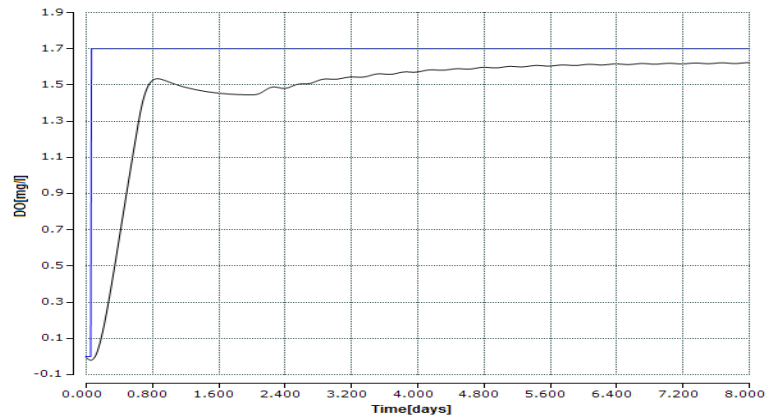


Figure 8.50: PLC Real-time simulation of the closed loop system with the NLPID2 (PP1) controller when the set-point is 1.7 mg/L , $s_{o,in} = 0.8 \text{ mg/L}$ and $r_{so} = -147.4477 \text{ mg/L/day}$

Comparison of the DO process closed loops behavior for the same set point and disturbances between the Matlab/Simulink and TwinCAT 3 platforms is done in Figure 8.51.

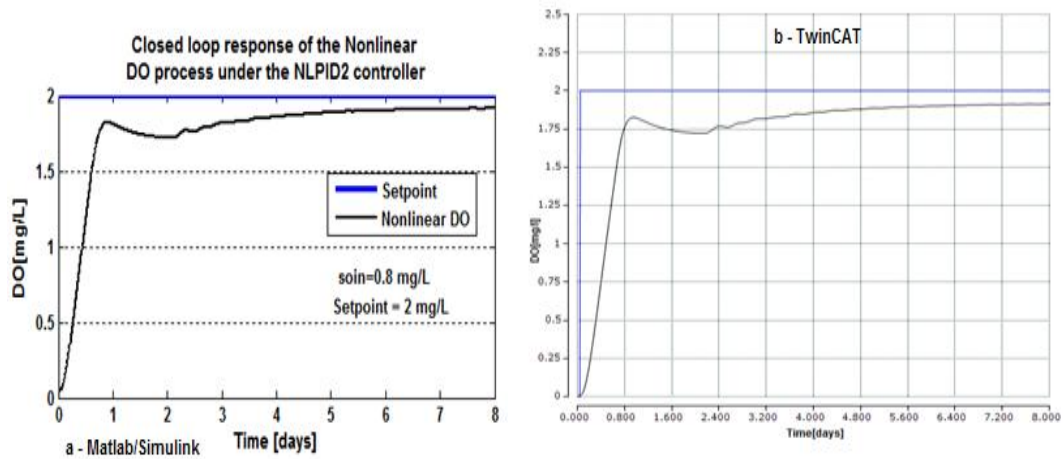


Figure 8.51: Comparison of two trajectories for comparison of the closed loop DO process response under the NLPID2 (PP1) controller, when the set-point is 2 mg/L , $s_{o,in} = 0.8 \text{ mg/L}$ and $r_{so} = -147.4477 \text{ mg/L/day}$ (Figure 8.51a- Simulink results and Figure 8.51b Real-time PLC results)

The comparison of the result from Simulink transformed to TwinCAT 3 environment shows the same behavior in the two platforms.

The real-time results of the DO process under the NLPID2 controller designed by the PP2 method (Pole-Placement method for the design of the NLPID2 controller based on the nonlinear DO model) are shown below, Figure 8.52 up to Figure 8.61 as follows:

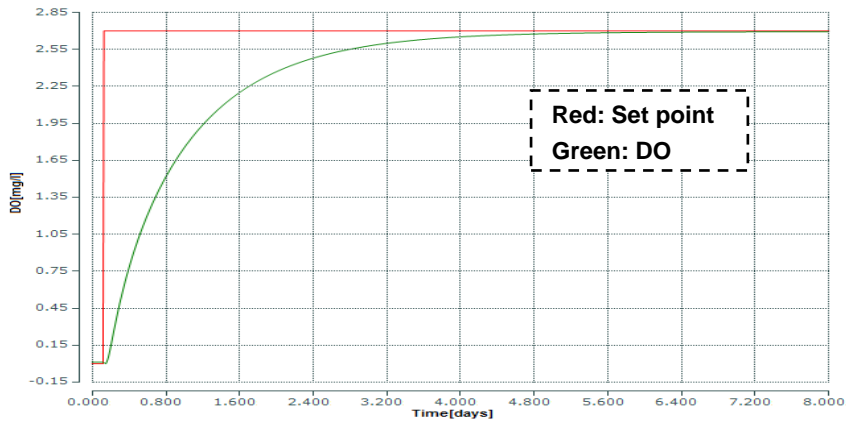


Figure 8.52: Real-time PLC simulation results of the closed loop system with NLPID2 (PP2) controller when the set-point is 2.7 mg/L , $s_{o,in} = 0.01 \text{ mg/L}$ and $r_{so} = -294.8954 \text{ mg/L/day}$

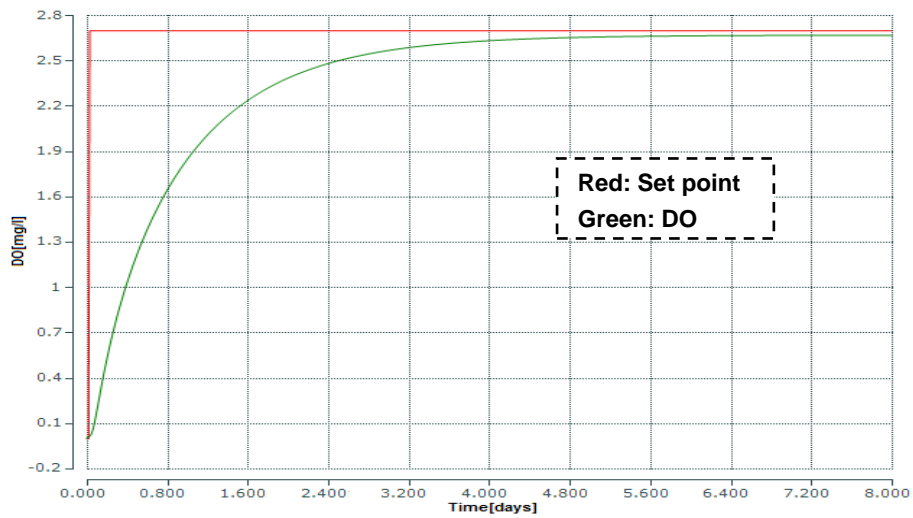


Figure 8.53: Real-time PLC simulation results of the closed loop system with NLPID2 (PP2) controller when the set-point is 2.7 mg/L , $s_{o,in} = 0.01 \text{ mg/L}$ and $r_{so} = -442.3431 \text{ mg/L/day}$

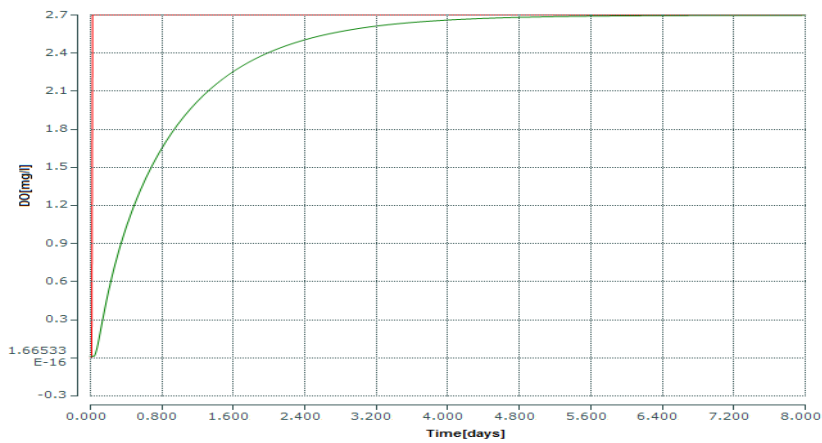


Figure 8.54: Real-time PLC simulation results of the closed loop system with NLPID2 (PP2) controller when the set-point is 2.7 mg/L , $s_{o,in} = 0.01 \text{ mg/L}$ and $r_{so} = -147.4477 \text{ mg/L/day}$

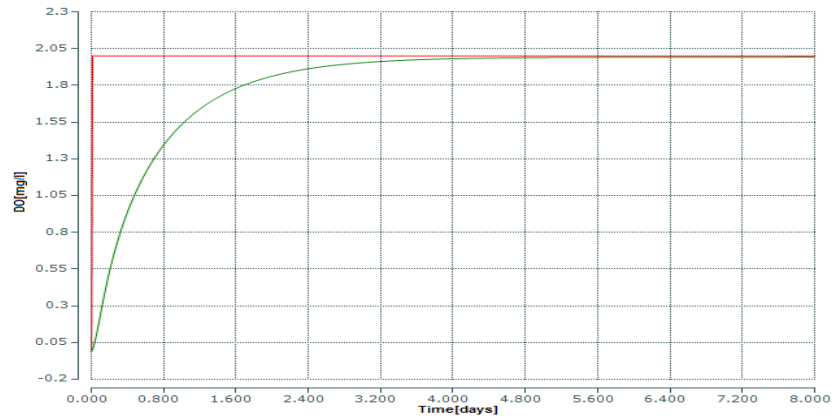


Figure 8.55: Real-time PLC simulation results of the closed loop system with NLPID2 (PP2) controller when the set-point is 2 mg/L , $s_{o,in}=0.8 \text{ mg/L}$ and $r_{so}=-294.8954 \text{ mg/L/day}$

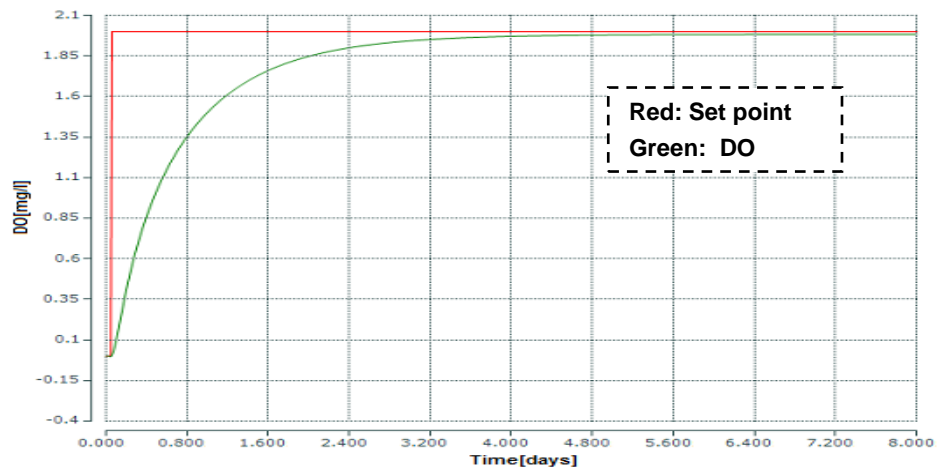


Figure 8.56: Real-time PLC simulation results of the closed loop system with NLPID2 (PP2) controller when the set-point is 2 mg/L , $s_{o,in}=0.8 \text{ mg/L}$ and $r_{so}=-442.3431 \text{ mg/L/day}$

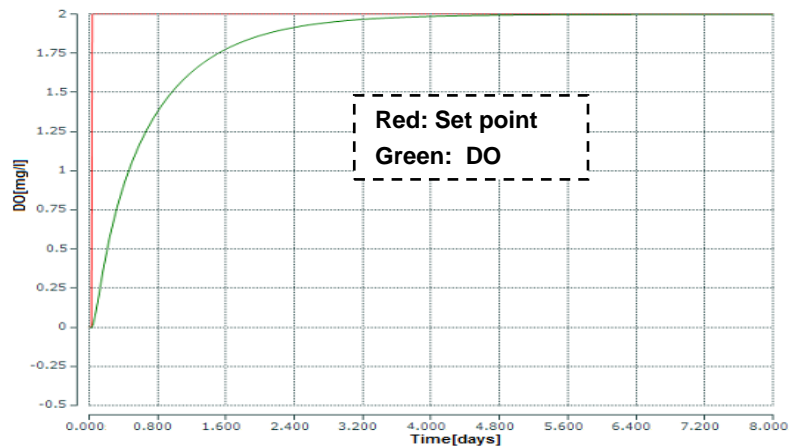


Figure 8.57: TwinCat 3 Real-time simulation of the closed loop DO process response under the NLPID2 controller, when the set-point is 2 mg/L and $r_{so}=-147.4477 \text{ mg/L}$

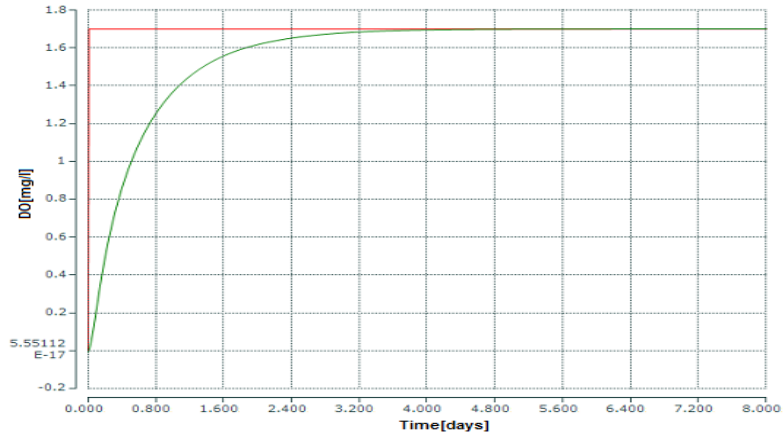


Figure 8.58: Real-time PLC simulation results of the closed loop system with NLPID2 (PP2) controller when the set-point is 1.7 mg/L , $s_{o,in} = 0.8 \text{ mg/L}$ and $r_{so} = -294.8954 \text{ mg/L/day}$

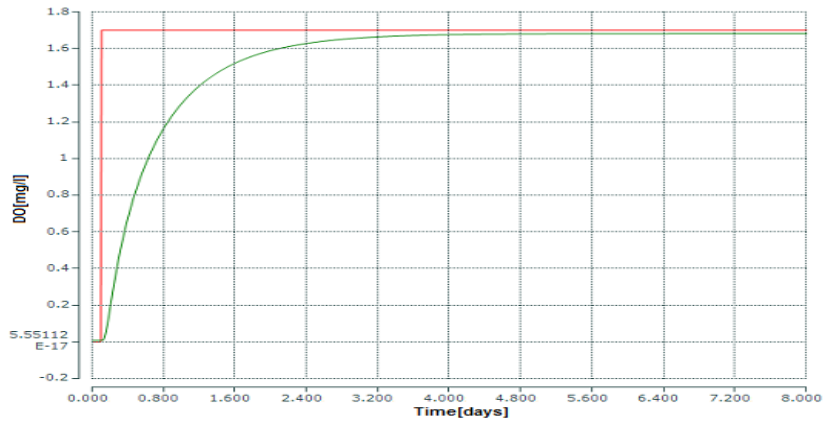


Figure 8.59: Real-time PLC simulation results of the closed loop system with NLPID2 (PP2) controller when the set-point is 1.7 mg/L , $s_{o,in} = 0.8 \text{ mg/L}$ and $r_{so} = -442.3431 \text{ mg/L/day}$

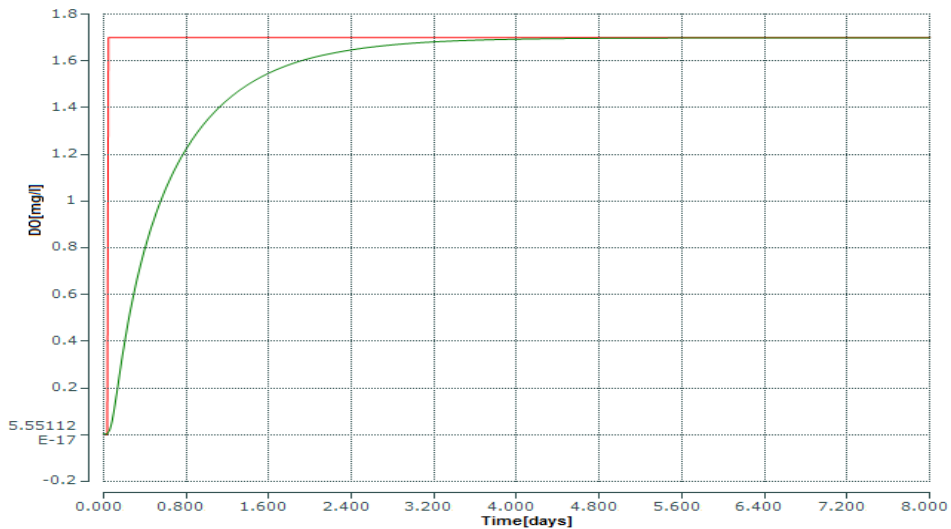


Figure 8.60: Real-time PLC simulation results of the closed loop system with NLPID2 (PP2) controller when the set-point is 1.7 mg/L , $s_{o,in} = 0.8 \text{ mg/L}$ and $r_{so} = -147.4477 \text{ mg/L/day}$

Figure 8.61 shows the comparison between the closed loop DO process trajectories for the same set point and disturbance. Again the behavior is the same on both platforms.

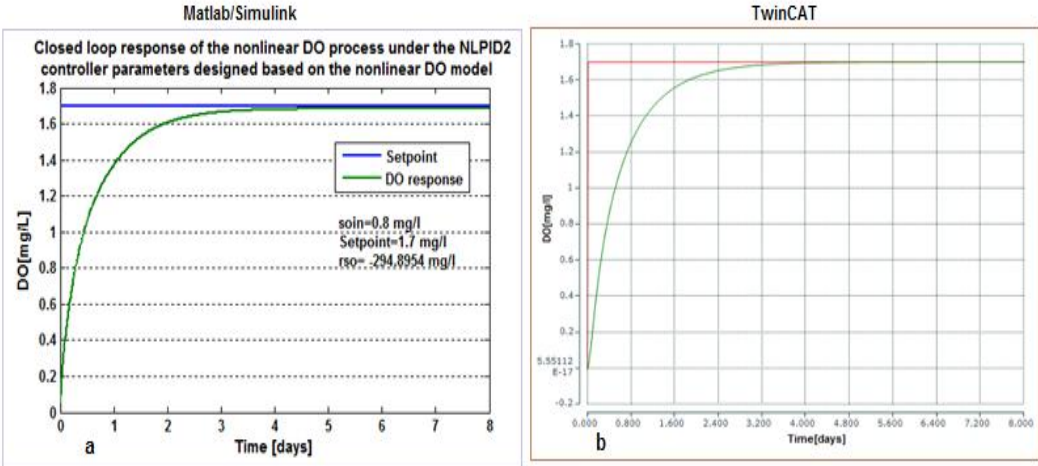


Figure 8.61: Comparison of two trajectories of the closed loop DO process response under the NLPID2 (PP2) controller, when the set-point is $1.7 \text{ mg} / \text{L}$, $s_{o,in} = 0.8 \text{ mg} / \text{L}$ and $r_{so} = -294.8954 \text{ mg} / \text{L} / \text{day}$ (Figure 8.61a- Simulink and Figure 8.61b- Real-time PLC)

The following Table 8.5 shows the real-time comparison based on the NLPID2 designed by the two different methods.

Table 8.5: Comparison between the DO processes characteristics behaviour obtained under the NLPID2 controller parameters designed by the PP1 and PP2 methods

NLPID2	Set-point	Disturbances		Simulink Results				TwinCat Results			
Method		$s_{o,in}$ [mg / L]	r_{so} [mg / L / day]	Time delay [days]	Rise time [days]	Settling time [days]	Steady state error [mg / L]	Time delay [days]	Rise time [days]	Settling time [days]	Steady state error [mg / L]
PP1	2.7	0.01	-294.8954	0.1	0.5	4.2	0.25	0.05	0.4	4.4	0.26
	2.7	0.01	-442.3431	0.1	0.5	4.5	0.45	0.05	0.49	4.9	0.45
	2.7	0.01	-147.4477	0.1	0.4	4	0.1	0.05	0.4	4	0.1
	2	0.8	-294.8954	0.1	0.5	4.1	0.2	0.05	0.4	3.5	0.2
	2	0.8	-442.3431	0.1	0.5	4.3	0.34	0.05	0.44	4.2	0.34
	2	0.8	-147.4477	0.1	0.4	4	0.1	0.05	0.4	3.4	0.1
	1.7	0.8	-294.8954	0.1	0.5	4	0.18	0.05	0.38	3.6	0.18
	1.7	0.8	-442.3431	0.1	0.5	4.2	0.305	0.05	0.4	4	0.3
	1.7	0.8	-147.4477	0.1	0.4	3.7	0.08	0.05	0.3	3	0.08
PP2	2.7	0.01	-294.8954	0.05	0.5	3.5	0.02	0.05	0.5	3.6	0.02
	2.7	0.01	-442.3431	0.05	0.5	4.4	0.04	0.05	0.5	4.4	0.04
	2.7	0.01	-147.4477	0.05	0.5	3.5	0.02	0.05	0.5	3.5	0.01
	2	0.8	-294.8954	0.05	0.5	3	0.001	0.05	0.5	3	0.001
	2	0.8	-442.3431	0.05	0.5	3	0.04	0.05	0.5	3	0.04
	2	0.8	-147.4477	0.05	0.5	2.8	0.0005	0.05	0.5	2.8	0.001
	1.7	0.8	-294.8954	0.05	0.5	2.8	0.001	0.05	0.5	2.8	0.001
	1.7	0.8	-442.3431	0.05	0.5	3	0.04	0.05	0.5	3	0.04
	1.7	0.8	-147.4477	0.05	0.5	2.7	0.0005	0.05	0.5	2.7	0

8.6.4.2 Discussion on the real-time simulation results of the closed loop system using the NLPID2 controller designed by the two design methods for different set point values

The real-time performance of the closed loop DO system is found to be the same as in Simulink, and then the conclusion can be drawn that the model implementation of the CX5020 PLC and its real-time simulation can be achieved successfully through the model transformation technique.

Figure 8.42 up to Figure 8.61 show PLC real-time simulation results of how the system responds in the CX 5020 Beckhoff PLC, under the same NLPID2 controller designed by the two design methods. On the basis of these methods the conclusion can be taken that the best real-time control is achieved when the design of the nonlinear controller is done on the basis of the nonlinear model of the process, this means PP2 control design performs very well in controlling the nonlinear DO process model. The steady state error when using the PP1 method is much bigger than the one when using the PP2 method.

8.7 Complete Result Discussion

The closed loop systems that are controlled by the controllers designed by the two (PP1 and PP2) methods are deployed on the Beckhoff PLC CX5020 physical platform and TwinCAT 3 real-time implementation software. As the different controller design methods are used, the results show that the best DO process control is achieved when the design of the nonlinear controller is done on the bases of the nonlinear model of the process, since it does not require any flexible and influential tuning in order to obtain good results for the plant. The Beckhoff PLC CX5020 platform is needed to cope with the increasing complexity of the industrial systems and it is built according to the new industrial standard.

The PLC CX5020 implementation results obtained in TwinCat 3 real-time environment are the same as the results obtained in Matlab/Simulink, this has let us come to conclusion that the Beckhoff PLC CX5020 which supports the IEC 61499 standard, has been the best platform in this thesis to accommodate the real-time simulation of the nonlinear control algorithms with the nonlinear plant.

8.8 Conclusion

The Beckhoff CX5020 PLC is used for the real-time simulation and comparison of the findings of the thesis. The CX5020 is used in conjunction with the TwinCAT 3 software from Beckhoff and offers the same functionalities as large industrial personal computers (PCs). This chapter has discussed a basic introduction of PLCs, TwinCAT 3 software; Beckhoff CX50x0 PLC and the model transformation technique to achieve real-time implementation of the closed loop Dissolved Oxygen (DO) system. As the nonlinear PID controllers and the DO system are implemented in the Beckhoff PLC (CX5020), the real-time implementation results are picked up, and plotted in TwinCAT 3 software. The real-time closed loop implementation results with both controllers (NLPID1 and NLPID2) show that the output of the DO process can be controlled to a desired value through a NLPID controller design based on the nonlinear model of the process to be controlled.

In the next chapter (Chapter 9) the findings of the thesis are outlined.

CHAPTER NINE

CONCLUSION AND FUTURE RECOMMENDATION

9.1 Introduction

This research project is motivated by the shortage of the existing controller design methods for general nonlinear processes and the difficulty of designing and implementing nonlinear model-based controller design. Investigation in nonlinear control is also motivated by the naturally nonlinear characteristics of the dynamic systems to be controlled. The reality says; many practical systems are significantly nonlinear in nature, so the important features of their performance may be completely overlooked if they are analyzed and designed through linear control techniques.

Effective control of nonlinear systems requires robust methods to accommodate system uncertainties and harsh environments. Wastewater Treatment Plants (WWTPs) are such nonlinear systems with complex multivariable processes which require effective control because of the increased requirements on the quality of the effluent concentrations imposed on the plants. There is a rising interest in research activities relating to finding better ways of controlling the WWTPs. The process of the Dissolved Oxygen (DO) concentration is chosen in the thesis to be controlled, because it has the potential to influence the behavior of the Activated Sludge Processes (ASP) as well as to ensure that the operational cost can be minimized.

Methods for the design of nonlinear PID controllers for the DO process concentration in the ASP are developed in the thesis. This Chapter describes the deliverables of the thesis, their applications and the future research in the field, as follows: Part 9.2 states the aim and objectives of the thesis, part 9.3 describes thesis deliverables, discussion of the importance of the thesis deliverables is given in part 9.4, part 9.5 describes the possible applications of the thesis results, the recommendation for future research are given in part 9.6, the publications on the thesis development are listed in part 9.7 and the conclusion is done in part 9.8.

9.2 Aims and Objectives:

Based on the statement of the problem, the thesis aim and objectives have been developed. The thesis aim is to develop methods for design of linear and nonlinear

controllers of the concentration of the DO process in the aeration tank of the ASP and to implement the designed controllers in the frameworks of Beckhoff CX5020 PLC, TwinCAT software environment and MATLAB/SIMULINK software. The objectives are as follows:

1. Evaluation of the literature for modeling and control of DO concentration.
2. Development of a model of the DO concentration process in the ASP and its simulation in Matlab/Simulink environment.
3. Investigation and development of the structure of nonlinear PID controllers for the purpose of the research study.
4. Development of a method for design of a linear PID (LPID) controller of the DO concentration process based on Ziegler-Nichols approach and applied to the nonlinear model of the DO process
5. Development of a method for design of Nonlinear PID (NLPID) controller of the DO process using Pole-Placement (PP1) method for design of LPID controller based on the linearized DO process model.
6. Development of a method for design of the LPID controller of the DO process using Pole-Placement method for design of LPID controller based on the nonlinear DO process model.
7. Development of a method for design of the NLPID controllers of the DO process using Pole-Placement (PP2) method for design of NLPID controller based on the nonlinear DO process model.
8. Development of the simulation models of the closed loop systems consisting of the developed controllers and nonlinear DO process model in Matlab/Simulink.
9. Implementation of the NLPID controllers in Beckhoff PLC (using IEC61499 standard approach) using a model transformation technique.
10. Real-time simulation of the closed loop system.

9.3 Thesis deliverables

The need for controlling and monitoring of the ASP has been emphasized in Chapter One. Therefore, the deliverables of this project are based on the aim and objectives as highlighted above. The initial step involved a review of the activated sludge process as an object of control. The different control approaches with different control variables were investigated and compared to each other.

The different control strategies available in the literature are discussed in Chapter two. MATLAB/Simulink is selected as a simulation environment to test the closed loop system

under the selected controllers, because it follows the principles of functional block programming, and the model transformation method. Model transformation automatically translates each state flow block into customized basic IEC 61499 function blocks with exactly, the same inputs, outputs and parameters as their Simulink counterparts.

9.3.1 Modeling and Simulation

The nonlinear mathematical model of the DO concentration process has been developed in Chapter 3. The oxygen transfer function is represented as a function of the control input to the process. The process open loop response of the DO concentration is simulated in Matlab/Simulink software environment in order to obtain the DO process trajectories; this is done in order to obtain the data for the controller design and development. The developed model is documented in Chapter 3.

9.3.2 Review of control theory for the design of nonlinear controllers

Chapter 4 gives a short overview of the linear and nonlinear control theory background. This chapter provides also the background for the design of the nonlinear PID controllers.

9.3.3 Controller Design and Implementation

As a practical, accurate mathematical model of the process has been tested through simulation and the problem now was how to make use of this model to find out what typical control actions, can be used to make the process of DO to operate according to the desired requirements. Chapter 5, 6 and 7 describe the design methods developed and used to control the DO process concentration. The type of control that is convenient for nonlinear systems is the nonlinear control; three methods were used and developed to design the nonlinear controllers in the thesis. The deliverables are:

9.3.3.1 The Ziegler-Nichols method for design of the LPID controller

The Ziegler-Nichols step response method is used to design the controller parameter of the LPID controller. The obtained values of the LPID controller parameters are used directly as the values of the parameters on the NLPID controllers and simulations of the closed loop system are performed. The results show that additional tuning is necessary to be performed for the NLPID controllers. The closed loop system with the tuned NLPID parameters is simulated under various values of the process set point and the process internal disturbances.

9.3.3.2 Pole Placement method for the design of the LPID controller based on the linearized DO model.

This method is named as a PP1 controller design method based on the linearized DO process model. The pole placement method is applied to the linearized DO model of the DO process to design the parameters of the linear PID controller. The obtained values of the LPID controller parameters are directly used as the value of the parameters of the NLPID controllers and simulations of the closed loop system are performed. The results show that additional tuning is necessary to be performed for the NLPID controllers. The closed loop system with the tuned NLPID parameters is simulated under various values of the process set point and the process internal disturbances.

9.3.3.3 Novel Pole Placement based method for direct design of the parameters of the LPID and NLPID parameters are unknown

This is called as a PP2 controller design method. The approach of the Pole Placement is applied directly to the nonlinear equation of the closed loop system. Then solution of this nonlinear differential equation according to the controller parameters in the case of known values of the process state determines the solution of the controller design problem. The controller parameters are obtained for every value of the DO concentration open loop trajectory and after some simulations of the closed loop system with the obtained parameters, the best one are selected. They are used to investigate the behavior of the closed loop DO process under different set point and internal process disturbances.

The new method determines the optimal values of the linear and nonlinear PID controllers. No additional tuning is needed.

9.3.4 Matlab codes for Simulation

The methods developed for simulation of the DO model as well as for the controller parameters design are implemented in the Matlab simulation environment. The software programs developed in MATLAB for the above-mentioned thesis deliverables are shown in Table 9.1. The corresponding Simulink models are shown in Table 9.2.

Table 9.1: Matlab script file developed

Matlab script file name	Function	Simulink model developed
DO_last.m	Script file for simulation of the DO process using	DO_model.mdl

	ASM1 biological model parameters	
LPID_DO.m	Script file for simulation of the closed loop DO process under the LPID controller.	LPIDwithDO.mdl
NLPID1withDOzn.m	Script file for simulation of the closed loop DO process using ASM1 biological model parameters under the NLPID1 controller based on Ziegler-Nichols tuning method.	nlpid1_DOmodelzn.mdl
NLPID1pp1withDOpar.m	Script file for simulation of the DO closed loop process using ASM1 biological model parameters with the NLPID1 controller based on Pole-Placement (PP1) method for design of LPID controller based on the linearized DO model.	"nlpid1_DOmodelpp1.mdl"
"myfun1".	This file is used to solve for unknown control parameters in Equation 7.9, following the design procedure in Figure 7.1.	
"Findnlpid1par_PP2.m"	This is a script file used to call myfun1, which will work with the DO process to find suitable controller parameters for the NLPID1 controller to control the DO process.	
nlpid1_DOmodelpp2.m	Script file for simulation of the DO closed loop system with NLPID1 based on PP2 method.	"nlpid1_DOmodelpp2.mdl"
NLPID2znwithDO.m	This program contains parameters for simulation of the DO process closed loop behavior under the NLPID2 controller. The model "NLPID2zn_DO.mdl" has been built in Simulink. The plant parameters are those one of the DO process as taken from ASM1 biological model no.1	"NLPID2zn_DO.mdl"
"NLPID2pp1withDO.m"	Script file for simulation of the closed loop DO process behavior under the NLPID2 controller based on Pole-Placement method for design of the LPID controller for the linearized model of the DO process (PP1 method).	"NLPID2pp1_DO.mdl"
"myfun2".	This file is used to solve for unknown control parameters in Equation 7.12, following the design procedure in Figure 7.1.	
"findnlpid2par.m"	This is a script file used to call myfun1, which will work with the DO process to find suitable controller parameters for the NLPID1 controller to control the DO process.	
"NLPID2DOpp2.m"	Script file for simulation of the closed loop DO process behavior under the NLPID2 controller built on Pole-Placement method for design of the NLPID for the nonlinear DO model (PP2 method).	"NLPID2pp2DO.mdl"

Table 9.2: Simulink Models

Simulink model developed	Description
DO_model.mdl	This Simulink model is the open loop nonlinear DO process.
LPIDwithDO.mdl	This is the closed loop Simulink model of the nonlinear DO process under the LPID controller.
nlpid1_DOmodelzn.mdl	This is the closed loop Simulink model of the nonlinear DO process under the NLPID1 controller that uses the tuned control parameters from Ziegler-Nichols method design for LPID controller.
“nlpid1_DOmodelpp1.mdl”	Simulink model that contains the NLPID1 controller, which is applied to control the process model of dissolved oxygen.
“nlpid1_DOmodelpp2.mdl”	Closed loop Simulink model of the nonlinear DO process under the NLPID1 controller design based on the PP2 method
“NLPID2zn_DO.mdl”	This is the closed loop Simulink model of the nonlinear DO process under the NLPID2 controller.
“NLPID2pp1_DO.mdl”	This is the closed loop Simulink model of the nonlinear DO process under the NLPID2 controller design based on the PP1 method.
“NLPID2pp2_DO.mdl”	This is the closed loop Simulink model of the nonlinear DO process under the NLPID2 controller design based on the PP2 method.

9.3.5 Real-Time simulation of the closed loop system models

Models of the closed loop system were developed in the MATLAB/Simulink software environment based on the control algorithms and the Simulation block diagram developed and shown in Chapter 5, Chapter 6, and Chapter 7. Then these models are transformed using model transformation technique from Simulink to TwinCAT 3 software environment of the Beckhoff PLC CX5020. Model transformation technique keeps the same data and parameter connections in order for Simulink and TwinCAT 3 to produce the same output data; the wrong mapping of the data type will make the algorithm computation to perform incorrectly. These two software environments (Simulink and TwinCAT 3) have their own basic data type defined. The transformed models to TwinCAT 3 environment are illustrated in the following Table 9.3:

Table 9.3: TwinCAT 3 Environment Models

Models in TwinCAT 3	Description
nlpid1_DOpp1	This model was transformed to TwinCAT for the

	real-time simulation of the DO model under the NLPID1 controller designed based on the PP1 method.
nlpid1_DOpp2	This model is deployed into a PLC for a real-time simulation. This is done in order to view the performances of the closed loop system implemented in a framework of the PLC, the result are viewed in TwinCAT software environment.
NLPID2pp1_DO	This model is transformed to TwinCAT for the real-time simulation of the DO model under the NLPID2 controller designed based on the PP1 method. Through TwinCAT the system was varied between different set point and disturbance values.
NLPID2pp2DO	This is the closed loop DO model under NLPID2. It was deployed into a PLC for a real-time simulation. This was performed in order to make an examination of how is the nonlinear process would perform under the framework of the PLC, the result are shown in TwinCAT 3 software environment.

9.4 Importance of the deliverables

Linear PID and the two nonlinear PID controllers were designed and investigated by off-line and real-time simulation. The two nonlinear controllers designed are also compared, in order to achieve a system that can have a reliable control performance.

Through Matlab/Simulink it is also proven that the parameters as designed for the linear PID controller cannot be directly used in the nonlinear PID controllers to control the DO process, and adjustments are needed to be made in order to succeed in controlling the DO process.

Simulation results confirm that the NLPID control algorithm can enhance the damping features and stabilize the system under different set-points, and disturbances.

The advantage of using a controller that can control the plant under different operation conditions and changing set-points is that only the needed energy is used. A controller that works well only under one operating condition and one DO set point and cannot handle changed disturbances can lead to energy loss, because the process can be supplied with control action which is not required.

The Beckhoff PLC CX5020 is a reliable platform and it is built according to the new industrial standard IEC 61499. The Real-Time implementation results also show that the Dissolved Oxygen is controlled very well under the developed two NLPID control algorithms which are capable to control the dissolved oxygen concentration for different operating conditions with almost zero steady state error.

9.5 Application of the nonlinear PID controllers

The following applications are considered:

- In nonlinear frameworks, where NLPID control is utilized for accommodation of any system nonlinearity and is used to accomplish steady reaction over a some different scope of conditions
- In linear systems, where nonlinear PID control is utilized to attain execution not achievable by a direct PID control, for example, expanded damping, reduced rise time for step or quick inputs, enhanced tracking accuracy, and contact remuneration.
- The main algorithm of the NLPID controller is formed based on a nonlinear function and is an inherent part of the controller. The fundamental objective is to accomplish a desired reaction in the output of the plant when traditional PID could not achieve it.

9.6 Application of the thesis results

The developed models, nonlinear PID algorithms and PLC software serve for the following:

- Understanding: Gives insight into the wastewater treatment processes and how suitable mathematical models are derived.
- Industrial applications: This investigation presents a solution to the problem of tuning NLPID controllers for a nonlinear system. Many systems in industrial applications use LPID controllers. A conventional PID controller works in linear systems and is less effective when the plant is nonlinear because the linear PID controllers cannot adapt the gain parameters as needed.

Education and training: Operators are not continuously sufficiently trained to operate advanced control equipment and many environmental engineers would require more basic understanding of the system dynamics and control so as to appreciate the potential of instrumentation, control and automation.

- PLC and visualization: The CX5020 offers the same functionality as the large Industrial PCs. In terms of PLC, up to four virtual IEC 61131 CPUs can be programmed with up to four tasks each, with a minimum cycle time of 50 μ s. All IEC 61131-3 languages can be used. In addition to real-time execution of control the tasks, the TwinCAT real-time seed ensures that enough time remains for the user

interface (HMI), to communicate with the real-time components via software interfaces.

9.7 Future recommendation

The next study is to apply the developed methods to a pilot plant. This will involve online estimation of the parameters. It will be interesting to see how quickly the system keeps up with the delays, disturbances and set point changes on a real ASP plant. The topic for future research can be on real-time implementation of NLPID controllers to control the DO process using any of the software that can support IEC 61499 standard, TwinCAT 3, NXT, FBDK or ISaGRAF and with Beckhoff PLC CX5020 to control the nonlinear process.

9.8 Publication

Tshemese, N., and Tzoneva, R. 2014. Design and real-time PLC simulation of the linear and nonlinear PID controllers for nonlinear dissolved oxygen process. The paper is sent to the European Journal of Control.

9.9 Conclusion

This chapter describes the aim and objectives of the thesis and gives the direction for the thesis deliverables for the methods and algorithms developed, together with software programs written. The application of the thesis results and the future research direction are outlined.

BIBLIOGRAPHY

- Abdelhadi, A., Gomm, J.B., Yu, D. & Rajarathinam, K. 2014. Nonlinear system identification and control of a pH process using Local Linear Model Networks strategy. In Automation and Computing (ICAC), 2014 20th International Conference on. IEEE: 254–259.
- Ali Bozorgmehr, Kaveh Kianfar and Reza Amiri., 2011. Designing the Non-Linear PID Controller for a Missile. Bandung, Indonesia, pp171-175.
- Amunrud, A. 2002. Programmable Logic Controllers. EE, paper 1, February 27.
- Audun Faanes, 2003. Controllability Analysis for Process and Control System Design. Department of Chemical Engineering Norwegian University of Science and Technology.
- Alex, J., Benedetti, L., Copp, J., Gernaey, K.V., Jeppsson, U., Nopens, I., Pons, M.N., Rieger, L., Rosen, C., Steyer, J.P., Vanrolleghem, P., and Winkler, S. 2008. Benchmark Simulation Model no. 1 (BSM1). Dept. of Industrial Electrical Engineering and Automation, Lund University
- Astrom, Karl J. Hagglund, T. 1995. Automatic Tuning of PID Controllers. Chapter 52, *The Control Handbook*, IEEE/CRC Press, William S. Levine ed.
- Atherton, Derek P., 1996. Early Developments in Nonlinear Control. IEEE Control Systems.
- Aydogdu, O and Korkmaz, M. 2011. A Simple Approach to Design of Variable Parameter Nonlinear PID Controller. *IPCSIT vol.20, pp 81-85, IACSIT Press, Singapore. International Conference on Advancements in Information Technology With workshop of ICBMG*
- Panagopoulos, H., Astrom, Karl J. Hagglund, T. 2002. Design of PID controllers based on constrained optimisation. IEE Process Control Theory Application, Vol. 149, No.1, pp 32-40.
- Anthony S. McCormack and Keith R. Godfrey, 1998. Rule-Based Autotuning Based on Frequency Domain Identification. IEEE Transactions on Control Systems Technology, Vol 6 no 1, January, pp 43-61.
- Barbu, M., Caraman, S., and Ceanga, E. 2005. Robust multi-model control using QFT techniques of a Wastewater treatment process. Control Engineering and Applied Informatics. CEAI, Vol. 7, No. 2, pp. 10-17.
- Bayrak, G., Murr, P.J., Ulewicz, S., Vogel-Heuser, B. 2012. Comparison of a transformed Matlab/Simulink model into the programming language CFC on different IEC 61131-3 PLC environments. IEEE. Boltzmannstrae 15, D-85748 Garching
- Brian, R. Copeland, 2008. The Design of PID Controllers using Ziegler Nichols Tuning. The Department of Electrical & Computer Engineering, University of the West Indies, March, pp 1-4.
- Bushnell, Linda G., 1996. On the History of Control. IEEE Control Systems.
- Chanin, P., 2005. Model-Based Controller Design for General Nonlinear Processes. Ph.D. Thesis, September

Caraman S., Sbarciog M and Barbu M. 2007. Predictive Control of a Wastewater Treatment Process. *International Journal of Computers Communications & Control*, ISSN 1841-9836, 2(2):132-142.

Chang, WD., and Yan, JJ. 2005. Adaptive robust PID controller design based on a sliding mode for uncertain chaotic systems. *Chaos, Solitons and Fractals* 26, pp 167-175, Journal – Elsevier. Available online at www.sciencedirect.com.

John, B. Copp. 1998, European Cooperation in the field of Scientific and Technical Research. Action 682. www.cs.mcgill.ca/~hv/articles/WWTP/

Copp, J.B. (editor). 2002. The cost simulation benchmark: description and simulator manual. ISBN 92-894-1658-0, Official Publications of the European Communities, Luxembourg. European Cooperation in the field of Scientific and Technical Research. Action 682

Copp, J.B., Jeppsson, U., and Vanrolleghem, P.A. 2008. The Benchmark Simulation model – A Valuable Collection of Modelling Tools. International Congress on Environmental Modelling and Software Integrating Science and Information Technology for Environmental Assessment and Decision Making., <http://www.iemss.org/iemss2008>

Dai, W.W. & Vyatkin, V. 2010. Redesign distributed IEC 61131-3 PLC system in IEC 61499 function blocks. In *ETFA*. 1–8.

Esfahani, P. M., Karimi-Ghartemani, M., 2008. A Suboptimal Controller Design Methodology for Input-Output Feedback-Linearizable Systems. Proceedings of the 17th World Congress, the International Federation of Automatic Control, Seoul, Korea, July 6-11.

Ender, D.B. 2001, "Special nonlinear PID Controllers", Application Manual, ch.6.

Fall, .2006. Basics of PLC Programming. MME 486

Feng, W., O'Reilly, J., and Ballance D.J. 2002. MIMO nonlinear PID predictive controller. *IEE Process Control Theory Application*.,Vol. 149, No. 3., pp 203-208.

Ferrer, J. Rodrigo, M. A. Seco, A. Penya-roja, J. M. 1998. Energy saving in the aeration process by fuzzy logic control, *Wat. Sci. Tech.* 38 (3) 209-217.

Fikar, M., Chachuat, B., and Latifi, M.A. 2005. Optimal operation of alternating activated sludge processes. *Control Engineering Practice* 13, pp 853-861. Available online at www.sciencedirect.com.

Gambier, Adrian. 2008. MPC and PID Control Based on Multi-objective Optimization. American Control Conference Westin Seattle Hotel, Seattle, Washington, USA June 11-13,

Glad, T., and Ljung, L. 2000. *Control Theory Multivariable and Nonlinear Methods*. 11 New Fetter Lane, London EC4P 4EE, Taylor and Francis.

Gao, Z. 2002. From linear to nonlinear control means: A practical progression. *ISA Transactions* 41, pp 177-189.

Gaonkar, P., Kande, M. 2014. Challenges and Opportunities of Automation System for Water and Waste

Water Applications. IEEE International Conference on Industrial Technology (ICIT), Feb. 26 – Mar. 1, Busan, Korea

GE, S., PENG, Y., LU, C., WANG, S. 2012. Practical consideration for design and optimization of the step feed process. *Front. Environ. Sci. Eng.* DOI 10.1007/s11783-012-0454-3. Higher Education Press and Springer-Verlag Berlin Heidelberg, pp 1-8.

Grigorieva, E.V., Khailov, E.N. 2010. Optimal control of a Wastewater cleaning plant. UAB Conference on Differential Equations and Computational Simulations. *Electronic Journal of Differential Equations*, Conf. 19, pp. 161–175. ISSN: 1072-6691. URL: <http://ejde.math.txstate.edu> or <http://ejde.math.unt.edu>

Hai-bin, D., Dao-bo, W., and Xiu-fen, Y. 2006. Novel Approach to nonlinear PID parameter optimization using Ant Colony Optimization Algorithm. *Journal of Bionic Engineering* 3, Vol.3 No.2. pp 73-78.

Henze, M., P. Harremoës, J. la Cour Jansen and E. Arvin (1995a). *Wastewater treatment, biological and chemical processes*. Springer-Verlag Berlin Heidelberg, Germany.

Henze, M., W. Gujer, T. Mino, T. Matsuo, M. C. Wentzel and G. v. R. Marais (1995b). *Activated sludge model no. 2*. Scientific and Technical Report No. 3. IAWQ, London, Great Britain.

Holenda, B., Domokos, E., Rédey, Á. And Fazakas, J. 2007, Dissolved oxygen control of the activated sludge wastewater treatment process using model predictive control. *Computers & Chemical Engineering*, 32 (6), 1270-1278.

Husmann, M., Orth, H., Schlegel, S. & Teichgräber, B. (1998). Application of process control for improved nitrogen removal. *Water Science & Technology*, 38 (3), 263-269.

Han, J., Wang, W. 1994. Nonlinear Tracking Differentiator. *System Science and Mathematics*, Vol14, No. 2, pp.177-183., (In Chinese).

Han, J. and Yuan, L., 1999. The discrete form of the tracking differentiator. *Syst. Sci. Math. Sci.* 19(3), 268–273.

Henson, M. A. and Seborg, D.E., 1994. Adaptive nonlinear control of pH neutralization process. *IEEE Transacation on control systems Technology* Vol. 2, No. 3., August 1994.

Henze, M., Petersen, B., Gernaey, K and Vanrolleghem, P.A. 2002. Evaluation of an ASM1 model calibration procedure on a municipal-industrial wastewater treatment plant. IWA Publishing. *Journal of Hydroinformatics* -04.1. 2002.

Holenda, B. (2007/2008). Development of modeling, control and optimization tools for the activated sludge process. PhD dissertation, University of Pannonia.

Han, J, 2009. From PID to Active Disturbance Rejection Control. *IEEE Transaction on Industrial Electronics*, Vol.56, no.3 (translation from Chinese).

Han, Y., Brdys, M. A. and Piotrowski, R., 2008. Nonlinear PI control for dissolved oxygen tracking at wastewater treatment plant. IFAC. Proceedings of the 17th World Congress. The International Federation of Automatic Control Seoul, Korea, July 6-11, pp 13587-13592.

Han Y, Wang Wei. Nonlinear Tracking Differentiator, Science and Math. Scis., v.14, No. 2.

Hua, M.D., and Samson, C. 2011. Time sub-optimal nonlinear PI and PID controllers applied to longitudinal headway car control. International Journal of Control Vol. 84, No. 10, pp 1717-1728. Taylor and Francis Group.

Hung, ML., Lin, JS., Yan, JJ., and Liao, TL. 2008. Optimal PID control design for synchronization of delayed discrete chaotic systems. Chaos, Solitons and Fractals 35, pp 781–785.

IEC International Standard IEC 61131–3: Programmable Controllers, Part 3: Programming Languages”, IEC, 2003. International Electro-technical Commission. www.plcopen.org/

Ito, H. 2004. A Dissipative Approach to Control of Biological Wastewater Treatment Plants Based on Entire Nonlinear Process Models. Proceeding of the American Control Conference Boston, Massachusetts June 30 –July 2, pp 5489-5495.

Ingildsen, P., Jeppsson, U. & Olsson, G. (2002). Dissolved oxygen controller based on on-line measurements of ammonia combining feed-forward and feedback. Water Science and Technology, 45 (4-5), 453-460.

Jiang. F., Gao. Z., 2001. An Application of Nonlinear PID Control to a Class of Truck ABS Problem. Proceedings of the 40th IEEE Conference on Decision and Control, pp 516 – 521 vol.1.

Joo, D.S., Park, H. 1998. Control of the Dissolved Oxygen Concentration in the Activated Sludge Process. Department of Civil Engineering, KAIST, Taejon Korea, 305-701. Korean Society of Environmental Engineers. Volume 3, No.2, pp 115-121.

Kang, J., Wang, M., Xiao, Z., and Zhao, Y., 2009. Fuzzy PID control of the PH in an Anaerobic wastewater treatment process. ©2009 IEEE., pp 1-4

Kurfess, Thomas R. PhD, 2007. Getting in tune with Ziegler-Nichols. Academic Viewpoint column, Control Engineering magazine, Feb, issue, p. 28, <http://www.controleng.com/article/CA6412703.html>.

Khadir, M.T., Ringwood, J.V. 2003. Linear and nonlinear model Predictive control design for A milk pasteurization plant. Control and Intelligent Systems, Vol. 31, No. 1,

Kongo. K. 2008, Design and Control of a Nonlinear Control of the Dissolved oxygen in the Wastewater Treatment plant.

Krause, K., Bocker, K., Londong, J. 2002, Simulation of a nitrification control concept considering influent ammonium load. *Water Science and Technology*, 45 (4-5), 413-420.

Kandare, G. 2008. Oxygen control in a wastewater treatment plant using adaptive predictive controllers. Department of systems and control, Jozef Stefan Institute, Jamova 39, 1000 Ljubijana, Slovenia.

Kotze. W. 2005. Design and Control of a nonlinear predictive Control of the Dissolved oxygen concentration in the Wastewater Treatment process.

Amand. L., 2008. Control of aeration systems in activated sludge processes – a review. IVL Swedish Environmental Research Institute, Department of Information Technology, Uppsala University.

- Lee, N., la Cour Jansen, J., Aspegren, V. Henze, M. Nielsen, P.H. and Wagner, M. 2002. "Population dynamics in wastewater treatment plants with enhanced biological phosphorus removal operated with and without nitrogen removal", *Water Science & Technology* Vol 46 No 1-2 pp 163–170 IWA Publishing.
- Liu, G.P., Daley, S., 2001. Optimal-tuning PID control for industrial systems. School of Mechanical, Materials, Manufacturing Engineering and Management, University of Nottingham, University Park, Nottingham NG7 2RD, UK. *Control Engineering Practice* 9 (1185–1194).
- Liu, G.P., Daley, S., 2000. Optimal-tuning PID control for hydraulic systems. School of Mechanical, Materials, Manufacturing Engineering and Management, University of Nottingham, Nottingham NG7 2RD, UK, ALSTOM Energy Technology Centre Cambridge Road. *Control Engineering Practice* 8 (1045–1053). 2000 Elsevier Science Ltd
- Lindberg, C.F. 1997: Control and Estimation strategies applied to the Activated Sludge Process. PhD thesis. Uppsala University. Department of Materials Science Systems and Control Group. SE-751 03 Uppsala. Sweden.
- Lindberg, C.F, Carlsson, B. 1996. Nonlinear and Set-Point control of the dissolved oxygen concentration in activated sludge process. *Water science and Technology*, 34 (3-4):135-142.
- Lindberg, C.F, Carlsson, B. 1996. Estimation of the respiration rate and oxygen transfer function utilizing a slow DO sensor. *Water science and Technology*, 33(1):325-333.
- Lewis, R. 2001. Modelling control systems using IEC 61499 – Applying function blocks to distributed systems. London, UK: The Institution of Electrical Engineers, 2001, ISBN 0-85296-796-9.
- Lu, W., Yang, J., and Liu, X. 2012. The PID Controller Based on Artificial Neural Network and the Differential Evolution Algorithm. *Journal of Computers*, Vol. 7, No. 10, October.
- Luo, X., and Si, J. 2013. Stability of Direct Heuristic Dynamic Programming for Nonlinear Tracking Control Using PID Neural Network
- Macnab, CJB., 2014. Stable Neural-Adaptive Control of Activated Sludge Bioreactors. American Control Conference (ACC) June 4-6, Portland, Oregon, USA
- Muga. J. 2009, "Investigation of artificial neural networks for modeling, identification and control of nonlinear plant". Thesis, CPUT, Bellville, South Africa
- Mhaskar, P., El-Farra, N.H., and Christofides, P.D. 2004. A Method for PID Controller Tuning Using Nonlinear Control Techniques. *Proceeding of the 2004 American Control Conference* Boston, Massachusetts June 30 – July 2, pp 2925-2930.
- Nketoane, P.A. 2009, "Design and Implementation of a nonlinear controller in PLC as part of an Adroit Scada system for optimal adaptive control of activated sludge process." Thesis, CPUT, Bellville, South Africa
- Ostace, G.S, Cristea, Mircea. V., Agachi, P.S. 2010. Investigation of different strategies for the BSM1 WWTP with Reactive Secondary Settler Model. 20th European Symposium on Computer Aided Process

Engineering – ESCAPE20 S. Pierucci and G. Buzzi Ferraris (Editors). Elsevier B.V.

Qi, WM., Cai, WY., Ji, Q., and Cheng, YC. 2006. A design of nonlinear adaptive PID controller based on genetic algorithm. Proceedings of the 25th Chinese Control Conference 7-11 August, Harbin, Heilongjiang, pp 175-178. IEEE Catalog Number: 06EX13 10.

Pang, C., and Vyatkin, V. 2009. Automatic Model Generation of IEC 61499 Function Block Using Net Condition/Event Systems. Senior Member IEEE

Prakash, J., and Srinivasan, K. 2009. Design of nonlinear PID controller and nonlinear model predictive controller for a continuous stirred tank reactor. ISA Transactions 48, pp 273-282. www.elsevier.com/locate/isatrans

Primbs, J. A., Nevistic, V and Doyle, J.C. 1999. Nonlinear optimal control: a control Lyapunov Function and receding horizon perspective. Asian Journal of Control, Vol. 1, No. 1, pp. 14-24, March 1999.

Peng, X and Cheng, S. 2005. Application of nonlinear PID Controller in Superconducting Magnetic Energy Storage. Journal of Electrical and Electronics Engineering. Vol. 5, No. 1, pp 1271-1278.

Rahmat, M.F., Samsudin, S.I., Wahab, N.A., Salim, Sy and Gaya, M.S. 2011. Control Strategies of Wastewater Treatment Plants. *Australian Journal of Basic and Applied Sciences*, 5(8): pp 446-455, ISSN 1991-8178.

Ren, Y., Li, Z and Zhang, F., 2010. A New Nonlinear PID Controller and its Parameter Design. World Academy of Science, Engineering and Technology 72, pp 884-889

Rodrigo, M. A. Seco, A. Ferrer, J. Penya-roja, J. M. 1998. "Control difuso de la aireacion en tratamientos biológicos de depuración de aguas residuales. Information Technology 9 (4) 221±228.

Rodrigo, M.A., Seco, A., Ferrer, J., Penya-roja, J.M., and Valverde, J.L. 1999. Nonlinear control of an activated sludge aeration process: use of fuzzy techniques for tuning PID controllers. Elsevier Science, ISA Transactions 38, pp. 231-241. www.elsevier.com/locate/isatrans

Reemtsma, T and Jekel, M. 1997. Dissolved organics in tannery wastewaters and their alteration by a combined anaerobic and aerobic treatment. Department of Water Quality Control, Technical University of Berlin, D-10623 Berlin, Germany., Vol. 31, No. 5, pg. 1035-1046., Elsevier Science Ltd.

Sanchez, A., and Katebi, M.R. 2003. Predictive Control of Dissolved Oxygen in an Activated Sludge Wasterwater Treatment Plant.

Selvabalan, M., Dhayalan, S., and Shimpi, J.A., 2012. Application of knowledge based engineering techniques in water resources development. India Water Week – *Water, Energy and Food Security: Call for Solutions*, 10-14 April 2012, pp 1-8, New Delhi.

Slotine JE, Li W. Applied nonlinear control. Englewood Cliffs, New York: Prentice-Hall; 1991.

Shinners. Stanley. M. 1989. Modern Control System Theory and Application 2nd Edition, published by, Addison Wesley, page: 368-371.

Singh, A., Bisht, G., Padhy, P.K. 2013. Neural network based adaptive Non- linear PID

Controller for non-holonomic mobile robot. International Conference on Control, Automation, Robotics and Embedded System (CARE). IEEE

Shuhua, M., and Wei, L., 2009. Non-linear PID Control Method with Feed-forward in Smart Car. Chinese Control and Decision Conference (CCDC). ©2009 IEEE, pp 462-465.

Skogestad, S, and Jacobsen, E.W. 1995. Multiple steady states and instability in distillation – Implications for operation and control. Ind. Eng. Chem. Res., Vol. 34, pg 4395-4405.

Su, Y.X., Sun, D., and Duan, B.Y., 2005. Design of an enhanced nonlinear PID controller. Published by Elsevier Ltd. Mechatronics 15, pp 1005-1024.

Tzoneva, R. 2007. Method for real time optimal control of the Activated Sludge Process. Proceeding of the 15th Mediterranean Conference on Control and Automation, July 27 – 29, Athens – Greece. IFAC.

Vanrolleghem P.A. 2003. Models in advanced WWTP control. *Colloque Automatique et Agronomie Montpellier 22-23-24 Janvier*. <http://hdl.handle.net/1854/LU-167374>

Wahab, N.A., Katebi, MR., and Balderud, J. 2007. Multivariable PID control design for wastewater systems. Mediterranean Conference on Control and Automation, July 27-29, 2007, Athens-Greece, T04-012. ©2007 IEEE.

Wahab, N.A., Gaya, M.S., Sam, Y.M., Jeppsson, U., and Katebi, R. 2012. A LabView-Based Simulation for the Activated Sludge Process

Wright, R.A., 2001. Model-Based Synthesis of Nonlinear PI and PID Controllers. AICHE Journal, Vol. 47, No.8.

www.beckhoff.com

<http://www.plcs.net/>

www.yisi.com/index.php/spring

Yang, Chia-han., and Vyatkin, Valeriy. 2012. Transformation of Simulink models to IEC 61499 Function Blocks for verification of distributed control systems

Yang, T., Zhang, L., and Chadli, M. 2013. Fuzzy Modeling of Activated Sludge Wastewater Treatment Processes and Predictive Control of Dissolved Oxygen. Process System Engineering Laboratory in MIT, USA

Ye, H., Luo F, and Xu, Y. 2010. Dissolved Oxygen Generic Model Control of Wastewater Treatment Process Based on Immune Optimization Least Squares Support Vector Machine. Proceedings of the 8th World Congress on Intelligent Control and Automation July 6-9, Jinan, China.

Yoo, Chang Kyoo., Lee, Jong-Min., and Lee, In-Beum. 2004. Nonlinear Model-based Dissolved Oxygen Control in a Biological Wastewater Treatment Process. Korean J. Chem. Eng., 21(1), pp.14-19.

Zaidner, G., Korotkin, S., Shteimberg, E., Ellenbogen, A., Arad, M and Cohen, Y. 2010 Nonlinear PID and its application in process control. IEEE 26th Convention of Electrical and Electronics Engineers in

Israel, pp 574-577.

Ziegler, J. B., Nichol, N. B. 1942. Optimum settings for automatic controllers. *ASME Transactions*, v64, pp. 759-768.

Zhao, H., Isaacs, S. H, Soeberg, H, and Kummel, M., 1994. Nonlinear optimal control of an alternating activated sludge process in a pilot plant. Department of chemical engineering, Technical University of Denmark, building 229. *J. Proc. Cont.* Volume 4, Number 1.

Zhou, K. Doyle, J.C., Glover, K. 1946/ 1996. *Robust and Optimal Control*. Prentice Hall, Upper Saddle River, New Jersey 07458.

APPENDICES

APPENDIX A: MATLAB PROGRAM

Appendix A: present the Matlab program for simulation of the DO open loop process using ASM1 parameters, the Matlab script file for this program is named as - *DO_last.m*

```
%=====2014=====
%                               Nomzamo Tshemese
%                               Cape Peninsula University of Technology
%=====
%---Parameters for simulation of the Dissolved Oxygen Concentration
%=====
clear all
clc
%=====
%                               System Variables
%=====
Sosat=8;           % Dissolved oxygen saturation
K1=240;           % Constant calculated from KLa=240 metres cubed per day
K2=1.0961e-004;   % Constant calculated from KLa=240 metres cubed per day
Soo=005;%0.49;    % Oxygen
V=1333;          %Volume of Tanks 3,4&5
soin=0.01;%0.8;%2 % Internal disturbance
t=0:1:8;         %time
u=50000.0*ones(1,9); % Air flow rate
Qq=55338;        % Internal recycle flow rate
Qr=18446;        % Influent flow rate
Qo=18446;        % Recycle flow rate
Q=Qq+Qr+Qo;     % Total flow rate
D=Q/V;          %
%=====
%                               State variables and kinetic values for ASM1
%=====
muA=0.9; %0.5;   %The maximum autotrophic growth rate
muH=6; %4;      %The maximum heterotrophic growth rate
Koh=0.20;       %Half-saturation heterotrphic oxygen growth rate
Yh=0.67;       %Heterotrophic yield
Ya=0.24;       %Is the autotrophic yield
Ks=10; %20     %Half-saturation heterotrphic growth rate
Knh=1.0; %0.2; %Half-saturation autotrophic growth rate
Koa =0.4;%0.3; %Half-saturation autotrophic oxygen growth rate
%-----
Xbhs=2559.4; %3839.166; % Active heterotrophic biomass
Xbas=149.8; %78.8985; % Active autotrophic biomass
Snhs=1.73;   % Ammonia and ammonium nitrogen
Sss=0.89;   % Readily biodegradable substrate
Snh=Snh*ones(1,9); %
Ss=Ss*ones(1,9); %
Xba=Xbas*ones(1,9); %
Xbh=Xbhs*ones(1,9); %
T=t'; %
U=u'; %
Ass=Ss'; %
Asnh=Snh'; %
Axba=Xba'; %
Axbh=Xbh'; %
```

```

rso=(-muH*((1-Yh)/Yh)*(Ss/(Ks+Ss))*(Soo/(Koh+Soo))*Xbhs-muA*((4.57-
Ya)/Ya)*(Snhs/(Knh+Snhs))*(Soo/(Koa+Soo))*Xbas);
DO_M %call DO
%=====

```

APPENDIX B: MATLAB/SIMULINK SOFTWARE SCHEDULE

The appendix B presents some Simulink models and MATLAB script files that are used in the development of the mathematical algorithms of the linear and nonlinear PID for control of the dissolved oxygen concentration trajectories. The description of these script files is contained in Chapter 5, Chapter 6 and Chapter 7, as well as the Table 9.1 in Chapter 9. The script files supply data to the Simulink environment.

Appendix B1: Matlab script - LPID_DO.m

The following program file shows the designed controller parameters of the linear PID controller through Ziegler-Nichols (ZN) method. These parameters are used to control the nonlinear process of the Dissolved Oxygen (DO) concentration.

```

%=====
%the script file for the LPID controller based on Z-N method to control
%DO process;
clc %clear the command window
%=====
%Parameters for simulation of the NLPID controller with DO
%=====
kp = 120; %calculated proportional gain;
ki = 50; %designed integral gain;
kd = 0.005; %calculated derivation part;
%=====
plot(time,DO); %plotting the output of the nonlinear DO process under LPID
grid on
xlabel('Time [days]','FontSize',11);
ylabel('DO[mg/L]', 'FontSize',11);
title(' Closed loop DO process response under the LPID
controller','FontSize',11');
gtext({'Kp= 120','Ki= 50','Kd= 0.005'});
legend('DO');

```

Appendix B2: Matlab script - NLPID1withDOzn.m

This program is for simulation of the Nonlinear PID controller using the final adjusted parameters based on the Ziegler-Nichols method, this controller is used to control the nonlinear process of DO that has the system parameters shown in Appendix A.

```

%=====
%the script file for the NLPID1 controller based on Z-N method;
%=====
%Parameters for simulation of the DO process under NLPID1 controller

```

```

%=====
kp = 120;      %120 %calculated proportional gain;
ki = 0.5;     % 50  %designed integral gain;
kd = 0.005;   %calculated derivation part;
%=====
%   Nonlinear Function parameter values
%=====
ap= 0.9;
ai= 0.9;
ad= 1.9;
dp= 0.005;
di= 0.05;
dd= 0.05;
%===== Nonlinear Differentiator Parameters
alfa1 = 0.5;
alfa2 = 0.5;
M1= 100; %
M2= 100; %
%=====
%   Copy and use the DO parameters in Appendix A
%=====
NLPID1zn_DOmodel %simulate the closed loop model in Simulink;
%=====

```

Appendix B3: NLPID2zn_DO.m

This program is for simulation of Nonlinear PID2 controller. It uses the final adjusted parameters based on Ziegler-Nichols method. These parameters are used in the controller to control the nonlinear process of DO.

```

%-----Mfile: Description-----%
%-----Test NLPID2 Ziegler-Nichols with DO-----%
% this program is for simulation of Nonlinear PID2 uses the used final
% adjusted parameters based on Ziegler-Nichols method
clear all
clc
%=====
%Parameters for simulation of the NLPID2 controller only
%=====
kp   = 200; %120  %100;
ki   = 0.5; %50;  %0.5;
kd   = 0.005;
%=====
%   Nonlinear Function and Nonlinear Differentiator values
%=====
ap= 0.9;
ai=0.9;
ad=1.9;
dp=0.005;
di=0.05;
dd= 0.05;
%===
alfa1 = 0.5;

```

```

alfa2 = 0.5;
M1= 100; %
M2= 100; %
%=====
%   Copy and use the DO parameters in Appendix A
%=====
nlpid2_DOmodel.mdl %simulate the closed loop model in Simulink;
%=====

```

Appendix B4: LPIDpp1.m

This program uses the calculated values of the matrices A and B through the Taylor series to find the controller parameters.

```

A=-3;
B=200; %
kp= (4+A)/B
ki= (6/B)
(1+Bkd) =1;
Kd=(1-1)/B; kd=0
%=====
%   Copy and use the DO parameters in Appendix A
%=====
LPID_DO.mdl %simulate the closed loop model in Simulink;
%=====

```

Appendix B5: - NLPID1pp1withDOpar.m

```

%----- Matlab script file: Description-----%
%Test DO closed loop under NLPID1 based on Pole-Placement -----%
% this program is for simulation of the DO process under the Nonlinear PID controller (NLPID1) uses
% the designed control parameters of Pole-Placement method for the
% LPID controller based on the linearized DO model.

```

```

clear all % clear the workspace
clc
%=====
%Parameters designed for LPID controller and were later tuned for NLPID1 to control DO
%=====
A=-3;
B=200; %
kp= (4+A)/B
ki= (6/B)
(1+Bkd) =1;
Kd=(1-1)/B; kd=0
%-----
%   Nonlinear Function parameter values
%=====
ap= 0.9;
ai=0.9;
ad=1.9;
dp=0.005;
di=0.05;
dd= 0.05;
%===== Nonlinear Differentiator Parameters
alfa1 = 0.5;
alfa2 = 0.5;

```

```

M1= 100;
M2= 100;
%soin = 0.01;% 0.8;% Internal disturbance
%=====
% Copy and use the DO model parameters in Appendix A
%=====

Appendix B6: - NLPID2pp1_DOpar.m

%----- Matlab script file: Description-----%
%Test DO closed loop process under the NLPID2 based on the Pole-Placement method (PP1)-----%
clear all % clear the workspace
clc
%=====
%Parameters designed for LPID controller and were later tuned for NLPID1 to control DO
%=====
A=-3; %-0.8;
B=200; %0.03;% 15000;
kp= (4+A)/B
ki= (6/B)
(1+Bkd) =1;
Kd=(1-1)/B; kd=0
%-----
% Nonlinear Function parameter values
%=====
ap= 0.9;
ai=0.9;
ad=1.9;
dp=0.005;
di=0.05;
dd= 0.05;
%===== Nonlinear Differentiator Parameters
alfa1 = 0.5;
alfa2 = 0.5;
M1= 100;
M2= 100;
%soin = 0.01;% 0.8;% Internal disturbance
%=====
% Copy and use the DO model parameters in Appendix A
%=====

```

```

%%%%%%%%%%=====

```

Appendix B7: - findLPIDpar.m

This section is used to find the controller parameters of the LPID controller through the PP2 method

```

clear all
clc
%=====
% System Variables from ASM1
%=====
setpoint=2; %Set point value
Sosat=8; %Dissolved oxygen saturation
K1=240; %Constant calculated from KLa=240 metres cubed per day
K2=1.0961e-004; % Constant calculated from KLa=240 metres cubed per day
Soo=0.05;%0.49; % Oxygen
V=1333; % Volume of Tanks 3,4&5
soin=0.01; %Internal disturbance

```

```

%e=setpoint-So;      %error
Qq=55338;           %Internal recycle flow rate.
Qr=18446;           %Influent flow rate
Qo=18446;           %Recycle flow rate
%ratios used in the equations
Q=Qq+Qr+Qo;        %Total flow rate
D=Q/V;%
t=0:1:8; %
So= 4.3203;         %Oxygen
u=50000.0*ones(1,9);% Air flow rate
%=====
%----- FOR rso -----%
muA = 0.9; %0.5      %the maximum autotrophic growth rate
muH = 6; %4          %the maximum heterotrophic growth rate
Koh = 0.20;          %Half-saturation heterotrphic oxygen growth rate
Yh = 0.67;           %Heterotrophic yeild
Ya = 0.24;           %the autotrophic yield
Ks = 10;             %Half-saturation heterotrphic growth rate
Knh = 1.0;           %Half-saturation autotrophic growth rate
Koa = 0.4;           %Half-saturation autotrophic oxygen growth rate
%-----
%====Active heterotrophic biomass and Active autotrophic biomass====%
%-----Ezi right-----%
%-----
Xbhs=2559.4; %3839.166; % Active heterotrophic biomass
Xbas=149.8; %78.8985; % Active autotrophic biomass

% Xbhs=2.68737;Xbas=0.15729; % -186.4457
% Xbhs=2.43143;Xbas=0.14231; % -168.6890
% Xbhs=3.8391;Xbas=0.2247; % -266.3510
% Xbhs=1.2797;Xbas=0.0749; % -88.7837

Snhs=1.73;          %Ammonia and ammonium nitrogen
Sss=0.89;           %Readily biodegradable substrate
Snh=Snhs*ones(1,9);%
Ss=Sss*ones(1,9);%
Xba=Xbas*ones(1,9);%
Xbh=Xbhs*ones(1,9);%
T=t';%
U=u';%
Ass=Ss';%
Asnh=Snh';%
Axba=Xba';%
Axbh=Xbh';%
V=1333;            % Volume of Tanks 3,4&5
rso=(-muH*((1-Yh)/Yh)*(Ss/(Ks+Ss))*(Soo/(Koh+Soo))*Xbhs-muA*((4.57-
Ya)/Ya)*(Snhs/(Knh+Snhs))*(Soo/(Koa+Soo))*Xbas);
x = [1,1];         %Make a starting guess at the solution
kp = x(1);
ki = x(2);
%ki=(kp/Ti);%; %x(2); Ti = 0.5;
kd=0.01;
%kd = kp*Td;
SimOut= sim('closedloop', 'ReturnWorkspaceOutputs', 'on'); % Return all
Simulink SimulationOutputs
So=SimOut.get('Ao'); % Output of So and the setpoint
Time=SimOut.get('time');
Sol=So(:,1); % So alone
So2=SimOut.get('Ao1');

```



```

L=[Time So1 So2]; % Take time, So1, So2 and store them to L
integral = 0;
previous_error = 0;
error=0;
    r=2; %set-point
dt = 0.01;
n=801;
for i=1:n
    S01=So1(i);
    S02=So2(i);
    previous_error = error;
    integral = integral + error*dt; % integral term
    error = r-S01;
    [x,FVAL,EXITFLAG] = fsolve(@(x)
myfun5(S01,S02,D,soin,rso,K1,K2,Sosat,x,integral,error,previous_error),[30,10]
,optimset('Display','iter')); % initial guess values: Kp=30,Ti=10;
    KpI=x(1);
    TiI=x(2);
    Kp2(1,i)= KpI;
    Ti2(1,i)= TiI;

% Ki2(1,i)= KpI/TiI;
%SS1(i,1)=S01; SS2(i,1)=S02;
end
    Kp2=Kp2';
    Ti2 = Ti2';
% Ki2=Ki2';
plot(Time,Kp2,'r',Time,Ti2,'b')
ff=[Kp2 Ti2];
%ff=[Kp2 Ki2 Ti2];

```

The function file used/called above "myfun5" is:

```

function F =
myfun5(S01,S02,D,soin,rso,K1,K2,Sosat,x,integral,error,previous_error)
Kd = 0.01; %0; % derivative term is not necessary in this problem
% previous_error = 0;
% integral = 0;
dt = 0.01;
derivative = (error-previous_error)/dt; % derivative term
F=S02-(D)*(soin-S01)-rso-K1*(1-exp(-
K2*(x(1)*error+x(2)*integral+Kd*derivative)))*(Sosat-S01);
end

```

Appendix B8: Findnlpid1par_PP2.m

```

%-----Mfile: Description-----%
%-----Test fsolve control parameter with DO-----%
% this program tries to find the Nonlinear PID controller (NLPID1) parameters
% designed based on the nonlinear DO model.
%-----
clear all % clear the workspace
clc
%=====
%Find Optimal value through fsolve function simulation
%=====
%===== Nonlinear Differentiator Parameters
alfal = 0.5;

```

```

alfa2 = 0.5;
M1= 100;
M2= 100;
%=====
Sosat=8;
K1=240;% Constant calculated from KLa=240 metres cubed per day
K2=1.0961e-04;% Constant calculated from KLa=240 metres cubed per day %
Soo=0.05; %0.491;%0.05; %Oxygen
V=1333;
soin=0.01;%2;%0.01; Internal disturbance
t=0:1:8; %time interval or range.
u=50000.0*ones(1,9); %Air flow rate
Qq=55338; %555338;
Qr=18446;
Qo=18446;
Q=Qq+Qr+Qo;
D=Q/V;
%=====
% State variables and kinetic values for ASM
%=====
muA=0.9; %0.5
muH=6; %4;
Koh=0.20;
Yh=0.67;
Ya=0.24;
Ks=10; %20;
Knh=1.0;
Koa =0.4; %Half-saturation autotrophic oxygen growth rate
Xbhs=2559.4;Xbas=149.8; %
Snh=1.73;% Ammonia and ammonium nitrogen
Sss=0.89;
Snh=Snh*ones(1,9);
Ss=Sss*ones(1,9);
Xba=Xbas*ones(1,9);
Xbh=Xbhs*ones(1,9);
T=t';
U=u';
Ass=Ss';
Asnh=Snh';
Axba=Xba';
Axbh=Xbh';
rso=(-muH*((1-Yh)/Yh)*(Ss/(Ks+Ss))*(Soo/(Koh+Soo))*Xbhs-muA*((4.57-
Ya)/Ya)*(Snh/(Knh+Snh))*(Soo/(Koa+Soo))*Xbas);
% NLPID1_NLDO2
%-----
% Nonlinear Function parameter values
%=====
ap= 0.9;
ai=0.9;
ad=1.9; % 1.9
dp=0.005;
di=0.05;
dd= 0.05;
x = [1,1]; %Make a starting guess at the solution
kp = x(1);
Ti = x(2);
ki = kp/Ti;
Td = 0.01;
kd=kp*Td;

```

```

SimOut= sim('closedloop2', 'ReturnWorkspaceOutputs', 'on'); % Return all
Simulink SimulationOutputs
So=SimOut.get('Ao'); % Output of So and the setpoint
Time=SimOut.get('time');
So1=So(:,1); % So alone
So2=SimOut.get('Ao1');
L=[Time So1 So2]; % Take time, So1, So2 and in store them to L

integral = 0;
previous_error = 0;
error=0;
r=2; %setpoint
dt = 0.01;
n=801;
% delta_x=0.01;
for i=1:n
    S01=So1(i);
    S02=So2(i);
    previous_error = error;
    error2=(sign(error)*(abs(error))^ap);%Kp
    integral=integral+(sign(error)*(abs(error))^ai)*dt; % integral term
    error = r-S01;
    [x,FVAL,EXITFLAG] =
fsolve(@(x)myfun1(S01,S02,D,soin,rso,K1,K2,Sosat,x,integral,error,error2,previ
ous_error), [52,10],optimset('Display','iter'))% % initial guess values:
Kp=52,Ti=10;
KpI=x(1);
    TiI=x(2);
    Kp2(1,i)= KpI;
    Ti2(1,i)= TiI;
end
Kp2=Kp2';
Ti2=Ti2';
plot(Time,Kp2,'r',Time,Ti2,'b');
FF=[Kp2 Ti2]; %store the outcome of the needed value in FF

```

Appendix B8b: - Myfun1.m

Matlab function file for the nonlinear PID equation used for the controller parameters design through *fsolve* Matlab function

```

function F =
myfun1(S01,S02,D,soin,rso,K1,K2,Sosat,x,integral,error,error2,previous_error)
    Td = 0.01;
    %Kd = 0.01;%0; % derivative term is not necessary in this problem
    dt = 0.01;
    ad=0.9;
    %derivative = (error-previous_error)/dt; % derivative term
    derivative = (((sign(error))*(abs(error))^ad)-((sign(error-
previous_error)*abs(error-previous_error)^ad)))/dt; % derivative term

F=S02-(D)*(soin-S01)-rso-(K1*(1-exp(-
K2*((x(1)*error2)+((x(1)/x(2))*integral)+(x(1)*Td*derivative))))*(Sosat-S01);
%F=S02-(D)*(soin-S01)-rso-(K1*(1-exp(-
K2*((x(1)*error2)+((x(2))*integral)+(Kd*derivative))))*(Sosat-S01);
%F=S02-(D)*(soin-S01)-rso-K1*(1-exp(-
K2*(x(1)*error+x(2)*integral+Kd*derivative)).*(Sosat-S01);
end

```

Appendix B8c: - *nlpid1_DOmodelpp2.m*

Matlab script file to simulate the closed loop DO process under the NLPID1 (PP2)

```
%=====
%--Description: Test NLPID1 controller of fsolve parameter with DO --%
% This program is for closed loop system simulation of the NLPID1 controller
% with DO plant. The control parameters are design using Pole Placement
% method (PP2) based on the nonlinear DO plant.
%=====
clear all % clear the workspace
clc
%=====
%Controller Parameters for simulation of the NLPID1 to control DO process
%=====
kp = 24.66; %
Ti = 66.66; %iki=0.5
ki=kp/Ti; %ki=0.369
kd =0.01; % 0.005
%=====
% Nonlinear Function parameter values
%=====
ap= 0.9; %
ai=0.9; %
ad=1.9; %
dp=0.005; %
di=0.05; %
dd= 0.05; %
%===== Nonlinear Differentiator Parameters
alfa1 = 0.5; %
alfa2 = 0.5; %
M1= 100; %
M2= 100; %
%=====

% copy and use ASM1 parameters in Appendix A
%=====
% System Variables
%=====

Sosat=8; % Dissolved oxygen saturation
K1=240;% Constant calculated from KLa=240 metres cubed per day
K2=1.0961e-04;% Constant calculated from KLa=240 metres cubed per day
Soo=0.05; % Oxygen initial condition
V=1333; % volume of the aeration tanks (3,4&5)
Soin=0.01; % Internal disturbance
t=0:1:8;
u=50000.0*ones(1,9); % Air flow rate
Qq=55338; % Internal recycle flow rate
Qr=18446; % Influent flow rate
Qo=18446; % Recycle flow rate
Q=Qq+Qr+Qo;
D=Q/V;
%=====
% State variables and kinetic values for ASM
%=====
muA=0.9; % Maximum autotrophic growth rate
muH=6; % Maximum heterotrophic growth rate
Koh=0.20; % Half-saturation heterotrophic oxygen growth rate
```

```

Yh=0.67; % Heterotrophic yeild
Ya=0.24; % Autotrophic yield
Ks=10; % Half-saturation heterotrphic growth rate
Knh=1.0; % Half-saturation autotrophic growth rate
Koa =0.4; % Half-saturation autotrophic oxygen growth rate
Xbhs=2559.4;Xbas=149.8; % % heterotrophic biomass% autotrophic biomass

Snhs=1.73;% Ammonia and ammonium nitrogen
Sss=0.89; % Readily biodegradable substrate
Snh=Snh*ones(1,9);
Ss=Sss*ones(1,9);
Xba=Xbas*ones(1,9);
Xbh=Xbhs*ones(1,9);
T=t';
U=u';
Ass=Ss';
Asnh=Snh';
Axba=Xba';
Axbh=Xbh';
%=====
=====plotting graphs=====

```

Appendix B9: Matlab script – *findnlpid2par*

```

%-----Mfile:Description-----%
%-----Test fsolve control parameter with DO-----%
% This program is for the simulation of the Nonlinear PID controller (NLPID2).
% It uses the designed control parameters of optimal (fsolve) method for a
% NLPID controller based on the nonlinear DO model.

clear all % clear the workspace
clc
%=====
%Parameters for simulation of the NLPID1 controller only
%=====
%===== Nonlinear Differentiator Parameters
alfa1 = 0.5;
alfa2 = 0.5;
M1= 100;
M2= 100;
%=====
Sosat=8;
K1=240;% Constant calculated from KLa=240 metres cubed per day
K2=1.0961e-04;% Constant calculated from KLa=240 metres cubed per day
%rSo=0.5
Soo=0.05; %0.491;%0.05; %Oxygen
V=1333;
soin=0.01;%2;%0.01; Internal disturbance
t=0:1:8; %time interval or range.
u=50000.0*ones(1,9); %Air flow rate
%u=82.000000*ones(1,9);
Qq=55338; %555338;
Qr=18446;
Qo=18446;
Q=Qq+Qr+Qo;
D=Q/V;
% D=Q/V;
%=====

```

```

%           State variables and kinetic values for ASM
%=====
muA=0.9; %0.5
muH=6; %4;
Koh=0.20;
Yh=0.67;
Ya=0.24;
Ks=10; %20;
Knh=1.0;
Koa =0.4; %Half-saturation autotrophic oxygen growth rate
Xbhs=2559.4; %3839.166;% Active heterotrophic biomass
Xbas=149.8; %78.8985;% Active autotrophic biomass
Snhs=1.73;% Ammonia and ammonium nitrogen
Sss=0.89;
Snh=Snhs*ones(1,9);
Ss=Sss*ones(1,9);
Xba=Xbas*ones(1,9);
Xbh=Xbhs*ones(1,9);
T=t';
U=u';
Ass=Ss';
Asnh=Snh';
Axba=Xba';
Axbh=Xbh';
rso=(-muH*((1-Yh)/Yh)*(Ss/(Ks+Ss))*(Soo/(Koh+Soo))*Xbhs-muA*((4.57-
Ya)/Ya)*(Snhs/(Knh+Snhs))*(Soo/(Koa+Soo))*Xbas);
% NLPID1_NLDO2
%-----
% Nonlinear Function parameter values
%=====
ap= 0.9;
ai=0.9;
ad=0.9;
dp=0.005;
di=0.05;
dd= 0.05;
x = [1,1]; %Make a starting guess at the solution for closed loop model
kp = x(1);
ki = x(2);
% ki = 1/Ti; %x(2); Ti = 0.5;
kd = 0.01;
SimOut= sim('closedloop3', 'ReturnWorkspaceOutputs', 'on'); % Return all
Simulink SimulationOutputs
So=SimOut.get('Ao'); % Output of So and the setpoint
Time=SimOut.get('time2');
Sol=So(:,1); % So alone
So2=SimOut.get('Ao1');
L=[Time Sol So2]; % Take time, Sol, So2 and instore them to L
integral = 0;
previous_error = 0;
error=0;
r=2; %setpoint
dt = 0.01;
n=801;
% delta_x=0.01;
for i=1:n
    S01=Sol(i);
    S02=So2(i);
    previous_error = error;

```

```

% integral      = integral + error*dt;      % integral term
errorp=(sign(error)*(abs(error))^ap);%Kp
integral=integral+(sign(error)*(abs(error))^ai)*dt; % integral term
error = r-S01;
[x,FVAL,EXITFLAG] = fsolve(@(x)
myfun2(S01,S02,D,soin,rso,K1,K2,Sosat,x,integral,error,errorp,previous_error),
[30,10],optimset('Display','iter'))%inial Kp=30;Ki=10

KpI=x(1);
KiI=x(2);
Kp2(1,i)= KpI;
Ki2(1,i)= KiI;
% SS1(i,1)=S01;
% SS2(i,1)=S02;
end
Kp2=Kp2';
Ki2=Ki2';
plot(Time,Kp2,'r',Time,Ki2,'b');
FF=[Kp2 Ki2];

```

Appendix B9b: “myfun2”

```

function F =
myfun2(S01,S02,D,soin,rso,K1,K2,Sosat,x,integral,error,errorp,previous_error)
Kd = 0.01; %0;      % derivative term is not necessary in this problem
dt = 0.01;
lamda=0.5; %ap= 0.9;
          %ai=0.9;
          %ad=0.9;
%derivative = (((sign(error))*(abs(error))^ad)-(sign(previous_error)^ad))/dt;
% derivative term
          %derivative = (error-previous_error)/dt; % derivative term
derivative = (((sign(error))*(abs(error))^ad)-((sign(error-
previous_error)*abs(error-previous_error)^ad)))/dt; % derivative term
F=S02-(D)*(soin-S01)-rso-(K1*(1-exp(-
K2*((x(1)*errorp)+(x(2)*integral)+(Kd*derivative)))))*(Sosat-S01);
end

```

Appendix B9c: “NLPID2PP2par_DO”

```

Matlab script file to simulate the closed loop DO process under the NLPID2 (PP2)
%=====
%--Description: This program is for the closed loop system simulation of the closed loop system of the
NLPID2 controller the with DO plant. The control parameters are design using Pole Placement
% method (PP2) based on the nonlinear DO plant.
%=====
clear all % clear the workspace
clc
%=====
%Controller Parameters for simulation of the NLPID2 to control DO process
%=====
kp = 30.118; %
ki = 0.52; %
Ti=kp/ki; %
kd =0.01; %

```

```

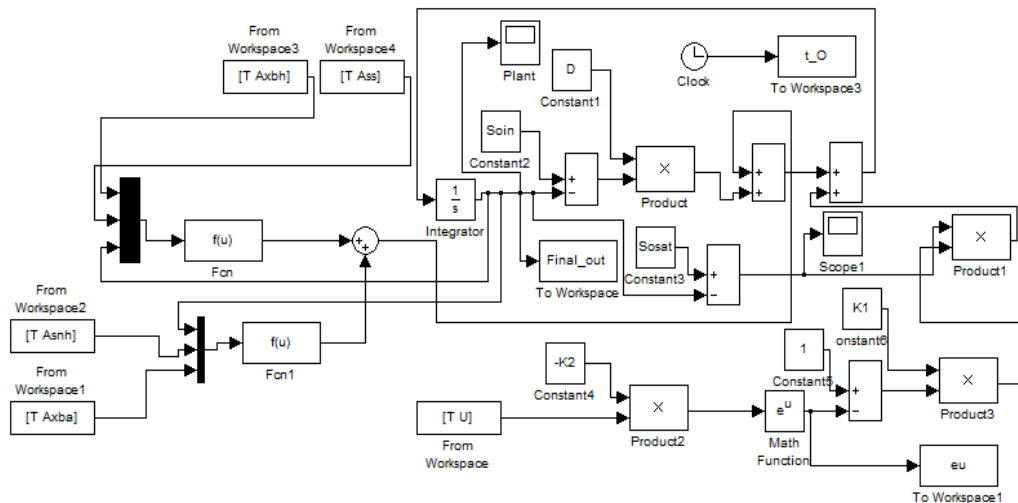
%=====
% Nonlinear Function parameter values
%=====
Lamda=0.05
% ap= 0.9; ai=0.9; ad=1.9;
dp=0.005; %
di=0.005; %
dd= 0.005; %
%===== Nonlinear Differentiator Parameters
alfa1 = 0.5; %
alfa2 = 0.5; %
M1= 100; %
M2= 100; %
%=====

```

% copy and use ASM1 parameters in Appendix A

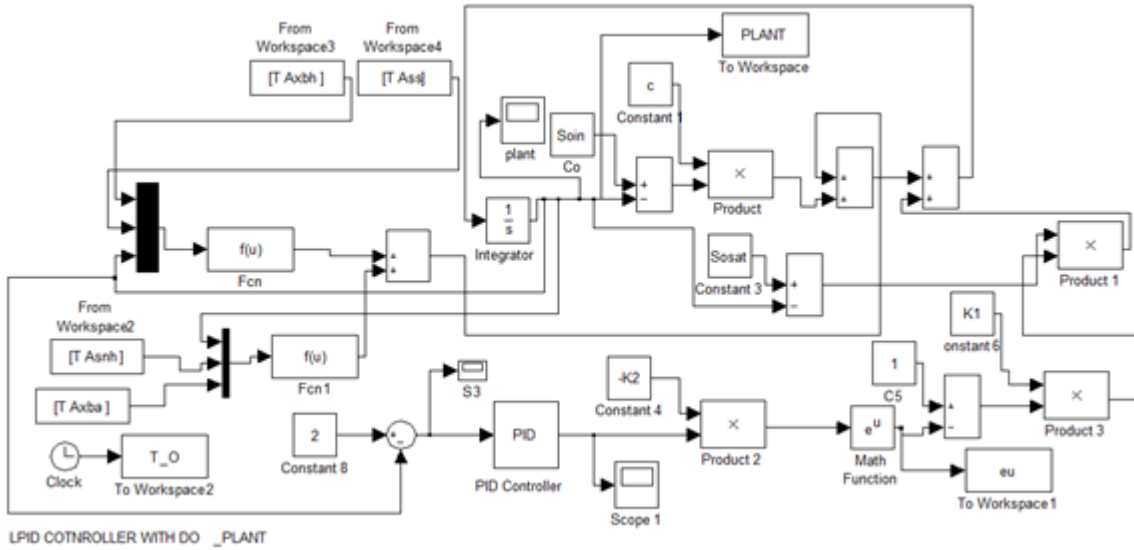
APPENDIX C: THIS PRESENTS THE SIMULINK MODELS USED WITH THE MATLAB SCRIPT FILES PRESENTED IN APPENDIX B

Appendix C1: DO model.mdl



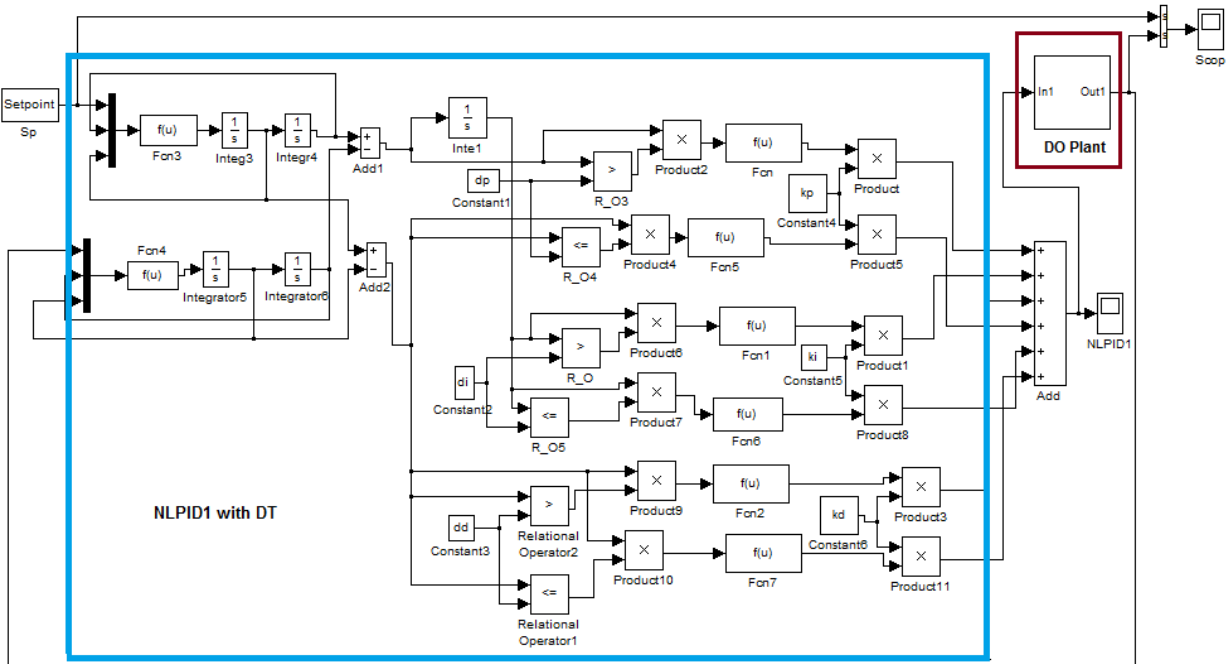
Appendix C2: LPIDwithDO.mdl

Simulink model of the LPID with DO process



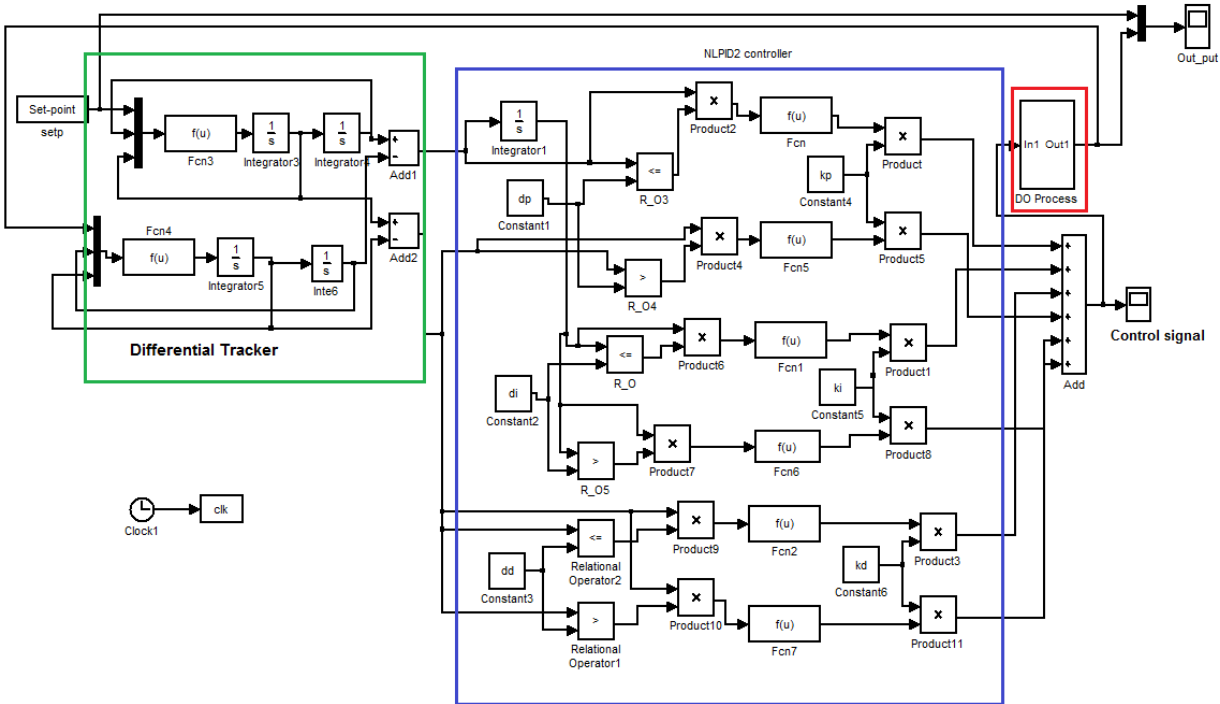
Appendix C3: NLPID1zn_DOmodel

Simulink model of the NLPID1 controller with the DO process closed loop system



Appendix C4: nlpid2_DOmodel.mdl

Simulink model of the NLPID2 controller with the DO process closed loop system



APPENDIX D: PLC HARDWARE

